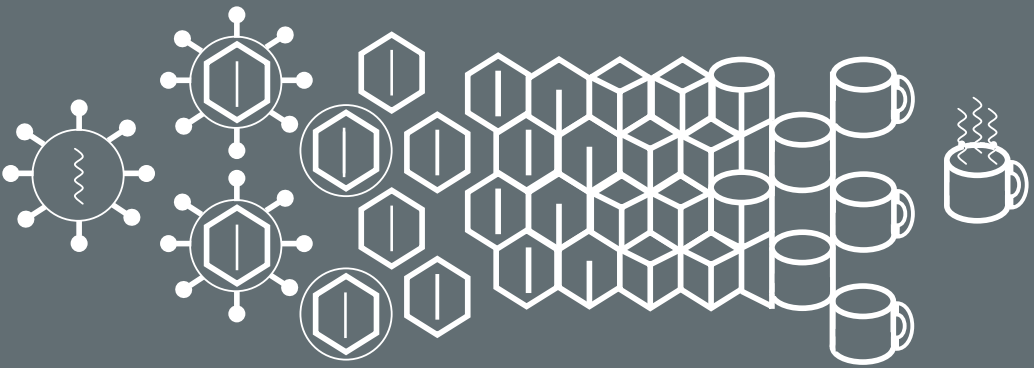


PATHOGENESIS OF ROTAVIRUS INFECTION



JOS BOSHUIZEN

PATHOGENESIS OF ROTAVIRUS INFECTION

J.A. Boshuizen

Pathogenesis of Rotavirus Infection

Thesis, Erasmus University Rotterdam – with references – with summary in Dutch

ISBN 90-9019438-X

© 2005 J.A. Boshuizen, Rotterdam, The Netherlands.

All rights reserved. No part of this theses publication may be reproduced or transmitted in any form, by any means, electronic or mechanical, including photocopy, recording or any information storage and retrieval system, without permission of the author.

Cover illustration by Mireille Boshuizen.

Printed by HAVEKA BV, Alblasserdam, The Netherlands (www.haveka.nl).

Pathogenesis of Rotavirus Infection

Pathogenese van Rotavirus infecties

Proefschrift

ter verkrijging van de graad van doctor aan de

Erasmus Universiteit Rotterdam

Op gezag van de rector magnificus

Prof.dr. S.W.J. Lamberts

en volgens besluit van het College voor Promoties

De openbare verdediging zal plaatsvinden op

woensdag 8 juni 2005 om 13.45 uur

door

Jacobus Antonius Boshuizen

geboren te Boxmeer

Promotiecommissie

Promotor: Prof.dr. H.A.Büller

Overige leden: Prof.dr. A. van Belkum
Prof.dr. J.B. van Goudoever
Prof.dr. A.D.M.E. Osterhaus

Copromotor: Dr. A.W.C. Einerhand

The research described in this thesis was performed at the Laboratory of Pediatric of Pediatrics, Pediatric Gastroenterology & Nutrition, of the Erasmus MC, Rotterdam, The Netherlands and was financially supported by the Sophia foundation for medical research, The Netherlands (grant 254) and the Netherlands Digestive Diseases Foundation.

The printing of this thesis was financially supported by: Section Experimental Gastroenterology of the Netherlands Society of Gastroenterology (NVGE).

Contents

| | Page |
|---|-------------|
| Chapter 1: General introduction | 7 |
| Aims and outline of this thesis..... | 28 |
| Chapter 2: Changes in small intestinal homeostasis, morphology, and gene expression during rotavirus infection in infant mice | 29 |
| Chapter 3: Goblet cell homeostasis and gene expression during rotavirus infection in infant mice | 51 |
| Chapter 4: Rotavirus infection induces mucin gene expression via a prostaglandin-mediated mechanism | 69 |
| Chapter 5: Systemic immune response after rotavirus inoculation of neonatal mice depends on source and level of purification of the virus: implications for the use of heterologous vaccine candidates | 83 |
| Chapter 6: Rotavirus enterotoxin NSP4 interacts with extracellular matrix proteins | 97 |
| Chapter 7: Summary and General discussion | 113 |
| Chapter 8: Samenvatting | 129 |
| References..... | 135 |
| Dankwoord & Curriculum vitae | 159 |
| Appendix: Color figures..... | 163 |

Chapter 1

General introduction

History

Today, rotaviruses are recognized as the single most significant cause of severe gastroenteritis, malnutrition and diarrhea in young children in both developed and developing countries worldwide (28, 122, 203, 312). Although rotavirus can infect older children and adults, diarrheal disease is primarily observed in children under 2 years of age (122, 123, 203). Each year about 440.000 children <5 years of age die mainly in developing countries, because of an infection with rotavirus (313). Mortality rates in developed countries on the other hand are very low and illness is usually self limiting (429).

In 1963 Adams and colleagues observed virus-like particles in intestinal tissue from mice infected with epizootic diarrhea of infant mice (EDIM) virus (1) (Figure 1). Ten years after Bishop and colleagues reported the discovery of human rotavirus and its association with severe endemic diarrhea in infants and young children (33). The identification of rotavirus in mucosa of infected children was achieved without the benefit of tissue culture technology and relied only on visualization by electron microscopy (EM). After this, rotavirus was also identified in feces by EM by several studies (32, 135, 207). Using EM, the viral particles observed above resembled a short-spiked wheel, which led to the name rotavirus (from the latin *rota*, meaning wheel)(136). After its discovery, it became obvious that rotavirus, was an important etiologic agent of diarrhea of infants and young children, causing about 35% to 50% of the hospitalizations for severe diarrhea during the first 2 years of life (202).

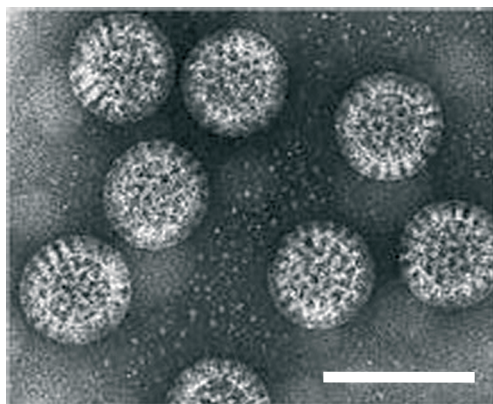


Figure 1. Negative stain electron micrograph showing infectious triple-layered (double-shelled) rotavirus particles. Picture modified from (122). Bar, 100 nM.

Structure, protein function and classification

Rotaviruses comprise a genus within the family of the *Reoviridae*, which contains eight other genera (122). There are common morphologic and biochemical features that classify rotavirus in a separate genus; (i) the complete rotavirus particle, which is approximately 70 nm in diameter, consists of a three-layered non-enveloped protein capsid; ii) from the outer layer, 60 spike-like projections extend from the surface; (iii) the virus genome consists of 11 double-stranded RNA (dsRNA) segments and the virus can reassort these genome segments; (iv) within the inner shell, mature virus particles contain an RNA-dependent RNA polymerase and other enzymes to produce capped RNA transcripts; (v) virus replication occurs in the cytoplasm within distinct viral organelles called viroplasms (vi) rotavirus morphogenesis is unique in the way that immature double layered particles (formed in the cytoplasm) are translocated across the endoplasmic reticulum (ER) and transiently obtain an

envelope. Mature particles however are nonenveloped and are released from infected cells by a nonclassical vesicular transport pathway that bypasses the Golgi apparatus (198).

Structure

The complete rotavirus particle, which is approximately 70 nm in diameter, consists of a three-layered non-enveloped protein capsid that is composed of an outer layer, an intermediated layer and an inner core layer (Figure 2). The inner core contains the 11 dsRNA segments that code for six structural proteins (VP) that make up the virus particles and for six non-structural proteins (NSP) that are found in infected cells harbouring replicating viruses. The structural proteins are designated VP1 to 8 as originally proposed by Mason et al. (256). Two peptides VP5* and VP8* are formed by proteolytical cleavage of VP4 and are therefore not present as distinctive dsRNA segments (125). The presently accepted nomenclature for the non-structural proteins is NSP1 to NSP6 as proposed by Mattion et al. (262) (Figure 2).

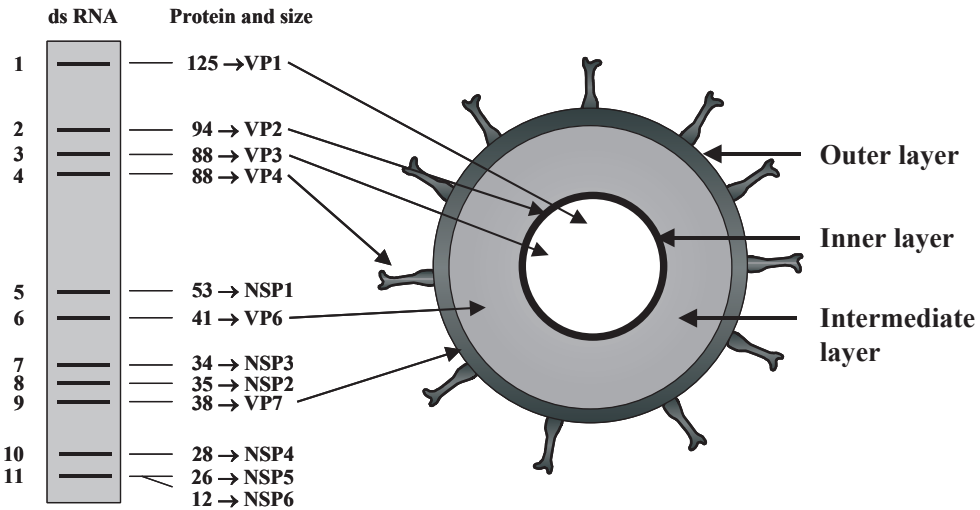


Figure 2. Schematic presentation of the rotavirus triple layered particle and the gene coding assignment. The 11 dsRNA segments are presented as typically obtained by polyacrylamide gel electrophoresis. Proteins encoded by the gene segments are shown together with their apparent molecular mass and position within the capsid structure. Modified from (122, 205).

Structural proteins

The inner core consists of the structural proteins VP1 and VP3 and is surrounded by a layer of VP2. These proteins have affinity for ssRNA, and play a role in the processes of RNA transcription and replication (Figure 3). VP1 is thought to be the viral RNA polymerase and functions as both the viral transcriptase and replicase (83, 315, 433). For replicase activity however, VP1 requires VP2 and the vital role of VP2 in replication is linked to its ability to bind the mRNA template for minus strand synthesis (316). In contrast to VP1, VP2 binds RNA nonspecifically (48, 328) and interacts with the dsRNA lining the VP2 shell (338). Very little is known about VP3. VP3 can bind to the N-terminus of VP2, involving a region of the innershell protein to which VP1 and ssRNA also bind and is required for RNA

replication (225, 478). VP3 also binds [α - 32 P] GTP, indicating that VP3 is the viral guanylyltransferase (237, 327) and VP3 was identified as a methyltransferase (73), indicating that VP3 is a multifunctional capping enzyme.

VP6 is the major component of the mature virus particle. VP6 forms the middle shell or intermediate layer of the virus particle and is found in trimers, which it forms spontaneously *in vitro* (124). VP6 plays a key role in virion structure, since it interacts with the outer capsid (VP4, VP7) and the inner layer (VP2) (122, 124). The fact that VP6 is extremely stable and contains epitopes that are conserved in many virus strains makes it the most important antigen used in diagnostic assays. VP6 is probably also involved in polymerase activity as removal of VP6 from double-layered particles results in a loss of viral polymerase activity (30, 372). It is however unclear whether VP6 plays a structural or functional role in this process.

VP4 the product of gene segment 4, is a nonglycosylated outer capsid protein which forms 60 homodimeric spikes that project from the surface of the virus (9, 256, 467). VP4 is also responsible for rotaviral hemagglutinin activity (200) and it is the protein responsible for cell attachment (93, 362). VP4 has been implicated as a virulence determinant in mice, calves, piglets, and humans (52, 277, 283, 300). VP4 is comprised of about 775 amino acids and it is proteolytically cleaved into two polypeptides VP5* (~60KD) and VP8* (~28KD) (125). Cleavage of VP4 results in an increase of viral infectivity (121, 125) and enhances penetration of virus into cells (81, 141, 201). Cell binding however is not dependent upon cleavage of VP4 (81, 121).

For the SA11 strain, the cleavage sites have been located at two arginine residues (Arg 241 and Arg 247), creating VP8* from the N-terminal portion, and VP5* from the C-terminal portion of the primary VP4 protein (241). In some cases, a third cleavage may occur at arginine 231 (10).

The mechanism underlying cleavage-induced activation of infectivity is not apparent, but it is assumed that cleaved VP4 activates an early step of viral replication that may be triggered by one or both terminal regions generated by cleavage (122). Recently it was shown that cleavage of VP4 confers correct conformation of the VP4 spikes, which is essential for the virus to enter the cell (94)

Why the virus produces a single translate, which is subsequently cleaved is not known. It has been postulated that the full length VP4 is more stable upon entry into the host (291). However, it was shown that infectivity using cleaved virus was not significantly different from uncleaved virus (245). Therefore, it seems unlikely that greater stability in the external environment explains the need to translate VP5* and VP8* as the single peptide VP4. Ludert et al., showed that VP4 is already cleaved upon release from the intestinal cells and that virus shed into the lumen of the gastrointestinal tract of infected mice do not contain intact VP4 (245). Therefore, a hypothesis in which an intact VP4 peptide is needed as the outer capsid is assembled or as the virus particles are transported intracellularly, seems more feasible. Another explanation may be that the individual VP5* and VP8* proteins are somehow toxic for the host cell. Prasad and coworkers localized the VP5* and VP8* proteins by three-dimensional cryo-electron microscopy using neutralizing antibodies that recognize different epitopes of VP4 (337). It appeared that part of VP8* may interact with VP6, while VP5* seemed to be more externally exposed on the virus particle near the tips of the spikes (122, 337). Hemagglutination activity has been mapped to VP8* (133). Monoclonal antibodies directed against VP8* more efficiently prevent binding of rhesus rotavirus to target cells than do antibodies against VP5* or VP7 (362). This indicates an important role for VP8* in cell

binding. In contrast, monoclonal antibodies directed against VP5*, but not VP8*, prevent release of the fluorophore CF (6-carboxyfluorescein) from isolated pig intestinal membrane vesicles (364). Recent studies have shown that VP5* can permeabilize lipid membrane vesicles and that there are at least two domains within VP5* required for pore formation. An N-terminal basic domain permits VP5* to associate with membranes and an internal hydrophobic domain that is essential for altering membrane permeability (108, 146). These findings point to a prominent role for VP5* in cell penetration and membrane destabilization rather than cell binding.

The glycoprotein VP7, the product of gene segment 9, is the major outer capsid protein and it forms trimers on the viral surface (122, 249). During morphogenesis, VP7 is directed to the ER by a cleavable signal peptide. As it is inserted in the membrane of the ER, VP7 is cotranslationally glycosylated (45, 119, 199). VP7 only contains N-linked high mannose oligosaccharides that are processed by trimming in the ER (9, 118, 199). VP7 does not contain the sequence KDEL found to confer retention for other ER proteins (122, 285). Instead, two hydrophobic domains that are only present in the pre-mature VP7 are thought to act as the signal sequence that directs VP7 to and across the ER membrane (122, 456). So far, two regions within VP7 (amino acids 51-61, and 61-111) are known to mediate retention in the ER (333, 336, 456). VP7 is processed exclusively in the ER, and rotaviruses are not transported to the Golgi apparatus during morphogenesis. Deletion of the two retention regions of VP7 however result in transport of VP7 through the Golgi and into the extra cellular medium (336). VP7 is resistant to proteolytic enzymes after insertion into membranes and remains membrane associated after high salt treatment or at alkaline pH (118, 199). This suggests that VP7 is not a membrane spanning protein but an integral membrane protein. VP7 also forms oligomer complexes with other proteins (VP4 and NSP4) in infected cells (249). These interactions together with the interaction of VP7 with calcium, appear to be important in the assembly of VP7 into the outer capsid (115, 334, 335, 381).

Nonstructural proteins

The rotavirus genome codes for six nonstructural proteins (NSP1-6). The proteins are involved in replication (NSP1, 3, 5, 6) and morphogenesis (NSP4) and except for NSP4, interact with nucleic acid (Figure 3) (122). NSP1 is the least conserved of the rotavirus proteins. It seems to be nonessential for virus replication, although it was recognized as a virulence factor in mice (53), but not in piglets or rabbits (51, 80). NSP1 contains a relatively conserved zinc finger domain, but this domain is missing in some virus strains, showing it is not essential for virus replication and genome segment reassortment (304, 425). NSP2 is an oligomeric NTPase, is localized to viroplasms, possesses helix-destabilizing activity, and is possibly involved in RNA encapsidation and virulence (412). NSP3 is a sequence-specific RNA-binding protein that requires only four nucleotides at the 3' end for RNA recognition (331). NSP3 functions similarly to the cellular poly (A)-binding protein (PABP). It binds to eIF4G and thereby inhibits cellular RNA translation and protein synthesis, while enhancing the translation of viral mRNA (325, 326, 330, 445). NSP5 is an O-glycosylated phosphoprotein. It self-assembles into dimers, has autokinase activity and exists in several phosphorylated isomers in infected cells (3, 36, 148). NSP5 interacts with NSP2 (147), and when co-expressed, NSP2 induces hyperphosphorylation of NSP5 (2, 332, 454). NSP6 is encoded in an alternative ORF on gene segment 11 of most rotaviruses and is known to interact with NSP5 and accumulate in viroplasms (264, 424). NSP2, NSP5, and NSP6 are

associated with viroplasm and co-expression of NSP2 and NSP5 is sufficient for the formation of viroplasm (127).

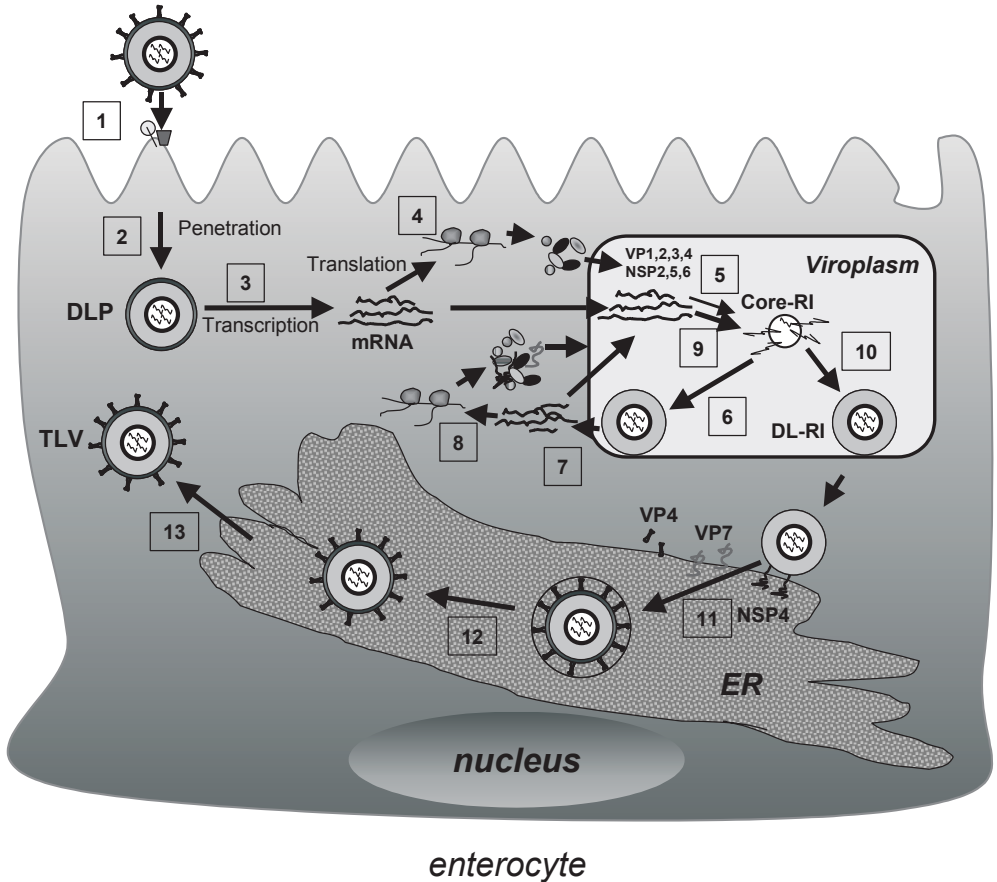


Figure 3. Major features of the replication cycle of rotaviruses. The different steps in the replication cycle of the virus are indicated by numbers. **1:** attachment of the virion to the cell surface; **2:** penetration and uncoating of the virus particle to yield double layered particle's (DLP); **3:** primary transcription of the genomic dsRNA; **4:** synthesis of viral proteins; **5:** assembly of core replication intermediates (Core-RI) and negative strand RNA synthesis; **6:** assembly of double-layered core replication intermediates (DL-RI); **7:** secondary transcription from double-layered RIs; **8:** secondary, enhanced synthesis of viral proteins; **9:** secondary, increased assembly of core RIs and negative strand RNA synthesis; **10:** secondary, increased assembly of DL-RIs; **11:** budding of DL-RIs through the membrane of the endoplasmic reticulum (ER), and acquisition of a transient membrane envelope; **12:** loss of the membrane envelope and generation of mature triple-layered virions; **13:** virions are released by a nonclassical vesicular transport mechanism that bypasses the Golgi apparatus (198).

These proteins may therefore function to recruit other viral proteins into the viroplasm, or enhance RNA encapsidation or movement of nascent viral particles from the viroplasm to the ER membrane. In contrast, NSP1 and NSP3 show a diffuse cytoplasmic staining in cells (7, 180, 261). NSP4 is the only nonstructural protein that does not bind to RNA. The nonstructural protein NSP4 encoded by gene 10 is 175 amino acids in length and has been shown to play a key role in viral morphogenesis (11, 12, 122, 271). The primary product of gene 10 is a 20kD protein that is cotranslationally glycosylated to a 29kD species.

Oligosaccharide processing then eventually yields the mature 28kD protein (118, 199). NSP4 is an ER glycoprotein that has been proposed as a receptor for double-layered particles (lacking the outer capsid proteins VP4 and VP7) and is crucial to translocate these immature viral particles across the endoplasmic reticulum membrane (11). During the process of budding, the subviral particles, assembled in the viroplasm adjacent to the ER, acquire a transient membrane envelope, which is lost when the two outer capsid proteins VP4 and VP7 are assembled. The receptor role for NSP4 is further confirmed by the observation that double-layered particles bind to ER membranes containing only NSP4 (11, 122, 271). Glycosylation of NSP4 is required for removal of the transient envelope from the budding particles (118, 324). The topography of NSP4 in the ER membrane indicates that the hydrophilic carboxy terminus is projected into the cytoplasm and that the amino acid terminus, containing three hydrophobic domains, is responsible for maintenance in the ER membrane (67, 420). The carboxy terminus (amino acids 161-175) was found to be responsible for binding to VP6 present on nascent particles (12, 414, 415). NSP4 contains a VP4 binding domain between amino acids 112 and 146 (12) and forms heterooligomeric complexes with VP4 and VP7 (249, 334). This association however is transient and NSP4 is not incorporated in the mature virion (249).

The amphipathic α -helix region is predicted to adopt an α -helical coiled-coil structure, and this region is thought to mediate oligomerization of the virus-binding domains into a homotetramer (416). Glycosylation of NSP4 is required for interaction with calnexin, but is not required for its binding activity to double-layered particles or for oligomerization (11, 273, 415).

Increasing lines of evidence show that the NSP4 protein is involved in pathogenicity of rotaviral infection and that it acts as a viral enterotoxin and can induce age-dependent diarrhea (see section mechanisms of rotavirus pathogenesis) (16, 173, 276, 374). Reassortment analyses showed that NSP4 might function as a virulence factor (174). Mutations in NSP4 have been associated with avirulence, and sequence changes correlated with an altered protein function (216, 479). Not all attenuated (avirulent) viruses however have been shown to contain mutations in NSP4 (5, 68). This is most probably caused by the fact that there are many mechanisms of virus attenuation, and other viral proteins (NSP1, NSP2, VP3, VP4, VP7) are also virulence factors (58).

Classification

Rotavirus can be classified serologically into seven distinct groups named A to G. This classification is according to antigenic groups detectable by a number of serologic tests, such as immunofluorescence, enzyme-linked immunosorbent assay (ELISA), and immunoelectron microscopy (122). The antigenic groups are mainly present on the major inner capsid protein VP6. Group A, B, and C rotaviruses are found in both humans and animals, whereas viruses in groups D, E, F, and G have been found only in animals to date (122). Group A has been established as the predominant group causing human rotavirus diarrheal disease and almost all information presented further in this thesis regards group A rotavirus. Group B seems to be limited to causing epidemic infection in Asia and the Indian subcontinent, whereas group C rotavirus causes endemic infections that frequently go unrecognized (204). Although coding assignments have been obtained for non-group A rotaviruses, information on these viruses have been hampered due to the inability to cultivate most of the non-group A viruses (122).

Within each group, rotaviruses can be further classified into serotypes defined by reactivity of viruses in plaque reduction neutralization assays using polyclonal or monoclonal antisera raised against the viral capsid proteins VP7 and VP4 (177, 263). In this way, serotype designation reflects the expression of neutralizing epitopes on VP4 (designated a P serotype because VP4 is protease sensitive) and VP7 (designated a G serotype because VP7 is a glycoprotein) as defined by reactivity of viruses in plaque reduction neutralizing assays (177). Lack of readily available typing serum or monoclonal antibodies to different VP4 types has hindered classification of VP4 (P) serotypes. Therefore, serogroups can also be classified into genotypes by use of sequence analysis. Genotypes of VP4 and VP7 are determined by sequence or hybridization analysis, whereas serotypes are determined by reactivity with polyclonal or monoclonal antisera (122). For VP7, a correlation between genotype and serotype has been established. Such a correlation is less clear for VP4, although sequence variation between amino acids 84 and 180 has been suggested to be useful to define P-type-specific epitopes (227). An important feature of rotaviruses is that they can reassort (rearrange) their genes independently (176). Viruses within each group are capable of genetic reassortment, but reassortment does not occur among viruses in different groups (468). The great genetic diversity created in this way and the existence of numerous G- and P serotypes within group A rotaviruses, indicates that the development of a successful vaccine, which is usually based on neutralizing the outer capsid proteins VP4 and VP7, is therefore challenging.

Binding and entry

Rotavirus predominantly infects the mature enterocytes in the mid and upper part of the villi of the small intestine, which ultimately leads to diarrhea. Rotavirus binding and entry of host cells is thought to be a multifactorial process (240). Some animal rotavirus strains require sialic acid (SA, N-acetylneuraminic acid) residues on the surface of target cells for initial attachment (107, 356, 410). The infectivity of these rotavirus strains is greatly diminished by the treatment of cells with neuraminidase, and consequently, these strains are neuraminidase-sensitive. In contrast, many animal strains and most strains isolated from humans are neuraminidase-resistant (79). This does not mean that these strains do not use sialic acid for cell attachment because sialic acid moieties that are internal in oligosaccharide structures are either less sensitive or not sensitive at all to neuraminidase (107).

In their review, López and Arias proposed a model describing rotavirus-host cell interactions (240). For neuraminidase sensitive rotavirus strains, initial binding to the cell surface is through a sialic acid (SA)-containing cell receptor, using the VP8 domain of VP4. This initial cell surface receptors containing sialic acid may be either glycolipids (gangliosides) or glycoproteins (107, 133, 356, 410, 472). The interaction with sialic acid probably induces a conformational change in VP4. This change allows the virus to subsequently interact with the integrin $\alpha 2\beta 1$. This binding is mediated by the integrin ligand sequence DGE on VP5 (150). Neuraminidase-resistant rotavirus strains have been hypothesized to use either a neuraminidase-resistant sialic acid-containing molecule (i.e. GM1) or a non-acidic sugar residue (i.e. galactose) for initial cell attachment or may be able to entirely bypass the binding to sialic acid and directly interact with integrin $\alpha 2\beta 1$ (150, 167).

After this second interaction, three more interactions are thought to take place; binding of VP5 and the ligand-binding domain of cell-surface heat shock cognate protein hsc70 (158, 477), binding of VP7 (through its CNP region) and integrin $\alpha v\beta 3$ (477), and binding of VP7

(via its integrin ligand sequence GRP) integrin $\alpha\beta 2$ (150). The order of these events however has not been established. The initial interactions of the virus with the cell surface might trigger conformational changes in VP4 to facilitate subsequent interactions of VP5 with hsc70 and VP7 with integrins.

Host cell binding ultimately leads to penetration and uncoating of the virus (removal of VP4 and VP7 proteins from the virus to yield the transcriptionally active double-layered particles). There are several hypotheses on how rotavirus enters host cells. Virus internalization was previously thought to happen via direct entry or fusion (201) or through Ca^{2+} -dependent endocytosis (70, 71, 363). In the latter process, the virus is internalized within clathrin-coated endocytic vesicles. Within these vesicles a decrease in the calcium concentration, solubilizes the surface proteins from the virus particle. The solubilized outer layer proteins then permeabilize the vesicle's membrane to release the double-layered particle into the cytosol (71). A recent study however, showed that specific drugs that are known to impair clathrin- and caveolae-mediated endocytosis, did not affect rotavirus cell infection (371). Instead cholesterol and dynamin seemed to play a role in the entry of rotaviruses.

The entry process was recently proposed to be mediated by lipid rafts (240). The pathway described as raft-dependent endocytosis is clathrin and caveolin independent (229, 240). Cellular lipid rafts are membrane lipid microdomains enriched in glycosphingolipids (gangliosides among others), cholesterol and a specific set of associated proteins. Rafts have been implicated in a variety of cellular functions such as apical cell-sorting of proteins, signal transduction, and endocytosis (240). In the rotavirus entry process, the rafts are also thought to serve as platforms to facilitate the efficient interaction of cell receptors with the virus particle (240). It however still remains ambiguous how virus particles penetrate the plasma membrane and how they lose the outer layer.

Mechanisms of rotavirus pathogenesis

Acute diarrhea caused by many viruses has been given significant attention in recent years. This section, in particular, describes the pathophysiological mechanisms proposed to underlie the intestinal fluid secretion and subsequent diarrhea caused by rotavirus. Several reviews have proposed the following hypotheses explaining age-dependent rotavirus diarrhea in young children and animals (126, 280). The watery diarrhea may be caused by i) reduction in total small intestinal surface area, leading to a decrease in net fluid absorption. This may especially have an impact at young age at the time when the absorptive capacity of the colon is not yet fully developed, ii) changes in the osmotic permeability of the mucosa secondary to destruction, and iii) changes in fluid and electrolyte secretion. All these phenomena may contribute to diarrhea at different times during infection.

i) reduction in total small intestinal surface area, leading to a decrease in net fluid absorption.

Histological changes during rotavirus infection

Most knowledge of pathological changes that occur during rotavirus infections comes from animal studies. Most severe intestinal damage is observed in piglets, where intestinal villi can be completely eroded (389). Macroscopic changes in the pig intestine also include thinning of the intestinal wall, and microscopic changes include the conversion to a cuboidal

epithelium (85). In calves, infection also leads to a change in the villus epithelium from columnar to cuboidal, and villi become stunted and shortened (63). Histological changes in calves are not limited to a symptomatic response; in fact asymptotically infected calves show also villus blunting (347). Compared with infections in piglets and calves, rotavirus infection in lambs results in less severe histopathological changes and mild clinical disease (151, 399). Rabbits and rats infected experimentally with rotavirus show normal intestinal histology, while vacuolation of enterocytes in the ileum was observed in rats (77, 171).

Rotavirus infections have been studied most extensively in mice. The pathology of murine rotavirus is generally similar to that of lambs, pigs and calves, but differs in certain aspects. During infection, histologic changes are characterized by swollen and vacuolated enterocytes (306). Vacuolation of enterocytes is most prominent on the villus tip, but can occur in enterocytes throughout the villus. While vacuolation can also be observed in other species like rats, it is most extensive in mice (77, 302, 306). Vacuolation is absent in calves, lambs, and piglets (268, 389, 398). These differences have been attributed to the specific nature of the host response and not to the virus, since vacuolization is also a characteristic feature of heterologous infections in mice (24, 149, 251). Thus far, the origin and nature of the vacuoles remains ambiguous. Mice usually do not develop any symptoms when infection occurs beyond 2 weeks of age, and infection of adult mice occurs without disease or histopathological lesions (59, 130, 306, 341, 402, 453). Unlike other species, villus blunting is limited in mice (33, 59, 236, 389, 399, 402).

In contrast to animal studies, there are few reports of the pathological changes in intestinal mucosa of infants infected with rotavirus. Studies of biopsies have revealed blunting and atrophy of villi, distended endoplasmic reticulum, mononuclear cell infiltration, mitochondrial swelling and denudation of microvilli (33, 97, 171).

Histological changes would be expected to be associated with activation of significant immune responses, as is observed for bacterial toxins during for example dysentery and invasive diarrheal syndromes. This inflammatory component of diarrhea however, does not seem to occur in children and in many animal models. In mice, rotavirus infection is not associated with mucosal inflammation and only mild mononuclear infiltration of the lamina propria is seen (65, 126, 138). Moreover, diarrheal onset in animals regularly occurs during subclinical levels of infectious load, before alterations in cytopathology. Treatment of infected pigs with cytoprotective growth factors can inhibit histologic changes but fails to influence the occurrence of diarrhea (126). These observations suggest that there is no absolute correlation between histological lesions and clinical symptoms and led to the assumption that mucosal destruction is unlikely to play a primary role in the induction and/or propagation of diarrhea in animals (65, 126, 279).

ii) changes in the osmotic permeability of the mucosa secondary to destruction

Epithelial permeability

Epithelial permeability is important for intestinal epithelial transport. Several studies report that transepithelial electrical resistance (TER) is decreased after rotavirus infection in enterocyte-like Caco-2 cells. Intestinal permeability to mannitol and dextran was also increased in these cells (112, 296). This increased paracellular permeability is possibly caused by a disorganization of tight junction associated proteins claudin, occludin and ZO-1 (112, 296). The disorganization of the cytoskeleton and effects on TER are also activities that are attributed to NSP4, as will be discussed below (411, 465). In Ussing chamber

experiments, a transient increase in absorption of horseradish peroxidase (HRP) has also been observed *ex vivo* in piglets and mice after infection with rotavirus (168, 211). Intestinal permeability has also been investigated in young children with rotavirus diarrhea using polyethylene glycols (PEGs) (405). PEG absorption was significantly lower during the acute phase of virus infection than 3 to 5 weeks after infection. This observation was largely ascribed to the decreased surface area for absorption. However the relationship between the rates of absorption of large and small PEG molecules indeed suggested increased permeability especially for the small PEGs in acute disease (405).

iii) changes in fluid and electrolyte secretion

Effect of rotavirus infection on fluid/electrolyte transport and apical symporters

Several reports show that rotavirus evokes *in vivo* a net secretion of fluid, caused by an attenuated uptake of sodium and secretion of chloride. When perfusing the rat intestinal lumen with an isotonic electrolyte solution devoid of glucose, net fluid secretion and a significantly decreased net sodium uptake was observed after rotavirus inoculation (370). In contrast, net fluid and sodium uptake was observed in control rats. At the peak of net fluid secretion, villus height was decreased to one third of control, whereas crypt depth was unaltered in infected rats. Mouse intestinal segments perfused with an isotonic electrolyte solution containing mannitol showed a significant secretion of fluid, sodium and chloride ions at 72 h post infection, when clinical signs of diarrhea were most pronounced (306, 401). In accordance with this finding, Lundgren et al. showed that rotavirus induced a net fluid secretion and increased electrolyte secretion at 48 to 60 h after infecting newborn mice (246).

A mechanism that in part may explain the virus-induced attenuation of electrolyte and fluid absorption is an inhibition of the symporters for sodium and glucose/amino acids. Apical symporters in villus enterocytes transport sodium ions together with glucose or amino acids and numerous studies indicate that the co-transport of glucose and sodium is impaired in intestinal segments exposed to rotavirus. Using Ussing chambers, McClung et al. found a defect in glucose-stimulated sodium absorption in intestinal segments isolated from pigs with viral enteritis (265). In line with this, the glucose effect on intestinal net sodium and water flux, measured in infected piglets *in vivo*, was absent or considerably smaller than that seen in normal intestines (417). The influence of the virus infection on glucose transport has also been investigated in brush border membrane vesicles. Keljo et al. (212) were unable to demonstrate a high-affinity sodium-dependent glucose transporter in virus-infected intestines. In agreement with this, rotavirus infection was shown to impair intestinal brush-border membrane Na (+)-solute co-transport activities of the Na-D-glucose symporter (SGLT1) in rabbits. This effect was found to be mediated by a direct inhibiting effect of NSP4 on SGLT1 (see also below) (162, 163). The apical membrane of enterocytes also harbors sodium/amino acids symporters. Na-L-alanine symport was reported to be inhibited in rotavirus-infected young rabbits (162), but not in infected pig intestines (348).

A lowered activity of the brush border enzymes probably also contributes to a diminished absorptive capacity during rotavirus infection. The disaccharidases localized at the apical brush region of enterocytes are factors of importance for the absorption of glucose and other sugars. Several reports demonstrated that viral enteritis attenuates the activity of mucosal disaccharidases like sucrase, lactase, and maltase (84, 99, 172, 213, 389, 390). Decreased levels of disaccharidase activity have also been measured in biopsies from patients (97).

Decreased disaccharidase activity may be the consequence of decreased expression of these enzymes in infected mature enterocytes. A mechanism at work during rotavirus infection involves the nonstructural protein NSP3 and probably results in the reduction of mRNA translation through hijacking of the host cell machinery (Box1, Figure 4) (272, 326, 445). In Summary, the blunting of villi induced by rotavirus infection merely leads to a decrease in the surface area for fluid and solute uptake and probably also to the diminished absorptive capacity during infection.

Sodium-potassium ATPase

The sodiumpotassium pump (Na, K ATPase) situated on the basolateral membrane of enterocytes is essential for the electro-chemical gradient across the apical membrane. This gradient is largely important for the transport across the polar epithelium of the gut. Many studies report that the activity of Na, K ATPase is attenuated in rotavirus infected intestines (162, 172, 349, 389, 390). This observation may be caused by a decrease of ATPase pump activity but again this event, may also be explained by the blunting of the intestinal villi and the reduced numbers of enterocytes. The relative decrease in Na, K ATPase activity nevertheless is much smaller than observed, for sucrase or lactase (84, 212, 349, 390).

Secretory diarrhea

Secretory diarrhea is caused by electrogenic exit of Cl⁻ across the apical plasma membrane of epithelial cells. The additional paracellular movement of Na⁺ and H₂O leads to accumulation of fluid within the lumen of the gastrointestinal tract and, subsequently, diarrhea. Clinically, secretory diarrhea is diagnosed when fecal fluid Na⁺, K⁺, and accompanying anions are in isosmotic balance with plasma. In contrast in osmotic diarrhea an osmotic gap exists as nonabsorbed solutes within the lumen (in the colon) prevent fluid absorption. At least in mice, there exists no osmotic gap between luminal and plasma anion and cation concentrations and alternatively, electrolyte levels in the lumen exceed plasma levels, pointing to the presence of secretory diarrhea (401). At least two mechanisms seem to attribute to rotavirus induced secretory diarrhea; the viral nonstructural protein NSP4 and the enteric nervous system.

NSP4

As they expressed several individual rotavirus genes in cells, Ball and coworkers coincidentally discovered that intra-peritoneal or intra-ileal delivery of NSP4 as well as a 22 amino acid synthetic peptide corresponding to residues (114-135), induced diarrhea in young mice (16). Since the diarrhea inducing effects of NSP4 were age dependent, it therefore mimicked the diarrhea provoked by virulent homologous rotavirus infections, although the time course was less prolonged. Moreover, the NSP4 114-135 peptide was shown to potentiate chloride secretion of unstripped mouse mucosal sheets, by a calcium dependent signaling pathway. Interestingly, chloride secretion and induction of diarrhea were shown to be age and dose dependent and specific. Specificity was further demonstrated by the fact that substitution of lysine for tyrosine at amino acid position 131, resulted in complete abolishment of the diarrheal inducing effect of NSP4 114-135 (16).

Box**Hijacking the host cell translation machinery.**

Viruses do not harbor functional ribosomes in their virions, successful amplification of the viral genomes thus requires that viral mRNAs compete with cellular mRNAs for the host cell translation apparatus. Therefore, many viruses (HIV, influenza, poliovirus, adenovirus, and herpes simplex) are known to interfere with the host cell translational machinery, and shut off gene expression in a variety of ways (35, 223, 244, 258, 463). In most eukaryotic mRNAs, translation initiation starts with the recruitment of the cap binding protein complex eukaryotic initiation factor (eIF)4F, composed of factors eIF4E (cap binding protein), eIF4A, and eIF4G (Figure 4), to the capped 5' end of the mRNA (166). The 40S ribosomal subunit, carrying eIF3 and the ternary initiator tRNA-eIF2-GTP complex, are recruited to the 5' end of the mRNA via interaction of eIF3 with eIF4G (166). When the 40S subunit finds a start codon in the mRNA, the large ribosomal 60S subunit joins the complex and protein synthesis begins (166). Additionally, the polyadenosine binding protein (PABP) interacts with eIF4G (Figure 4A) (366). In this way, circularization of the mRNA is accomplished, which may lead to increased mRNA translation or mRNA stability (365).

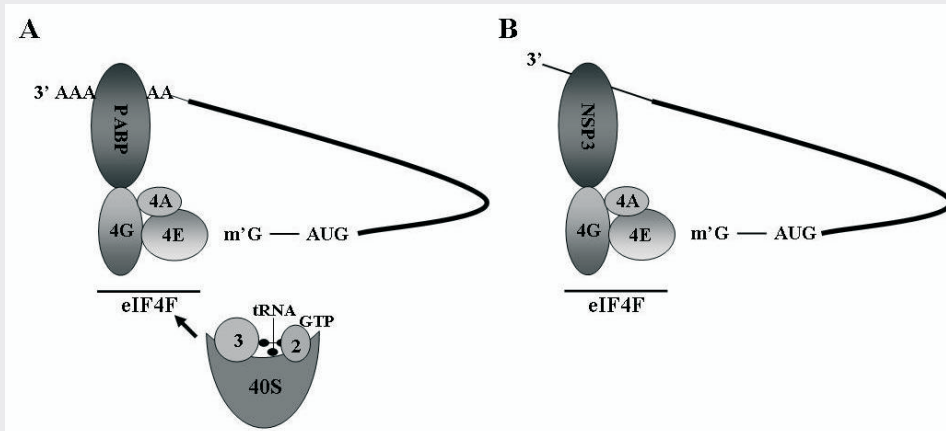


Figure 4 A. Model depicting the major participants that are involved in translational initiation in eukaryotic mRNAs. Interactions of eukaryotic translation initiation factors eIF2 (2), eIF3 (3), and initiator tRNA with a 40S ribosomal subunit, eIF4E (4E), eIF4A (4A), and eIF4G (4G) with the m7G cap structure, and the polyadenosine binding protein PABP with the polyadenosine tail in an mRNA are shown. B. Substitution of PABP by NSP3. Eviction of PABP by viral NSP3 from the cap binding protein complex eIF4F in rotavirus-infected cells. Interactions of eukaryotic initiation factors eIF4G (4G), eIF4A (4A), eIF4E (4E), and eIF3 (3) are indicated. Modified from (61).

The eleven double-stranded RNA segments of rotavirus are transcribed into mRNAs that possess a 5' terminal cap structure but lack 3' terminal poly(A) tails (317). Instead, the 3' end sequences contain a tetranucleotide motif which is conserved among different groups of rotaviruses. It was discovered that the rotavirus protein NSP3 binds specifically to the conserved viral 3' end sequences (326). Using the two-hybrid system in yeast, it was found that NSP3 interacts with a binding site in eIF4G that overlaps with the binding site for PABP (Figure 4B) (326). Later it was found that eIF4G has a higher affinity for NSP3 than PABP. In this way, the interaction between PABP and eIF4G is disrupted in rotavirus-infected cells (272, 445). The replacement of PABP by NSP3 has two important consequences. First it achieves a circularization-mediated translational enhancement of rotavirus mRNAs, while the NSP3-RNA complex confers stability to the viral mRNAs by protecting them from 3'–5' exonucleases. (109). Second, eIF4F is known to modulate mRNA stability (343). Removal of the eIF4F complex from cellular mRNA by NSP3 therefore may lead to decreased stability of the mRNAs and a reduction in the efficiency of host mRNA translation.

Furthermore, pups born to dams immunized with the NSP4 peptide developed less severe diarrhea and with less frequency and duration, when challenged with a high dose of infectious rotavirus, reinforcing a major role of this peptide in the pathogenic process. The diarrhea inducing effects of NSP4 have subsequently also been confirmed by other groups (173, 276, 374). Diarrhea was observed using either group A or group C NSP4, indicating that the pathogenetic role of NSP4 is widespread between many rotavirus strains and groups. Recent studies indicate that a specific 7-kDa cleavage product of NSP4 (aa 112-175) is actively secreted from infected cells and that NSP4 is released from the apical side of infected epithelial cells via an atypical pathway that bypasses the Golgi apparatus and involves lipid microdomains called rafts (173, 373, 374). This suggests that NSP4 is extracellularly available for subsequent effects on the adjacent mucosa and provides a physiological basis for immunoprotection after NSP4 immunization (16, 279).

After being secreted from infected cells, NSP4 is thought to bind to an unidentified apical receptor and mediate phospholipase C (PLC) dependent cell signaling by increasing intracellular calcium levels leading to chloride secretion in adjacent uninfected cells (16, 114, 280, 421).

Studies with cystic fibrosis knockout mice imply that the age-dependent diarrhea inducing properties of NSP4 are due to age-dependent changes in calcium mediated anion permeability (280). Rotavirus and NSP4 alone, induce age-dependent diarrhea and age-dependent chloride permeability changes in these knockout mice (5, 280).

Together these findings lead to the conclusion that NSP4 is a new type of secretory agonist, since other known secretagogues induce chloride secretion by activating cyclic adenosine monophosphate (cAMP), instead of mobilizing intracellular calcium as a second messenger. Moreover, NSP4 fails to cause diarrheal disease in CFTR knockout mice (280). Thus rotavirus-induced secretory diarrhea is not mediated by CFTR, and the molecular identity of the responsible channel remains to be determined.

A secondary effect of NSP4 could also involve basolateral Ca^{2+} -sensitive K^+ conductances, which could facilitate transcellular Cl^- secretion via cellular hyperpolarization and the upregulation of basolateral secondary active Cl^- uptake (278).

Besides the role of NSP4 as a viral enterotoxin, NSP4 is involved in other pathogenetic phenomena that occur during rotavirus replication. Intracellular Ca^{2+} mobilization is expected to affect the functioning of a variety of host cell Ca^{2+} -sensitive processes, enzymes, and transporters (279). NSP4 was further found to have a direct inhibiting effect on the SGLT1, indicating that NSP4 inhibits water resorption (163).

Extracellular and/or intracellular NSP4 may also contribute to diarrheal pathogenesis by altering the dynamics of intracellular actin distribution as NSP4 has been identified along microtubule-like structures, where it disrupts microtubule-mediated membrane trafficking from the ER to Golgi complex (465). Furthermore, administration of NSP4 was found to cause a reduction in the transepithelial electrical resistance (TER) and redistribution of Zonula occludens-1 in MDCK-1 cells (411), indicating that it can increase epithelial permeability as has been observed during rotavirus infection in piglets, mice and humans (168, 211, 405).

An important recent finding is that crystal structure modelling predicts that the 95–137 region of NSP4, which includes the enterotoxic domain (114–135), may form a homotetrameric pore (47). This region could possibly act as a Ca^{2+} channel in the ER, since it was previously found that endogenously expressed NSP4 could induce Ca^{2+} release from the ER via a non-PLC-dependent pathway in insect cells (421). The induced intracellular Ca^{2+}

mobilization provoked by intracellular NSP4 could extend the signal of extracellular NSP4 or itself initiate disease.

The enteric nervous system

Current evidence point to a role of the enteric nervous system (ENS) in rotavirus induced secretory diarrhea. The gastrointestinal ENS functions fairly independently from the central nervous system as suggested by both morphological and functional studies and it is estimated that the ENS contains about as many neurons as the spinal cord (142). The ENS is composed of two major nerve plexuses that are interconnected, the myenteric plexus (between the circular and longitudinal muscle layers) and the submucosal plexus.

A recent study demonstrated that part of the fluid secretion induced by rotavirus in mice was also caused by an activation of ENS (246). Using Ussing chamber experiments Lundgren et al. demonstrated that tetrodotoxin (neuronal cation channel inhibitor), lidocaine (local anaesthetic) and mecamlamide (a nicotinic receptor blocker) could attenuate the increased potential difference across the epithelium observed in intestines exposed to rotavirus. Interestingly lidocaine was able to prevent the fecal fluid loss, when given intraperitoneally to mice inoculated with rotavirus (246). The authors furthermore calculated that at least two thirds of the fluid and electrolyte secretion caused by rotavirus could be attributed to the activation of the ENS. Similar levels of involvement of the ENS in fluid secretion were also found for many other luminal secretagogues (like bacterial enterotoxins) by these authors (247).

A major question about how rotavirus can activate enteric nerves to induce fluid loss remains to be elucidated. For bacterial enterotoxin-evoked fluid secretion it has been proposed that enterotoxins via their effects on intracellular second messengers induce the release of amines/peptides from the endocrine cells of the intestinal epithelium. Experimental evidence indicates that cholera toxin causes the release of 5-hydroxytryptamine (5-HT) from enteroendocrine cells (247, 320). The released 5-HT activates mucosal 5-HT₂ receptors or 5-HT₃ or 5-HT₄ receptors present on nervous dendrites located just underneath the intestinal epithelium (320). This elicits neuronal VIP release, which results in both protein kinase C and phosphoinositol hydrolysis-dependent increases in fluid (Cl⁻ or HCO₃⁻) secretion as well as decreases in transmucosal absorption (279, 320). A similar mechanism seems also involved in rotavirus diarrhea, as it was recently demonstrated that 5-HT₃ and VIP agonists were able to attenuate rotavirus-induced diarrhea. (218). This suggests that the neurotransmitter serotonin and VIP are involved in rotavirus disease. NSP4 might function in this mechanism by affecting intracellular second messenger in endocrine cells as it increases the intracellular calcium concentration (247, 279).

Other mechanisms may also explain how rotavirus activates the ENS. Normal epithelial cells can function as 'sensors' for microorganisms. As part of an innate defence mechanism, cells release a wide range of biologically active compounds such as cytokines, prostaglandins and nitrous oxide when exposed to bacteria or viruses (128, 355). These compounds participate in the inflammatory response and result in impaired intestinal absorption and the initiation of a prosecretory state in the intestine (128).

Rotavirus was shown to promote the synthesis and release of chemokines, such as interleukin (IL)-8 (65, 355), by intestinal epithelial cells. IL-8 is a known potent chemoattractant for polymorphonuclear leucocytes that enhance the inflammatory cascade and produce further mucosal and epithelial damage by release of reactive oxygen species. Interestingly, activation of the ENS by chemokines is one of the mechanisms that may explain the

rotavirus-induced age dependent diarrhea in mice (<15 days old), since chemokines were only shown to be released from epithelial cells during the first 2 weeks of life (355).

Early studies have correlated rotavirus infection in mice with changes in vascular circulation and reversible cellular ischemia in the villus tips (306, 307, 402). It was proposed that diarrhea was likely to result from the release of a vasoactive substance from epithelial cells, causing villus ischemia and subsequent functional damage to enterocytes (307). It later was proposed that VIP and/or prostaglandins could exemplify the above suggested vasocative agent (279). Similar to rotavirus-induced damage, microbial organisms like cholera, also cause extensive structural changes in human small intestinal villi (257). A further similarity between cholera and rotavirus is that the duration of diarrheal illness is reduced after oral administration of aspirin (nonsteroidal anti-inflammatory), and elevated levels of prostaglandins (notably PGE2 and PGF2a) have been recorded in the plasma and stool of rotavirus-infected children (466) and cholera-infected adults (254). Moreover, rotavirus infection was shown to induce PGE2 production in infected enterocytes in vitro and was inhibitable by indomethacin, a COX1/2 inhibitor like aspirin (358). Therefore, there possibly exist similar prostaglandin-dependent cellular mechanisms that mediate the histological changes observed during both infections and contribute to the diarrhea.

A clinical observation that supports the involvement of the ENS in rotavirus-induced diarrhea involves the enkephalinase inhibitor risedotril (acetorphan) (368). In hospitalized rotavirus-infected children this drug was shown to reduce the duration of diarrhea from an average of 48 to 24 h after admission (368). Risedotril, is used for the treatment of a variety of acute and chronic infectious and inflammatory diarrheas. It prevents the breakdown of endogenous enkephalins within the gastrointestinal mucosa, particularly those that interact with antisecretory (cAMP lowering) δ -receptors expressed on mucosal epithelial cells. This prevents elevations in cAMP levels and, therefore, cAMP dependent anion secretion.

In some diarrheal infections intestinal motility is significantly increased. For various enterotoxins (like cholera toxin), experimental evidence shows that enterotoxins influence intestinal motility via the ENS since the motility pattern can be attenuated by lidocaine and by nicotinic receptor blockade ((247), and references therein). The molecular stimulator of motility however, is not known.

Whether rotavirus infection affects intestinal transit time is not known. It was however recently reported that peristaltic activity in the distal small intestine was not altered during acute rotavirus infection children when compared to the convalescent period (19).

Clinical features

Infection with rotavirus typically occurs in infants between ages 6 months and 2 years, although severe infection in infants younger than 6 months and infection in neonatal intensive-care units are frequently observed (95, 384). Rotavirus infection results in responses that vary from subclinical infection to mild diarrhea to a severe and occasionally fatal dehydrating illness. In all age groups, the classic presentation of rotaviral infection is fever and vomiting for 2–3 days, followed by non-bloody diarrhoea (152).

In an early study examining patients hospitalized with rotavirus diarrhea and patients hospitalized with a diarrheal illness that could not be associated with rotavirus, vomiting was significantly more frequently observed in rotavirus-infected patients. These patients also became dehydrated significantly more often than the rotavirus-negative group. (354). Especially when associated with vomiting, rotavirus diarrhea can lead to severe and even

life-threatening dehydration. Infants with repeated rotavirus infections are generally less severely affected than those with primary disease (444).

Rotaviruses can produce a chronic symptomatic infection in immunodeficient children (190, 303, 377, 461). For example, chronic diarrhea associated with prolonged shedding of rotavirus was described in children with primary immunodeficiency, T-cell immunodeficiency, or severe combined immunodeficiency (SCID). Rotaviruses also are a threat to patients who are immunosuppressed for bone marrow transplantation, and adult renal transplant recipients (319, 470). Rotaviruses do not appear to play an important role in diarrhea occurring in adults infected with human immunodeficiency virus (HIV) (153).

Recent studies indicate that rotavirus infection is not confined to the intestine, but instead is able to leave the intestine and enters the circulatory system (40, 282, 342). Rotavirus has been detected in cerebral spinal fluid (188, 248, 294, 310, 474), liver and kidney (145), extra-intestinal lymphoid tissue (54), and serum of infected children and animals (40, 431). Using in situ RT-PCR, rotavirus was also found in the heart (282). Further studies are needed to determine the significance of these findings.

Epidemiology

It was estimated that each year, rotavirus causes approximately 111 million episodes of gastroenteritis requiring only home care, 25 million clinic visits, 2 million hospitalizations, and 352,000–592,000 deaths (median, 440,000 deaths) in children below 5 years of age. By age 5, nearly every child worldwide will have had an episode of rotavirus gastroenteritis, 1 in 5 will visit a clinic, 1 in 65 will be hospitalized, and approximately 1 in 293 will die as result of the infection. Children in underdeveloped countries account for 82% of rotavirus deaths ((313), and references therein).

The contribution of rotavirus as a cause of endemic gastrointestinal disease varies according to geographic distribution and characteristics of patients. In the United States, rotaviruses cause about 5% to 10% of all diarrheal episodes in infants and children under 5 years old, and account for 30% to 50% of severe diarrheal episodes (87). Several long-term (6-8 years) and short-term (1 year) studies in the USA, Japan, Australia, the UK and Finland demonstrated that rotaviruses was associated with disease in about 35-52% cases of hospitalized infants with diarrhea,(49, 98, 217, 231, 448). A recent study in The Netherlands investigated a broad range of pathogens recovered from an unselected population of patients who had consulted general practitioners because of gastroenteritis (101). From this study it was found that in children <5 years of age with gastroenteritis, rotavirus was the most common pathogen (21% of patients), followed by Norwalk-like virus (NLV; 15% of patients). In older patients (>5 years), *Campylobacter* species and *Giardia lamblia* were the most common pathogens (101). Rotaviruses have also been documented consistently as the most important etiologic agents of diarrheal illnesses in developing countries (27). In a study performed over a 1-year period in Bangladesh, rotaviruses were the most frequently detected pathogen in children under 2 years of age, as 46% of the studied group was rotavirus positive (34). The next most important agent was enterotoxigenic *E. coli*, detected in 28%. In the over-2-year age group, bacterial agents were recovered more frequently than rotavirus. Similar results were obtained in an analysis in a hospital in Cairo, Egypt, where rotavirus was most frequently detected, accounting for 34% of the cases. Enterotoxigenic *E. coli* ranked second (27%) (393).

Rotavirus infection in children is seasonal, with peak incidence in winter months in temperate climates. In the United Kingdom and in the USA, increasing numbers of infections begin in December or January, with peaks in March or April and incidence falling to almost zero by July (189, 206). Several studies suggest that rotavirus disease in adults do not mirror the winter seasonality of infection in children (92, 288).

Among adults, endemic outbreaks of rotavirus infections seem to occur most frequently in communities that are more or less sheltered from routine exposure to rotavirus-infected children. These communities may be college communities, military bases, long-term health-care facilities (especially those with compromised host immunity), and geriatric facilities ((4), and references therein). Rotavirus has been implicated as an important cause of travellers' diarrhea among adults, especially among those visiting Central America and the Caribbean (for a review see (4), and references therein). Interestingly these rotavirus-infected adults shed 10–100 times less rotavirus than do infected children (41, 449).

Immunity

The mechanisms responsible for immunity to rotavirus infections are not completely understood. However, animal models have been particularly useful in elucidating the role of antibodies and in exploring the relative importance of systemic and local immunity (299, 367). The immunological response of the host to infection with rotavirus results in rotavirus antigens being transported to Peyer's patches, undergo processing by B cells, macrophages, or dendritic cells and are presented to helper T cells. This cascade culminates in stimulation of rotavirus-specific B cell and cytotoxic T-lymphocyte-precursor expansion (298). Polyclonal B cell activation was induced by the rotavirus outer capsid protein VP7 (39). Although many physicians presume that rotavirus infection will confer lifelong immunity, several investigations show that (multiple) re-infection(s) can occur. (31, 444, 473).

A symptomatic infection with rotavirus stimulates a strong humoral IgG, but protection from rotavirus disease is however primarily thought to be mediated by local IgA antibodies. Several studies demonstrated that local IgA is important or at least a good predictor of protection (29, 451). A recent study in which IgA knockout mice were challenged with murine rotavirus showed that in the absence of IgA, other compensatory antibody isotypes, IgG in particular, were able to mediate protection against homologous rotavirus challenge (305).

VP4 and VP7 were shown to be very important in inducing neutralizing antibodies and they can do so independently from each other (122, 175, 204). Children infected with a particular serotype of rotavirus are more likely to be protected against challenge with the same serotype than against re-infection with a different serotype. However, heterotypic protection is operating, as has been demonstrated in several studies. It appears that predominantly homotypic immunity is induced following the first naturally occurring or vaccine-induced rotavirus infection (204) and this immunity is mediated by antibodies against VP7 and VP4 (175). In both infants and animals, subsequent rotavirus infections increase antibodies that cross-react with multiple serotypes. (192, 204). Several other rotavirus proteins could also play a role in mounting a protective immune response and mediate heterotypic protection. VP6 is a hydrophobic protein that is highly antigenic and immunogenic and may play a role in inducing protective immunity and modulate protection (122). NSP4 could also be involved in this process as immunization with NSP4 can induce immunity that protects neonatal mice from disease induced by virus (16, 122). The role of cell-mediated immunity in the immune

response to rotavirus infection is under investigation in humans and in animal models (204). Following studies using adult mice infected with a selected murine rotavirus strain and SCID mice, it was shown that cytotoxic T-lymphocytes play a major role in resolution of primary rotavirus infection ((204), and references therein). It was shown that VP7 is the dominant target for cytotoxic T-lymphocyte (CTL) activity in mice (139, 301).

Diagnosis, treatment, and prevention

Initially, diagnosis of rotavirus infection was performed using electron microscopy, by the visualization and observation of the rotavirus wheel-like appearance (457, 469). Nowadays, ELISA or EIA have become more commonly used. The commercial assays are reliable, and inexpensive, but require at least 10^4 – 10^7 virions to generate a positive result (457, 469). A more sensitive and newer method is PCR, which is up to 1000 times more sensitive than immunoassays (457). A further major limitation of most commercial assays is that they only detect group A rotavirus. (178, 344).

Treatment of rotavirus infections is mainly aimed at symptom relief and restoration of normal physiological function. Oral rehydration is by far, the most commonly used treatment and oral rehydration salt solutions are extensively used in children in developing countries. If rotavirus infected patients become dehydrated, administration of intravenous fluids and hospital admission might be necessary. An additional intervention that has been used is administration of *Lactobacillus* spp bacteria that shorten the duration of diarrhea (155, 392). Codeine, diphenoxylate and loperamide, were reported to result in symptom relief and decrease in diarrheal fluid loss (111), although the latter appeared to have no significant effect on the course of acute gastro-enteritis in an earlier study (308). Bismuth salicylate, was successful in treating the symptoms of rotavirus diarrhea (400).

As mentioned above, the enkephalinase inhibitor ricedotril has successfully been used for the treatment of a variety of infectious and inflammatory diarrheas and was found to reduce the duration of diarrhea in rotavirus-infected children (368). Several studies report the oral administration of human serum immunoglobulins that show anti-rotavirus activity by binding free rotavirus antigen. This approach was able to shorten the duration of diarrhea and clear rotavirus antigen (154, 242).

Although not used on a regular basis, the following agents could be useful in effective treatment of rotavirus-induced diarrhea. Diarrheal illness was reduced after oral aspirin, a non-specific COX inhibitor as elevated levels of PGE₂ and PGF₂ were observed in the plasma and stool of rotavirus-infected children (466). Furthermore, indomethacin and a NFκβ inhibitor have been shown to inhibit rotavirus infection in vitro (358).

Various carbohydrates including mucins were shown to inhibit rotavirus infection in vivo and vitro (72, 289, 323, 440, 459, 471, 472). Mucins serve protective functions in the gut (438). The secretory mucin Muc2, which is the most important structural component of the intestinal mucus layer (426, 427, 438, 440), is secreted into the lumen and forms a protective mucus gel layer that acts as a selective barrier to protect the epithelium from mechanical stress, noxious agents, viruses, and other pathogens (116, 137, 407, 426, 438, 440). Muc2 and other mucins contain many O-linked sialic acid moieties and are important inhibitors of rotavirus infection (72, 289, 323, 440, 459, 471, 472). It was suggested that intestinal mucins represent a barrier to rotaviruses via binding of rotavirus to sialic acid moieties thereby hindering virus-to-cell attachment (72, 472).

Prevention of rotavirus infection can be facilitated by avoiding exposures and faecal-oral spread. It was shown that 43% of rotavirus virions placed on human fingers survive for 1h (6), and rotavirus survives best in low humidity on non-porous surfaces at room temperature or cooler (376). Phenolic disinfectants fail to inactivate rotavirus, instead hypochlorite or sodium dichloroisocyanurate are effective (344). Ethanol (70%) is also effective in inactivation of rotavirus and can help to prevent environmental spread (318).

Since there is a significant disease-related morbidity and mortality associated with rotavirus, the development of an effective vaccine is a priority. Several rotavirus vaccines candidates have been developed and tested (312). However, there has been variable efficacy with the use of some live-attenuated rotaviruses developed for oral administration and at present no effective rotavirus vaccine is available (18, 186).

Up till now, a live attenuated tetravalent rhesus-human reassortant rotavirus vaccine (Rotashield) seemed to produce the best results and prevented about half of rotavirus infections, while it was in particular effective in preventing severe disease (194, 321). This vaccine was the first licensed rotavirus vaccine in the United States and recommended for routine immunization of U.S. infants in 1998. Shortly after the vaccine was approved, the use of Rotashield was suspended because reports suggested a possible association with intussusception (287). After the association was established, the recommendation for use of Rotashield was withdrawn and the manufacturer stopped vaccine production. Efforts are ongoing to develop other rotavirus vaccines, and several candidates are undergoing clinical testing (50).

Aims and outline of this thesis

Our overall aim was to attain a more profound understanding of rotavirus pathogenesis.

Chapter 2 focuses on the effect of rotavirus infection on epithelial homeostasis and dysfunction during rotavirus infection in neonatal mice. To get insight in the pathogenesis of infection, the induction of diarrheal illness, timing and extent of rotavirus replication in the mice small intestine are related to viral replication and alterations in mucosal structure, epithelial homeostasis, kinetics, and differentiation.

The study outlined in **Chapter 3** was performed to evaluate whether goblet cells and mucins play a role in the active defense against rotavirus infection. The chapter describes the changes in goblet cell homeostasis during rotavirus infection in neonatal mice. Different experiments are performed to examine structural changes of mucins during rotavirus infection. Moreover, by isolating mucins from infected and control mice, it is determined whether age-dependent differences in mucin composition and/or structure alter the anti-viral capabilities of small intestinal mucins. Next in **Chapter 4**, our goal was to evaluate the role of prostaglandins in mucin expression during rotavirus infection. **Chapter 5** focuses on the effects of rotavirus exposure on immune maturation in young mice. As a model for vaccination, we examined the immune responses in infant mice following oral inoculation with standardized amounts of different fractions of purified simian rotavirus SA11 that differed in antigen composition. Finally, in **Chapter 6** we aim to identify cellular proteins that interact with the rotavirus enterotoxin NSP4. Identifying these proteins is important since it might lead to new therapeutic approaches and viral intervention in order to reduce and prevent rotavirus disease.

Changes in small intestinal homeostasis, morphology, and gene expression during rotavirus infection in infant mice

Jos A. Boshuizen, Johan H.J. Reimerink, Anita M. Korteland-van Male, Vanessa J.J. van Ham, Marion P.G. Koopmans, Hans A. Büller, Jan Dekker, Alexandra W.C. Einerhand

Abstract

Rotavirus is the most important cause of infantile gastroenteritis. Since *in vivo* mucosal responses to a rotavirus infection thus far are not extensively studied, we related viral replication in the murine small intestine to alterations in mucosal structure, epithelial cell homeostasis, cellular kinetics, and differentiation. Seven-day-old suckling BALB/c mice were inoculated with 2×10^4 ffu of murine rotavirus and were compared to mock-infected controls. Diarrheal illness and viral shedding were recorded and small intestinal tissue was evaluated for rotavirus- (NSP4 and structural proteins) and enterocyte specific (Lactase, SGLT1, LFABP) mRNA and protein expression. Morphology, apoptosis, proliferation and migration were evaluated (immuno-) histochemically. Diarrhea was observed from day 1 to 5 post infection, and viral shedding from day 1 to 10. Two peaks of rotavirus replication were observed at 1 and 4 days post infection. Histological changes were characterized by the accumulation of vacuolated enterocytes. Strikingly, the number of vacuolated cells exceeded the number of cells in which viral replication was detectable. Apoptosis and proliferation were increased from day 1 to 7, resulting in villus atrophy. Epithelial cell turnover was significantly higher (<4 days) than in controls (7 days). Since epithelial renewal occurred within 4 days, the second peak of viral replication was most likely caused by infection of newly synthesized cells. Expression of enterocyte specific genes was downregulated in infected cells at mRNA- and protein-levels starting as early as 6 h after infection.

In conclusion, we show for the first time that rotavirus infection induces apoptosis *in vivo*, an increase in epithelial cell turnover and a shut-off of gene expression in enterocytes showing viral replication. The shut-off of enterocyte specific gene expression, together with the loss of mature enterocytes through apoptosis and the replacement of these cells by less differentiated dividing cells, likely lead to a defective absorptive function of the intestinal epithelium, which contributes to rotavirus pathogenesis.

Introduction

Rotaviruses are one of the most significant causes of gastroenteritis, malnutrition and diarrhea in young children and animals (123, 203). Mortality rates are low in developed countries where illness is usually self limiting (429). However, each year more than 600.000 young children die in developing countries throughout the world (269). Rotavirus infection in children is mainly restricted to the small intestinal villus epithelium, resulting in the occurrence of total villus atrophy (33). Although rotavirus can infect older children and adults, diarrheal disease is primarily observed in children under 2 years of age (122, 123, 203).

Rotavirus induced diarrhea is thought to be caused by a combination of factors (369), which include a reduction in epithelial surface area, replacement of mature enterocytes by immature (crypt-like) cells (306), an osmotic effect resulting from incomplete absorption of carbohydrates from the intestinal lumen in combination with bacterial fermentation of these non-absorbed compounds, secretion of intestinal fluid and electrolytes through activation of the enteric nervous system (ENS)(246), and the effect of the rotavirus non-structural protein 4 (NSP4), which is thought to act as a viral enterotoxin (16).

Since the epithelium is the primary target of rotavirus infection, epithelial dysfunction plays an important role in rotavirus pathogenesis. However thus far, *in vivo* data concerning specific epithelial responses are rather limited (84, 162, 209, 306, 355, 389). Studies on the effect of infection on epithelial homeostasis *in vivo* are mainly restricted to studies in piglets, young rabbits and mice (84, 162, 209, 389). In piglets, sucrase-isomaltase activity was found decreased, whereas thymidine kinase activity was increased during rotavirus infection (389). In rabbits, rotavirus infection was shown to impair epithelial homeostasis and intestinal brush-border membrane Na (+)-solute co-transport activities were affected (162, 163). In young mice, homologous rotavirus infection affects the small intestinal epithelium by reducing leucine uptake, lactase and alkaline phosphatase activities, whereas the maturation of sucrase-isomaltase activity was found to be precocious (84, 209).

Vacuolization of enterocytes during rotavirus infection is observed in mice and rats (77, 302, 306), but is not a feature of rotavirus infection in calves, lambs, and piglets (268, 389, 398). These differences have been attributed to the specific nature of the host response and not to the virus, since vacuolization is also a characteristic feature of heterologous infections in mice (24, 149, 251). Mice usually do not develop any symptoms beyond 2 weeks of age, and infection of adult mice occurs without disease or histopathological lesions (59, 130, 306, 341, 402, 453).

The present study was designed to get more insight into the pathogenesis of rotavirus infection by studying epithelial homeostasis and dysfunction during rotavirus infection in mice. We examined the induction of diarrheal illness, timing and extent of rotavirus replication in the murine small intestine, and related viral replication to alterations in mucosal structure, epithelial homeostasis, kinetics, and differentiation.

Materials and Methods

Animals

Pregnant dams were obtained from Harlan (Zoetermeer, The Netherlands). Dams, either with their control or inoculated litters, were housed in micro-isolator cages under negative pressure in a specified pathogen-free environment. Rodent chicken-protein free chow (9605/9608; Harlan Teklad TRM (A)) and deionized water were autoclaved and provided *ad libitum* until the end of the experiment. All dams were rotavirus antibody negative as measured by enzyme-linked immunosorbent assay (ELISA, as described below). All the experiments were performed with the approval of the Animal Studies Ethics Committee of the National Institute of Public Health and the Environment.

Virus

The EDIM (Epizootic Diarrhea of Infant Mice) mouse rotavirus strain was obtained from Dr. R. Ward, Children's Hospital Research Foundation, Cincinnati, USA (266). The strain used is an unpassaged virus isolated directly from the stools of ill mice.

Virus inoculations and subsequent animal-handling procedures

Seven-day-old BALB/c mice were inoculated intra-gastrically with 2×10^4 focus forming units (ffu) of the EDIM rotavirus strain. Control mice were mock infected through inoculation with PBS. To analyze epithelial proliferative kinetics, 30 mg/kg body weight 5-bromo-2'-deoxyuridine (BrdU; Sigma, St Louis, USA) was injected intraperitoneally just

before inoculation. After inoculation and injection of BrdU, the mice were returned to their mothers and allowed to suckle. After 6 h and at days 1, 2, 4, 7, 10, and 14 5 infected and 3 control mice were sacrificed per time point. Segments of jejunum (anatomic middle of the small intestine) and ileum (distal 2 cm of the small intestine) were rinsed in PBS and fixed for 4 h in 4% (wt/vol) paraformaldehyde (Merck, Darmstadt, Germany) dissolved in PBS. The segments were then dehydrated through a graded series of ethanol and xylene (Merck), and embedded in Paraplast Plus (Sherwood Medical, Den Bosch, The Netherlands) as previously described (446). In addition, adjacent segments of the jejunum and ileum were dissected and snap frozen in liquid nitrogen and stored at -80°C for RNA and protein isolation.

Detection of rotavirus in stools

To determine the rotavirus shedding, fecal samples were collected from each individual sacrificed mouse at 0-14 days post infection (dpi) and stored at -20°C. Samples were then homogenized in PBS in a 10% (wt/vol) solution/suspension and centrifuged (1000 g for 5 min) to remove debris before being analyzed. The presence of rotavirus antigen in fecal samples was determined by enzyme-linked immunosorbent assay (ELISA) using the Premier rotaclone kit (Meridian Diagnostics, Cincinnati, Ohio). The test was considered positive if the optical density (OD, at 450 nm) of the well containing stool minus the OD of control wells was ≥ 0.1 .

Diarrhea score

The severity of diarrheal illness was assessed by examination of fecal material. Stools were scored from 1 to 4 based on color, texture and amount of stool. Normal feces was defined as a score of 1, exceptionally loose feces was scored as 2, loose yellow-green feces was scored 3, and watery feces was defined as a score of 4. Stools with a score of ≥ 2 were considered as diarrhea. The percentage diarrhea was calculated by dividing the number of diarrheic samples by the total number of mice scored for diarrhea each day. Mice from which no stool could be obtained were considered as mice with no diarrhea. The diarrhea severity was determined by dividing the sum of all scores by the number of total stool samples collected each day.

Antibody production

Polyclonal rabbit hyperimmune sera were raised against cesium chloride purified simian rotavirus (SA11) or a synthetic peptide corresponding to amino acids 114-135 of NSP4 from the SA11 strain (KLTREIEQVELLKRIYDKLTV). The NSP4 peptide was coupled to keyhole limpet hemocyanin using the EDC-kit from Pierce (Pierce, Rockford, IL), following the manufacturer's protocol. Purified rotavirus or the NSP4 peptide were emulsified with Freund's adjuvant and injected subcutaneously into rabbits following the method we have described previously (426). The polyclonal serum raised against purified rotavirus was used for quantifying rotavirus protein in intestinal homogenates. The polyclonal serum raised against the NSP4 peptide was used for immunohistochemistry.

Histology and morphometry

For standard histochemical staining or immunohistochemistry, paraffin-embedded tissues were sectioned (5 μ m), deparaffinized with xylene (Merck) and rehydrated in graded ethanol solutions as previously described.(346) Epithelial morphology was analyzed after Gill's

hematoxylin (Vector Laboratories, Burlingame, England) and eosin (Merck) staining (HE). Crypt depth and villus height were measured manually in well-orientated sections (10 measurements per region per mouse) using a micrometer (Nikon, Bunnik, The Netherlands) mounted in an Eclipse E600 Microscope (Nikon). By dividing the crypt-villus axis into 5 equal regions, the position of vacuolated cells and cells containing replicating virus along the crypt-villus axis were assessed. The positions were scored from 1 to 5 representing the tips of the villi to the crypts, respectively. The presence of vacuoles was judged by standard HE staining. The vacuoles were examined for the presence of acid and neutral carbohydrates using a combined alcian blue-periodic acid-Schiff (PAS) staining. The presence of replicating virus was determined by immunohistochemistry using the antibody against the non-structural protein NSP4 (see below). Ten crypt-villus units per segment of the small intestine per animal were analyzed. All scores were averaged per intestinal segment per animal, and subsequently averaged between animals to calculate the mean score per segment per time-point (\pm SEM).

Immunohistochemistry

Deparaffinized and rehydrated sections were incubated overnight at 4°C using the primary mouse monoclonal antibodies anti-human proliferating cell nuclear antigen (PCNA, 1:1500; Boehringer), anti-BrdU (1:250; Boehringer), anti-rat lactase (1:1000;(339)) or the rabbit polyclonal antibodies, anti-(cleaved) caspase-3 (1:500; Cell Signaling Technology, Beverly, USA), anti-NSP4 (1:1000), anti-rat liver fatty acid binding protein (L-FABP, 1:2000;(359)), or anti-rabbit sodium glucose co-transporter 1 (SGLT1, 1:1000;(169)). Immunohistochemistry was carried out as described previously (346).

Epithelial proliferation and apoptosis

The effects of rotavirus infection on intestinal epithelial cell migration kinetics were analyzed through detection of BrdU, a nucleotide analog that is incorporated into the DNA of proliferating cells. At different time-points after injection of BrdU the position of the foremost and least advanced-BrdU labeled cells in ten crypt-villus units per animal were expressed as the number of cell-positions from the crypt-villus axis. Proliferating (PCNA-positive) and apoptotic (caspase-3-positive) cells were counted in villi and crypts of the jejunum until 14 dpi, of respectively 10 and 30 well-oriented crypt-villus units per animal per time-point.

***In situ* hybridization and probe preparation**

Non-radioactive *in situ* hybridization was performed using the method as previously described (233, 346). Digoxigenin (DIG)-11-UTP labeled RNA probes were prepared according to the manufacturer's protocol (Boehringer Mannheim GmbH, Mannheim, Germany) using T3, T7 or SP6 RNA polymerase. The following probes were used: A 1 kb NcoI fragment based on a 2.4 kb rat SGLT1 cDNA ligated in pBluescript (88), a 350 bp fragment of rat L-FABP cDNA ligated in pBluescript,(394) a 250 bp EcoRI/HindIII mouse beta-actin fragment ligated in pSP65 (221), and a 750 bp NcoI/SmaI NSP4 (SA11 strain) fragment ligated in pBluescript (see below). Transcripts longer than 450 bp were hydrolyzed in 80 mM NaHCO₃ and 120 mM Na₂CO₃, pH 10.2 to obtain probes of various lengths \leq 450 bp (91).

Quantitation of mRNA

Total RNA was isolated from frozen small intestinal segments, using Trizol reagent (Gibco-BRL, Gaithersburg MD) following the manufacturer's protocol. Integrity of the RNA was assessed by visual analysis of the 28S and 18S ribosomal RNAs after electrophoresis and staining with ethidium bromide. Subsequently, 1 µg of total RNA was dot-blotted on Hybond-N⁺ (Amersham, Bucks, England) using a vacuum-operated manifold (BioDot, BioRad, Hercules, CA). All blots were hybridized using specific ³²P-labeled cDNA probes as described previously (446). To correct for the amount of RNA that was spotted, hybridized signals were corrected for glyceraldehyde-3-phosphate dehydrogenase (GAPDH) mRNA expression using a 1.4 kb human GAPDH probe (446). Hybridization signals were measured through autoradiography using a PhosphorImager and ImageQuant software (Molecular Imaging, Sunnyvale CA, USA). The following probes were used: a 394 bp NcoI fragment of rat SGLT1 (obtained from Charles Burant), a 400 bp XhoI/EcoRI fragment of rat LFABP,(394) a 1.8 kb EcoRI fragment of rat lactase (57). For the construction of the NSP4 probe, RT-PCR was performed on RNA from simian rotavirus (SA11 strain) infected MA104 monkey kidney cells. NSP4 was cloned using the primers GGAACCATGGAAAAGCTTACCGACCTC (nt 46-62) and TCCCCGGGTACATTAA-GACCGTTCCT (nt 730-750), based on the NSP4 SA11 coding sequence (46). PCR fragments were cloned into the EcoRI sites of PCR 2.1 (Invitrogen).

Quantitation of rotavirus protein

Proteins were isolated from frozen segments by homogenization of the tissue in 500 µl (Tris-) homogenization buffer containing Triton X-100 (BDH, Poole, England), 1% SDS and various protease inhibitors as previously described (252). Protein concentration was measured using a bicinchoninic acid (BCA) protein assay reagent kit (Pierce). Bovine serum albumin was used as a standard. To quantify rotavirus structural protein contents, protein homogenates were dot-blotted on nitrocellulose (Nitran; Schleier & Schuell, Dassell, Germany). The blots were blocked for 1 h with blocking buffer (50 mM Tris-HCl, pH 7.8, 5% (wt/vol.) nonfat dry milk powder (Lyempf, Kampen, The Netherlands), 2 mM CaCl₂, 0.05% (vol./vol.) Nonidet P40 (BDH), and 0.01% (vol./vol.) antifoam (Sigma)), and incubated for 18 h with rabbit hyperimmune serum raised against SA11 rotavirus particles (1:1000). After being washed in blocking buffer, the blots were incubated with ¹²⁵I-labeled protein A (specific activity 33.8 mCi/mg; Amersham) for 2 h. Bound ¹²⁵I-labeled protein A was then detected and the elicited signals were quantified using a PhosphorImager and ImageQuant software (Molecular Imaging).

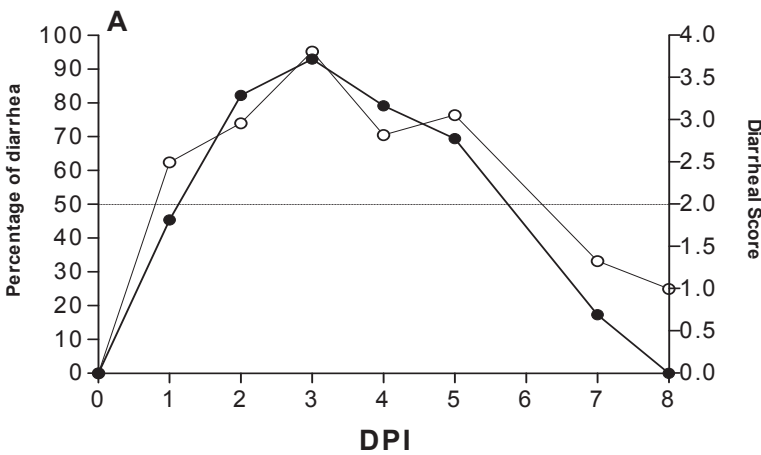
Statistical analysis

Statistical analysis of all data from control and infected groups was performed using Student's *t*-test for unpaired data (two-tailed). To compare three or more groups, data were analyzed by ANOVA followed by an unpaired *t*-test. Data were expressed as the mean ± SEM and *P* values of ≤ 0.05 were considered statistically significant.

Results

Rotavirus infection of 7-day-old mice caused diarrhea and virus shedding starting at 1 day post-infection

To be able to study rotavirus infection *in vivo*, 7-day-old suckling mice were inoculated orally with 2×10^4 ffu of EDIM rotavirus. As a control, mice of the same age were PBS inoculated. Control mice did not develop diarrhea at any time-point, and did not shed rotavirus antigen over a period of 14 days after PBS inoculation as measured by ELISA (data not shown). Mice inoculated with rotavirus, developed diarrhea over a period of 5 days (Figure 1A).



| | | | | | | | | |
|------------------|---|----|----|----|----|----|----|----|
| diarrheic stools | 0 | 15 | 28 | 27 | 23 | 16 | 4 | 0 |
| total stools | 0 | 33 | 34 | 29 | 29 | 23 | 23 | 17 |

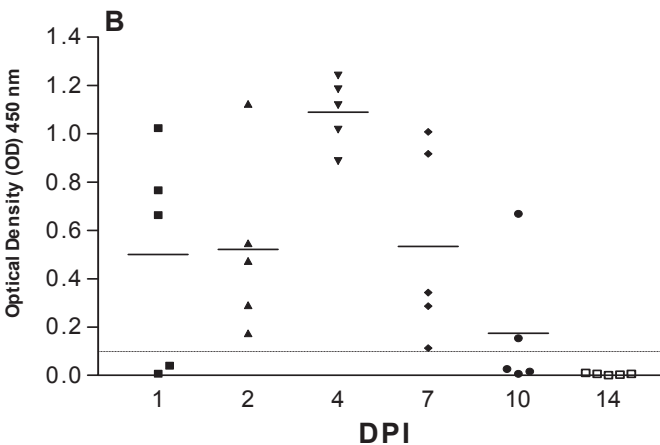


Figure 1. Percentage diarrhea (●) and mean diarrheal score (○) (A), and viral antigen-shedding (B) in neonatal mice inoculated with rotavirus. Percentage of diarrhea per day was calculated by dividing the number of diarrheic samples by the number of total samples collected each day. A score of ≥ 2 was considered diarrhea, whereas a score of < 2 was considered normal. The mean diarrheal score was determined by dividing the sum of all diarrhea or non-diarrhea scores (1 to 4) by the number of total samples scored each day (numbers are listed at the bottom of the figure). Fecal samples ($n=5$ per day) from 0 to 14 dpi were assayed for rotavirus antigen shedding by ELISA (B). Data are expressed as net and mean OD readings at 450 nm and represent individual values obtained for fecal samples. Readings of ≥ 0.1 are considered positive.

The onset of diarrhea occurred as early as 1 day post infection (dpi). The highest percentage of diarrhea occurred at 3 dpi, reaching 93% (Figure 1A). At this time-point also the severity of diarrheal illness was maximal. The duration of viral antigen shedding was maximally 10 days (Figure 1B).

At 1 dpi three of the five animals examined shed virus and at 4 dpi viral shedding was maximal. At 10 dpi only two of five examined animals still shed virus. None of the infected mice died spontaneously. Thus, the onset of diarrhea occurred approximately at the same time as viral antigen shedding began.

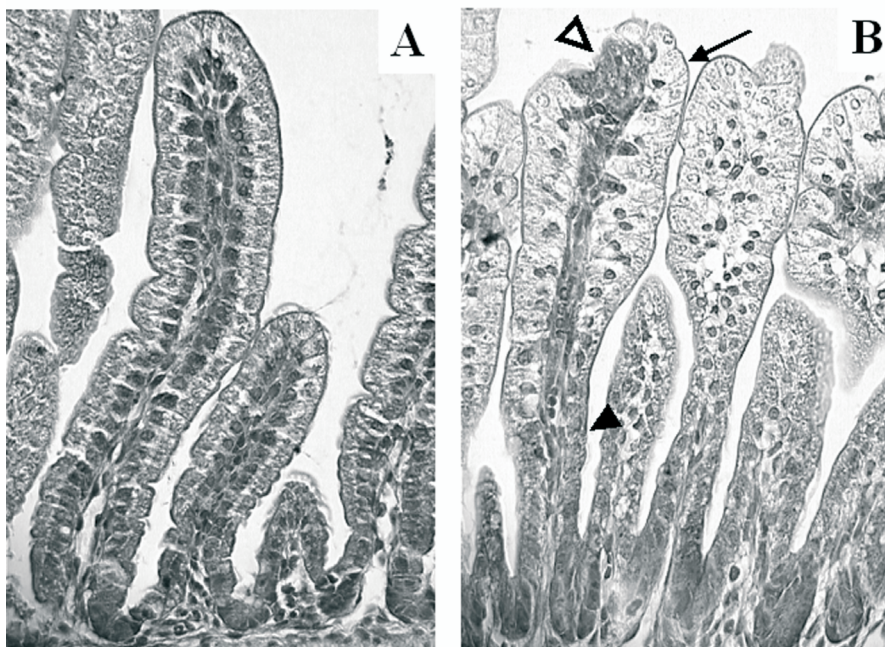


Figure 2. Histopathological lesions in mouse small intestine (jejunum) during rotavirus infection at 1 dpi. Sections were stained with hematoxylin and eosin. In control animals (A), enterocytes were clearly polarized and the nuclei were localized at the base of the enterocytes. In infected mice at 1 dpi (B), histopathological changes were characterized by vacuolization of the enterocytes, swelling of the villus tips (arrow), constriction of the bases, and nuclei that were irregularly positioned within the cells (arrowhead). In many villi, lesions seemed to be present at the tips (open arrowhead). Original magnification, X 250.

Histopathological lesions in mouse small intestine during rotavirus infection

At necropsy, accumulation of fluid in the small intestine was observed in infected mice. This was first observed at 1 dpi, persisted through 4 dpi, and was accompanied by distention of

the ileum and large intestine. At these time points the diameter of the duodenum of infected mice however, appeared smaller when compared to controls (data not shown). In control animals, jejunal enterocytes were clearly polarized and the nuclei were localized at the base of the enterocytes (Figure 2A). Histopathological changes in the small intestine of rotavirus infected mice, were characterized by swollen villus tips and constricted villus bases. In many villi, lesions seemed to be present at the tips (Figure 2B, open arrowhead). In infected mice at 1 dpi, nuclei were enlarged and irregularly positioned within the cells. At the constricted bases of the jejunal villi, the cells were flattened and rounded (Figure 2B, arrowhead). During infection, large vacuoles occurred in the enterocytes lining most of the surface of the villi in the small intestine (Figure 2B, arrow). Particularly in the ileum, accumulation of supra-nuclear vacuoles was observed, while in the duodenum histological changes were mainly restricted to rounding of enterocytes (data not shown). Vacuolization was observed from 1 to 7 dpi and was most pronounced in the ileum at 2 dpi. Almost complete resolution of the histopathological changes was observed by 7 dpi. At the start of the weaning period at 10 dpi, when the pups were 17 days old, minimal vacuolization was noticeable at the tips of the villi in (formerly) infected and control animals. These vacuoles however were only detected in the ileum, morphologically different from-, and always far less in number than the vacuoles observed in the inoculated mouse pups before 7 dpi (data not shown). The vacuoles observed during infection and during the start of the weaning period did not stain for acid or neutral carbohydrates using a combined alcian blue-periodic acid-Schiff (PAS) staining (data not shown).

Kinetics of rotavirus replication in the mouse small intestine

To determine the kinetics of rotavirus replication in young mice, the presence of replicating virus in small intestinal tissue was determined by detection of rotavirus structural proteins and NSP4. NSP4 is not found in mature infectious virus particles and is only synthesized within host cells during virus replication. The presence of NSP4 is therefore an incontrovertible indication for viral replication. At 6 hours post infection (hpi), NSP4 was detected at RNA and protein level in an occasional epithelial cell in the duodenum and jejunum of infected mice, as observed by *in situ* hybridization and immunohistochemistry, respectively (data not shown).

At 1 dpi rotavirus NSP4 protein and mRNA was detected in almost all the epithelial cells located in the upper part of the small intestinal villi of rotavirus infected mice (Figure 3A and B, jejunum). At 2 dpi, when vacuolated cells were still abundantly present, NSP4 expression was only detected in a few cells in the villus epithelium. At 4 dpi, a second peak of rotavirus replication was observed (Figure 3A and B). No rotavirus antigen was detected beyond 7 dpi in any part of the small intestinal epithelium. Analysis of adjacent sections revealed that the localization of NSP4 RNA and protein within the small intestinal epithelium correlated well and matched with that of the structural proteins (data not shown). Viral replication was not observed in the crypt compartment at any time during infection and replication was confined solely to the villus epithelium. No rotavirus structural proteins (data not shown), or NSP4 mRNA or protein could be detected in the vacuoles at any time-point. Quantitatively, very low expression of NSP4 mRNA was first observed in gut homogenates of the jejunum at 6 hpi (Figure 3C). In agreement with the histological data, two peaks of viral replication were observed in both the jejunum and ileum. At 1 dpi there was a first peak of NSP4 mRNA expression. Expression was low at 2 dpi, and a second peak of replication was observed at 4 dpi. At 1 dpi, expression of NSP4 mRNA was statistically significantly higher in the ileum

than the jejunum. Quantitative data of rotavirus structural protein expression in gut homogenates correlated well with the expression of NSP4 mRNA (Figure 3D). Some animals did not shed rotavirus at 1 dpi (Figure 1). However, NSP4 mRNA and rotavirus structural protein expression was observed in the duodenum and jejunum, but not ileum, of these animals (data not shown). Rotavirus antigen was not detected in any section of the small intestine of control mice.

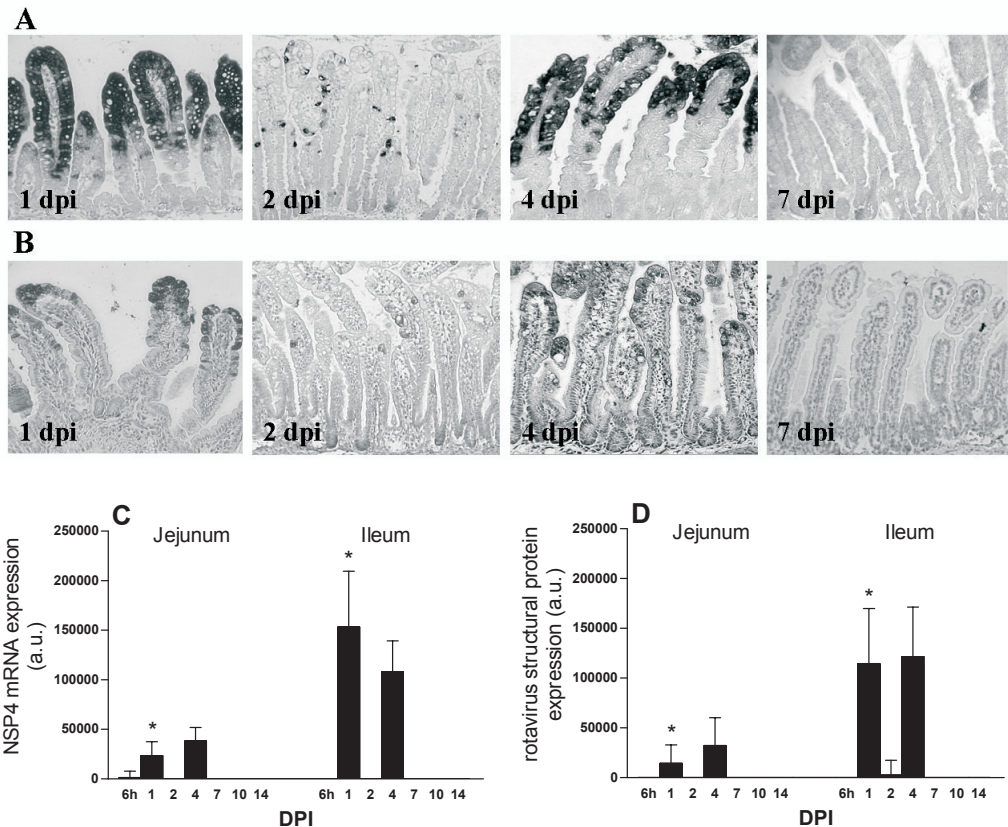


Figure 3. Kinetics of rotavirus replication in the mouse small intestine. NSP4 mRNA (panel A) and protein (panel B) expression in jejunum at several days post infection were detected by *in situ* hybridization and immunohistochemistry respectively. No rotavirus antigen was detected beyond 7 dpi in any part of the small intestinal epithelium. Quantitative expression of NSP4 mRNA and structural rotavirus proteins were analyzed by RNA- and protein dot-blotting respectively (panels C and D). At 1 dpi, the levels of NSP4 mRNA and structural protein expression were significantly higher in the ileum compared to the jejunum, * $P < 0.05$, using Student's *t*-test. Original magnification, X 150. a.u., arbitrary units.

The pattern of epithelial vacuolization is more extensive than the pattern of replicating virus

To determine whether replicating virus and vacuolated cells were found in the same region along the villi, crypt-villus units in the jejunum were divided into 5 regions of equal length. The positions were scored from 1 to 5 representing the tips of the villi to the crypts, respectively (Figure 4). As stated earlier, the first infected cells were observed at 6 hpi and

vacuolated cells were first observed at 1 dpi. At 1 and 2 dpi, infected cells were exclusively found in the upper halves of the villi. However, vacuolated cells were observed along the entire villi, even at the base of the villi where no rotavirus was detected. At 4 dpi, infected and vacuolated cells were found in the same region. At 7 dpi, no virus antigen was detected, but occasionally there was still some vacuolization of the enterocytes in the upper villus regions. A very similar pattern of vacuolization and replicating virus was observed in the ileum (data not shown). Note that these scores do not present data on the severity of histological pathology but rather present information on where the pathology was observed.

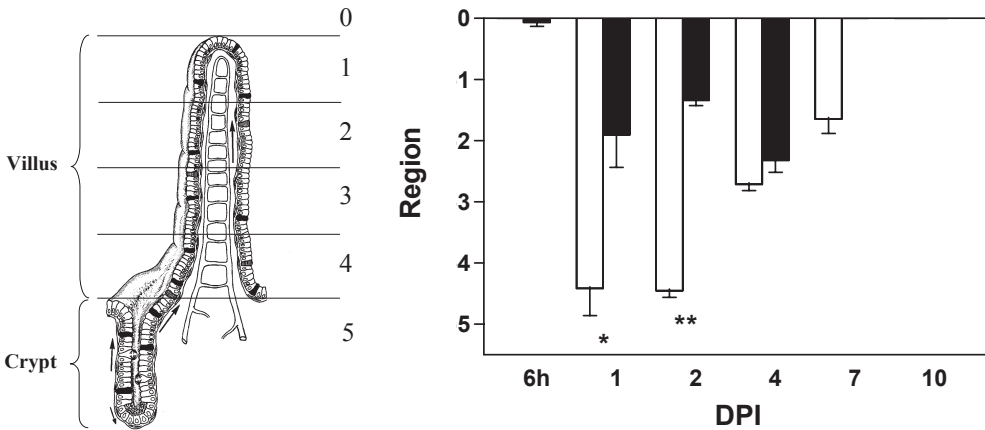


Figure 4. The pattern of epithelial vacuolization is more extensive than the pattern of replicating virus. Crypt-villus units in the jejunum were divided into 5 regions of equal length (see left part of the figure). The position of the vacuolated cells (open bars) and virus-containing cells (solid bars) on the crypt-villus axis was scored from 1 to 5 representing the regions from the tips of the villi to the crypts. At 1 and 2 dpi, infected cells were exclusively found in the upper part of the villi, whereas vacuolated cells were observed along the entire villi and even at the base of the villi. Values are means \pm SEM. * $P < 0.01$, ** $P < 0.001$ using Student's *t*-test. At the left, a crypt/villus unit is shown and the different regions are indicated.

Villus and crypt length during rotavirus infection

We wanted to examine whether villus atrophy occurred in our homologous rotavirus model. In control mice, villus length in the jejunum remained constant during development in the second week after birth (i.e. 6 hpi to 7 dpi, Figure 5A). Then, when the control mice were 17 and 21 days old (i.e. 10- and 14 dpi), villi became significantly shorter (74-78%) when compared to control length at 6 hpi-7 dpi. In control mice, the crypts of the jejunum increased in depth by about 100% during development in the period between 1 and 3 weeks (i.e. 6 hpi to 14 dpi) after birth. During infection, villus atrophy was observed as villi in the jejunum were shortened to 69-75% (i.e. at 6 hpi to 4 dpi) of control length. Villus length of infected and control mice were comparable at 7 to 14 dpi. Crypt depth increased from 6 hpi to 14 dpi in control as well as infected mice. During infection there was a trend towards an increased crypt depth at 1 (142%) and 2 dpi (134%) compared to control mice, however this did not reach statistical significance. From day 4 to 14 crypt depth of infected mice was comparable to controls.

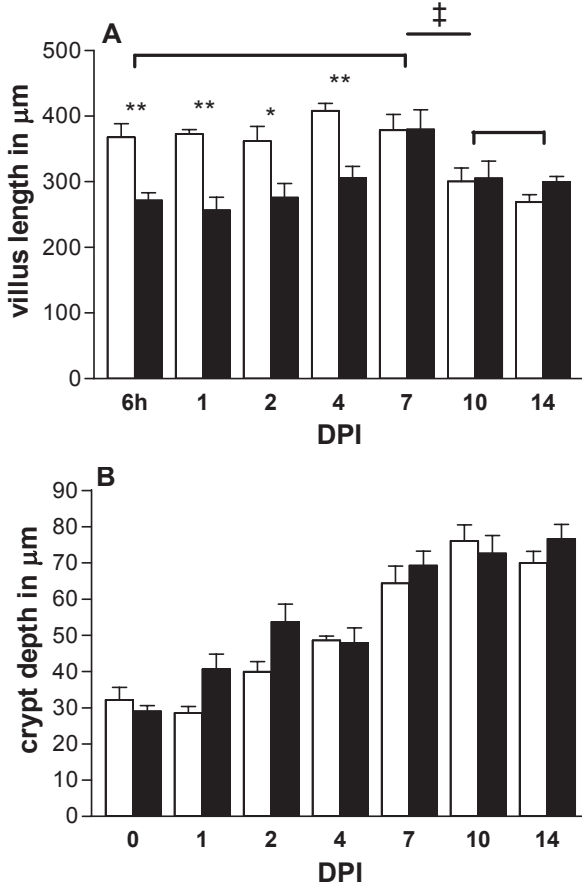


Figure 5. Villus length (A) and crypt depth (B) in the jejunum of control mice (open bars) and during rotavirus infection (solid bars). Data from 3-5 animals at each time point are expressed as mean villus height and mean crypt depth (µm) ± SEM. *P<0.05, **P<0.01 using Student's *t*-test. Controls at 6 hpi to 7 dpi were compared to controls at 10 and 14 dpi, and analyzed by ANOVA followed by an unpaired *t*-test, ‡P<0.05.

Apoptosis and proliferation of intestinal epithelial cells are increased during rotavirus infection

To analyze jejunal epithelial proliferation and apoptosis during the course of rotavirus infection, proliferating cells were identified by expression of PCNA and apoptotic cells were identified by expression of cleaved caspase-3. In control animals, proliferating cells were almost exclusively observed in the crypt compartment (Figure 6A, arrow). However in infected animals at 1 and 2 dpi, proliferating cells were abundantly covering the crypt epithelium and reached up to two-third of the length of the villi (Figure 6B, arrows). The number of proliferating cells were strongly increased at 1 (153%) and 2 (206%) dpi, but were returned to control numbers from 4 to 14 dpi (Figure 6E). Note that the number of proliferating cells in control animals is gradually declining during development in the second week after birth. Apoptotic cells were rarely observed in control animals (Figure 6C). During infection, apoptotic cells were particularly observed in the upper parts of the villi (Figure 6D, arrow). Quantitative analysis of the number of cleaved caspase-3 positive cells showed that

apoptosis follows the course of infection (Figure 6F). At 1 and 4 dpi, there was a strong increase in the number of apoptotic cells. At 2 dpi, the number of apoptotic cells was not increased. Apoptosis was still slightly but significantly increased at 7 dpi, but thereafter at 10 and 14 dpi normalized.

Rotavirus infection alters epithelial cell migration kinetics in mouse small intestine

As rotavirus infection caused increased epithelial proliferation as well as apoptosis, we wanted to investigate the effects of infection on intestinal epithelial cell migration kinetics. Cell kinetics were analyzed through detection of incorporated BrdU that was injected at $t=0$ just before inoculation. The position of the foremost- as well as least progressed BrdU-labeled cells in a crypt-villus unit in the ileum was expressed as the number of cell-positions from the crypt-villus boundary. There was no significant difference in the number of cells that had incorporated BrdU during the first 6 h after inoculation (data not shown). At 6 hpi, BrdU-positive cells in control- and infected animals were restricted to the crypt compartment (Figure 7). At 1 dpi, there was no difference between the position of BrdU-labeled cells in infected and control animals. From 2 to 7 dpi, BrdU-positive cells in infected animals migrated significantly faster up the villi than in respective controls. During infection, also the number of cell positions between the foremost cells and least advanced cells was increased at 2 dpi. In control animals, BrdU-labeled cells were observed until 7 dpi. However in infected animals, most of the BrdU-labeled cells were lost from the tips of the villi already at 4 dpi.

Analysis of enterocyte gene expression in mouse small intestine during infection

In order to examine enterocyte gene expression during rotavirus infection, we analyzed serial small intestinal sections (jejunum) by *in situ* hybridization. As markers for enterocyte gene expression we used lactase (the brush border protein that hydrolyzes the milk-sugar lactose), SGLT1 (the brush border protein involved in the uptake of sodium, glucose and water), and L-FABP (a cytoplasmic protein involved in fatty acid metabolism). L-FABP- (Figure 8C), SGLT1- (Figure 8G), and beta-actin mRNA (data not shown) expression was detected in all enterocytes along the entire small intestinal villi of control animals. At 1 dpi, there was massive expression of NSP4 mRNA in the upper halves of the intestinal villi (Figure 8A). In cells and areas on the villi that were NSP4 positive, there was an apparent downregulation of enterocyte (L-FABP and SGLT1) and housekeeping (beta-actin) mRNA expression (Figure 8B, F, and E). At subsequent days after inoculation this phenomenon was also observed, although not as prominent as during the first replication peak at 1 dpi. During infection, lactase mRNA expression followed the same pattern as SGLT1 and L-FABP mRNA expression (data not shown).

To examine whether enterocyte-specific gene expression in the jejunum was also quantitatively affected during infection, expression of lactase-, L-FABP-, and SGLT1 mRNA was assessed by RNA spot blotting. Since the expression of the housekeeping gene beta-actin was also affected by rotavirus infection, the amount of RNA spotted was corrected for GAPDH mRNA- and 28S rRNA expression. Only data from spot blots normalized to GAPDH mRNA are shown, since spot blots normalized to 28S rRNA gave very similar results. Already at 6 hpi all three markers were downregulated (Figure 9). During massive viral replication at 1 dpi, mRNA levels were decreased to 15-22% of control levels. The mRNA levels were significantly decreased until 7 dpi (L-FABP and SGLT1) and 10 dpi (lactase). Notice that at 4 dpi, when there was a second peak of viral replication, no second

decline of marker mRNA levels was observed. This suggests that mRNA levels in the remaining cells on the villi were increased at this time-point.

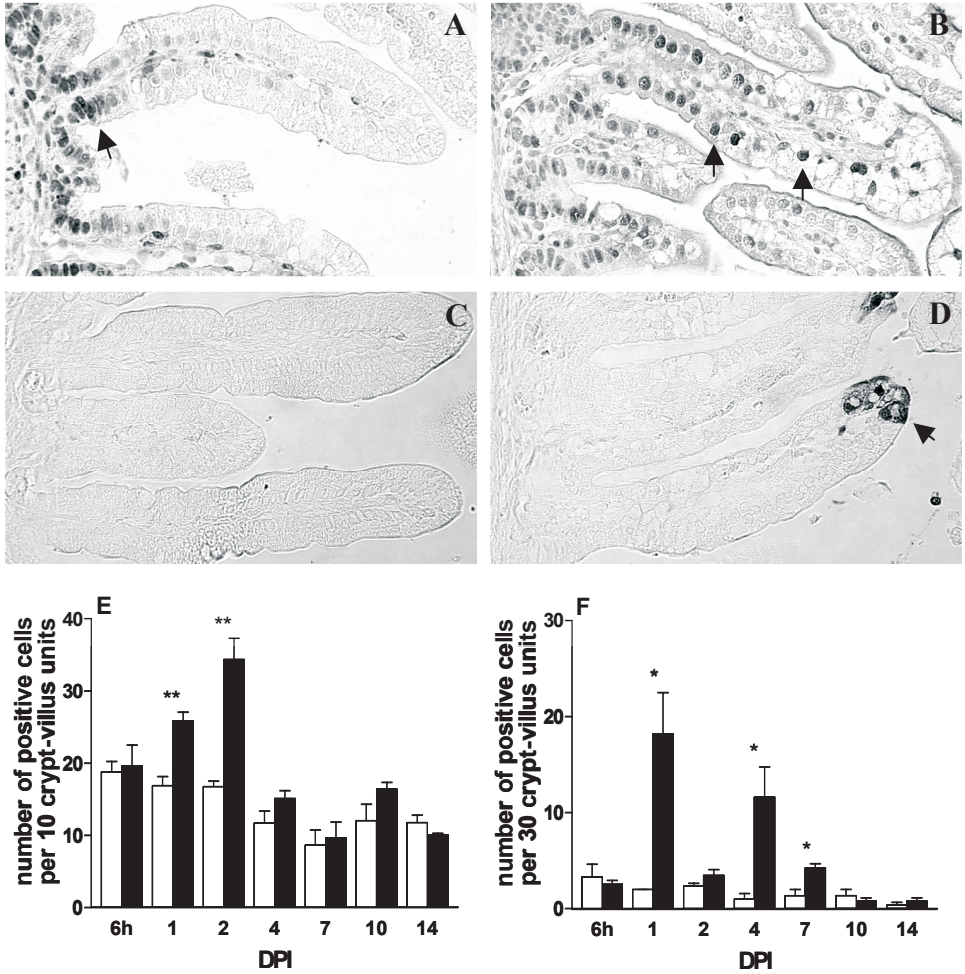


Figure 6. Proliferation and apoptosis in jejunum during rotavirus infection as analyzed by staining of PCNA and cleaved caspase-3 respectively. In control animals, proliferating cells were exclusively found in the crypt compartment (A, arrow). In infected animals at 1 dpi, proliferating cells were observed up to two-third of the length of the villi (B, arrows). The number of proliferating cells in infected animals were strongly increased at 1 and 2 dpi (solid bars), and were comparable to control numbers (open bars) between 4 to 14 dpi (E). Apoptotic cells were rarely observed in control animals (C and F open bars). During infection at 1 dpi however, apoptotic cells were abundantly observed at the villus tips (D, arrow) and the number of apoptotic cells were significantly increased at 1, 4, and 7 dpi (F solid bars). *P<0.05, **P<0.01 using Student's *t*-test. Original magnification, X 250.

In addition to the mRNA expression, SGLT1 protein expression was examined by immunohistochemistry. In the jejunum of control animals, SGLT1 membrane protein was expressed in the enterocyte brush border (Figure 8D). During rotavirus infection at 1 dpi, SGLT1 expression was almost completely lost from the brush border of enterocytes along the villi (Figure 8H). Expression of SGLT1 protein was largely recovered by 4 dpi and was

completely recovered by 7 dpi (data not shown). Lactase and LFABP protein expression was also affected by rotavirus infection, and expression largely followed the pattern seen for SGLT1 (data not shown).

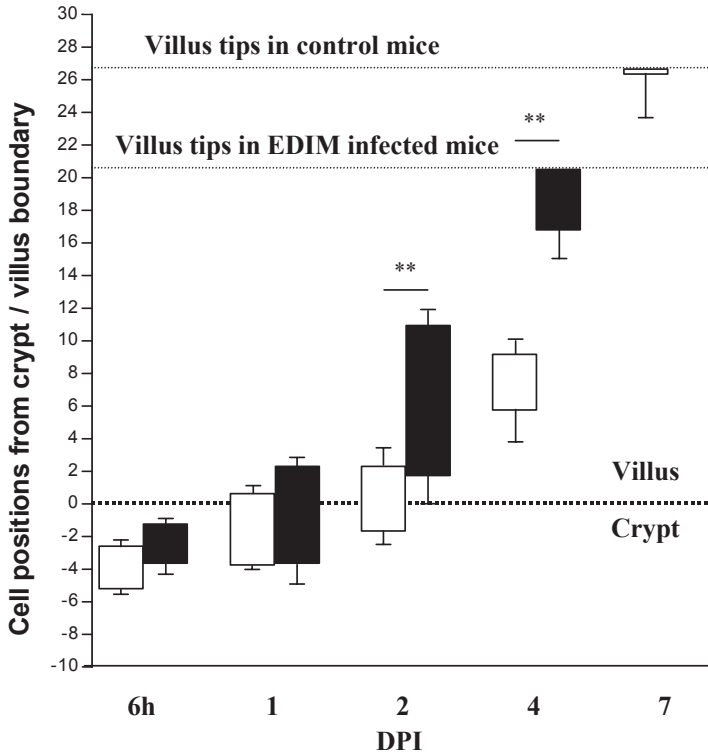


Figure 7. Cell migration kinetics in the mouse small intestine (ileum) during rotavirus infection. Just before inoculation, mice were injected with BrdU. The position of the foremost - as well as least progressed BrdU-labeled cells in each crypt-villus unit are expressed as the number of cell-positions from the crypt-villus boundary (shown as a dotted line at 0 in the graph). At 6 hpi, BrdU-positive cells in control- (open bars) and infected animals (closed bars) were restricted to the crypt compartment. From 2 to 7 dpi, BrdU-positive cells in infected animals migrated significantly higher up the villi than in respective controls (* $P < 0.05$, ** $P < 0.01$). The number of cell positions between the foremost- and least-advanced cells was also increased at 2 dpi (‡ $P < 0.05$). However, in infected animals, BrdU-labeled cells were predominantly lost from the villi at 4 dpi.

Discussion

In this study, we infected suckling mice with a homologous rotavirus strain. All phenomena that are presented in this paper were at least observed in 2 independent experiments.

Mice developed diarrhea over a period of 5 days, starting at 1 day after inoculation. The onset of diarrhea coincided with the onset of viral shedding, however rotavirus antigen was shed for a total period of maximally 10 days. This means that after 5 dpi to 10 dpi, virus antigen was shed, while no diarrheal illness occurred. Viral antigen in small intestinal tissue

however, was only observed until 4 dpi, indicating that diarrhea correlated with the presence of replicating virus in the intestinal tissue.

Two peaks of viral replication in small intestinal tissue were observed at 1 and 4 dpi. The occurrence of two antigen peaks during homologous (murine) rotavirus infection is in agreement with electron microscopic studies in infant mice (306, 402). The second peak of viral replication at 4 dpi is most likely caused by infection of newly formed cells, since we show that most BrdU-labeled cells, present during inoculation, were lost within 4 days.

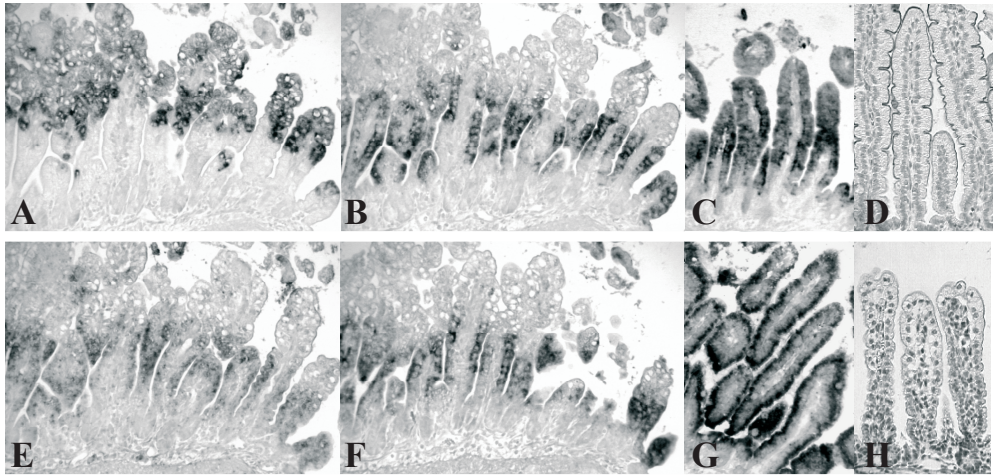


Figure 8. Histological analysis of enterocyte gene expression during rotavirus infection. NSP4 (A), L-FABP (B), beta-actin (E), and SGLT1 (F) mRNA expression in serial small intestinal (jejunum) sections during rotavirus infection as examined by *in situ* hybridization (at 1 dpi). During massive expression of NSP4 in enterocytes in the upper halves of the villi at 1 dpi (A), enterocyte specific L-FABP, beta-actin and SGLT1 mRNA expression was downregulated in these cells (B, E, and F). In control animals, L-FABP mRNA (C), SGLT1 mRNA (G), and beta-actin mRNA (data not shown) were expressed in all enterocytes along the entire villi. SGLT1 protein was observed in the brush border of control animals (D). At 1 dpi, expression of SGLT1 protein was almost completely lost in infected animals (H). Original magnification: A, B, C, E, F, and G, X 150; D and H, X 175.

During both peaks of infection, levels of NSP4 mRNA and structural rotavirus proteins were higher in the ileum than in the jejunum. Although some animals did not shed rotavirus at 1 dpi, replicating virus was observed in the duodenum and jejunum, but not ileum, of these animals (data not shown). These findings suggest that infection begins in the proximal small intestine, but eventually is more severe in the distal small intestine at later stages during infection.

With respect to the exact timing of the induction of damage and viral replication, it is important to note that it appears that the initial load of viral inoculum is of particular importance. From previous experiments, we observed that when mice were inoculated with less ffu (2×10^3 or 5×10^2), the development of histological damage and the first peak of viral replication were delayed by one day compared to mice inoculated with the high dose of 2×10^4 ffu. Interestingly, the mice inoculated with the lower virus load eventually developed peaks of infection that were comparable with that of the higher load (unpublished data).

During infection at 1-7 dpi, large vacuoles were observed in enterocytes lining most of the surface of the villi in the small intestine. The vacuoles seemed largely devoid of rotavirus

antigen as determined by immunohistochemistry. This observation is in agreement with other studies in mice and rats (157, 306, 341), although rotavirus particles were observed by electron microscopy to be associated with intracytoplasmic vacuoles in canine rotavirus infected gnotobiotic dogs (195). At 1 and 2 dpi, many vacuolated cells were found lower on the villi than infected cells. Moreover, vacuolization was observed in many cells in which no NSP4 or structural proteins were detected, and cells that were strongly positive for rotavirus antigen seemed histologically undamaged. In agreement with other studies, these findings suggest that there is no direct correlation between the occurrence and severity of vacuolization of the enterocytes and the presence of virus (77, 82, 306). The vacuoles do not stain for acid or neutral carbohydrates with alcian blue or periodic acid-Schiff (PAS), respectively. Others found that the vacuoles in infected neonatal rats also did not contain neutral lipids (77). Therefore, the origin and nature of these vacuoles remains obscure.

It has been suggested that vacuolization is a late state of infection preceding extrusion (82). However, the fact that the vacuolated cells were found lower on the villi than virus-infected cells at various time-points during infection, suggests that vacuolization is not directly caused by infection of these cells. Therefore, vacuolization might be caused by a systemic mechanism or by a secreted (viral) factor. One such viral factor could be the non-structural protein NSP4. After being secreted from infected cells, NSP4 is thought to mediate cell signaling by increasing intracellular calcium levels leading to chloride secretion in uninfected cells (16).

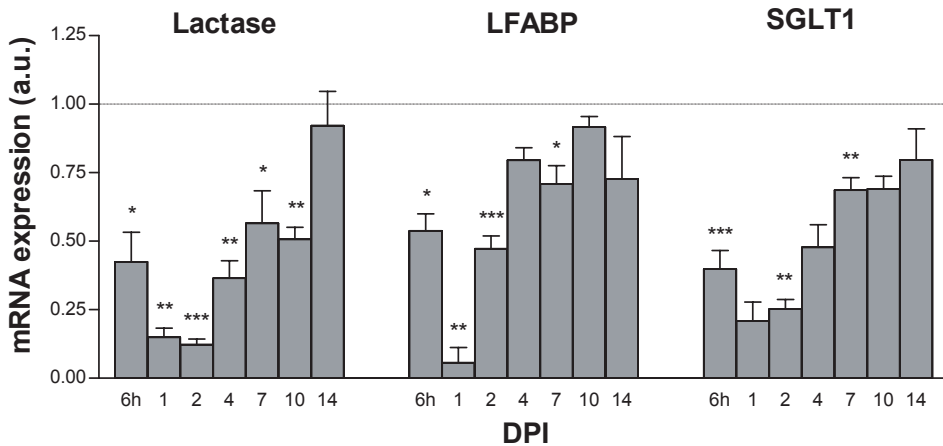


Figure 9. Quantitative analyses of enterocyte mRNA expression during rotavirus infection. Control values per day were arbitrarily set at a relative expression of 1 and are represented as a dotted line. At 6 hpi enterocyte mRNA levels in the jejunum of infected animals were decreased compared to controls (dotted line). mRNA levels remained significantly decreased until 7 dpi (L-FABP and SGLT1) and 10 dpi (lactase). The amount of RNA spotted was corrected for GAPDH mRNA expression. * $P < 0.05$, ** $P < 0.01$, *** $P < 0.001$ vs. control using Student's *t*-test. a.u., arbitrary units.

In addition to the morphological damage, we analyzed the changes in epithelial homeostasis during rotavirus infection by studying epithelial proliferation, migration and apoptosis. In our study, the rate of proliferation during infection was strongly increased at 1 and 2 dpi as

indicated by increased numbers of PCNA-positive cells. Indications for increased proliferation rates in mice during rotavirus infection, also come from studies showing that the activity of thymidine kinase is increased (84, 99, 306). Epithelial migration was also drastically increased as indicated by the BrdU-labeling study. Overall, this led to an increase in epithelial cell turnover from 7 days in control mice to 4 days in infected mice.

To our knowledge, this is the first study to describe increased apoptosis during rotavirus infection *in vivo*. Apoptotic cells were mainly observed in the upper parts of the villi where most infected cells were observed. The number of apoptotic cells followed the course of infection. These findings indicate that rotavirus is directly causing the increased apoptosis of villus enterocytes. In HT-29 human adenocarcinoma cells, SA11 rotavirus infection was also found to trigger apoptosis, and the authors stated that the specific histological features of rotavirus infected enterocytes may be a consequence of virus-induced apoptosis (409). However, in our study most damaged and vacuolated cells were not caspase-3-positive and also were found lower on the villi than infected cells. Moreover, many apoptotic cells were not morphologically damaged upon histological examination. This suggests that vacuolization is not a direct consequence of apoptosis, but rather precedes it.

Rotavirus infection in children can result in the occurrence of a flat mucosa with total villus atrophy (33), and the most severe form of villus atrophy is observed in piglets, where small intestinal villi can be completely eroded (389). Villus atrophy in mice is mild when compared to observations in other mammalian species (33, 59, 236, 389, 399, 402). Villus atrophy in our model occurred as early as 6 hpi, before the onset of massive viral replication. At this stage of infection, no obvious histological damage or increased apoptosis was observed. The shortening of the villi is therefore possibly caused by an effect of infection on the smooth muscle cells or the subepithelial network of myofibroblasts within the villi. Speculatively this rapid villus contraction involves the enteric nervous system (ENS).

On the subsequent days, villus atrophy is likely attributed to the strong increase in apoptosis. One of the most plausible explanations for the relatively minor villus atrophy in mice is our observation of a very strong increase in the number of proliferating cells and cellular migration that potentially counteracts the increased number of shed and apoptotic cells. The pathogenesis of this enhanced proliferation is unknown, but a negative feedback from mature villus epithelium has been postulated (210, 351, 378). The shedding of differentiated enterocytes may result in a deficient negative feedback of mature enterocytes, resulting in enhanced proliferation. In our model, the small intestinal epithelium likely responds to the increased loss of epithelial cells by enhancing the replacement of these cells through induction of proliferation in the crypts, as well as at the base of the villi. As has been proposed by others, we think that the basal region of the villi might constructively contribute to the process of enhanced renewal of villus cells (306, 353).

We studied the expression of enterocyte-specific Lactase, LFABP and SGLT1 mRNAs as markers for the absorptive and metabolic functions of the enterocytes. Lactase is essential for the hydrolysis of lactose (434), the most important sugar in milk. LFABP is a protein that is involved in the uptake and intra-cellular transport of fatty acids (179) and SGLT1 is a glucose co-transporter involved in the uptake of glucose, salts and water (104). Already after 6 hours, we observed reduced levels of these enterocyte specific mRNAs. The downregulation of these genes *in vivo* persisted till 10 dpi. The most prominent effect of viral infection was observed at 1 dpi. At this time-point there was a very distinct downregulation of enterocyte gene expression in cells that harbored replicating virus. Enterocyte-specific

protein levels were also reduced at days 1 and 2 dpi, following the reduced levels of the cognate mRNAs. This is in agreement with an earlier study where mice were infected with a homologous (murine) rotavirus, lactase and alkaline phosphatase activities were reduced, whereas sucrase-isomaltase activity showed a precocious maturation (84). Katyal and co-workers found that there was a reduced amino acid (leucine) uptake in the jejunum and ileum of mice infected with a homologous rotavirus (209). In rabbits, rotavirus infection was shown to impair intestinal brush-border membrane Na (+)-solute co-transport activities of SGLT1. This effect was found to be mediated by a direct inhibiting effect of NSP4 on SGLT1 and not by means of reduced levels of SGLT1 in brush border vesicles (162, 163). Our data however, show that these observed reduction of Na (+)-solute co-transport activities, at least in mice, are probably not only caused by a direct inhibitory effect of rotavirus proteins (NSP4) on SGLT1 activity, but also by reduced levels of SGLT1 transcripts and SGLT1 protein in the brush border of enterocytes. So from our study, it seems that a reduced amount the transporter (SGLT1) in the brush border membrane of enterocytes might be one of the mechanisms underlying the reduced Na⁺ solute transport activity observed during rotavirus infection in rabbits (162).

Together these findings suggest that the enterocyte absorptive- and metabolic capacity are affected, which might contribute to pathogenesis of rotavirus infection.

Many viruses (HIV, influenza, poliovirus, adenovirus, and herpes simplex) are known to interfere with the host cell translational machinery, and shut off gene expression in a variety of ways (35, 223, 244, 258, 463). The rotavirus non-structural protein NSP3 is capable of inducing the shut off of host cell translation during *in vitro* rotavirus infection, by interacting with the eukaryotic initiation factor eIF4GI, which is part of the eIF4F holoenzyme complex (326). Since eIF4F modulates mRNA stability (343), the shut off of enterocyte gene expression during rotavirus infection we observed here *in vivo*, might also be mediated by NSP3. Furthermore, we hypothesize that NSP3 could mediate this shut off by removing eIF4F from cellular mRNA resulting in decreased stability of these mRNAs and subsequently a decreased translation. However this shut off might not be absolute, since several *in vitro* studies indicate an upregulation of specific genes in infected cells (96, 464).

Based on the presented data we suggest that the hypothesis of Hamilton and colleagues (164, 212, 350) to explain one of the mechanisms for rotavirus induced diarrhea, that is decreased solute absorption and water reabsorption in the intestine through substitution of mature enterocytes by non-transporting crypt cells needs further refinement. In relation to the inhibitory effect of rotavirus on the absorptive function of the small intestinal epithelium, we propose that in addition to the direct inhibition of Na (+)-solute co-transport activities through NSP4, at least 3 sequential processes are implicated in this mechanism of rotavirus induced diarrhea. (i) Early on during infection, enterocyte specific gene expression is directly downregulated in infected cells at the mRNA level. This results in reduction of mature enterocyte specific protein levels and thus in a functional less differentiated status relatively early during infection while there is still little histological damage. (ii) Mature enterocytes are lost from the villi through apoptosis and shedding. (iii) These mature enterocytes are replaced by immature and actively dividing cells.

In summary, we report that during a homologous rotavirus infection in mice, villus atrophy and an increase in crypt depth are accompanied by highly induced epithelial apoptotic- and proliferation rates. Epithelial cell turnover was increased from 7 days in controls to 4 days in infected mice, indicating that the second peak of viral replication was most likely caused by infection of newly synthesized epithelial cells. Rotavirus infection caused a downregulation

of enterocyte specific gene expression *in vivo* in infected cells. This suggests that rotavirus infection causes a shut-off of endogenous gene expression in favor of viral gene expression. The shut-off of enterocyte specific gene expression, together with the loss of mature enterocytes through apoptosis and the replacement of these cells by less differentiated dividing cells, likely lead to a defective absorptive function of the intestinal epithelium, which contributes to rotavirus pathogenesis.

Acknowledgements

The authors would like to thank Dr. R. Ward for donating the EDIM mouse rotavirus strain. We thank Dr A. Quaroni and Dr. B.Hirayama for kindly providing the anti-rat lactase antibody, and the anti-rabbit SGLT1 antibody, respectively. We are grateful to Dr J. Gordon for providing both the anti-rat L-FABP antibody and the rat L-FABP probe, Dr C.F. Burant for providing the rat SGLT1 probe, and Dr S.D. Krasinski for donating the beta-actin probe. The authors thank G. van Amerongen, M. van der Sluis and D.J.P.M. van Nispen for excellent technical assistance. This work was supported by grants from the Sophia Foundation for Medical Research and the Netherlands Digestive Diseases Foundation.

Chapter 3

Homeostasis and function of goblet cells during rotavirus infection in mice

Jos A. Boshuizen, Johan H.J. Reimerink, Anita M. Korteland-van Male, Vanessa J.J. van Ham, Janneke Bouma, Gerrit J. Gerwig, Marion P.G. Koopmans, Hans A. Büller, Jan Dekker, Alexandra W.C. Einerhand

Virology 2005: *in press*

Abstract

Rotaviruses are the leading cause of severe viral gastroenteritis in young children. To gain insight in goblet cell homeostasis and intestinal mucin expression during rotavirus infection, 6-day-old mice were inoculated with murine rotavirus. To determine epithelial cell migration, mice were injected with BrdU just before inoculation. Small intestines were isolated at different days post infection (dpi) and evaluated for rotavirus and goblet cell specific gene-expression. Small intestinal mucins of control and infected animals at 1, 2, and 4 dpi were isolated and tested for their capability to neutralize rotavirus infection *in vitro*. After inoculation, two peaks of viral replication were observed at 1 and 4 dpi. During infection, the number of goblet cells in infected mice was decreased in duodenum and jejunum, but was unaffected in the ileum. Goblet cells in infected animals accumulated at the tips of the villi. Muc2 mRNA levels were increased during the peak of viral replication at 1 dpi, whereas at other time-points Muc2 and Tff3 mRNA levels were maintained at control levels. Muc2 protein levels in the tissue were also maintained, however Tff3 protein levels were strongly decreased. The number of goblet cells containing sulfated mucins was reduced during the two peaks of infection. Mucins isolated at 1 and 2 dpi from control and infected mice efficiently neutralized rotavirus infection *in vitro*. Moreover, mucins isolated from infected mice at 4 dpi were more potent in inhibiting rotavirus infection than mucins from control mice at 4 dpi. In conclusion these data show that during rotavirus infection goblet cells, in contrast to enterocytes, are relatively spared from apoptosis especially in the ileum. Goblet cell-specific Muc2 expression is increased and mucin structure is modified in the course of infection. This suggests that goblet cells and mucins play a role in the active defense against rotavirus infection, and that age-dependent differences in mucin quantities, composition and/or structure alter the anti-viral capabilities of small intestinal mucins.

Introduction

Rotavirus is the major infectious agent in the development of gastroenteritis, malnutrition and diarrhea in young children and animals (122, 204). In developed countries mortality rates are low and illness is usually self-limiting (429). In developing countries however, each year about 440.000 children of under 5 years of age die due to infection with rotavirus (313). Mortality is essentially related to dehydrating diarrhea. So far, no vaccine is available. Therefore it is important to develop alternative therapies, based on a better knowledge of rotavirus pathogenesis.

Rotavirus binding and entry of host cells is thought to be a multifactorial process (240). Sialic acid-dependent rotavirus strains use sialic acid (SA) residues on the surface of target cells for initial attachment (107, 356, 410). The initial cell surface receptors containing sialic acid may be either glycolipids or glycoproteins (107, 133, 356, 410, 472). For SA-dependent strains, these receptors are thought to play a key role in cellular entry, since SA-independent strains can infect cells through either the apical or basolateral membrane, while SA-dependent strains infect cells only through the apical membrane (78). Most animal and human rotaviruses nevertheless, are SA-independent (79). It is however important to realize that apparently most rotavirus strains, SA-dependent as well as SA-independent, indeed bind to SA, but rather have different requirements regarding sialic acids on the host cell (23, 196).

For glycolipids it was found that the position of SA residues influenced the binding capacity of the different rotavirus strains. SA-dependent rotavirus strains bind to terminal SA residues in glycolipids, while SA-independent rotavirus strains bind glycolipids with internal sialic acids (which are resistant to neuraminidase treatment) (107). The fact that many glycoproteins can inhibit rotavirus infection *in vivo* and *in vitro* is possibly based on the ability of rotavirus to bind to SA residues, since treatment with neuraminidase abolishes the inhibitory effect of these agents (72, 289, 323, 459, 472). Some studies however indicate that removal of sialic acid from glycoproteins does not significantly alter the inhibitory properties of these compounds (471).

Previous studies have shown that rotavirus infection has a profound effect on small intestinal epithelial homeostasis. It was found that rotavirus induced apoptosis, mild villus atrophy, increased epithelial cell turnover and hampered enterocyte gene expression (43, 84, 209, 306, 389, 402). Rather than concentrating on enterocyte cell function, we wanted to focus our attention on the function of goblet cells during rotavirus infection and the expression of specific gene products that are secreted by these cells. Goblet cells are characteristic for the intestinal epithelium and are known to secrete molecules such as mucins and trefoil factor family peptides that serve protective and healing functions in the gut, respectively (419, 438). The secretory mucin Muc2, which is the most important structural component of the intestinal mucus layer, is exclusively and abundantly expressed by goblet cells in the small intestine (426, 427, 438, 440). After synthesis, Muc2 is secreted into the lumen and forms a protective mucus gel layer that acts as a selective barrier to protect the epithelium from mechanical stress, noxious agents, viruses, and other pathogens (116, 137, 407, 426, 438, 440). Muc2 and other mucins contain many O-linked SA moieties and are important inhibitors of rotavirus infection (72, 289, 323, 440, 459, 471, 472). It was suggested that intestinal mucins may represent a barrier to certain rotaviruses by neutralizing rotavirus infection through direct interaction with the virus, whilst hindering virus-to-cell attachment (72, 472). Interestingly, it was found that mucins isolated from suckling mice neutralize rotavirus more effectively than adult mucins (72). Besides Muc2, the trefoil factor family peptide 3 (Tff3) is another secretory protein synthesized by goblet cells. Tff3 is a small bioactive peptide that is involved in epithelial repair (255, 419). Because Tff3 acts as a motogen, i.e., promotes cell migration without promoting cell division, it stimulates epithelial restitution and thus epithelial repair (460). Therefore, Tff3 could also be involved in both protection against rotavirus infection as well as epithelial restitution after rotavirus-induced injury.

In this paper we examined the timing and extent of rotavirus replication in the murine small intestine, and related this to the number of goblet cells and the production of the goblet cell-specific markers Muc2 and Tff3. Moreover, we performed qualitative analyses of the structural changes of mucins through histochemical staining, and we assessed the ability of isolated intestinal mucins to inhibit rotavirus infection *in vitro*.

Materials and Methods

Animals

Pregnant dams were obtained from Harlan (Zoetermeer, The Netherlands). Dams, either with their control or inoculated litters, were housed in micro-isolator cages under negative pressure in a specified pathogen-free environment. Rodent, chicken protein-free, chow

(9605/9608; Harlan Teklad TRM (A)) and deionized water were autoclaved and provided *ad libitum* until the end of the experiment. All dams were rotavirus antibody negative as measured by enzyme-linked immunosorbent assay (ELISA, as described below). All the experiments were performed with the approval of the Animal Studies Ethics Committee of the National Institute of Public Health and the Environment.

Virus inoculations and subsequent animal-handling procedures

The EDIM (Epizootic Diarrhea of Infant Mice) mouse rotavirus strain was obtained from Dr. R. Ward, Children's Hospital Research Foundation, Cincinnati, USA (266). This strain is an unpassaged virus isolated directly from the stools of ill mice. Six days-old BALB/c mice were inoculated intra-gastrically with 2×10^4 focus forming units (ffu) of the EDIM rotavirus strain, as described previously (43). To analyze epithelial proliferative kinetics, 30 mg/kg bodyweight 5-bromo-2'-deoxyuridine (BrdU; Sigma, St Louis, USA) was injected intraperitoneally 5 minutes before inoculation. Control mice were mock infected through inoculation with PBS. After 6 h and at days 1, 2, 4, 7, and 14, three infected and three control mice were sacrificed per time point. The infection of mice and all subsequently experiments and data analysis, except the experiment measuring the mucin inhibitory capacities, were performed twice independently. The results of the independent experiments were comparable in all aspects. Segments of duodenum (i.e. proximal 2 cm of the small intestine), jejunum (i.e. 2 cm intestine taken from the anatomic middle of the small intestine) and ileum (i.e. distal 2 cm of the small intestine) were rinsed in PBS and fixed for 4 h in 4% (wt/vol.) paraformaldehyde (Merck, Darmstadt, Germany) dissolved in PBS. The segments were subsequently dehydrated through a graded series of ethanol and xylene (Merck), and embedded in Paraplast Plus (Sherwood Medical, Den Bosch, The Netherlands) as previously described (43, 446). In addition, adjacent segments of the jejunum and ileum were dissected and snap frozen in liquid nitrogen and stored at -80°C for RNA and protein isolation.

Histology

Paraffin-embedded tissues were sectioned (5 μm), deparaffinized with xylene (Merck) and rehydrated in graded ethanol solutions as previously described (43, 346). Histochemical staining was performed by using: Alcian blue (AB) at pH 2.5 followed by periodic acid-Schiff's reagent (PAS), or high iron diamine (HID) followed by AB at pH 2.5 as previously described (252). The numbers of goblet cells per villus were counted after AB-PAS staining in 20 well-oriented crypt-villus units of the duodenum, jejunum, and ileum, respectively, per animal per time point until day 7 dpi. The numbers of HID positive goblet cells were counted in 10-well-oriented crypt-villus units per animal in the ileum per animal per time point until day 7 dpi.

Immunohistochemistry

Deparaffinized and rehydrated sections were incubated overnight at 4°C using the primary mouse antibody anti-BrdU (1:250; Boehringer, Mannheim GmbH, Mannheim, Germany), caspase-3 (1:500; Cell Signaling Technology, Beverly, USA), or a rabbit hyperimmune serum raised against SA11 rotavirus particles (1:1500; (43)). Immunohistochemistry was carried out as described previously (43, 346). Sections that had been incubated with the anti-BrdU antibody were washed with PBS and subsequently treated with AB at pH 2.5.

***In situ* hybridization and probe preparation**

Non-radioactive *in situ* hybridization was performed using the method as previously described (233, 346). Digoxigenin (DIG)-11-UTP labeled RNA probes were prepared according to the manufacturer's protocol (Boehringer) using T3, T7 or SP6 RNA polymerase. The following probes were used: a 244-bp murine Muc2 probe (440) and a 901 bp VP4 fragment (EDIM strain) ligated in pBluescript (see below). Transcripts longer than 450 bp were hydrolyzed in 80 mM NaHCO₃ and 120 mM Na₂CO₃, pH 10.2 to obtain probes of various lengths \leq 450 bp (91).

Quantitation of mRNA

Total RNA was isolated from frozen small intestinal segments, using Trizol reagent (Gibco-BRL, Gaithersburg MD, USA) following the manufacturer's protocol. Integrity of the RNA was assessed by visual analysis of the 28S and 18S ribosomal RNAs after electrophoresis and staining with ethidium bromide. Subsequently, 1 micro-g of total RNA was dot-blotted on Hybond-N⁺ (Amersham, Bucks, England) using a vacuum-operated manifold (BioDot, BioRad, Hercules, CA). All blots were hybridized using specific ³²P-labeled cDNA probes as described previously (446). To correct for the amount of RNA that was spotted, hybridized signals were standardized by glyceraldehyde-3-phosphate dehydrogenase (GAPDH) mRNA levels using a 1.4 kb human GAPDH probe (43, 446). Hybridization signals were measured through autoradiography using a PhosphorImager and ImageQuant software (Molecular Imaging, Sunnyvale CA, USA). The following probes were used: The pBluescript cDNA probes that were used were the 244-bp murine Muc2 probe (440), a 438-bp rat Tff3 probe (408), or a 900 bp VP4 probe. For construction of the VP4 probe, RT-PCR was performed on RNA isolated from EDIM infected neonatal mice. VP4 was cloned using the primers TATACCATGGCTTCACTCATTTATAGAC and TTGGTAGTTCGCTGGTTTGAA, based on the EDIM VP4 coding sequence accession number AF039219 (GenBank). PCR fragments were TA-cloned into the PCR 2.1 vector (Invitrogen, Breda, The Netherlands) and sequenced.

Quantitation of rotavirus protein

Proteins were isolated from frozen segments by homogenization of the tissue in 500 μ l (Tris-) homogenization buffer containing Triton X-100 (BDH, Poole, England), 1% SDS and various protease inhibitors as previously described. (43, 345). Protein concentration was measured using a bicinchoninic acid (BCA) protein assay reagent kit (Pierce, Rockford, IL, USA). Bovine serum albumin was used as a standard. To quantify rotavirus structural protein contents, protein homogenates were dot-blotted on nitrocellulose (Nitran; Schleier & Schuell, Dassel, Germany). The blots were blocked for 1 h with blocking buffer (50 mM Tris-HCl, pH 7.8, 5% (wt/vol.) nonfat dry milk powder (Lyempf, Kampen, The Netherlands), 2 mM CaCl₂, 0.05% (vol./vol.) Nonidet P40 (BDH), and 0.01% (vol./vol.) antifoam (Sigma, St Louis, USA), and incubated for 18 h with anti-mouse Muc2 serum (1:500) (440), or anti-rat Tff3 serum (1:1500), a generous gift from Daniel K. Podolsky (408). After being washed in blocking buffer, the blots were incubated with ¹²⁵I-labeled protein A (specific activity 33.8 mCi/mg; Amersham) for 2 h. Bound ¹²⁵I-labeled protein A was then detected and the elicited signals were quantified using a PhosphorImager and ImageQuant software (Molecular Imaging).

Isolation of mucins

Mouse colonic mucin was isolated and prepared from mucosal scrapings, as described previously (440). Mucins from the small intestine (distal jejunum) of rotavirus-infected or control mouse neonatal pups were isolated with the following procedure. Whole tissue segments were homogenized at 4°C in 6M guanidium hydrichloride (Sigma). The mucins were reduced by addition of 100 mM dithiotreitol (Sigma) to enhance solubility. Sulfhydryde groups were carboxymethylated through addition of 250 mM iodoacetamide (Sigma) and stirring for 24 h at 4 °C. Mucins were then fractionated by gelfiltration on a sepharose column (Bio-Gel A-50m; Bio-Rad, Veenendaal, The Netherlands). Fractions were analyzed for purity and mucin content by SDS-polyacrylamide gel electrophoresis (SDS-PAGE) followed by periodic acid–Schiff (PAS) staining. Mucin containing fractions were pooled and dialyzed extensively against distilled water at 4°C. Mucin preparations were quantified as described previously by a hexose assay using orcinol (Sigma) and galactose:fuose (3:2) as standard (426).

Cell culture, rotavirus infection and immunofluorescence assay to measure the protective capacities of mucins

Human colonic adenocarcinoma Caco-2 cells (ATCC, Manassas, VA, USA) were grown and maintained in 75 cm² tissue culture flasks in DMEM (Dulbecco's Modified Eagle's Medium; Gibco BRL) with glutamax-1, pyridoxine, sodium pyruvate, and 4.5 g/l glucose, supplemented with 10% fetal calf serum (Integro, Zaandam, The Netherlands), 100 U/ml penicillin (Sigma), 100 micro-g/ml streptomycin (Sigma) and non-essential amino acids (Bio Whittaker Europe, Verviers, Belgium) at 37°C, 5% CO₂ in a humidified atmosphere. One day prior to infection, Caco-2 cells were seeded on 10 well heavy Teflon-coated microscopic slides (7mm, Nutacon, Leimuiden, The Netherlands) at 10⁴ cells/well as described previously (358). One hour prior to infection, the Caco-2 cells were rinsed 3 times in serum free DMEM and incubated together with diluted purified mucins. Meanwhile, the human rotavirus strain Wa was activated using 10 mg/ml trypsin (Sigma) at 37°C for 1 hour. Rotavirus was diluted to 2 x 10² ffu/ml (corresponding to about 100 ffu per well) in serum free DMEM containing the diluted mucins. Cells were infected with rotavirus at 37°C, 5% CO₂ in a humidified atmosphere. After 15 hours of incubation, infection was terminated using ice-cold methanol and cells were stored for 10 minutes at -20°C. The microscopic slides with the methanol-fixed infected Caco-2 cells (358) were rinsed 3 times in PBS and then incubated for 90 minutes at RT with rabbit hyperimmune serum raised against SA11 rotavirus particles (1:1600) (43, 358). Slides were then rinsed again 3 times and incubated with a secondary anti-rabbit Texas Red conjugated antibody (1:200; Jackson Immuno Research laboratories inc., West Grove, PA, USA). Slides were mounted with a solution containing Mowiol (Sigma), 2.5% DABCO (1,4-Diazabicyclo[2.2.2]octane, Sigma) and 0.5 micro-g/ml DAPI (4',6'-Diamidino-2-phenylindole Dihydrochloride:Hydrate, Sigma) (165). Fluorescence was observed using a Nikon Eclipse 800 microscope and the number of foci was determined at 200X magnification.

Statistical analysis

Statistical analysis of all data from control and infected groups was performed using Student's *t*-test for unpaired data (two-tailed). To compare three or more groups, data were analyzed by ANOVA followed by an unpaired *t*-test. Data were expressed as the mean ± SEM and *P* values of ≤ 0.05 were considered statistically significant.

Results

Kinetics of rotavirus replication in the mouse small intestine

In the present study we used 6-day-old suckling mice and inoculated them orally with 2×10^4 ffu of EDIM rotavirus. As a control, mice of the same age were PBS inoculated. As in a previous study (43), rotavirus-inoculated mice, developed diarrhea over a period of 5 days starting at 1 day post infection (dpi). Control mice did not develop diarrhea at any time-point (data not shown). As observed by immunohistochemical staining of rotavirus particles or detection of VP4 RNA by *in situ* hybridization, rotavirus replication was confined solely to the upper-villus epithelium (Figure 1A and B). To determine the kinetics of rotavirus replication in the present experiment, replicating virus in small intestinal tissue was determined by detection of VP4 RNA. In agreement with previous studies (43, 306, 402), two peaks of viral replication were observed in both the jejunum and ileum. At 6 hours post infection (hpi), very low levels of VP4 RNA were detected in each segment (Figure 1C). At 1 dpi there was a first peak in the amount of VP4 RNA. The VP4 mRNA level was low at 2 dpi, and a second peak of replication was observed at 4 dpi. Thereafter replication decreased to very low (7 dpi) and finally undetectable levels (14 dpi). As in our previous studies, the extend of virus replication in the ileum was more extensive than in the jejunum.

Number of goblet cells during rotavirus infection

We performed AB-PAS staining on intestinal tissue sections and counted the number of goblet cells per villus in duodenum, jejunum, and ileum. In control mice, the number of goblet cells per villus in the duodenum, jejunum and ileum remained constant during development in the second week after birth (i.e. 6 hpi to 7 dpi, Figure 2). We however observed a difference in goblet cell numbers during infection, when the duodenum and jejunum were compared to the ileum. During infection, the number of goblet cells in the duodenum and jejunum were significantly decreased at 1 and 2 dpi and 1, 2, and 4 dpi respectively. In contrast, in the ileum numbers of goblet cells in infected animals remained comparable to controls during infection. Thus, in the proximal parts of the small intestine there seems to be an early loss of goblet cells. In order to detect apoptotic goblet cells in the different regions of the small intestine in control and infected mice, we performed a double staining of alcian blue and the apoptotic marker (cleaved) Caspase-3. With this double staining however we never observed apoptotic goblet cells (i.e. Caspase-3 positive AB staining cells, data not shown) after screening numerous intestinal sections.

Rotavirus infection alters goblet cell survival and migration kinetics

In order to investigate the effects of rotavirus infection on goblet cell survival and migration in the small intestine, mice were injected with BrdU just before inoculation with rotavirus. Goblet cell kinetics were analyzed by combined AB staining of the goblet cells and detection of incorporated BrdU in epithelial cells. Brdu-labeled goblet cells are recognized by blue-stained granula and brown-stained nuclei. In control animals, BrdU-labeled enterocytes migrated in cohorts along the villus epithelium (Figure 3 A-D, see *Appendix*), and at 7 dpi the enterocytes had reached the villus tips. Goblet cells had a different migration pattern and remained evenly distributed in the villus epithelium as can be seen at 7 dpi (Figure 3D,

Appendix). BrdU-labeled cells in infected mice in general migrated faster up the villus than in control animals. BrdU-labeled enterocytes were already lost from the villi in infected animals at 4 dpi.

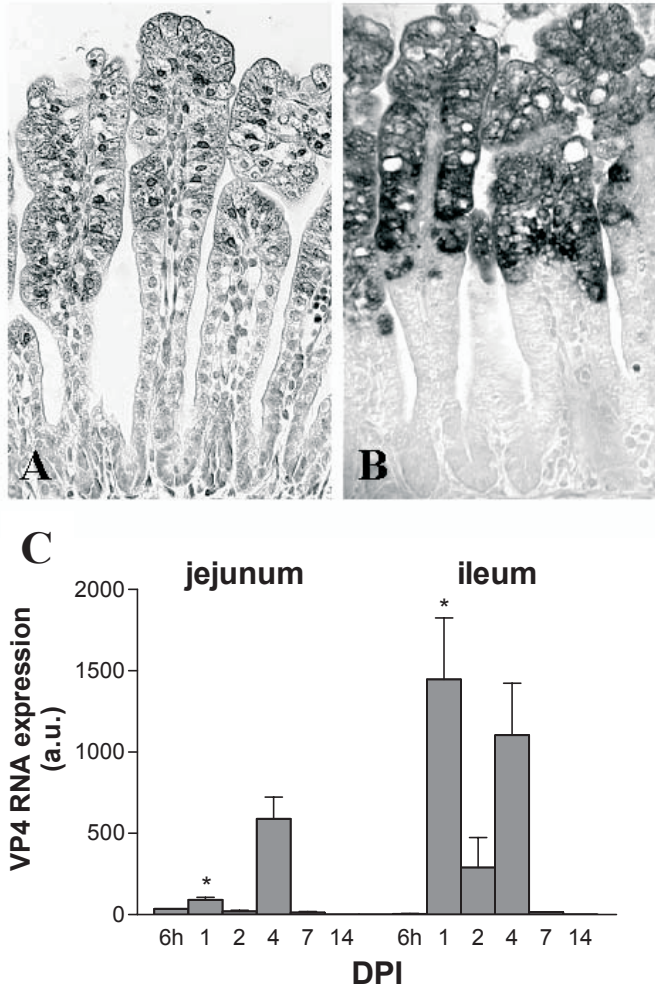


Figure 1. Rotavirus replication in the mouse small intestine. Rotavirus protein (panel A) and VP4 RNA (panel B) expression in ileum at 1 dpi were detected by immunohistochemistry and *in situ* hybridization, respectively. Virus replication was solely confined to the upper villus epithelium. Quantitative expression of VP4 RNA at several days post infection was analyzed by RNA dot-blotting (panel C). VP4 showed two peaks of expression at 1 and 4 dpi in both jejunum and ileum. At 1 dpi, the level of VP4 RNA was significantly higher in the ileum compared to the jejunum, * $P < 0.05$ (using Student's *t*-test). No VP4 RNA was detected beyond 7 dpi in any part of the small intestinal epithelium. Error bars in panel C represent \pm SEM.

In infected mice, goblet cells were not evenly distributed along the villi during infection (1, 2, and 4 dpi). Instead the goblet cells tended to accumulate at the tips of the villi (Figure 3 E-H, *Appendix*). This was most prominent in the ileum, but was also observed in the duodenum

and jejunum. At 4 dpi almost all BrdU-labeled cells, that were still present in the villus epithelium, were goblet cells, located at the tips of the villi. BrdU-labeled goblet cells were even found at the tops of the villi in infected animals at 7 dpi, when all BrdU-labeled enterocytes were lost from the epithelium (Figure 3H, *Appendix*).

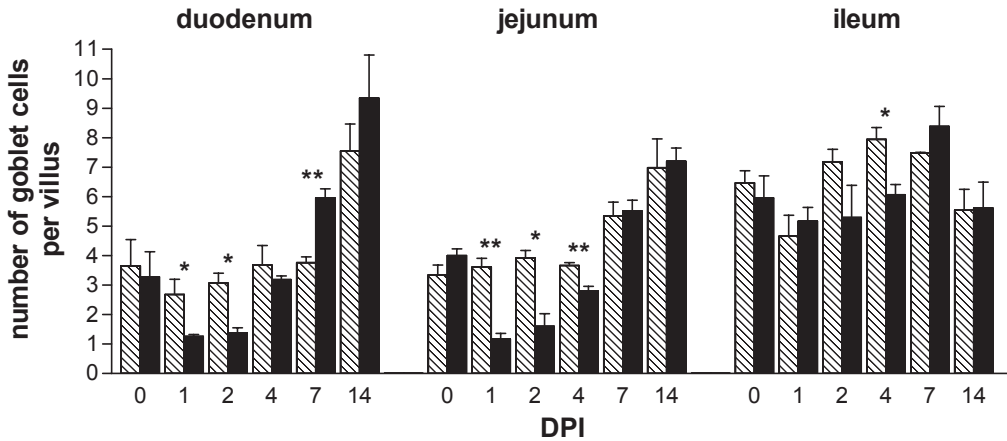


Figure 2. The numbers of goblet cells per villus in the duodenum, jejunum, and ileum of control mice (hatched bars) and during rotavirus infection (solid bars). During infection, goblet cell numbers in the duodenum and jejunum were significantly decreased at 1 and 2 dpi and 1, 2, and 4 dpi, respectively. In the ileum, goblet cell numbers in infected animals were only significantly decreased at 4 dpi. Data from 3 animals at each time-point are expressed as mean number of goblet cells per villus as analyzed after AB-PAS staining \pm SEM. Statistical significance in the infected tissue relative to the control tissue is indicated per time-point per tissue, * $P < 0.05$, ** $P < 0.01$ using Student's *t*-test.

Muc2 and Tff3 mRNA and protein levels in jejunum and ileum during rotavirus infection

Our previous findings showed that enterocyte gene expression rapidly deteriorated during rotavirus infection (43). In contrast, infection did not seem to have large effects on goblet cell gene expression. Muc2 mRNA remained detectable in goblet cells during the course of infection even at time-points of extensive damage and vacuolization of enterocytes (Figure 4). To examine whether goblet cell-specific expression was quantitatively affected during infection, Muc2 and Tff3 mRNA and protein levels in jejunum and ileum were assessed by RNA and protein spot blotting, respectively. Subsequently the expression levels were corrected for the numbers of goblet cells in the tissue, as shown in Figure 2, to obtain values for Muc2 on Tff3 expression per goblet cell. In general, there were only minor differences in the levels of Muc2 and Tff3 mRNAs in the jejunum versus the ileum. Muc2 mRNA levels were decreased in the jejunum of infected animals when compared to controls (Figure 5A). In ileum the Muc2 mRNA levels were comparable with controls, with exception of the Muc2 mRNA levels 1 dpi that were significantly increased. When these Muc2 mRNA values were corrected for the number of goblet cells in the respective tissues, it appeared that the level of Muc2 mRNA per goblet cell was similar in jejunum and ileum (Figure 5C). In both jejunum and ileum there was a peak increase in Muc2 mRNA level per goblet cell at 1 dpi. Tff3 mRNA levels in the jejunum as well as in the ileum remained largely unaltered during infection, i.e. the levels of Tff3 mRNA did not differ from the control values (Figure 5B). We normalized the Tff3 mRNA levels for the number of goblet cells, and found that the Tff3

mRNA levels per goblet cell were not statistically different from control levels (Figure 5D). The Muc2 protein levels appeared different in jejunum and ileum. In the jejunum the Muc2 protein levels were decreased in infected tissue at 1 to 4 dpi, and after correction for the number of goblet cells the Muc2 protein levels appeared to be significantly increased at 1 and 2 dpi (Figures 6A and 6C). In the ileum the Muc2 protein levels remained largely unaltered during infection both before and after normalization for the number of goblet cells (Figures 6A and 6C). Tff3 protein levels were decreased compared to controls at 6 hpi to 4 dpi (Figures 6B and 6D).

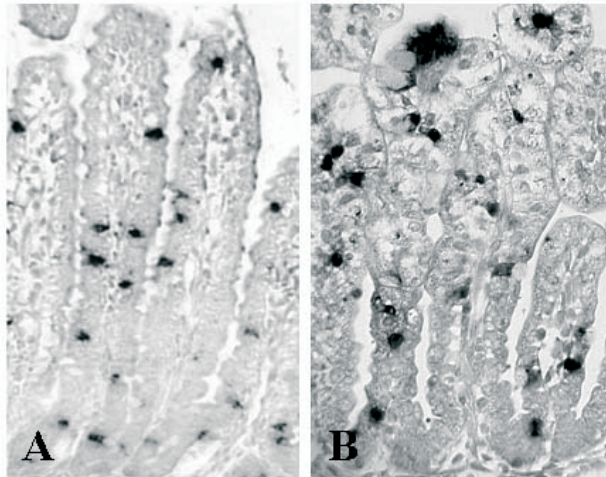


Figure 4. Muc2 mRNA levels in jejunal sections in control mice (A) and during rotavirus infection (B) as examined by *in situ* hybridization at 1 dpi. At the time-point of massive expression viral replication and extensive damage and vacuolization of enterocytes, goblet cell-specific Muc2 mRNAs remained detectable and comparable with controls. Original magnification: X 200.

Sulfated mucins and sialylated mucins during rotavirus infection

To analyze mucins qualitatively, mucins in control and infected tissues were detected with a combined AB-PAS staining (Figure 7, see *Appendix*). With this staining neutral mucins stain magenta, whereas acid mucins stain purple/blue. In the control animals at 4 dpi, goblet cells stained pink, indicating that they primarily contain neutral mucins (Figure 7A, *Appendix*). In infected animals at 4 dpi however, goblet cells stained blue in the crypt region or dark purple on the villi indicating that these goblet cells contained abundantly acidic mucins (Figure 7B, *Appendix*). The increase in AB-stained cells, further suggests that the fraction of acidic mucins increased during rotavirus infection. This phenomenon was observed from 1 to 4 dpi in all analyzed sections from infected animals (Figure 7B, *Appendix* and data not shown). To further examine mucins qualitatively, the mucins in control and infected ileum were detected with a combined High Iron Diamine-alcian blue (HID-AB) staining. With the HID-AB staining, sulfated mucins stain black or brown, whereas sialomucins stain blue (Figure 7C-E, *Appendix*). In control mice at 7 dpi, goblet cells predominantly stained black/brown indicating that they contained sulfated mucins (Figure 7C, *Appendix*). In infected mice at 7 dpi however, many goblet cells stained blue indicating that they predominantly contained sialomucin (Figure 7D, *Appendix*). We then counted the number of HID positive goblet cells and represented them as percentage of all goblet cells that were detected by AB-PAS at the

villi of control- and infected animals (Figure 7E, *Appendix*). During infection, the fraction of HID-stained goblet cells was decreased at 1 and 7 dpi. At 2 dpi there was a trend towards a decreased number of HID-stained goblet cells compared to controls, but this did not reach statistical significance. These results indicate that at specific time-points during rotavirus infection, mucins become less sulfated.

Protective capacities of mucins during rotavirus infection

As an initial experiment, we serially diluted mucin isolated from adult mouse large intestine (440) and assayed viral (Wa strain) infectivity in Caco-2 cells in the presence of mucin (data not shown). The mucin preparation was able to neutralize rotavirus infection in a concentration dependent manner. The concentration at which viral infectivity was reduced by 50% of this mucin preparation was 10 micro-g/ml.

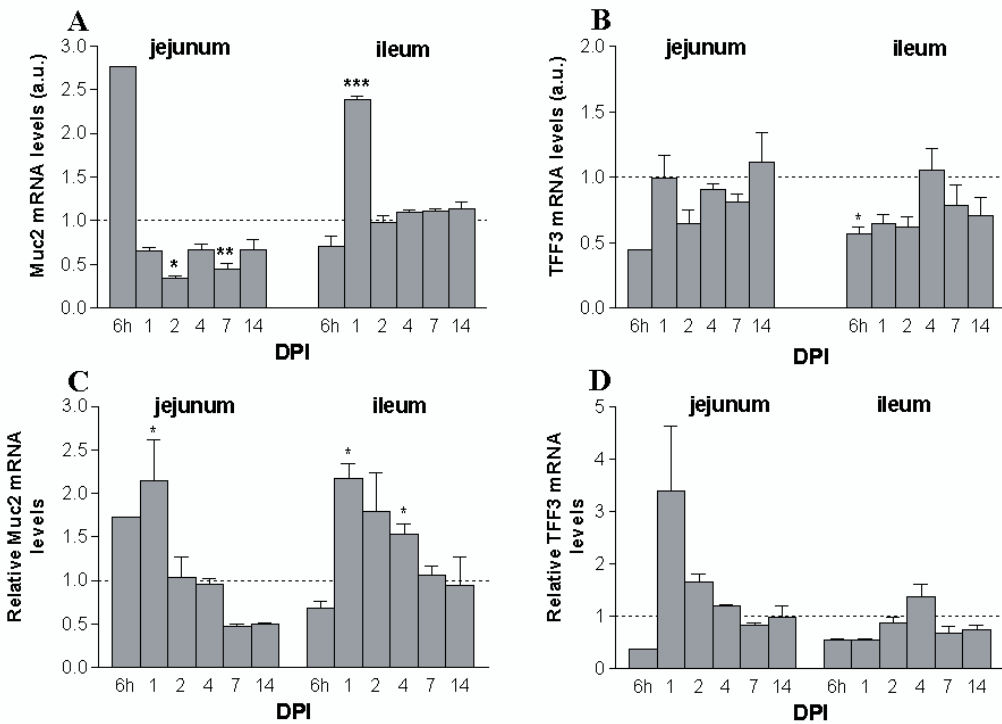


Figure 5. Quantitative analyses of goblet cell-specific mRNA levels during rotavirus infection. Muc2 (A) and Tff3 (B) mRNA levels in jejunum and ileum during rotavirus infection as measured by RNA-dot blot analysis and after normalization by the number of goblet cells in the respective tissue (C and D, respectively). Control values per day were arbitrarily set at a relative expression of 1 and are represented as a dotted line. The amount of RNA spotted was corrected for GAPDH mRNA expression. * $P < 0.05$, ** $P < 0.01$, *** $P < 0.001$ vs. control using Student's *t*-test. a.u., arbitrary units. Error bars in represent \pm SEM.

We determined if the changes in mucin structure during rotavirus infection in neonatal mice had functional implications, in particular on the mucin's capability to inhibit rotavirus infection. We isolated mucins from the small intestines (distal jejunum) of three control and three infected animals per time-point at 1, 2, and 4 dpi. These mucin preparations were tested for neutralization of the rotavirus Wa strain (SA-independent) at a concentration of 10 micro-

g/ml. Note that we could not use the mouse EDIM strain for our *in vitro* experiments, since this strain is not cell culture-adapted and does not infect or replicate within the Caco-2 cell line.

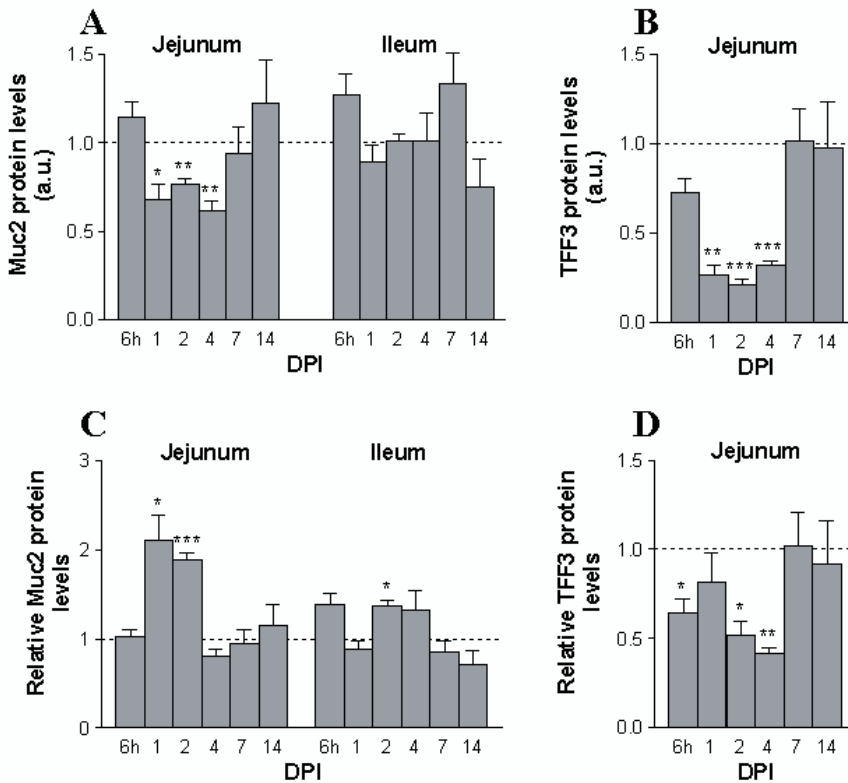


Figure 6. Quantitative analyses of goblet cell-specific protein levels during rotavirus infection. Muc2 (A) protein levels in jejunum and ileum, and Tff3 (B) protein levels in jejunum during rotavirus infection as determined by protein dot-blot analysis and after normalization by the number of goblet cells in the respective tissue (C and D, respectively). Control values per day were arbitrarily set at a relative expression of 1 and are represented as a dotted line. * $P < 0.05$, ** $P < 0.01$, *** $P < 0.001$ vs. control using Student's *t*-test. a.u., arbitrary units. Error bars represent \pm SEM.

Mucins isolated from control and infected mice were able to significantly neutralize Wa rotavirus infection in Caco-2 cells when compared to a similar amount of cells incubated with virus in the absence of mucins. Inhibiting effects of the individual mucin isolates ranged from 78.3% to 27.3% (Table 1). Mucins isolated at 4 dpi from control and infected mice were less efficient in inhibiting rotavirus infection than the respective mucins isolated from control and infected mice at 1 and 2 dpi ($P < 0.05$). At 4 dpi, mucins isolated from infected mice were capable of inhibiting rotavirus infection more efficiently (57.1%) than mucins isolated from control mice (27.3%). We also performed an inhibition study using the rotavirus SA11 (SA dependent) strain and obtained similar results as for the Wa strain (data not shown).

All abovementioned experiments, i.e. the infection of mice and the whole data analysis, except the isolation and subsequent measurement of the mucin inhibitory capacities, were

performed twice independently. The results of both experiments were comparable in all aspects.

Discussion

Previous studies demonstrated that rotavirus infection has a profound effect on small intestinal epithelial homeostasis. It was found that rotavirus infection induces apoptosis at the tips of the villi, increases epithelial cell turnover and hampers enterocyte gene expression (43, 84, 209, 306, 389, 402). Rather than concentrating on enterocyte cell function, we focused on goblet cell homeostasis during rotavirus infection and on the expression of specific gene products that are secreted by these cells. In the present study, we investigated changes in the number of goblet cells, goblet cell migration kinetics, *Muc2* and *Tff3* mRNA and protein levels, and analyzed the qualitative changes in intestinal mucin glycosylation and sulfation during rotavirus infection in neonatal mice.

Neonatal mice infected with EDIM rotavirus developed diarrhea over a period of 5 days starting at 1 -day post infection (dpi). As in other studies, viral infection occurred in two peaks of replication at 1 and 4 dpi (43, 306, 402). Our previous findings demonstrated a severe loss of enterocytes during infection, through increased apoptosis (43). In these infected mice the expression of specific enterocyte markers was reduced to only 10-20% of control levels. We found in the duodenum and jejunum that also the number of goblet cells decreased significantly between 1 and 4 dpi. In the ileum however infection had little effect on the number of goblet cells. Epithelial cells in infected mice migrated faster up the villus than in control animals, a process during which the goblet cells accumulated at the tips of the villi. This phenomenon was most prominent in the ileum, but occurred in all of the small intestine. At 4 and 7 dpi all BrdU-labeled cells that were still present at the villus tips of infected mice were goblet cells. These findings suggest that, at least in the ileum (where we found the highest levels of viral replication) goblet cells, in contrast to enterocytes, are comparatively spared from the apoptosis during severe rotavirus infection. The sparing of goblet cells could be a mechanism within the epithelium to uphold their protective function in epithelial defense. This event was also observed in rats during severe intestinal damage induced by the cytostatic drug methotrexate (446). The potential protective role of goblet cells and their products was further corroborated by our observation that *Muc2* and *Tff3* levels produced by these cells were maintained or even enhanced during infection. *Muc2* mRNA levels per goblet cell in the small intestine were increased during most severe damage and viral replication. Moreover, *Tff3* mRNA levels were maintained during rotavirus-induced damage at levels not different from control levels. Interestingly in the jejunum, total *Muc2* protein levels were decreased during viral replication at 1 and 2 dpi, probably due to the observed decrease in the number of goblet cells. However, when the jejunal *Muc2* protein levels were considered in relation to their numbers, it appeared that the *Muc2* protein production per cell was even increased. This was in contrast to the *Tff3* protein levels that were decreased during rotavirus infection. Given the fact that the expression patterns of *Muc2* and *Tff3* differ in space and time, our results suggest that the *Muc2* and *Tff3* genes are not coordinately regulated in goblet cells during rotavirus infection. This was also observed in a methotrexate-induced damage and regeneration model in rats (447).

| Inhibition of rotavirus infection by mucins isolated from neonatal mice | | | |
|---|------------------------|----------------|------------------|
| | % inhibition \pm SEM | | |
| | 1 dpi | 2 dpi | 4 dpi |
| control mice | 68.2 \pm 2.9 | 78.3 \pm 2.0 | 27.3 \pm 6.1 a |
| infected mice | 78.1 \pm 2.1 | 69.1 \pm 2.9 | 57.1 \pm 4.1 a |

Table 1. Inhibition of rotavirus infection by mucins. Mucins were isolated from the small intestines (distal jejunum) of three control and three infected animals per time-point at 1, 2, and 4 dpi. Mucin preparations (10 micro-g/ml) were tested to neutralize infection of rotavirus Wa strain in the Caco-2 cell line. Mean \pm SEM percentages inhibition of infection in Caco-2 cells incubated with and without mucins are indicated. Mucins isolated from control and infected mice at 4 dpi were less efficient of inhibiting infection than mucins isolated from control and infected mice at 1 and 2 dpi (a, $P < 0.05$). The experiments were performed in at least ten-fold. a $P < .005$, using Student's *t*-test.

The increased Muc2 mRNA levels observed during infection could be mediated through several mechanisms. Mucus overproduction has long been recognized as an important symptom of respiratory viral infections, but only recently it was shown that mucin is induced as a direct effect of viral double stranded RNA (dsRNA) on airway epithelial cells (238). The signaling pathways mediating MUC2 transcription by dsRNA were shown to resemble those shown previously to mediate cytokine induction and include the activation of mitogen-activated protein kinases (MAPK) and nuclear factor kappa-B (NF- κ B)(238). Rotavirus is also able to rapidly activate NF- κ B during infection (355). Instead of via dsRNA, however this activation was shown to be provoked primarily via binding of its outer capsid protein VP4 to the TNFR-associated factor 2 (TRAF2) and activation of TRAF signaling (226). The above-mentioned pathways are also known to induce the expression of cyclooxygenase 2 (COX2) a key enzyme for the production of prostaglandins (PGs). Our group recently demonstrated that COX2 mRNA and PGE₂ levels are increased during rotavirus infection in Caco-2 cells and that PGE₂ and COX activity is crucial for rotavirus replication (358). Interestingly, MUC2 protein expression is mediated through PGE₁ and PGE₂ (458) and moreover, PGE₂ was shown to enhance mucin release via a cAMP-dependent mechanism (25).

Bacteria were also shown to induce MUC2 transcription mainly via production of NF-kappaB and various cytokines (110, 113, 232, 250). Among the many (pro-inflammatory) cytokines that stimulate mucin gene expression are IL-1, IL-4, IL-6, IL-9 and tumor necrosis factor alpha (TNF-alpha), (110, 443) and references therein. It still has to be defined which of these multiple pathways and to what extent are mediating the increased levels of Muc2 mRNA at 1 dpi in this study.

Mucins can roughly be classified into neutral and acidic subtypes. Acidic mucins can further be distinguished by sulfated (sulfomucins) or non-sulfated (sialomucins) groups. In most mammalian species, neutral mucins appear to be the predominant subtype expressed in gastric mucosa, whereas acidic mucins dominate in the small and large intestine (386). During rotavirus infection, we found a reduction in the number of goblet cells producing sulfated mucins. Studies of SA11 rotavirus infection in rats also showed a reduction in the number of sulfated mucin-containing cells (156). SA11-infected rats fed with milk fermented by *Lactobacillus casei*, had less diarrhea and the number of sulfated mucin-containing cells

was comparable to controls (156). We observed that the small intestinal mucins particularly were less sulfated during or after the two replication peaks. At these time-points, sulfated mucins could have been preferentially secreted or the mucin molecules could be undersulfated as has been observed in patients with ulcerative colitis or in a rat model for colitis (191, 345, 442). Sulfate content of mucins is thought to present resistance to (bacterial) enzymatic degradation of the mucus layer (293, 352) and therefore the decrease in sulfated mucins could influence the consistency of the mucus layer. Changes in mucin sulfation particularly will be of relevance in the colon where sulfate-reducing bacteria reside. It will therefore be of special interest to determine whether sulfation is also reduced in the colon during rotavirus infection.

AB-PAS staining suggested that the fraction of acidic mucins was strongly increased during rotavirus infection in mice. Since we found that the number of goblet cells producing sulfated mucins was decreased, these acidic mucins most probably embody heavily sialylated mucins. Several studies have reported that glycosylation and sialylation of mucins changes during bacterial or parasite infections (100, 170). Davril et al. reported that in patients who were severely infected with *Pseudomonas aeruginosa*, mucins isolated from bronchial mucosa had a higher sialic acid content than mucins from non-infected patients (100). The authors also concluded that bacterial infection influences the expression of sialyltransferases and fucosyltransferases in the human bronchial mucosa. In vitro, cytokines have been implicated in the sialylation of mucins (106). In particular, TNF-alpha was shown to upregulate mRNA levels of sialyl- and of fucosyl-transferases and increase the sialylation of mucins in a human respiratory gland cell line. Interestingly TNF-alpha levels were found increased in rotavirus-infected children and increased levels correlated with the severity of the symptoms (193).

Mucins of various origins have been implicated in the inhibition of rotavirus infection (72, 289, 323, 459, 471, 472). Mucins are thought to present a barrier for infection through direct interaction with the virus, thereby preventing virus-cell attachment (72, 472). The changes in mucin sulfation and especially sialylation during rotavirus infection in mice suggested that these mucins would have an altered competence to inhibit rotavirus infection. Mucins isolated at 4 dpi from control and infected mice were less efficient in inhibiting rotavirus infection than mucins isolated from control and infected mice at 1 and 2 dpi. Our data therefore suggest that, as was previously found (72), age-dependent differences in mucin composition alter the inhibitory capabilities of small intestinal mucins. Mucins isolated from infected mice at 4 dpi were more efficient in neutralizing rotavirus infection than mucins isolated from control mice at 4 dpi. This implies that the increase in sialylated mucins in infected animals at 4 dpi, results in the increased protective capacity compared to controls at this time-point. This observation could represent part of an innate defense mechanism to remove pathogens. The specific relationship between mucin oligosaccharide composition alterations and susceptibility to infection however is still the subject of ongoing investigations. Additionally, more experiments have to be performed in order to substantiate the possible role of the rotavirus-increased occurrence of acid mucins and their role in the defence against rotavirus infection.

In conclusion our data show that during rotavirus infection goblet cells, in contrast to enterocytes, are spared from apoptosis in the ileum, Muc2 levels are up-regulated and mucin structure is changed. This suggests that mucins and in particular Muc2, play an important role in the active defense against rotavirus infection. The data further imply that age-dependent differences in mucin composition and increased occurrence of acidic (most likely

sialylated) mucins alter the inhibitory capabilities of mucins isolated from the small intestine. This suggests that posttranslational modification in glycosylation of mucins during infection, may affect specific epithelial barrier function against intestinal pathogens.

Acknowledgements

Dr D.K. Podolsky is acknowledged for providing both the Tff3 probe and the anti-Tff3 antibodies. This work was supported by grants from the Sophia Foundation for Medical Research (SSWO), the Netherlands Digestive Diseases Foundation (MLDS), and the Netherlands Foundation for Scientific Research (NWO).

Rotavirus infection induces mucin expression via a prostaglandin-mediated mechanism

Jos A. Boshuizen, Janneke Bouma, Hans A. Büller,
Alexandra W.C. Einerhand

Submitted for publication

Abstract

Rotaviruses are recognized as the leading cause of severe viral gastroenteritis in young children. Previously we have shown that cyclooxygenase (COX) 2 mRNA and secreted prostaglandin (PG) E₂ levels are increased after rotavirus infection in Caco-2 cells. PGs have been implicated in production and secretion of mucins. Mucins are the key components of the intestinal mucus layer and represent a barrier to rotavirus infections. The purpose of this study was to determine whether PGs and COX could be involved in rotavirus-induced mucin expression. Using quantitative RNA dot blotting and semi-quantitative RT-PCR, we determined Cox2 and mucin mRNA expression during rotavirus infection in neonatal mice and in Caco-2 cells. The results showed that Cox2 mRNA expression is strongly enhanced during rotavirus infection in mice, implying increased PG production. Infected mice also showed increased levels of Muc2, Muc3 and Muc5AC mRNAs. As an enterocyte model, Caco-2 cells “mirrored” the observations in mice and showed increased enterocyte-specific MUC3 mRNA expression during rotavirus infection. In the goblet cell line LS174T, PGE₁ and PGE₂ were able to induce MUC2, -3, and -5AC mRNA expression in a time and concentration dependent manner. These findings suggest that mucin upregulation during rotavirus infection is mediated through upregulation of rotavirus-induced Cox2 and PG levels.

Introduction

Rotavirus is the major infectious agent in the development of gastroenteritis, malnutrition and diarrhea in young children and animals (122, 204). By the age of 5, nearly every child worldwide will have had at least one episode of rotavirus gastroenteritis, whereas approximately 1 in 300 of these children will die as result of the infection. Children in developing countries account for 82% of the 440,000 children younger than 5 years of age that annually die worldwide because of an infection with rotavirus (313). Rotavirus infection in children and animals is mainly restricted to the small intestinal villus epithelium. Replication generally occurs in mature enterocytes and leads to the induction of a variety of pro-inflammatory cytokines, reduction of enterocyte gene expression, and vacuolization and apoptosis of enterocytes. As a result of enhanced cell death villus atrophy occurs (33, 43, 65, 355). Recently however, it was reported that rotavirus infection is not confined to the intestine, but in addition is able to leave the intestine and enters the circulatory system resulting in antigenaemia and possible viraemia (40, 282, 342).

Prostaglandin E₂ levels rise early after rotavirus infection in pigs (481). Furthermore, elevated levels of the prostaglandins PGE₂ and PGF₂ have been reported in the plasma and stool of rotavirus-infected children (466), indicating that cyclooxygenases (COXs) and prostaglandins (PGs) might be involved in rotavirus pathogenesis. PGs are lipid mediators that are produced through cyclooxygenases (COXs). The COX1 gene is constitutively expressed, whereas in most cell types, COX2 is induced by pro-inflammatory or mitogenic activators including cytokines, endotoxin, and inflammatory molecules (74). Especially PGE₂ was shown to be involved in regulation of viral replication. Aside from a few exceptions, increased production of PGE₂ or exogenously added PGE₂ leads to increased replication of most viruses, e.g., Herpesvirus (CMV), Retrovirus (HIV), and Rhabdovirus

(403). We recently demonstrated that COX2 mRNA and PGE₂ levels are increased during rotavirus infection in the enterocyte-like cell line Caco-2. PGE₂ and COXs activity were shown to be crucial for rotavirus replication via a post-binding mechanism (358).

The intestinal epithelium is covered by mucus that primarily consists of mucus glycoproteins (mucins) (137, 438). Mucins play a crucial role in epithelial protection against luminal bacterial compounds (116), and references therein), and it was suggested that mucins represent a barrier to rotavirus infections by neutralizing rotavirus infection through direct interaction with the virus, by hindering virus-cell attachment (72, 472). Mucins are encoded by the MUC-gene family and are classified into either membrane-bound or secretory glycoproteins (105). The secretory mucin MUC2, the most important structural component of the intestinal mucus layer, is exclusively and abundantly expressed by goblet cells in the large and small intestine (426, 427, 438, 440). In the human small intestine, the membrane bound mucin MUC3 is mainly confined to the more mature enterocytes at the tips of the villi, although occasional expression in goblet cells has been observed (69). The secretory mucin MUC5AC is normally confined to gastric epithelium (437), but is aberrantly expressed in Barrett's oesophagus, gastric metaplasia in the duodenum, the colon in inflammatory bowel disease (IBD) and colorectal adenomas (55, 239, 382, 435, 436). Mucin gene expression patterns in mouse are very similar to those described in humans (13, 116, 120, 197, 387, 440, 443).

PGs were previously shown to play a role in the production and secretion of mucins, as PGE₂ enhanced mucin release via a cAMP-dependent mechanism in LS174T cells and in the rat colon (25), and MUC2 protein expression is enhanced by short chain fatty acids through PGE₁ and PGE₂ produced by myofibroblasts (458).

In this study we wanted to evaluate the role of PGs in mucin expression during rotavirus infection. We examined whether COX and mucin mRNA expression were enhanced during rotavirus infection in neonatal mice and during rotavirus infection of Caco-2 cells, as PG levels are elevated in both rotavirus-infected children and the enterocyte-like cell line Caco-2 (358, 466). We furthermore wanted to determine if the prostaglandins PGE₁ and PGE₂ could differentially regulate mucin mRNA expression in the goblet cell-like cell line LS174T. Our findings suggest that the increased intestinal mucin mRNA expression during rotavirus infection *in vivo* is mediated by rotavirus-induced increase in PG levels.

Materials and Methods

Animals and virus inoculations

Seven-day-old BALB/c mice were inoculated intra-gastrically with 2×10^4 focus forming units (ffu) of the EDIM rotavirus strain as previously described (43). Control mice were mock infected through inoculation with PBS. At different time points after infection, mice were sacrificed and segments of the ileum were dissected and snap frozen in liquid nitrogen and stored at -80°C for RNA isolation.

Cell culture and rotavirus infection

The human colonic adenocarcinoma cell lines Caco-2 and LS174T (American Type Culture Collection, Manassas, VA, USA) were grown and maintained in 75 cm² tissue culture flasks in DMEM (Dulbecco's Modified Eagle's Medium; Gibco BRL, Paisly, Scotland) containing 10% (v/v) fetal bovine serum (FBS, Integro, Dieren, The Netherlands), 100 U/ml Penicillin,

100 µg/ml Streptomycin and 1% (v/v) Non-Essential Amino Acids (BioWhittaker, Verviers, Belgium) at 37°C and 5% CO₂. One day prior to infection, Caco-2 cells were seeded on 10 wells heavy teflon coated microscopic slides (7mm, Cel-line/Erie Scientific, Portsmouth, NH) at 10⁴ cells/well. One hour prior to infection, the Caco-2 cells were rinsed 3 times in serum free DMEM. Simultaneously, the human rotavirus strain Wa, obtained from Dr. M. Koopmans (National Institute for Public Health and the Environment, Bilthoven, The Netherlands), was activated at 37°C for 1 h using 10 µg/ml trypsin (Sigma) diluted in DMEM-FCS. Viral infectivity in culture media and cells were determined as previously described (358). Rotavirus was diluted to 2 x 10³ ffu/ml (corresponding to 100 ffu per well) in serum-free DMEM and cells were subsequently infected with rotavirus at 37°C, 5% CO₂ in a humidified atmosphere. After 15 hours of incubation, infection was terminated using ice-cold methanol and cells were stored for 10 minutes at -20°C. Five to seven days after seeding, LS174T cells were incubated with 0, 1.4, 2.8 or 28 µM PGE₁ or PGE₂ (Sigma-Aldrich; St. Louis, MO) for 8, 16 or 24 h. Cells were then rinsed 3 times with PBS and RNA was isolated using RNeasy (QIAGEN, Venlo, The Netherlands) following the manufacturer's instructions.

RNA isolation, RNA dot blotting, and RT-PCR

Total RNA from frozen small intestinal segments, was isolated using Trizol reagent (Gibco-BRL, Gaithersburg MD) following the manufacturer's protocol. Total RNA from LS174T or Caco-2 cells was isolated with the RNeasy RNA isolation kit according to the manufacturer's protocol (Qiagen, Hilden, Germany). Integrity of the RNA was assessed by visual analysis of the 28S and 18S ribosomal RNAs after electrophoresis and staining with ethidium bromide. Random and oligo(dT)15 primers (ratio of 2:1) were used to synthesize cDNA by the M-MLV Reverse Transcriptase according to the manufacturer's protocol (Promega, Madison, WI). Mouse Muc3 was amplified using the oligo's 5'-GAGACATGCAAGAAGGAGGC-3' and 5'-CCAAGTCCATACACCAGGCT-3' (nucleotide positions 786-805 and 1011-1030, accession number [AF027131](#) (387), resulting in a 245 bp product. Mouse Muc5ac was amplified using the oligo's 5'-CCAATTGGCTAGATGGCAGT-3' and 5'-CAGATCAAACCCTCTCTCG-3' (nucleotide positions 373-393 and 553-575, accession number [L42292](#); (388)) resulting in a 175 bp product. The temperature cycling protocol for these PCR reactions consisted of 10 min pre-heating at 96°C followed by 30 cycles of 1 min denaturation at 96°C, 1 min primer annealing at 60°C and 1 min primer extension at 72°C.

The mouse Cox1 orthologue prostaglandin-endoperoxide synthase 1 (Ptgs1) was amplified using the oligo's 5'-TGTTTCAGCTTCTGGCCCAAC-3') and 5'-ATCAACACGGACGCC-TGTTTC-3' (nucleotide positions 561-580 and 841-860, respectively, accession number [NM008969](#); (286) resulting in a 300 bp product. The mouse Cox2 orthologue prostaglandin-endoperoxide synthase 2 (Ptgs2) was amplified using the oligo's 5'-TTCAAAGAAGTGCTGGAAAAG-3' and 5'-AGATCATCTCTACCTGA-GTGTCTT-3' (nucleotide positions 577-598 and 858-881, accession number [NM011198](#); (222)) resulting in a 305bp product. The temperature cycling protocol for the Cox1 and 2 PCR reactions consisted of 4 min pre-heating at 94°C followed by 35 (Cox1) or 40 (Cox2) cycles of 1 minute denaturation at 94°C, 45 seconds primer annealing at 51 (Cox1) or 56 °C (Cox2) and 1 min primer extension at 72°C. The efficiency of the PCR reactions on mouse cDNA was determined by amplifying β-actin using the oligo's 5'-CAAGCCAACCGCGAGAA G-3' and 5'-CAGGGTACATGGTGGTGCC-3', resulting in a 587 bp PCR product, as described previously (439). The temperature cycling protocol for this PCR reaction consisted of 4 min

pre-heating at 94°C followed by 35 cycles of 45 seconds denaturation at 94°C, 1 min primer annealing at 60°C and 1 min primer extension at 72°C.

Human MUC2 and MUC3 were amplified using the oligo's 5'-CTGCACCAAGACCGTCCTCATG-3' and 5'-GCAAGGACTGAACAAAGACTCAGAC-3' (nucleotide positions 15291-15312 and nt 15667-15691, accession number [L21998](#) (160)) resulting in a 401 bp product, or 5'-AGTCCACGTTGACCACCACTGC-3' and 5'-TGTTACATCCTGGCTGGCG-3' (159) resulting in a 522 bp product, respectively. Human MUC5AC was amplified using the oligo's 5'-TGATCATCCAGCAGCAGGGCT-3' and 5'-CCGAGCTCAGAGGACATATGGG-3' (nucleotide positions 2897-2917 and 3284-3305, respectively, accession number [AJ001402](#); (56)), resulting in a 409 bp product. The efficiency of the PCR reactions performed on human cell line cDNA was determined by amplifying human 18S rRNA using the oligo's 5'-TCCTGCCAGTAGCATATGCTTG-3' and 5'-AGAGGAAGCGAGCGAC-3' and resulting in a 120 bp product (358). The temperature cycling protocol for the PCR reactions for MUC2, MUC3 and 18S consisted of 2 min pre-heating at 94°C followed by 30 (MUC2 and 18S) or 35 (MUC3) cycles of 45 seconds denaturation at 94°C, 1 min primer annealing at 60°C and 1 min primer extension at 72°C. The temperature cycling protocol for the MUC5AC PCR reaction consisted of 2 min pre-heating at 94°C followed by 35 cycles of 45 seconds denaturation at 94°C, 1 min primer annealing at 62°C and 1 min primer extension at 72°C. All PCR products were visualized and quantified using the Gel Doc 2000 system and Multi-Analyst software version 1.1 (Bio-Rad Laboratories, Inc., Hercules, CA).

For RNA blotting, 1 µg of total RNA was dot-blotted on Hybond-N⁺ (Amersham, Bucks, England) using a vacuum-operated manifold (BioDot, BioRad). All blots were hybridized using specific ³²P-labeled cDNA probes as described previously (43). To correct for the amount of RNA that was spotted, hybridized signals were corrected for glyceraldehyde-3-phosphate dehydrogenase (GAPDH) mRNA expression using a 1.4 kb human GAPDH probe (43). Hybridization signals were measured through autoradiography using a PhosphorImager and ImageQuant software (Molecular Imaging, Sunnyvale CA, USA). The following probes were used: The pBluescript cDNA probes that were used were the 244-bp murine Muc2 probe (440), and a 900 bp VP4 probe. For construction of the VP4 probe, RT-PCR was performed on RNA isolated from EDIM infected neonatal mice. VP4 was cloned using the primers 5'-TATACCATGGCTTCACTCATTATAGAC-3' and 5'-TTGGTAGTTCGCTG-GTTTGAA-3', based on the EDIM VP4 coding sequence (nucleotide positions 7-28 and 883-900, accession number [AF039219](#) (309)). PCR fragments were TA-cloned into the PCR 2.1 vector (Invitrogen) and sequenced.

Statistical analysis

Statistical analysis of all data was performed using Student's *t*-test for unpaired data (two-tailed). Data were expressed as the mean ± SEM and *P* values of ≤ 0.05 were considered statistically significant.

Results

Mucin gene expression increased during rotavirus infection in neonatal mice

Rotavirus infected 6-day-old suckling mice showed two peaks of viral replication in the ileum at 1 and 4 days post infection (dpi) as determined by rotavirus VP4 RNA expression (Figure 1A). Muc2 is the most prominent mucin in the small and large intestine in humans and mice (120, 426, 427, 438, 440). Using dot blotting, Muc2 mRNA levels in the ileum were found to be significantly increased 2.5 fold at 1 dpi (Figure 1B).

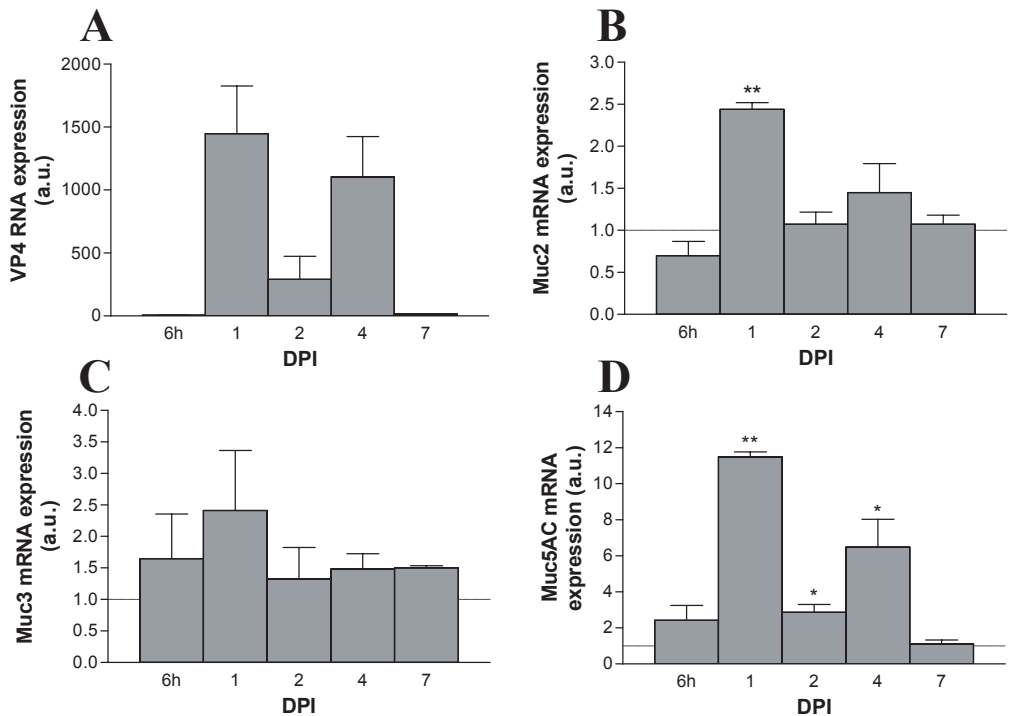


Figure 1. Analyses of rotavirus VP4 RNA and Muc2, Muc3 and Muc5ac mRNA expression in the ileum of rotavirus-infected neonatal mice. VP4 and Muc2 expression were quantitatively analyzed by RNA dot blotting. Muc3 and Muc5ac levels were semi-quantitatively determined by densitometric analysis of RT-PCR products. Control values per day were arbitrarily set at a relative expression of 1 and are represented as a dotted line. Rotavirus infected 7-day-old suckling mice showed two peaks of viral replication in the ileum at 1 and 4 dpi, as determined by VP4 RNA expression (A). Muc2 mRNA levels were found to be significantly increased 2.5 fold at 1 dpi (B). Muc3 mRNA levels were increased 1.5-fold at 6 hpi and nearly 2.5-fold at 1 dpi (C). Muc5ac expression was strongly increased in rotavirus infected neonatal mice (D). The amount of VP4 and Muc2 RNA spotted was corrected for GAPDH mRNA expression. The efficiency of the Muc3 and Muc5ac PCR reactions was verified by amplifying β -actin. * $P < 0.05$ vs. control using Student's *t*-test. a.u., arbitrary units. * $P < 0.05$, ** $P < 0.01$, vs. control using Student's *t*-test. a.u., arbitrary units.

The membrane-bound non-secretory mucin Muc3 was analyzed by semi-quantitative RT-PCR. Muc3 mRNA levels were increased 1.5-fold at 6 hpi and nearly 2.5-fold at 1 dpi (Figure 1C). The secretory mucin MUC5AC is normally confined to gastric epithelium (197, 388, 437), but its expression is altered in Barrett's oesophagus, gastric metaplasia in the

small intestine, in IBD and colorectal cancer (55, 239, 435, 436). Using RT-PCR, only minute expression of Muc5ac mRNA was observed in the ileum of control mice. Muc5ac expression was considerably and significantly increased in the ileum of rotavirus infected neonatal mice. At 1 and 4 dpi, during the two peaks of viral replication, expression was increased 12- and 6-fold respectively (Figure 1D).

Expression of cyclooxygenase 2 mRNA increased during rotavirus infection in neonatal mice

We previously showed that expression of COX2 mRNA is increased in the intestinal colon carcinoma cell line Caco-2 during rotavirus infection and that COX activity is crucial for rotavirus replication (358). In this study, we wanted to investigate whether cyclooxygenase expression is also increased during rotavirus infection in mice. Using semi-quantitative RT-PCR analysis, we determined that Cox1 mRNA levels were comparable to controls at 6 hpi and 1, 4, and 7 dpi (Figure 2). Only at 2 dpi, levels were decreased compared to controls. This is probably due to the extensive loss of epithelial cells due to increased apoptosis at this time point (43). Cox2 mRNA expression was significantly increased during rotavirus infection and peaked at 6 hpi and 4 dpi reaching a maximum of 8.5-fold increase (Figure 2). At 7 dpi, as there was resolution of rotavirus infection, Cox2 mRNA expression returned to control levels. These results show that Cox2 mRNA expression, but not Cox1 mRNA, is strongly enhanced during rotavirus infection in mice, implying increased PG production.

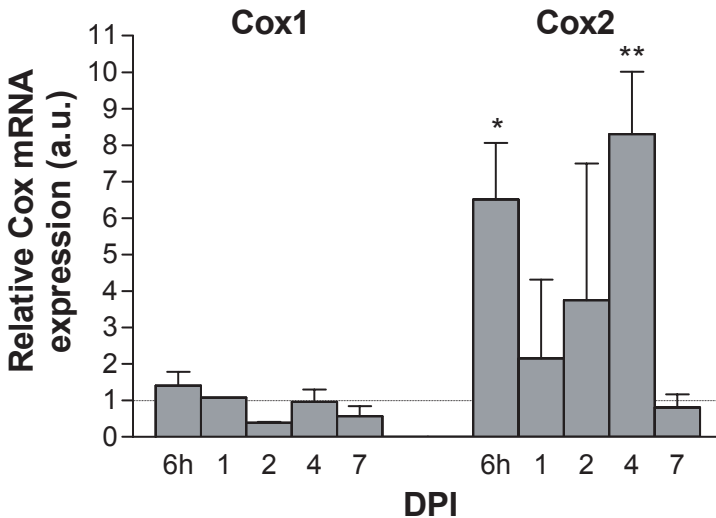


Figure 2. Analyses of Cox1 and Cox2 mRNA expression in the ileum during rotavirus infection in neonatal mice. Cox1 and Cox2 mRNA levels were semi-quantitatively determined by densitometric analysis of RT-PCR products. Control values per day were arbitrarily set at a relative expression of 1 and are represented as a dotted line. Cox1 mRNA levels were comparable to controls except for 2 dpi. Cox2 mRNA expression was significantly increased during infection and peaked at 6 hpi and 4 dpi reaching a maximum of 8.5-fold increase. The efficiency of the PCR reactions was verified by amplifying β -actin.* $P < 0.05$, ** $P < 0.01$, vs. control using Student's *t*-test. a.u., arbitrary units.

Mucin expression during rotavirus infection in colon carcinoma cell line Caco-2

To verify the effect on mucin expression in an *in vitro* model for enterocytes, enterocyte-like Caco-2 cells were infected with human rotavirus Wa. In this cell system, viral RNA and protein synthesis was first detected from 4 hpi by RT-PCR and Western blotting, respectively (358). Caco-2 cells are known to express MUC3 and low levels of MUC2 mRNA (295, 441). In rotavirus-infected Caco-2 cells, MUC3 mRNA expression was increased to 1.5- to 2-fold at 2 and 4 hpi, although this did not reach statistical significance (Figure 3). We did however not observe increased or induced expression of the secretory mucins MUC2 and MUC5AC in these cells, respectively. MUC2 mRNA expression remained unaltered (Figure 3), whereas MUC5AC mRNA could not be detected in mock infected or rotavirus infected Caco-2 cells (data not shown).

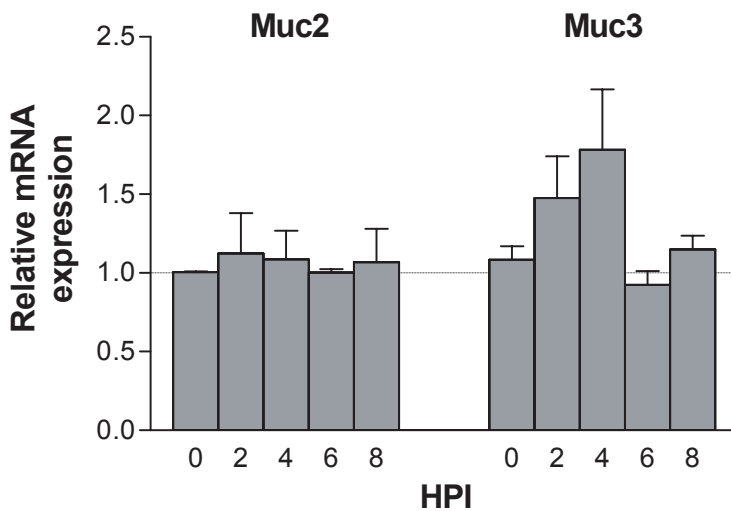


Figure 3. Analyses of mucin mRNA expression in rotavirus-infected Caco-2 cells. MUC2 and MUC3 mRNA levels were semi-quantitatively determined by densitometric analysis of RT-PCR products. Control values per day were arbitrarily set at a relative expression of 1 and are represented as a dotted line. MUC2 levels remained unaltered during infection. MUC3 expression was increased at 2 and 4 hpi. MUC5AC could not be detected in mock infected or rotavirus infected Caco-2 cells (not shown). The efficiency of the PCR reactions was verified by amplifying 18S ribosomal RNA.

Mucin expression by LS174T cells after incubation with prostaglandin

MUC2 and MUC5AC are not expressed by enterocytes *in vivo*. MUC2 is normally expressed by goblet cells (426), whereas MUC5AC is normally confined to gastric epithelium (437), but can atypically be expressed by goblet cells in Barrett's oesophagus, gastric metaplasia in the small intestine, in IBD and colorectal adenomas (55, 239, 382, 435, 436). The altered expression of Muc2 and Muc5ac found in infected mice can therefore not be explained by altered expression of these mucins in infected enterocytes, but are most likely brought about by goblet cells. Goblet cells are not a target for rotavirus infection. However, secreted PGE₂ and COX2 mRNA levels are increased between 2 and 8 hpi in rotavirus infection in Caco-2 cells (358) and we observed a strong increase in Cox2 mRNA expression in rotavirus infected mice, suggesting a role for PGs in the induction of mucin expression observed during rotavirus infection. To determine whether prostaglandins could induce mucin mRNA

transcripts, we used the goblet cell-like cell line LS174T. LS174T cells express MUC2 mRNA at a high level whereas MUC3 and MUC5AC mRNAs are present at low levels (441). Besides PGE₂, we also wanted to examine the role of PGE₁, since this PG was shown to induce MUC2 protein expression in the human adenocarcinoma cell line T84 (458). We therefore, incubated LS174T cells with different concentrations of the prostaglandins PGE₁ and PGE₂ and examined if they could differentially regulate MUC2, MUC3 and MUC5AC mRNA expression.

As an initial experiment, we incubated LS174T cells with PGE₂ for respectively 8, 16 and 24 hours (Figure 4). After 8 h induction with PGE₂ semi-quantitative analysis of MUC2 mRNA expression showed increased transcripts at a concentration of 2.8 and 28 μ M PGE₂. After 16 h no induction by PGE₂ was observed, whereas after 24 h incubation with PGE₂ resulted in a decrease of Muc2 mRNA expression compared to mock incubation. After 8 h of incubation PGE₁ was able to induce MUC2 (2-fold compared to controls) and MUC3 (2.5-fold compared to control) levels at all tested concentrations, while this was significant for both mucins at a concentration of 1.4 μ M (Figure 5A). PGE₁ was able to increase MUC5AC mRNA expression only at a concentration of 1.4 μ M (2-fold increase). However, this did not reach statistical significance. At all three concentrations, addition of PGE₂ gave induction of MUC2 and MUC3 expression to maximal levels of 2.6- and 2.8-times the control values respectively (Figure 5B). For both mucins, this increase was statistically significant at a concentration of 1.4 μ M. MUC5AC expression in LS174T was unaffected by addition of PGE₂.

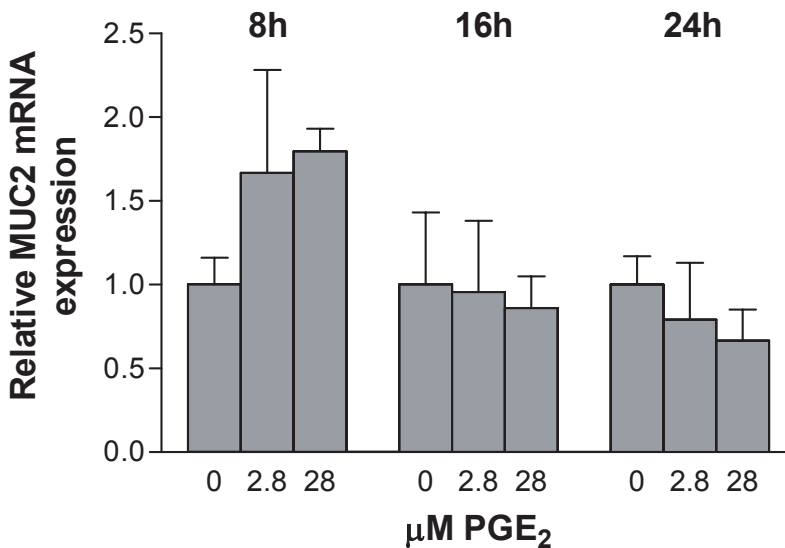


Figure 4. MUC2 expression in LS174T at different time-points after incubation with PGE₂. LS174T cells were incubated with 2.8 and 28 μ M of PGE₂ for respectively 8, 16 and 24 hours. MUC2 mRNA levels were semi-quantitatively determined by densitometric analysis of RT-PCR products. After 8 h induction with PGE₂, MUC2 mRNA levels were increased, whereas after 16 h or 24 h no induction with PGE₂ was observed. The efficiency of the PCR reactions performed on human cell line cDNA was determined by amplifying human 18S rRNA.

Discussion

We previously showed that COX2 mRNA and PGE₂ levels were increased after rotavirus infection *in vitro* (358), whereas elevated levels of PGE₂ and PGF₂ were observed in the plasma and stool of rotavirus-infected children (466). Moreover, PGE₂ and COX activity were shown crucial for rotavirus replication in Caco-2 cells and rotavirus illness in young children is reduced after oral aspirin, a non-specific COX inhibitor (358, 466). These findings strongly indicate that COX and PGs are involved in rotavirus replication and pathogenesis.

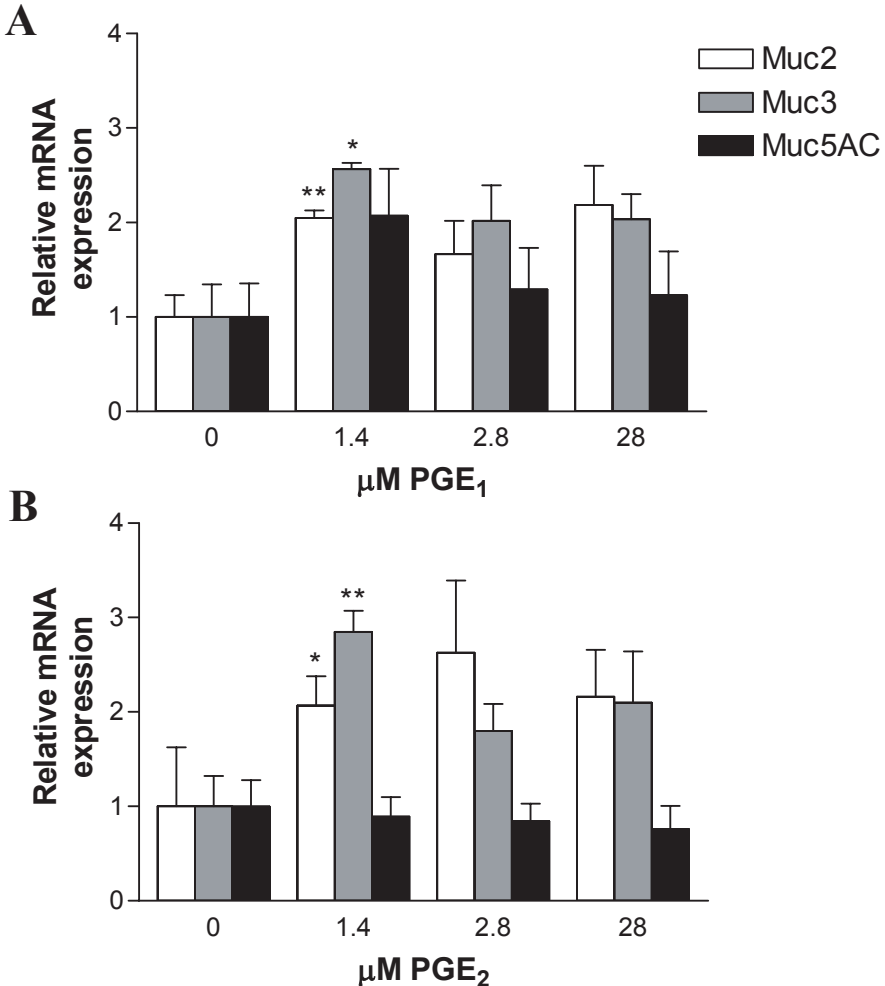


Figure 5. MUC2, MUC3, and MUC5AC expression in LS174T cells after 8 h of incubation with 0, 1.4, 2.8, or 28 μM of PGE₁ or PGE₂. Mucin mRNA levels were semi-quantitatively determined by densitometric analysis of specific RT-PCR products. PGE₁ was able to induce MUC2 and MUC3 mRNA significantly (A). PGE₁ induced MUC5AC expression only at a concentration of 1.4 μM. Addition of PGE₂ significantly increased MUC2 and MUC3 mRNA levels. MUC5AC expression in LS174T was unaffected by addition of PGE₂. The efficiency of the PCR reactions performed on human cell line cDNA was determined by amplifying human 18S. * P<0.05, ** P<0.01, vs. control using Student's *t*-test. a.u., arbitrary units.

In the present study, we found that Cox2 mRNA levels were also strongly increased in the ileum of rotavirus infected neonatal mice. Increased levels were found between 6 hours and 4 days after infection, with peaks at 6 hpi and 4 dpi, largely corresponding to the peaks of viral replication at 1 and 4 dpi. These results imply that following Cox2 mRNA induction, PG levels could also have been increased in the small intestine in infected mice as was observed in infected children and Caco-2 cells (358, 466). Cox1 expression was not induced during infection and instead was even found to be slightly decreased at 2 dpi, which is possibly caused by the loss of epithelial cells at the tips of the villi, as has been previously described (43).

Mucin mRNA levels were also found to be increased during rotavirus infection in mice. Goblet cell-specific Muc2 mRNA levels were found to be significantly increased at 1 dpi, whereas enterocyte-specific Muc3 mRNA levels were increased at 6 hpi and 1 dpi. The secretory mucin Muc5ac is normally confined to gastric epithelium (388) and expression in the small intestine of control mice was found to be extremely low as determined by RT-PCR. Expression of this mucin was however upregulated considerably in rotavirus infected neonatal mice. For all three mucins it was found that induction was observed at 1 dpi. Muc5ac levels followed the course of infection as expression of mRNA was provoked at both peaks of viral infection.

Previous studies demonstrated that rotavirus infection has a profound effect on intestinal epithelial homeostasis. It was found that rotavirus infection hampers the expression of enterocyte absorptive genes (43, 84, 209, 306, 389, 402). In contrast, we found in this study that goblet cell and enterocyte-specific mucin expression were upregulated during massive viral replication. As mucins are recognized to serve protective functions in the gut (438), the upregulation might indicate that this is part of an innate protective response against infections of the gut.

Mucin expression was also increased in the enterocyte-like Caco-2 cell line after infection with the rotavirus strain Wa. In accordance with the *in vivo* data, enterocyte-specific MUC3 mRNA levels were moderately increased at 2 and 4 hpi. However, MUC2 mRNA levels remained unaltered and MUC5AC mRNA could not be detected in mock infected nor rotavirus infected Caco-2 cells. MUC2 and MUC5AC are not expressed by enterocytes *in vivo*, which might explain the non-responsiveness of these genes in infected Caco-2 cells.

During rotavirus infection in Caco-2 cells, Cox2 mRNA and PGE₂ levels are increased from 2 to 8 hpi (358). Moreover, in this study we observed a strong increase in Cox2 mRNA expression in rotavirus-infected mice, suggesting a role for PGs in the induction of mucin expression observed *in vivo* during rotavirus infection. Whether PGE₁ levels are increased in infected mice and-or Caco-2 cells still has to be determined.

The induced expression of Muc2 and possibly also Muc5ac in rotavirus-infected mice was counted for by goblet cells. However, goblet cells are not a target for rotavirus infection, and therefore we aimed to determine whether PGs, that are apparently produced by infected enterocytes and secreted in the lumen during rotavirus infection, could induce mucin transcription in the goblet cell culture model LS174T. After incubation, PGE₁ and PGE₂ could directly induce MUC2 mRNA expression in LS174T cells in a dose-dependent manner. PGE₁ and PGE₂ were also able to induce MUC3 mRNA expression to a maximum increase of about three-fold. PGE₁ induced MUC5AC expression about 2-fold, and this was only observed at a concentration of 1.4 μ M. In contrast to studies in NCI-H293 airway epithelial cell (215), PGE₂ was unable to induce MUC5AC expression in LS174T cells.

Since the increase of MUC5AC by PGE₁ in LS174T cells was only moderate, other mediators are additionally involved in the induction of Muc5ac in infected mice. An interesting candidate that could be involved in the latter is TNF- α . TNF- α is found increased in rotavirus infected children (15) and is able to upregulate MUC5AC in airways via an epidermal growth factor receptor mediated route. Moreover TNF- α increases MUC5AC mRNA half-life (42) and induces MUC5AC secretion in HT29-MTX cells (397). The above findings suggest that the induction of mucin expression during rotavirus infection *in vivo* is to a large extent mediated by PGs.

The increased PG levels during rotavirus infection could be produced by either infected- or noninfected epithelial cells, and/or the underlying submucosa. In agreement with this and other studies (14, 396, 458), our previous data (358) indicated that PGs indeed can be derived from (infected) epithelial cells. Submucosal cells like myofibroblasts can also induce PGs and were shown to alter the PGE₁/PGE₂ ratio in response to short chain fatty acids in favor of PGE₁ (458).

COX2 expression is mediated through the activation of mitogen-activated protein kinases (MAPK) (like extracellular signal-regulated kinase ERK and p38) and nuclear factor κ B (NF- κ B) (215, 238). The increased COX2 transcription in rotavirus-infected mice and infected Caco-2 cells (358), could directly have been stimulated by double stranded viral RNA (dsRNA) as has been observed in macrophages (404). However, a recent study indicates that the activation of COX2 transcription during rotavirus infection is most probably not primarily provoked by dsRNA, but via binding of the rotavirus outer capsid protein VP4 to the TNFR-associated factor 2 (TRAF2) leading to activation of TRAF signaling (226). This is in agreement with our previous findings, since we found that COX2 levels were increased in Caco-2 cells after binding of rotavirus to the cells (358). Interestingly COX2 and PGE₂ were induced by mucins in macrophages (184), suggesting the existence of a forward-loop mechanism. In rotavirus-infected mice however, induced Cox-2 expression (6 hpi) preceded the increased mucin transcripts suggesting that a Cox-mediated pathway induced the mucin increase and not *visa versa*.

In summary, our data show that Cox mRNA expression correlates with Muc2, Muc3 and Muc5ac mRNA levels during rotavirus infection in mice, indicating that PGs are mediating the mucin induction. *In vitro* data showed that rotavirus infection of enterocytes led to MUC3 mRNA induction and that PGE1 and PGE2 are both important inducers of mucin expression in goblet cells. PGE1 was able to induce MUC2, MUC3 and MUC5AC mRNA levels, whereas PGE2 was able to induce MUC2 and MUC3 mRNA levels. The *in vitro* induction of MUC2 and MUC3 mRNA by PGE₁ and PGE₂ mirrored the *in vivo* induction. However, the increase of MUC5AC by PGE₁ in LS174T cells was only moderate, indicating that other pathways or other PGs (e.g. PGF) are likely to be involved in the induction of Muc5ac in infected mice. Moreover, it should be noted that although PGE₁ could be involved in the increase in mucin expression during rotavirus infection, it has to be determined whether PGE₁ levels are increased in infected mice and Caco-2 cells.

Additional experiments will be required to define the precise role of PGs in mucin induction, and which (other) pathways or effectors are involved in the observed induction of Muc5ac. The present study suggests that mucin upregulation during rotavirus infection is mediated through rotavirus-induced Cox2 and PG upregulation. The rotavirus-induced prostaglandin production and subsequent mucin induction could have beneficial effects on the gut by supporting mucosal barrier integrity.

Acknowledgements

The authors thank Dr Jan Dekker for critical reading of the manuscript. We would like to thank Dr Marion Koopmans for kindly providing the rotavirus Wa strain. This work was supported by grants from the Sophia Foundation for Medical Research (SSWO), the Netherlands Digestive Diseases Foundation (MLDS), and the Netherlands Society for Scientific Research (NWO).

Systemic immune response after rotavirus inoculation of neonatal mice depends on source and level of purification of the virus: implications for the use of heterologous vaccine candidates

Johan H. J. Reimerink, Jos A. Boshuizen, Alexandra W. C. Einerhand, Geert van Amerongen, Nico Schmidt and Marion P.G. Koopmans

Submitted for publication

Abstract

Rotavirus is an important cause of morbidity and mortality worldwide, and vaccines are currently under development. An unexpected side effect of the first licensed rotavirus vaccine, however, drew attention to possible effects of childhood infection or vaccination on the maturation of the immune system early in life. We examined the immune responses in infant BALB/c mice following oral inoculation with a standardized amount (2×10^6 CCID₅₀) of heterologous simian rotavirus SA11 as a model for vaccination. The SA11 infectious virus was presented in different backgrounds, which differed in antigen composition. Virus was purified from cell lysate by cesium chloride density gradient centrifugation. Fraction I was enriched for single shelled rotavirus particles, fraction II for double-shelled particles and fraction III consists mainly of infected-cell components. Inoculation with murine rotavirus EDIM (2×10^4 focus forming units) served as natural control infection.

Diarrhea was observed after inoculation with EDIM and all three SA11 fractions. Viral shedding was observed in the EDIM inoculated group but not in any of the SA11 inoculated mice. We could not detect virus replication in the small intestine either by immunohistochemistry or *in situ* hybridization in SA11-infected mice, in contrast to observations in the EDIM inoculated mice indicating extra-intestinal replication.

EDIM and SA11 fractions induced similar IgG responses but marginal IgA responses were found in the SA11 infected mice compared to the EDIM could be explained by the non-mucosal replication of SA11. The rotavirus specific IgG1/2a ratio were similar in the EDIM and SA11 fraction 2 but a higher ratio was found for SA11 fraction 3 and a lower ratio was observed for SA11 fraction 1. This data shows that the composition of the fractions influences the outcome of the immune responses following infection with the same amount of infectious virus. The effect of different preparations of orally administered (vaccine) virus has become increasingly relevant following the finding of an as yet unexplained adverse effect (i.e. intussusception) of oral rotavirus vaccine.

Introduction

Immune-mediated gastrointestinal disorders including classic IgE-mediated food allergy (275), eosinophilic gastroenteritis (423), allergic colitis (391) and eosinophilic esophagitis (360) are primarily polygenic allergic disorders that involve Th2-type immune responses and are occurring with increased frequency in the developed countries. In infants, the immune system is skewed towards Th2 and thereby set favourably for IgE-mediated responses. Immunologic maturation is stimulated by different types of microbial exposure in early life that induce Th1 responses (134, 224).

In the so called "hygiene hypothesis" (406) it has been postulated that reduced exposure of young children to common infections of childhood may lead to delayed maturation of the immune system, reflected by skewing of the Th1/Th2 balance in favor of Th2, and an increased likelihood of developing IgE mediated allergies in atopic individuals. Matricardi et al., suggested a role of enteric pathogens, following the observation of a 60% reduction of allergic diseases in 20 yr old military recruits that had a history of exposure to food and orofecal pathogens (259, 260). Rotavirus is a common enteric infection in early childhood, and even in developed countries the great majority of children under 5 years of age

experience at least one rotavirus infection (102). Therefore, the effect of a rotavirus infection in early life on the infant immune system may be important in relation to the hygiene hypothesis. Worldwide approximately 440,000 children die each year from rotavirus diarrhea, mostly in the developing countries (313). For that reason, rotaviruses have received a high priority as a target for vaccine development. Most current rotavirus vaccine strategies are based on the use of heterologous (animal) rotaviruses to immunize humans to prevent subsequent infections with homologous (human) rotavirus (reviewed by (452).

Studies of natural rotavirus infection have relied for a major part on the mouse model. Infections with murine rotavirus result in diarrhea through epithelial dysfunction and the effects of the virus-encoded enterotoxin NSP4 when given before 15 days of age, after which mice no longer experience clinical signs but shed the rotavirus in stools for 7 days after oral inoculation (59, 357, 453). Non-murine (heterologous) rotaviruses can be used in the same experimental design as a model for rotavirus vaccine, thus allowing us to compare wild-type (homologous) infection with vaccination (129, 140). For these infections, however, studies on the virulence and replication in the gastrointestinal epithelium *in vivo* are limited (24, 149, 251). The dose of heterologous simian strains required to induce diarrhea in suckling mice is about 10^5 to 10^6 times higher than that required for a homologous murine virus strain. For that reason most of the studies on the oral heterologous rotavirus infections are done with unpurified tissue culture concentrates of rotaviruses. These crude virus preparations contain a mixture of complete and incomplete viral particles, as well as cellular proteins, and therefore are very different in antigenic composition from the (low dose) inocula used in the natural rotavirus infection. This lack of standardization makes a direct comparison of the data on rotavirus pathogenesis and immune responses for the different viruses very difficult. As part of ongoing studies on the hygiene hypothesis in which we measure the effects of rotavirus exposure on immune maturation and allergic challenge in young mice, we analyzed differences in the immune responses stimulated by different purified simian rotavirus SA11 fractions. Furthermore we examined the pathogenesis of a heterologous rotavirus infection by examining the induction of diarrhea, and timing and extent of rotavirus replication in the gastrointestinal epithelium in mice.

Materials and methods

Virus and antigen preparation

Two viruses were used in this study: The simian rotavirus SA11 was obtained from the American Type Culture Collection (ATCC, Rockville, MD) and the murine EDIM (Epizootic Diarrhea of Infant Mice) strain was provided by Dr. R. Ward, Children's Hospital Research Foundation, Cincinnati, USA. The EDIM strain was titrated by fluorescent focus assay in monkey kidney MA104 cells (453). SA11 rotavirus was serially plaque purified three times by limiting dilution in MA104 cells. SA11 virus (trypsin-activated by adding $10\mu\text{g/ml}$ at 37°C for 1hr) was subsequently grown at a multiplicity of infection (m.o.i.) of 0.1 on MA104-cells attached to cytodex-3 microcarriers in a 3-liter spin culture flask (Wheaton Science products, Millville, USA) in Eagle MEM supplemented with, 2 mM glutamine, penicillin, streptomycin, 0.125% NaHCO_3 and 0.5 $\mu\text{g/ml}$ trypsin (Sigma Chemical Company St. Louis, MO.). Cells and medium were harvested when 100% cytopathological effect (CPE) was observed, and subjected to one cycle of freezing and thawing. The lysate was extracted with 10% arklone (tri-chloro-tri-floroethane, ICI), centrifuged 30 min 3000 rpm

and the aqueous phase was concentrated by ultrafiltration through a 10,000 MW membrane (Millipore Corporation, Bedford, MA). Finally cesium chloride (CsCl) was added to the suspension to reach a final density of 1.37 g/ml. Rotavirus particles and cellular components were separated by density gradient centrifugation (35,000 rpm, 18 hr, 4°C in a SW 40Ti rotor (Beckman)). Three fractions enriched for double-shelled (1.34 g/cm³) and single-shelled (1.36 g/cm³) rotavirus particles, and cellular/virus components (1.26 g/cm³) were collected and dialyzed extensively against PBS. For each preparation, the infectivity and (predominant) type of particles were determined by virus titration assays on MA104 cells and electron microscopy (EM). Purified SA11 rotavirus ELISA antigen was obtained by centrifugation of the concentrated virus suspension (ultrafiltrated as described above) through a 40% sucrose cushion. The pellet was resuspended in PBS by vigorous pipetting, and stored frozen in -20°C in aliquots.

Preparation of monoclonal antibody AC3H7

This antibody was used for many years in the lab and produced as follows. BALB/c mice (6-10 week old) were immunized subcutaneously with 30µg CsCl purified double-shelled (ds) SA11 rotavirus emulsified in complete Freund's adjuvant, a second immunization 2 weeks later with 60 µg, and a final intravenous injection 1 week later with 100 µg purified ds SA11 rotavirus. Fusion of single cell suspension of splenocytes with myeloma P3-X63-Ag8653 cells was performed 3 days after the last vaccination using 40% polyethylene glycol and selection in HAT medium (455). Supernatants of wells with cell growth were screened for rotavirus specific IgG antibodies in an EIA as described below. Antibody-secreting hybridomas were cloned twice by limiting dilution. Five million viable cells were injected intraperitoneally into BALB/c mice previously primed with pristane (Sigma-Aldrich, Saint Louis, MO, USA). Ascitic fluid was harvested 1-2 weeks after cell inoculation, and stored at -70°C.

Animals

Pregnant BALB/c dams were obtained from Harlan CPB (Zeist, the Netherlands) at least 1 week before partus and housed in microisolator cages containing sterile bedding, water and ovalbumin depleted food. All pups used in the experiments were between 6-8 days of age. Experiments were reviewed and approved by the ethics committee of the National Institute of Public Health and the Environment.

Virus inoculation

Litters of 6-8 days old BALB/c mice were orally infected with 100 µl EDIM (2×10^4 focus forming units (FFU) or one of the three different CsCl purified fractions of SA11 rotavirus. The infectious virus titers of the fractions administered were standardized to 2×10^6 CCID₅₀ (cell-culture infectious dose 50%) per mouse. Control animals were inoculated with mock-infected cell lysate. Infected pups were examined daily for diarrhea by gentle palpation of the abdomen. Stools were scored from 0 to 4 based on color, texture and amount of stool. Normal feces were scored as 1, loose feces as 2, yellow feces as 3 and watery feces as 4. Stools with a score of ≥ 2 were considered as diarrhea (16). The daily proportion diarrheal samples was calculated by dividing their total by the total number of samples collected each day. Mice were anaesthetized with barbiturate/chloral hydrate i.p. and sacrificed. Segments of jejunum and ileum were collected immediately after euthanasia at different time points (1, 2, 4, 7, 10 and 14 days post infection) for 5 infected and 3 control mice per time point. Gut

sections were flushed in cold PBS and fixed in 4% (wt/vol) paraformaldehyde (Merck, Darmstadt, Germany) for 4 hours and embedded in paraffin wax using routine procedures (446). Twenty-one days after oral infection, blood samples were taken by retro-orbital puncture. Sera were stored at -20°C before testing.

Immunohistochemistry and *in situ* hybridization

To determine the presence of replicating virus, immunohistochemistry and *in situ* hybridization were used. Paraffin-embedded tissues were sectioned (5 µm), deparaffinized with xylene (Merck) and rehydrated in graded ethanol solutions. Sections were incubated overnight at 4°C using the rabbit polyclonal antibodies K3PPIV (1/1000) directed against rotavirus SA11 and the rabbit polyclonal antibodies directed against the rotavirus non-structural protein NSP4 (1/1000) as previously described (43, 346). *In situ* hybridization was performed as previously described using non-radioactive digoxigenin (DIG)-11-UTP labeled 750 bp NSP4 (SA11 strain) hydrolyzed in 80 mM NaHCO₃ and 120 mM Na₂CO₃, pH10.2 to obtain probes of various lengths (43, 91).

Detection of rotavirus specific serum antibodies

Rotavirus specific IgG, IgG1, IgG2a and IgA were determined by enzyme-linked immunosorbent assay (ELISA). After each incubation step the microtiter plates were washed four times with wash buffer (PBS supplemented with 0.05% Tween-20). Optimal dilutions of antigen, serum and conjugate were determined by checkerboard titration. Rotavirus specific IgG levels were measured by coating 96-wells maxisorp microtiter plates (Nalgene Nunc International, Roskilde, Denmark) with 1/100 dilution of polyclonal rabbit anti SA11 serum (K3PPIV) in coating buffer (0.05 M sodium carbonaat buffer [pH 9.6]. After an overnight incubation at 4°C, 100 µl of sucrose purified SA11 virus, 1/100 diluted in dilution buffer (PBS plus 0.5% Tween-20 plus 1% BSA) was added and incubated for 1 hour at 37°C. Subsequently, plates were loaded with 1/50 diluted mouse serum samples in dilution buffer and a pool of known positive and negative sera from rotavirus infected and sham infected mice respectively as controls. Plates were incubated for 1 hour at 37°C. The detector, phosphatase-conjugated goat anti-mouse Immunoglobulin G (Sigma Chemical Company St. Louis, Mo.) was added for 1 hour at 37°C. Incubation of the substrate p-nitrophenylphosphate in a concentration of 1 mg/ml in 0.1 M glycine buffer (pH 10.4) was at room temperature for 10 min. The absorption values were measured at a wavelength of 405 nm in an ELISA reader (Organon Teknika, Boxtel, Netherlands). A sample was considered positive when the OD was above the cutoff levels (mean + 3 SD of the samples of non-immunized mice).

For the detection of rotaspecific IgA titers in serum a capture ELISA was performed. Briefly, 96-well microtiter plates (Nalgene Nunc International, Roskilde, Denmark) were coated overnight at 4°C with goat anti-mouse IgA (Sigma Chemical Company St. Louis, Mo.) in coating buffer. Serum samples were diluted 1/100 in dilution buffer and added to the plates. After an incubation of 1 hour at 37°C the plates were incubated with sucrose purified SA11 virus, 1/100 diluted in dilution buffer for another hour at 37°C. Monoclonal antibody anti-rotavirus SA11 [AC3H7] conjugated with horseradish peroxidase was added for 1 hour 37°C as a detector. After incubation with the substrate 3,3',5,5'-tetramethyl-benzidine (Sigma Chemical Company St. Louis, Mo.) for 5 min at room temperature the absorption values were measured at a wavelength of 450 nm in an ELISA reader (Organon Teknika, Boxtel, Netherlands). The test was valid when the OD of the known positive control serum was

above 1.000 and a sample was considered positive when the OD was above the cutoff levels (mean + 3 SD of negative sera from sham infected mice).

Detection of viral shedding

Intestinal contents were collected from each sacrificed mouse at different time points (0-14 days) post infection and stored at -20°C . Fecal suspensions (10%) were prepared in PBS, clarified by centrifugation (1000g for 5 min) and analyzed by ELISA using the Premier rotaclone kit (Meridian Diagnostics, River Hills, USA) according to the manufacturer's instructions or cultured on MA104 cells.

Statistical analysis

Statistical analysis of all data was performed using Student's *t*-test for unpaired data (two-tailed). Data were expressed, as the mean \pm SEM and P values of ≤ 0.05 were considered statistically significant.

Results

Virus preparation

CsCl fractionation of SA11-infected cell supernatant yielded three distinct visible bands in the gradient containing single shelled particles, double shelled particles and cell components respectively as determined by electron microscopy (EM) (Fig.1). Virus titers were $10^{9.1}$, $10^{10.0}$ and $10^{7.6}$ per ml, respectively. The final rotavirus antigen concentrations of the inoculated fractions as measured by ELISA were higher in fractions 1 (ss) (OD value 900) and 3 (mix) (OD >1400) compared to fraction 2 (ds) (OD 200) as shown in Fig. 1.

Diarrhea in newborn mice inoculated with different fractions of simian SA11 and murine EDIM rotavirus strains

The development and duration of diarrhea after inoculation with the different fractions of the heterologous SA11 rotavirus (2×10^6 CCID₅₀) and homologous EDIM (2×10^4 FFU) over a period of seven days varied among the different CsCl fractions compared with wild type virus strain (Fig. 2). All virus preparations induced diarrhea in the newborn animals. In mice inoculated with the EDIM strain and SA11 fraction 3 (enriched with cell components) diarrhea was observed from day 1 after inoculation in respectively 45 and 30% of the animals, whereas diarrhea was observed from day 2 onwards in the groups inoculated with the other gradient purified fractions of SA11. Viral shedding in the EDIM inoculated group was observed from day 2 up to day 10 as we reported earlier (43) and no viral shedding was found in the SA11 infected animals (data not shown).

Rotavirus-specific serum antibody responses in mice inoculated with different preparations of SA11 and the EDIM rotavirus strain

Systemic rotavirus specific antibody responses (IgA, IgG, IgG1 and IgG2a) were measured in serum of individual mice at day 21 after inoculation. High rotavirus specific IgG responses were obtained in the EDIM-infected group, and in mice inoculated with SA11 fractions 1,2 and 3 (Fig.3A). The mean IgG responses were significantly higher in the SA11 fraction 3 infected animals compared to EDIM or the other fractions ($p < 0.05$). The IgA responses on

the other hand were much lower in all SA11 infected animals compared to the EDIM infected animals (Fig. 3B).

To examine the role of replication in the induction of IgA and IgG responses we orally inoculated mice with UV inactivated SA11 triple layered virus particles (fraction 2) corresponding to an original titer of 2×10^6 CCID₅₀. We found a marginal IgG (one positive out of 25 mice) and no IgA responses in these mice (Fig.3), similar as in the mock-infected animals.

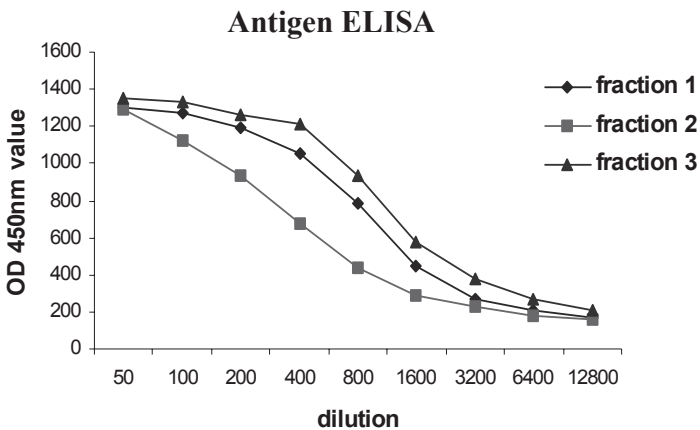
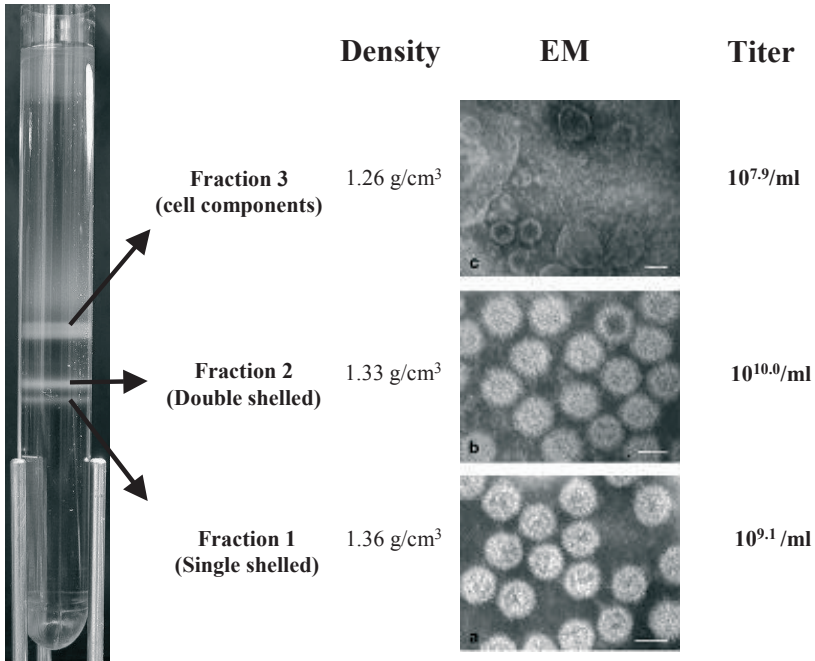


Figure 1. Virus preparations of SA11 infected cell supernatant. Virustitration, electron microscopy and rotavirus antigen ELISA determined the infectivity and type of particles and rotavirus antigen concentrations for each CsCl purified fractions of SA11.

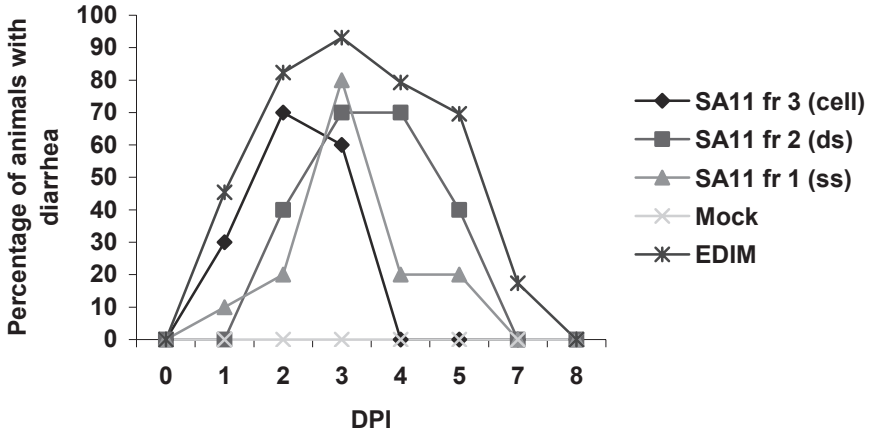


Figure 2. Proportion of neonatal mice with diarrhea following oral inoculation with rotavirus murine EDIM strain or different CsCl purified fractions of simian SA11 strain or mock control. All fractions contained 1×10^6 TCID₅₀ as determined by virus titration.

We then tested sera for specific IgG subtype responses, plotted as the IgG1/IgG2a ratio of SA11 compared to the EDIM group (Fig. 4). The IgG1/IgG2a ratio of specific antibodies in sera from mice inoculated with EDIM and fraction 1 (ss) of SA11 were similar but a significantly higher ratio was observed in the mice infected with fraction 3 of SA11. Furthermore the fraction 2 (ds) serum IgG1/IgG2a ratio of SA11 infected mice was significantly lower than that of EDIM infected mice and fraction 3 (Fig.4).

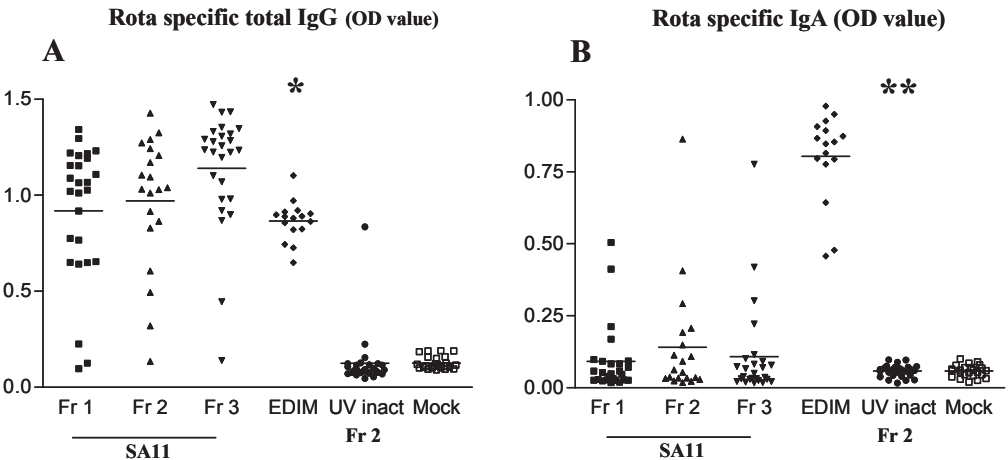


Figure 3. Systemic rotavirus-specific antibody responses in neonatal mice orally inoculated with rotavirus murine EDIM strain or different CsCl purified fractions of simian SA11 strain or mock control. Serum antirotavirus IgG (A) and IgA (B) levels were determined using ELISA from blood samples collected 21 days after inoculation. The data represent individual sera and the median. * ($p < 0.05$) fraction 3 compared to fr1, fr2 and EDIM. ** ($p < 0.01$) EDIM compared to fr1, fr2 and fr3.

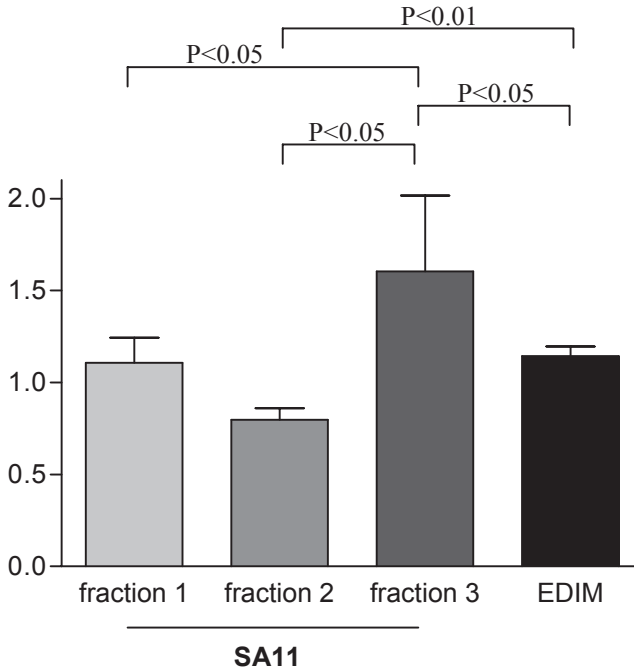


Figure 4. Ratio of anti rotavirus IgG1/IgG2a subclass responses in serum of neonatal mice orally inoculated with rotavirus murine EDIM strain or different CsCl purified fractions of simian SA11 strain. Serum anti-rotavirus IgG1 and IgG2a levels were determined using ELISA from a 1/50 dilution of blood samples collected 21 days after inoculation. The data represent the mean value \pm SEM. * ($p < 0.01$) fraction 1 compared with fraction 3; ($p < 0.05$) # EDIM compared to fraction 1.

Histological changes in the small intestine during rotavirus infection

Histopathological changes in the small intestine were observed at 1 day past infection (dpi), and persisted through 7 dpi. In the EDIM as in the SA11 rotavirus fraction 2 infected animals throughout the whole intestine (duodenum, jejunum and ileum), these changes were characterized by swollen villus tips with enterocytes containing large vacuoles shown for 1 dpi post infection in the jejunum (Fig.4). After 7 dpi almost complete resolution of the histopathological changes was observed (data not shown). In control animals no vacuoles were seen at any time-point. To determine the presence of replicating rotavirus in the small intestine, NSP4 and rotavirus structural proteins were detected by immunohistochemistry and NSP4 mRNA was detected by in situ hybridization. At 1 dpi rotavirus structural -protein, NSP4 protein and mRNA were detected in almost all epithelial cells of the upper part of the small intestinal villi of EDIM-infected mice. No rotavirus proteins or mRNA could be detected in any section of the small intestine of SA11-infected or control mice at any time-point (Fig.5).

Discussion

In most studies of immune response against heterologous rotavirus infections, crude concentrates of cell-culture grown virus are used (129, 140, 187, 209, 267, 270). That means

that in addition to the virus, these preparations contain unknown and non-standardized amounts of cellular proteins. We postulated that the type of purification of the viruses used in such infection experiments might influence the ensuing immune responses, thus leading to potentially ambiguous conclusions. The present study was designed to gain more insight into the influence of different preparations of the simian SA11 rotavirus on the immune response following oral delivery to suckling BALB/c mice. We found that each of the purified fractions of SA11, corresponding with the two forms of virus particles (double-shelled and single-shelled) and infected-cell components, are able to induce diarrhea in seven days old suckling BALB/c mice but with different kinetics. These fractions are enriched, but do not exclusively contain the specified components; infectious virus was present in all fractions administered but in different amounts. The preparations were standardized to 2×10^6 CCID₅₀ per mouse and effects were compared with those following infection with the murine EDIM strain (2×10^4 FFU per animal). This standardization resulted in great differences in antigen content of the preparations. Nevertheless, similar serum IgG antibody responses were found in the different groups with a slightly higher response in the mice infected with the fraction with the highest concentration of cell components, which had the highest antigen content (fr. 3). The IgG subtype responses were not equally distributed and we found a significantly higher IgG1/2a ratio in the animals inoculated with fraction 3 compared to the other fractions and the EDIM infected animals. This indicates an more Th2-like immune response following infection with rotavirus in the presence of abundant cell associated protein compared with infection with a more purified preparation or with EDIM (134). This shows that the composition of the fractions influences the outcome of the immune responses following infection with the same amount of infectious virus. This 'adjuvant' effect may be the result of the increased amount of antigen to which these mice are exposed, or result from adjuvant effect of an unknown component of infected cells. The effect of different preparations of orally administered (vaccine) virus has become increasingly relevant following the finding of an as yet unexplained adverse effect (i.e. intussusception) of oral rotavirus vaccine (287). This raised questions about the exact effect of heterologous rotavirus infection on the (neonatal) gut. There are additional reasons for this increased interest:

Immune-mediated gastrointestinal disorders including classic IgE-mediated food allergy (275), eosinophilic gastroenteritis (423), allergic colitis (391) and eosinophilic esophagitis (360) are primarily polygenic allergic disorders that involve Th2-type immune responses and are occurring with increased frequency in the developed countries. Concomitantly, an increased prevalence of Th1-driven diseases like inflammatory bowel disease (IBD) (413, 450) is seen. Therefore a better understanding of the factors that influence the development of a balanced mucosal immune response is essential. Mucosal vaccinations are part of the challenges of the immunological balance.

The IgA titers were lower for the three fractions of SA11 compared to the EDIM strain despite comparable IgG titers. This observation has been found previously (385) and may be related to reduced replication in the intestine of the heterologous SA11 strain compared to the murine EDIM strain since replication is an important determinant of IgA responses to rotavirus. Indeed we did not find measurable virus shedding in the SA11-infected animals whereas virus antigen was readily detected in feces of the EDIM-infected animals. Contradictory to this observation is the fact that we did find diarrhea in infected animals up to 1 week after oral delivery of the SA11 virus. This suggests that replication took place since NSP4, thought to be important for the induction of diarrhea in young siblings, is not found in mature infectious virus particles and is only synthesized within the host cells during

virus replication (16). We cannot exclude the possibility of contamination with a small amount of NSP4 protein in the double-shelled and single-shelled particle fractions produced during virus growth in cell culture. Ball et al. (16) reported that diarrhea was observed within 1 to 4 hours after inoculation of purified NSP4, which continued for up to 8 hours but occasionally persisted for 24 hours. Therefore, the diarrhea on day 1 in mice inoculated with fraction 3 may be explained by the presence of free NSP4. It seems unlikely that this was the case for mice inoculated with fraction 2 in our study as UV treatment resulted in abolishment of diarrhea and immune response.

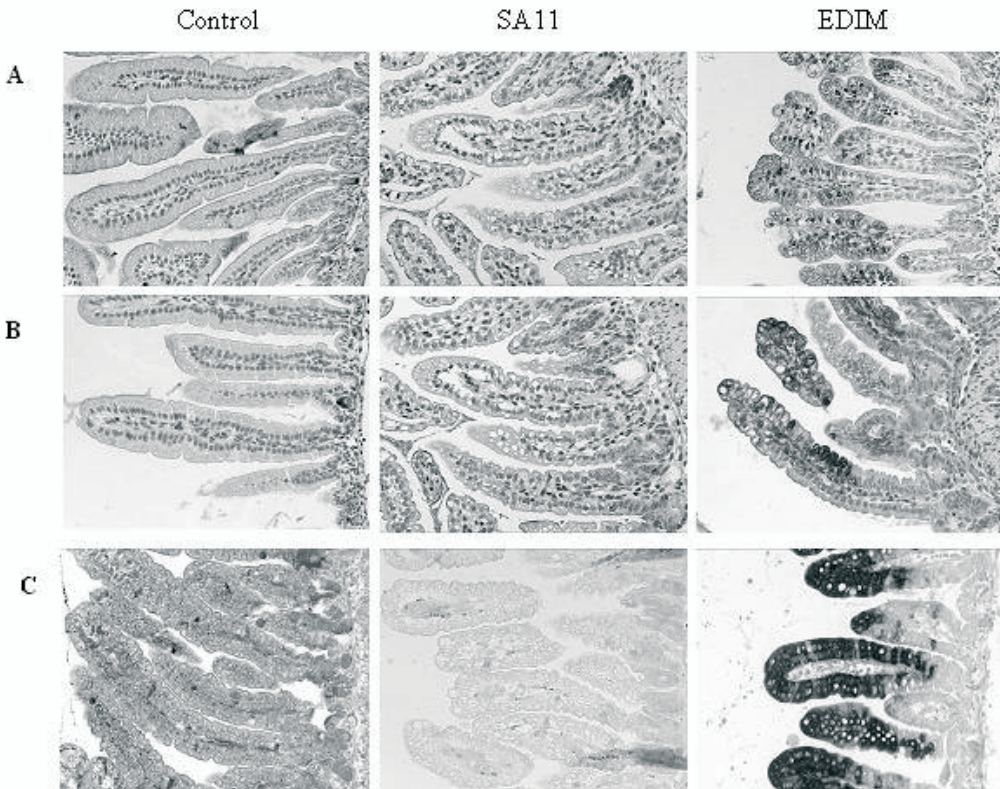


Figure 5. Histological analysis of rotavirus replication in the small intestine in neonatal mice 2 days post oral inoculation with rotavirus murine EDIM strain or CsCl purified fraction 2 of simian SA11 strain or mock control. Sections were stained using polyclonal anti-rotavirus antigen (A) and NSP4 protein expression in jejunum was detected by immunohistochemistry (B) and NSP4 mRNA was detected by in situ hybridization (C).

To further study the effects of heterologous infection, we examined intestinal sections from the mice infected with SA11 fraction 2 and EDIM. We observed large vacuoles in the small intestinal enterocytes of the villus following rotavirus exposure with the SA11, similar to those observed after EDIM infection (43). As indicated by the lack of viral shedding, we could not detect virus replication in the small intestine either by immunohistochemistry or *in situ* hybridization in SA11-infected mice, in contrast to observations in the EDIM inoculated mice. This suggests that replication may have occurred extraintestinally, as shown by Uhnoo et al. who found that infection with a heterologous rhesus rotavirus resulted in hepatitis in

84% of SCID and 21% of BALB/c mice (430). Furthermore, Blutt and coworkers showed viraemia and antigenaemia in infected patients and in animal models, suggesting that extraintestinal spread might be a common event (40). We cannot rule out intestinal replication as only a small segment of the different regions were analyzed by immunohistochemistry and *in situ* hybridization. However, replication of the heterologous SA11 virus at a non-mucosal site could explain the low induction of (mucosal) IgA with a high systemic IgG response. In case of extraintestinal replication of the virus, the histological damage and diarrhea might be induced by a secreted viral factor and not by direct viral cpe (77, 306). A candidate factor could be NSP4, which is thought to mediate cell signaling by increasing intracellular calcium levels leading to chloride secretion in uninfected cells and diarrhea in young mice (16).

Recently, we have shown that after EDIM infection of mice, NSP4 is produced in and secreted basolaterally from infected enterocytes (44). It is tempting to speculate that the basolaterally secreted NSP4 can subsequently be transported via the blood stream to the small intestine and initiate the pathological damage and diarrhea in inoculated mice. In summary, we show that the polarization of the immune response (Th1/Th2) against heterologous rotavirus is depending on the exact composition and the purification of the inoculum used, and that the level and possibly site of replication differs from wild-type rotavirus infection. Furthermore, it is demonstrated that the mucosal immune response is lacking after a heterologous infection by SA11. These factors should be evaluated with new rotavirus vaccines in upcoming trials, as they may have a significant impact on the neonatal immune system.

Acknowledgements

We would like to thank Rahena Binda for her excellent technical assistance and dr. P.J.M. Roholl for the EM pictures. This work was supported by grants from the Sophia Foundation for Medical Research (SSWO), and the Netherlands Digestive Diseases Foundation (MLDS).

The rotavirus enterotoxin NSP4 binds to the extracellular matrix proteins laminin- β 3 and fibronectin

J.A. Boshuizen^{§*}, J.W.A. Rossen[†], C.K. Sitaram[§], F.F.P. Kimenai[§], Y. Simons-Oosterhuis[§], C. Laffeber[§], H.A. Büller[§], and A.W.C. Einerhand[§].

Abstract

Rotavirus is the most important cause of viral gastroenteritis and dehydrating diarrhea in young children. The rotavirus non-structural protein 4 (NSP4) is an enterotoxin that was identified as an important agent in symptomatic rotavirus infection. To identify cellular proteins that interact with NSP4, a two-hybrid technique with *Saccharomyces cerevisiae* was used. NSP4 cDNA, derived from the human rotavirus strain Wa, was cloned into the yeast shuttle vector pGBKT7. An intestinal cDNA library derived from Caco-2 cells cloned into the yeast shuttle vector pGAD10 was screened for proteins that interact with NSP4. Protein interactions were confirmed in vivo by coimmunoprecipitation and immunohistochemical colocalization. After two-hybrid library screening, we repeatedly isolated cDNAs encoding the extracellular matrix (ECM) protein laminin- β 3 (aa 274–878) and a cDNA encoding the ECM protein fibronectin (aa 1755–1884). Using deletion mutants of NSP4, the region of interaction with the ECM proteins was mapped between aa 87–145. Deletion analysis of laminin- β 3 indicated that aa region 726–875 of laminin- β 3 interacts with NSP4. Interaction of NSP4 with either laminin- β 3 or fibronectin was confirmed by coimmunoprecipitation. NSP4 was present in infected enterocytes and in the basement membrane (BM) of infected neonatal mice and colocalized with laminin- β 3, indicating a physiological interaction. In conclusion, the two-hybrid screening with NSP4 yielded two potential target proteins, laminin- β 3 and fibronectin, interacting with the enterotoxin NSP4. The release of NSP4 from the basal side of infected epithelial cells and the subsequent binding to ECM proteins localized at the BM may signify a new mechanism by which rotavirus disease is established.

Introduction

Rotavirus is the most important cause of a severe, life-threatening viral gastroenteritis and dehydrating diarrhea in young children (123, 203). Mortality rates are low in developed countries, but about 440,000 children <5 years of age die each year in developing countries because of an infection with rotavirus (313). The high incidence of rotavirus disease, especially in developing countries, calls for the development of effective vaccines. However, efforts to develop safe and useful rotavirus vaccines are continuing, since the first vaccine routinely used in the U.S. was suspended in 1999 because of a possible association with intussusception (287).

The nonstructural protein NSP4 encoded by rotavirus gene 10 has been shown to play a key role in viral morphogenesis (11, 12, 122, 271). In the ER membrane, NSP4 functions as a receptor for newly formed virus particles that are translocated across the ER membrane (11). Increasing lines of evidence show that NSP4 is involved in pathogenicity of rotavirus infection and that it acts as a viral enterotoxin (16, 173, 276, 374). When administered to young mice, NSP4 from different rotavirus groups, or a synthetic peptide corresponding to aa 114–135 was able to induce age-dependent diarrhea (16, 173, 276, 374). After being secreted from infected cells, NSP4 is thought to mediate phospholipase C (PLC) dependent cell signaling by increasing intracellular calcium levels leading to chloride secretion in adjacent uninfected cells (16, 114, 280, 421). Studies with cystic fibrosis knockout mice imply that the age-dependent diarrhea-inducing properties of NSP4 are due to age-dependent changes in calcium-mediated anion permeability (280). Recent studies indicate that a specific cleavage

product of NSP4 (aa 112-175) is actively secreted from infected cells and that NSP4 is released from the apical side of infected epithelial cells via an atypical pathway that bypasses the Golgi apparatus and involves lipid microdomains called rafts (373, 480). Consistent with its proposed apical secretion, only apical but not basolateral administration of NSP4 was found to cause a reduction in the transepithelial electrical resistance (TER) and redistribution of Zonula occludens-1 in MDCK-1 cells (411). On the other hand, NSP4 is able to cause chloride secretion when added to either the apical (luminal) or basal (submucosal) surface of mouse mucosal sheets (16), indicating that NSP4 is possibly also active at the basal side of the intestinal epithelium.

Laminin and fibronectin are multifunctional proteins with diverse biological activities. They can influence cell adhesion, growth, morphology, differentiation, migration, and agglutination as well as the assembly of the extracellular matrix (ECM) (86, 329). Members of the laminin family of glycoproteins are major constituents of basement membranes (BMs), ECMs found in close contact with individual cells and cell layers. Each laminin is a heterotrimer assembled from α , β , and γ chain subunits, secreted and incorporated into cell-associated ECMs. Laminins can be found in association with other BM components (collagens, proteoglycans, and nidogens) and with a variety of other macromolecules including fibronectin and growth factors (422, 475). Through these interactions, laminins contribute to cell differentiation, cell shape and movement, maintenance of tissue phenotypes, and promotion of tissue survival. Laminin-5, a heterotrimer of $\alpha 2$, $\beta 3$, and $\gamma 2$ chain subunits, can bind to $\alpha 3\beta 1$, $\alpha 6\beta 4$, and $\alpha 6\beta 1$ integrins (64, 253, 292) and is distributed in BMs in several epithelial tissues including the intestine (75, 243). Fibronectin is a large multidomain protein that can exist in multiple forms that arise from alternative splicing of a single pre-mRNA (131, 220). Fibronectin mediates a wide variety of cellular interactions with the ECM and plays important roles in cell adhesion, migration, growth and differentiation (311). Each monomer consists of three types of repeating units (termed FN repeats): type I, type II and type III. These repeats account for approximately 90% of the fibronectin sequence and are also found in other molecules (311, 314). Fibronectin can be a ligand for many members of the integrin receptor family, including $\alpha 5\beta 1$, $\alpha 4\beta 1$, $\alpha 4\beta 7$, $\alpha 9\beta 1$ (329), and it has several heparin binding sites (17, 60, 185).

In this study, we used a two-hybrid system with *Saccharomyces cerevisiae* to identify proteins that interact with NSP4. After screening, we repeatedly isolated cDNAs encoding the ECM proteins laminin- $\beta 3$ and fibronectin. The region of NSP4 responsible for interaction with both proteins was mapped between aa 87-145. Binding of NSP4 to laminin- $\beta 3$ and fibronectin was further confirmed by coimmunoprecipitation in rotavirus-infected Caco-2 cells and colocalization in the BMs of neonatal mice infected with rotavirus. These findings might reveal a novel pathway via which NSP4 is involved in rotavirus-induced diarrhea.

Materials and Methods

Two-hybrid screening

The Matchmaker system 3 two-hybrid assay in the yeast *S. cerevisiae* (Clontech) (76, 132) was used to detect interactions between NSP4 and cellular proteins. An intestinal cDNA library derived from Caco-2 cells cloned into the yeast shuttle vector pGAD10 was obtained from C. Mitchelmore and O. Norén, Copenhagen, Denmark. The construct used as bait corresponded to the NSP4 protein of human rotavirus (Wa strain). The NSP4 bait lacked the

hydrophobic N-terminus (aa 1-86) and was designated NSP4 Δ N (nt 300-750 and corresponding to aa 87-175). To obtain the pGBKT7-NSP4 Δ N bait a RT-PCR was performed with RNA from rotavirus Wa infected MA104 monkey kidney cells. NSP4 Δ N was cloned using a NSP4 forward primer (5'-GGTACCATGGAGCAGGTTACTACAAAAGACG-3') based on the NSP4 Wa coding sequence (nt 300-321; accession number AF093200 (68) and a reverse primer (5'-TCCCCCCGGGTCACATTAAGACCGTTCCT-3') based on the SA11 coding sequence (nt 730-750) (46). With these primers a *Nco*I restriction site was introduced at the 5' (underlined) end and a *Sma*I restriction site was introduced at the 3' end to allow in-frame insertion into the plasmid pGBKT7 (Clontech) containing the GAL4 DNA binding domain. The *S. cerevisiae* AH109 strain (Clontech) containing the four reporter genes *ADE2*, *HIS3*, *MEL1* and *lacZ* was cotransfected with the pGBKT7-NSP4 Δ N bait plasmid and the pGAD10 Caco-2 cDNA library by the lithium acetate method (144, 379). AH109 cells were grown on plates containing medium lacking tryptophan and leucine (Trp⁻ Leu⁻) to select for the presence of both the bait and the library plasmids. 2 X 10⁶ of these double transformants were then grown on dropout medium deprived of tryptophan, leucine, histidine and adenine (Trp⁻ Leu⁻ His⁻ Ade⁻) to select for protein-protein interactions. Transformants that grew were assayed for α -galactosidase activity on X- α -Gal plates according to the manufacturer's instructions (Clontech). Plasmids were extracted from blue yeast clones and were then transfected into *Escherichia coli* DH5 α . Bacteria were grown on medium with ampicillin to select for bacteria containing library plasmids. The plasmid DNA was then isolated and sequenced with an ABI 310 sequencer using a primer identical to nt 788-820 of the pGAD10 cloning vector and a primer reverse complementary to nt 862-893 of the pGAD10 vector as a forward and reverse primer, respectively. Homology searches were performed using the National Center for Biotechnology Information database with Mega BLAST. All positive constructs were rescreened for their ability to grow on complete dropout medium when transfected together with the NSP4 bait or with the empty pGBKT7 plasmid to verify potential interactions and to eliminate false positives.

Serum and monoclonal antibodies

For immunostaining and immunoprecipitation experiments, we used the following antibodies: a NSP4 polyclonal rabbit hyper immune serum directed against aa 114-135 of the NSP4 SA11 strain (43), a rabbit polyclonal serum against aa 120-147 of SA11 NSP4 (480), a rabbit hyperimmune serum raised against SA11 rotavirus particles (43), the rabbit polyclonal anti-laminin- β 3 (H300, Santa Cruz), the rabbit polyclonal anti-fibronectin (Sigma), and the goat polyclonal anti-laminin- β 3 (C-19, Santa Cruz). Peroxidase-conjugated secondary antibodies were purchased from DAKO.

Immunohistochemistry

Tissue was obtained from 7-day-old BALB/c mice that were inoculated intra-gastrically with 2 x 10⁴ focus forming units (ffu) of the EDIM rotavirus strain as previously described (43). At different time points after infection, mice were sacrificed and tissue from the small intestine was fixed for immunohistochemistry as previously described (43). Deparaffinized and rehydrated sections of neonatal control mice and mice infected with the murine EDIM strain (43) were incubated overnight at 4°C using the following rabbit polyclonal antibodies, anti-NSP4 (114-135; 1:1000), anti-NSP4 (120-147; 1:1000), anti-SA11 (1:1500), or anti-laminin- β 3 (1:500). Immunohistochemistry was carried out as described previously (43,

346), however antigen unmasking for laminin- β 3 was carried out by heating the sections for 10 min in 0.01 M sodium citrate (pH 6.0) at 100°C and additional treatment with protease XXIV (Sigma) for 10 min at 37°C. The slides were analyzed by microscopy using a Nikon eclipse 800 microscope and Leica IM-500 software.

Infection of Caco-2 cells, co-immunoprecipitation, and Western blotting

Human colonic adenocarcinoma Caco-2 cells (Numico Research, Wageningen, The Netherlands) were grown and maintained in 75 cm² tissue culture flasks in DMEM (Dulbecco's Modified Eagle's Medium; Gibco BRL) with glutamax-1, pyridoxine, 0.11g/L sodium pyruvate, 4.5 g/l glucose, 10% fetal calf serum (Integro), 100 U/ml penicillin (Sigma), 100 μ g/ml streptomycin (Sigma) and non essential amino acids (Bio Whittaker Europe, Verviers, Belgium) at 37°C and 5% CO₂ in a humidified atmosphere. One day prior to infection, Caco-2 cells were seeded in 175 cm² tissue culture flasks at 2.6 X 10⁵ cells per cm².

The human rotavirus strain Wa was obtained from Dr. M.Koopmans (National Institute for Public Health and the Environment, Bilthoven, The Netherlands), was activated using 10 mg/ml trypsin (Sigma) at 37°C for 1 h. Rotavirus was diluted to 2 x 10² ffu/ml (corresponding to a multiplicity of infection of 0.5) in serum free DMEM. Cells were infected with rotavirus at 37°C, and 5% CO₂ in a humidified atmosphere. After 15 h of incubation, cells were washed in phosphate-buffered saline (PBS) and harvested into Tris lysis buffer (20mM Tris pH7.5, 100mM NaCl, 0.5% NP-40, 0.5 mM EDTA, 0.5 mM PMSF, 10 μ g/ml Leupeptin, 10 μ g/ml aprotinin and 10 μ g/ml SBTI). Cells were swelled on ice for 10 minutes and then lysed by 10 passages through a 23-gauge needle. The cellular homogenate was centrifuged at 10,000 X g for 10 min. Lysates (corresponding to 2.35 X 10⁶ cells) were immunoprecipitated with anti-NSP4 antibody for 2 h at 4°C, and then 25 μ l of protein A-Sepharose CL-4B beads (Pharmacia) was added to the mixture and incubated for another 2 h at 4°C. Beads coupled to immune complexes were washed three times with Tris lysis buffer. The immune complexes were then suspended in 3X SDS-PAGE sample buffer and analyzed by sodium dodecyl sulfate-polyacrylamide gel electrophoresis (SDS-PAGE; 7.5% or 10% polyacrylamide) and Western blotting. Proteins were transferred to nitrocellulose membranes (Nitran; Schleier & Schuell, Dassell, Germany) and were consecutively incubated with the rabbit polyclonal antibodies anti-NSP4 (114-135; 1:1000) and anti-fibronectin (1:500) or the goat polyclonal antibody anti-laminin- β 3 (1:500) and peroxidaseconjugated anti-rabbit or anti-goat secondary antibodies (1:2000). Bands were revealed by enhanced chemiluminescence (ECL), according to the instructions by the manufacturer (Amersham).

Deletion analysis of NSP4 and laminin- β 3

Five NSP4 deletion fragments and five laminin- β 3 deletion clones were obtained by PCR. For all forward primers used to create deletion mutants of NSP4 an *Nco*I site (underlined) was added at the beginning of the forward primer to direct in-frame subcloning in the pGBKT7 plasmid.

The NSP4 clones NSP4-(87-114), NSP4-(87-145), NSP4-(113-145), NSP4-(145-175), and NSP4-(113-175) were obtained using the following primers; 5'-GGTACCATGGAGCAG-GTTACTACAAAAGACG-3' and 5'-ATCAATCATCTCCAGCTGACCTCTC-3' (nt 301-321 and nt 359-383); GGTACCATGGAGCAGGTTACTACAAAAGACG-3' and 5'-CCTTCGACATATCTATAACG-3'(nt 301-321 and nt 461-480); 5'-ACGCCATGGT-

GATTGATAAACTAACTACTCG-3' and 5'-CCTTCGACATATCTATAACG-3'(nt 376-397 and nt 461-480); 5'-ATAGCCATGGCGAAGGAATTCAATCAGAA-3' and 5'-TCAACC TCTCACATGGATGC-3'(nt 475-493 and nt 558-577); 5'-ACGCCATGGGTG-ATTGATAAACTAACTACTCG-3' and 5'-TCAACCTCTCACATGGATGC-3' (nt 376-397 and nt 558-577), based on accession number AF093200 (68). Primers for human laminin- β 3 were based on the sequence with accession number NM_000228 (143). The laminin- β 3 fragments corresponding to aa regions 274-377 (nt 903 to 1212), 368-497 (nt 1185-1572), 488-618 (nt 1545-1935), 605-739 (nt 1896-2298), and 726-875 (nt 2259-2706) were obtained by PCR using the following oligonucleotides; 5'-GAATTCGTCCACGATGTCTGTGTCTGC-3' and 5'-GGTCTCCTGAATGGAAGCTCC-3'; 5'-GAATTCGGAGCTTCCATTCAGGAGACC-3' and 5'-CTGGTTGCACTGTGGGCTGAG-3'; 5'-GAATTCCTCAGCCCACAGTGCAACCA-3' and 5'-CTCCAGCC-CAGGCCCTGACCA-3'; 5'-GAATTCACCGCCAGCCTGTGGTCAGGG-3' and 5'-GCGCGAGCTGTCGGAGACCTG-3'; 5'-GAATTCAGGCTGCTCAGCAGGTCTCC-3' and 5'CCTGGGTCTCCAAGCGCTGGG-3', respectively. An *Eco*RI site (underlined) was added at the beginning of the forward primers to direct in-frame insertion in the pGADT7 plasmid containing the GAL4 activation domain. All constructs were controlled by DNA sequencing and expression of the corresponding fusion proteins in yeast cells.

We investigated the interaction of the fragmented NSP4 proteins with a pGAD10 laminin- β 3 library clone (D19), the fragmented laminin- β 3 clones in the PGADT7 vector, and the pGAD10 fibronectin library clone in yeast cells. Qualitative and quantitative results were obtained by assessing the ability of yeast to grow in the absence of histidine and adenine (Trp⁻ Leu⁻ His⁻ Ade⁻), by the appearance of blue colonies in the presence of X- α -Gal (5-bromo-4-chloro-3-indolylphosphate), and by assaying the α -galactosidase activity of yeast grown in liquid medium with the chromogenic substrate PNP- α -Gal (*p*-nitrophenyl- α -D-galactopyranoside; Sigma-Aldrich) according to the manufacturer's instructions (Clontech).

Statistical analysis

Statistical analysis of all data was performed using Student's *t*-test for unpaired data (two tailed). Data were expressed as the mean \pm SEM and *P* values of ≤ 0.05 were considered statistically significant.

Results

Identification of proteins binding to NSP4

To identify host cell proteins that interact with the NSP4 enterotoxin of rotavirus, we used the yeast two-hybrid approach. NSP4 cDNA, derived from the human rotavirus strain Wa, was cloned into the yeast shuttle vector pGBKT7. We used amino acid region 87-175 of NSP4 (NSP4 Δ N) to screen an intestinal Caco-2 cell cDNA library, since the first 86 amino acids of NSP4 contain three hydrophobic domains. These domains could possibly interfere with the two-hybrid system, since the fusion proteins have to travel into the nucleus of the yeast cell where transactivation of the reporter genes occurs. Additionally, many functionally properties of NSP4 are located between amino acid 112 and 175 (12, 16, 163, 480). The intestinal cDNA library derived from Caco-2 cells was screened for proteins that might interact with NSP4 Δ N. The Caco-2 cell line has enterocyte-like characteristics and can be infected by the human rotavirus Wa strain. In total 238 transformants were able to activate

transcription of all reporter genes (*MEL1*, *HIS3*, *ADE2*). These transformants grew in the absence of histidine and adenine and showed blue colonies in the presence of X- α -Gal substrate. After re-screening, restriction analysis, and sequencing, twenty-three clones fused to the activating domain of GAL4 were identified.

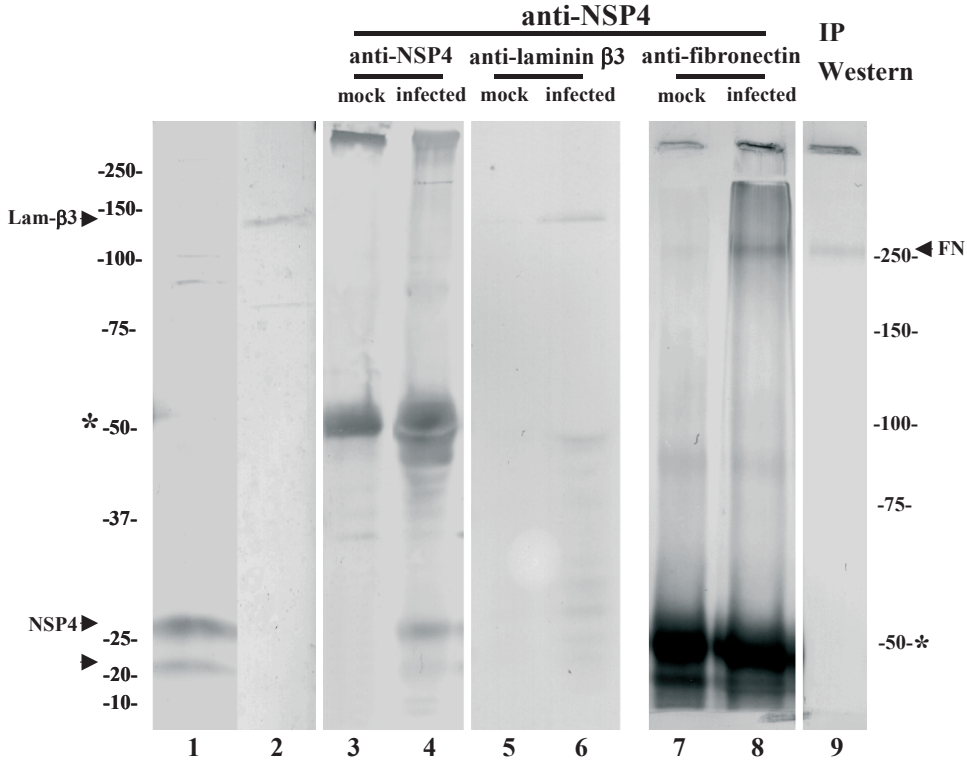


Figure 1. Coimmunoprecipitation of NSP4 and laminin- β 3, and NSP4 and fibronectin protein in infected Caco-2 cells. NSP4 (fully glycosylated form 28 kD, nonglycosylated form 20 kD, lane 1), laminin- β 3 (Lam β -3, 140 kD, lane 2) and fibronectin (FN, 250 kD, lane 9) were detected by Western blotting in lysates from respectively infected (NSP4) and mock-infected Caco-2 cells (laminin- β 3 and fibronectin) using specific antibodies. Lysates from infected or mock-infected Caco-2 cells were subjected to immunoprecipitation with protein A-Sepharose beads loaded with anti-NSP4 antibody (lanes 3 to 8). Immunoprecipitates were analyzed by SDS-PAGE and anti-NSP4 (lanes 3 and 4), anti-laminin- β 3 (lanes 5 and 6), or anti-fibronectin (lanes 7 and 8) Western blotting. The bands around 50 kD (asterisk; lanes 3-8) correspond to the immunoglobulin heavy chain. The immune complexes were analyzed on a 7.5% (lanes 7-9) or 10% (lanes 1-6) polyacrylamide gel.

Twenty-two of these clones encoded a 1172 aa protein identified as laminin- β 3 (accession number NM_000228). These clones were derived from three independent clones. The common overlapping sequence of these clones corresponded to aa 274 to 878 (nt 903-2716) of laminin- β 3. One clone encoded aa 1755 to 1884 of a protein identified as fibronectin (nt 5532-5919; accession number NM_002026).

NSP4 interacts with laminin- β 3 and fibronectin during rotavirus infection in Caco-2 cells

To establish that NSP4 associates *in vivo* with laminin- β 3 and fibronectin, we performed co-immunoprecipitation studies. Cell lysates from mock-infected or rotavirus Wa infected Caco-

2 cells were prepared in a mild Tris lysis buffer. NSP4 (fully glycosylated and nonglycosylated forms 28 kD and 20 kD, respectively), laminin- β 3 (140 kD) and fibronectin (250 kD) can be detected by Western blotting in lysates from respectively infected (NSP4) and mock-infected Caco-2 cells (laminin- β 3 and fibronectin) using specific antibodies (Fig. 1, lanes 1, 2 and 9). NSP4 was immunoprecipitated with hyper immune anti-NSP4 serum in lysates from infected Caco-2 cells, but not from mock infected Caco-2 cells (Fig 1, lanes 3 and 4). After immunoprecipitation with anti-NSP4 serum, both fibronectin and laminin- β 3 could be detected in coimmunoprecipitated material from infected cells by Western blotting with specific goat and rabbit polyclonal antisera (Fig.1, lanes 6 and 8, respectively). No coimmunoprecipitation of NSP4 and fibronectin or NSP4 and laminin- β 3 was observed in lysates from mock-infected Caco-2 cells (Fig.1B, lanes 5 and 7). Therefore, we demonstrated that NSP4 interacts with both fibronectin and laminin- β 3 during rotavirus infection in Caco-2 cells.

NSP4 co-localizes with the enterocyte basement membrane during rotavirus infection in suckling mice

As NSP4 interacts with laminin- β 3 and fibronectin, proteins that are localized in the extracellular matrix (ECM), we wanted to investigate whether NSP4 could be detected in the ECM *in vivo*. We used embedded tissue from 11-day-old BALB/c mice that had been inoculated with 2×10^4 focus forming units (ffu) of the EDIM rotavirus strain or tissue from control mice that were mock infected with PBS. In this mouse model that we previously described, virus replication occurs in two peaks at 1 and 4 days post infection (dpi) and mice develop diarrhea over a period of 5 days (43). The onset of diarrhea is at 1 dpi, with the highest percentage of diarrhea and maximal severity of diarrheal illness at 3 days post infection (dpi). In infected mice at 1 (data not shown) and 4 dpi, anti-NSP4 (114-135) rabbit polyclonal serum stained infected epithelial cells of the small intestine (jejunum) (Fig. 2A and C, see *Appendix*). The antiserum however also stained the BM of infected cells on the villi as well as the BM of non-infected cells further down the villus (Fig. 2C, *Appendix*). When infected cells were observed low on the villus, we could detect NSP4 in the BM of lower villus- and crypt cells (Fig 2F, *Appendix*). Pre-immune serum (obtained before antigen boosting with NSP4; Fig.2B, *Appendix*) did not stain an adjacent section of infected tissue, indicating that the NSP4 staining was specific. With control mice 4 days after mock infection with PBS, no staining was observed with the NSP4 antiserum (Fig. 2D, *Appendix*). Similar to the anti-NSP4 (114-135) rabbit serum, a rabbit polyclonal serum against SA11 NSP4 aa 120-147 (480), also stained the BM of uninfected as well as infected epithelial cells in infected mice (data not shown). A rabbit polyclonal antiserum against SA11 rotavirus only stained infected cells and not the BM (Fig 2E, *Appendix*), indicating that rotavirus structural proteins are not present in the BM and that BM staining was specific for the NSP4 antibodies. Using adjacent immunohistochemical sections NSP4 could be colocalized with laminin- β 3 in the BM of small intestinal epithelial cells (Fig 3). During rotavirus infection in neonatal mice, laminin- β 3 was detected in the BM of small intestinal epithelium at 4 days post infection (Fig 3A). In the adjacent section (Fig 3B), rotavirus-infected cells were detected with the anti-NSP4 antibody, whereas the BM of infected- and non-infected cells was also stained. During development, laminin-5 (or its single subunits) is initially present in the BM associated with both the villus- and crypt epithelium. Expression in the adult human small intestine is eventually mainly restricted to the villus region, with only weak expression in the BM of the upper crypt region (219, 230, 243). In agreement with these data, laminin- β 3 was

detected in the BM associated with villus- as well as crypt epithelium in eleven-day-old mice (Fig 3C). In twenty eight-day-old mice that are not susceptible to rotavirus-induced diarrhea (341), laminin- β 3 expression appeared decreased and was only weak in the BM of the villus and upper crypt region (Fig 3D). These observations suggest that NSP4 is released on the basal side from infected epithelial cells in neonatal mice and binds to laminin- β 3 in the extracellular matrix. We also tested several anti-fibronectin antibodies in order to stain the BM. Using paraffin embedded tissue all the antibodies failed to stain the BM. In contrast, using frozen tissue sections, numerous studies previously described expression of fibronectin in the BM of small intestinal tissue in different species (20, 22, 26, 219, 228, 340, 395). These studies point out that fibronectin is found predominantly in the crypt region while expression gradually decreases towards the tips of the villi. Therefore, it is apparent that NSP4, similar to laminin- β 3, also co-localizes with fibronectin in the extracellular matrix, although we could not detect fibronectin with our methods.

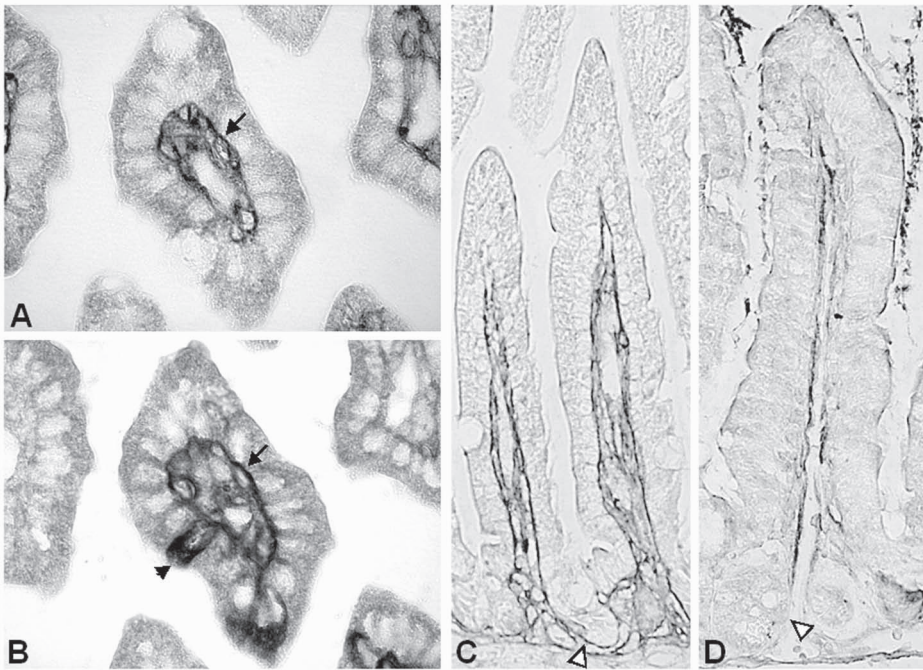


Figure 3. Colocalization of NSP4 with laminin- β 3 in the BM of small intestinal epithelial cells during rotavirus infection in neonatal mice. Laminin- β 3 was detected in the BM of small intestinal epithelium at 4 days post infection (A, arrow). In the adjacent section (B), rotavirus-infected cells were detected with the anti-NSP4 antibody (arrowhead), whereas the BM of infected- and non-infected cells were also stained (arrow). Laminin- β 3 was detected in the BM associated with the villus and crypt epithelium (open arrowhead) in eleven-day-old mice (C). In twenty eight-day-old old mice, laminin- β 3 expression was decreased in the BM of the villus region, weak in the upper crypt region, and not observed in the lower crypt region (D, open arrowhead). Panels A and B are cross-sectional slides, original magnification, X 600. Panels C and D are longitudinal slides, original magnification, X 200.

Characterization of the interacting domains of NSP4, laminin- β 3, and fibronectin

The laminin- β 3 aa 274-878 insert region contains four laminin-type epidermal growth factor like (EGF) domains (aa 277-304, aa 378-428, aa 431-478, and aa 533-570), an intermediate filament protein domain (aa 627-686), and a small region of the coiled-coil forming domain (myosin tail; aa 868-878) (Fig. 4; NM_000228; (143) and using the NCBI, conserved domain database). To evaluate which regions or domains of laminin- β 3 interact with NSP4 we constructed five different deletion fragments of the laminin- β 3 clones and tested them against NSP4 Δ N in the yeast-two-hybrid screening (Fig 4). The readout of the interaction between the various laminin- β 3 deletion mutants with NSP4 Δ N was the growth of yeasts harboring the two plasmids in His⁻ Ade⁻ medium and the development of a blue color in the presence of X- α -Gal substrate (Fig. 4). As a negative control, the laminin- β 3 clones were also screened against the pGBKT7 plasmid without NSP4 as bait. Only laminin- β 3 aa 274-878 or the laminin- β 3 clone aa 726-875 interacted with NSP4. None of the other constructs encoding a fragment of laminin- β 3 was able to interact with NSP4 (Fig. 4). This indicates that NSP4 interacts with the region between aa 726 and 875 of laminin- β 3.

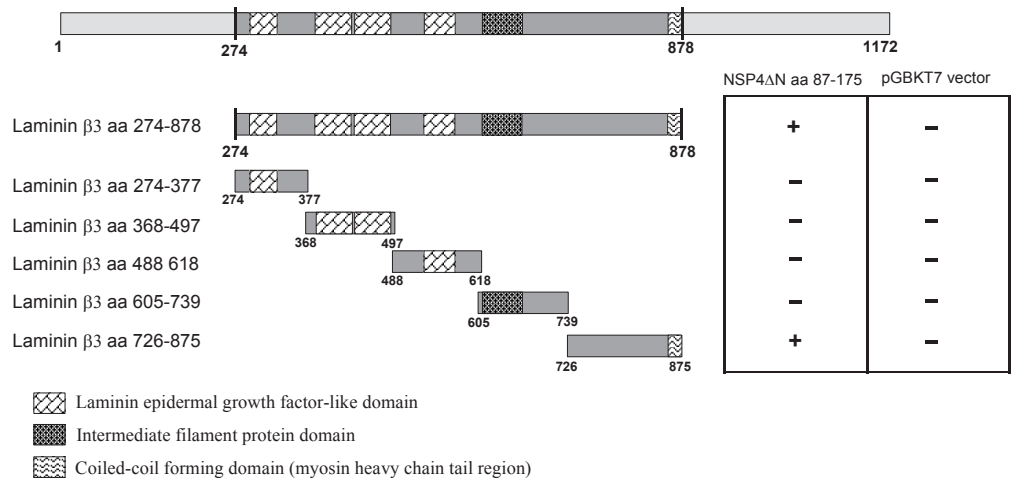


Figure 4. Binding domain analysis of laminin- β 3 with NSP4 Δ N. Laminin- β 3 insert of clone D19 (aa 274-875) was fragmented into 5 subclones using PCR. Bars represent truncated laminin- β 3 inserts fused to the GAL4 activation domain. Amino acid positions are indicated. AH109 yeast was cotransformed with the laminin- β 3 clones and pGBKT7-NSP4 Δ N. The interaction was assessed by checking for blue colonies in the presence of X- α -Gal. Functional and structural domains of laminin- β 3 are presented in boxes.

The NSP4 Δ N bait (aa 87-175) presents several previously described functional domains including: an amphipatic alpha helical region (aa 95-137) involved in the formation of a coiled coil domain, oligomerization and membrane destabilizing activities of NSP4 (290, 416, 420); an enterotoxigenic peptide sequence (aa 114-135) domain that was shown to induce diarrhea in young mice and potentiate chloride secretion (16), and seems to be involved in the direct inhibitory effect of NSP4 on the Na-D-glucose symporter (SGLT1) (163); a VP4 binding site (aa 112-146) (12); and a region that functions as a receptor for inner capsid particles (aa 156-175) (297). Using polymerase chain reaction (PCR), we constructed five mutants of NSP4. In order to map the sites of NSP4 involved in binding, these mutants were

sub-cloned in the pGBKT7 plasmid, to obtain deletion mutants of NSP4 fused to the DNA binding domain of the yeast transcription factor GAL4, and screened against the GAL4-activating domain fusion proteins laminin- β 3 aa 274-878, laminin- β 3 aa 726-875, and fibronectin in a yeast-two-hybrid screening (Fig 5A). The interaction of the five NSP4 deletion clones with laminin- β 3 aa 274-878, laminin- β 3 aa 726-875, or fibronectin was assayed on His⁻ Ade⁻ selection medium in the presence of X- α -Gal substrate through selection by growth and the development of blue colonies (Fig. 5A). Interactions were confirmed in a quantitative α -galactosidase assay based on the induction of the *Mell* gene (Fig. 5B). NSP4 Δ N was used as a positive control. Deletion of aa 87-114 of NSP4 in the NSP4 aa 113-175 subclone abolished or suppressed the interaction of NSP4 with laminin- β 3 274-878 and laminin- β 3 aa 726-875 respectively (Fig 5A and B). The laminin- β 3 aa 726-875 fragment was able to interact with the NSP4 truncated clones aa 87-114 and aa 113-145. These interactions however were significantly suppressed compared to the interactions with NSP4 Δ N and NSP4 aa 87-145. Interaction of laminin- β 3 aa 726-875 with NSP4 was much stronger than with the full length laminin- β 3 clone. This could be due to the fact that the laminin- β 3 subclones were constructed in the pGADT7 high copy number vector instead of the pGAD10 low copy number vector used for the construction of the Caco-2 cDNA library. However, on the other hand, shorter fragments frequently give stronger interactions than longer fragments when using the two-hybrid system, which can be caused by differences in folding of the fusion proteins (183, 326).

The fibronectin insert (aa 1755-1884) contains the last 57 aa of the fibronectin type III FN repeat FN12, and the first 72 aa of FN13 (383). This region of fibronectin lies within a region known as the heparin-binding site II (HepII) (17, 60, 185), and shown to be involved in the binding of fibronectin to syndecan-4 (462), tenascin-C (181), and the integrins α 4 β 1 and α IIB β 3, (274, 284). Interaction of NSP4 with fibronectin was only abolished when the C-terminal clone NSP4 aa 145-175 was used in the two-hybrid screening (Fig 5A and B). These data indicate that for the interaction of NSP4 with laminin- β 3 and fibronectin, aa 87-145 are sufficient and that for binding to laminin- β 3 aa 87-114 are most important.

Discussion

To date, several cellular partners of NSP4 have been identified. NSP4 has been shown to interact with the ER-associated lectin-like chaperone calnexin during infection in MA104 cells (273). For this interaction glycosylation of NSP4 was important and glucose trimming was necessary, indicating that the N-terminal domain of NSP4 is involved, and that binding to calnexin is of a carbohydrate nature. NSP4 has a direct inhibiting effect on the Na-D-glucose symporter (SGLT1), indicating that NSP4 inhibits water resorption and thus is crucial for rotavirus pathogenesis (163). However, whether or not the inhibition involves direct binding of NSP4 to SGLT1 has to be confirmed. Finally, NSP4 has been identified along microtubule-like structures, where it disrupts microtubule-mediated membrane trafficking from the ER to Golgi complex (465). Although several NSP4-interacting proteins have thus far been identified, none revealed more insight into the mechanism of NSP4-induced chloride secretion.

In the present work we, searched for cellular proteins that interact with the rotavirus protein NSP4, in order to gain more insight into rotavirus pathogenesis. For this purpose we used the two-hybrid technique in yeast and screened a human Caco-2 cell cDNA library fused to the

GAL4 activation domain with aa 87-175 of NSP4 fused to the DNA-binding domain of GAL4. As NSP4-interacting cDNA clones, laminin- β 3 and fibronectin were isolated. The interaction of NSP4 with the ECM proteins, laminin- β 3 and fibronectin, was confirmed by coimmunoprecipitation of infected Caco-2 cell lysates. The interaction with laminin- β 3 was further established by colocalization of NSP4 with laminin- β 3 in the basement membranes of infected neonatal mice. Deletion analysis showed that aa 87-145 of NSP4 were sufficient for interaction with laminin- β 3 and fibronectin. For binding to laminin- β 3 aa 87-114 of NSP4 were the most important. Interaction of NSP4 with laminin- β 3 and fibronectin was only abolished when the C-terminal clone NSP4 aa 145-175 was used in the two-hybrid screening, indicating that this C-terminal region is not involved in NSP4 binding. The insert of the laminin- β 3 clones encoded several conserved domains. NSP4 was only found to interact with a truncated laminin- β 3 fragment (aa 726-875) containing the N-terminal part of a domain involved in the formation of the triple-stranded α -helical coil-coiled structure that represents the rod of the long arm of laminins (182, 432).

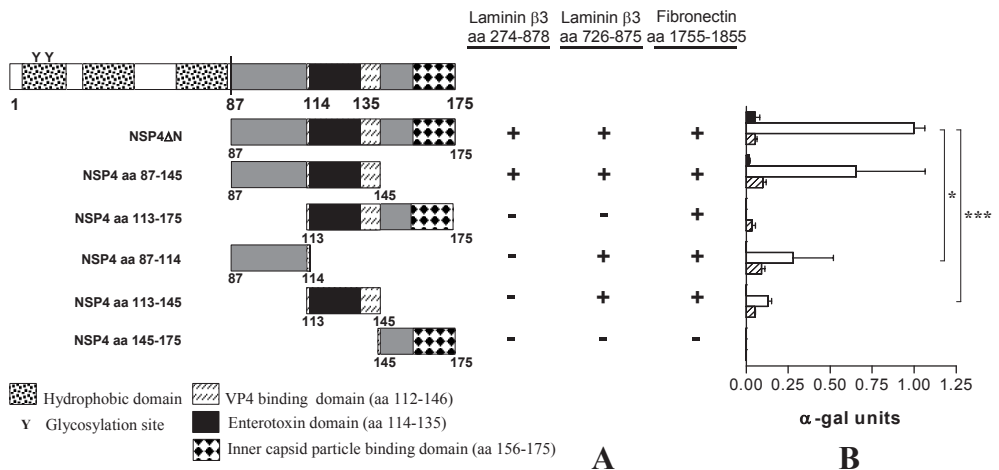


Figure 5. Binding domain analysis of NSP4 with laminin- β 3 (aa 274-878), laminin- β 3 (aa 726-875), and fibronectin (aa 1755-1885). NSP4 Δ N was fragmented into 5 subclones using PCR (A). Bars represent truncated NSP4 clones fused to the GAL4 binding domain. Amino acid positions are indicated. AH109 yeast was cotransformed with the laminin- β 3 clones and pGBKT7-NSP4 Δ N. The interactions were assessed by checking for blue colonies in the presence of X- α -Gal. Functional and structural domains of NSP4 are presented in boxes. Quantitative analysis of the interactions were obtained from independent yeast cotransformants assayed with *p*-nitrophenyl- α -D-galactosidase as substrate (B). α -Galactosidase activity was expressed in units and calculated by the following formula: $(OD_{410} \times V_f \times 1,000) / [OD_{600} \times T \times (\epsilon \times b \times V_i)]$, where OD_{410} is the absorbance of the reaction mixture, OD_{600} is the cell density of the culture, T is the reaction time (in minutes), V_f is the total volume (in milliliters) of the assay, V_i is the volume of culture medium supernatant added, ϵ is the molar absorptivity for *p*-nitrophenol, and b is the light path (in centimeters). Solid, open, and striped bars correspond to interactions of laminin- β 3 (D19 clone), laminin- β 3 aa 726-875, and fibronectin (clone D22) with the indicated NSP4 constructs, respectively. Standard error of the mean are shown ($n=3$). * $P < 0.05$, *** $P < 0.001$ using Student's t -test.

The fibronectin insert (aa 1755-1884) contains the last 57 aa of the fibronectin type III FN repeat FN12, and the first 72 aa of FN13 (383). This region of fibronectin called the HepII region, is known to be involved in cell binding and cell spreading (38, 462), and binds to heparan sulfate proteoglycans like syndecan-4 (17, 60, 185, 462), tenascin-C (181), and

integrins $\alpha 4\beta 1$ and $\alpha IIb\beta 3$, (274, 284), (17, 60, 185). The fibronectin insert found with the two-hybrid system, contains all six basic residues previously shown to be crucial for heparin binding (60) and thus represents the principal heparin-binding site of fibronectin. By binding to the HepII region in fibronectin, syndecan-4 has been shown to function as a co-receptor in integrin signaling (462). It might be possible that NSP4, through binding to fibronectin, could interfere with this interaction and influence integrin signaling. Such a mechanism was observed for tenascin-C as binding of tenascin-C interfered with fibronectin-syndecan-4 interaction and replaced syndecan-4, thereby influencing cell signaling and proliferation (181). The fibronectin type III domain is a very common constituent of animal proteins, and its main functions are to mediate protein-protein interactions and to act as a linker (62). Fibronectin type III domains have been found in intracellular, extracellular, and membrane-spanning proteins and are additionally found in many bacterial extracellular glycohydrolases (62, 235).

Rotavirus-induced disease is thought to be caused by a combination of factors (369), including a reduction in epithelial surface area, replacement of mature enterocytes by immature (crypt-like) cells (43, 306), an osmotic effect resulting from incomplete absorption of carbohydrates from the intestinal lumen in combination with bacterial fermentation of these non-absorbed compounds, secretion of intestinal fluid and electrolytes through activation of the enteric nervous system (ENS)(246), and the secretory effect of NSP4, which is thought to act as a viral enterotoxin (16). During rotavirus infection, there is an enhanced turnover of epithelial cells that is thought to result in the presence of immature cells on the villi (43, 306). Since laminin-5 and fibronectin are proteins involved in cell differentiation and cellular migration (20, 22, 311, 340, 395), it is possible that NSP4 could modulate migration and/or differentiation of epithelial cells via binding to fibronectin and laminin. The mechanism contributing to diarrheal disease and involving NSP4 is thought to occur through release of NSP4, or its cleavage product (NSP4 (112-175), from infected cells and binding to a yet-unidentified apical membrane receptor. Binding would directly or indirectly trigger a signal transduction pathway to enhance chloride secretion, eventually resulting in diarrhea (16, 126, 279, 480). This secretory mechanism however is thought to act in the intestinal crypts (247). It is still not clear if and how NSP4 reaches the intestinal crypts. However, it seems unlikely that this occurs via the luminal route since continuous abundant secretion from the crypts results in a hydrodynamic flow against which NSP4 has to diffuse (247). We observed a BM localization of NSP4 and colocalization with laminin- $\beta 3$ in the ECM during rotavirus infection in neonatal mice. BM localization was found underneath infected as well as non-infected cells. Our data therefore suggest that NSP4 is also released from the basal side of infected enterocytes. We currently can only speculate about whether NSP4, or a cleavage product, is being released from the basal side of infected cells. However, since we detected NSP4 *in vivo* at the BM with antibodies against aa 114-135 and aa 120-147, it can be concluded that the released peptide sequence at least contains the enterotoxic domain. After basal release, NSP4 would bind to the extracellular matrix proteins laminin- $\beta 3$ and fibronectin. Since, we could detect NSP4 in the BM of lower villus cells and occasionally underneath epithelial cells in the crypts, it is tempting to speculate that, via a route involving the ECM, NSP4 could travel towards the crypt region where it can induce fluid secretion. In concurrence with the hypothesis stated above and with our results, Ball and coworkers found that NSP4 is able to cause chloride secretion when added to the submucosal (basal) surface of mouse mucosal sheets (16).

Recent studies indicate that rotavirus infection is not confined to the intestine, but instead is able to leave the intestine and enters the circulatory system (40, 282). Rotavirus has been detected in cerebral spinal fluid ((188, 248, 294, 310, 474)), liver and kidney (145), extra-intestinal lymphoid tissue (54), and serum of infected children and animals (40, 431). Using in situ RT-PCR, rotavirus was also found in the heart, where it was mainly localized to endothelial cells (282). It was suggested that rotavirus, analogous to what has been found for reovirus, gets into the circulatory system through M cells that are present in the epithelium that overlies the Peyer's patches (40, 282). Our data also imply that NSP4 could be able to get into the circulatory system, as it is apparently at least partly secreted into the tissue underlying the enterocytes. If NSP4 is also able to get into the circulatory system, it is likely that it does so through release from the basal side of infected epithelial cells.

In summary, our results show that NSP4 binds to the ECM molecules laminin- β 3 and fibronectin in vitro and in vivo. Binding to the ECM and localization at the BM imply that NSP4 is released from the basal side of infected epithelial cells. From our data the significance of the deposition of NSP4 in the BM is still unclear, but it could possibly point to a new mechanism by which rotavirus disease is established. The involved mechanisms however, remain to be defined.

Acknowledgements

The authors are very grateful to C. Mithelmore and O. Noren for donating the Caco-2 cDNA library. We would like to thank Marion Koopmans for kindly providing the rotavirus Wa strain, and Mary Estes for donating the NSP4 (120-147) antibody. We also like to thank Jan Dekker for critical reading of the manuscript. This work was supported by grants from the Sophia Foundation for Medical Research (SSWO), the Netherlands Digestive Diseases Foundation (MLDS), and the Netherlands Society for Scientific Research (NWO).

Chapter 7

Summary and General discussion

Summary

Rotaviruses comprise a genus within the family of the *Reoviridae* and are recognized as the single most significant cause of severe gastroenteritis, malnutrition and diarrhea in young children. Each year rotavirus causes the death of about 440,000 children <5 years of age (313). The research described in this thesis focuses on the multifactorial process of rotavirus pathogenesis. This chapter summarizes and discusses the results of the preceding chapters and will focus on some aspects in more detail.

Chapter 1 provides a general overview on rotaviruses, describes the current “state of the art” on rotavirus pathogenesis and outlines the aims of this thesis. **Chapter 2** of this thesis describes the effect of rotavirus infection on epithelial homeostasis and dysfunction during rotavirus infection in neonatal mice. After inoculating seven-days-old suckling mice with a homologous rotavirus, virus replication occurred in two peaks, and histological changes were characterized by the accumulation of vacuolated enterocytes. During infection, apoptosis as well as proliferation were increased and epithelial cell turnover was significantly higher than in control mice. The overall outcome of these changes was an increase in crypt depth and the occurrence of villus atrophy. Rotavirus infection also caused a down regulation of enterocyte specific gene expression (mRNA and protein) in infected cells. This shut-off of enterocyte specific gene expression, together with the loss of mature enterocytes through apoptosis and the replacement of these cells by less differentiated dividing cells, are expected to lead to a defective absorptive function of the intestinal epithelium that contributes to rotavirus pathogenesis. In **chapter 3**, we evaluated the role of goblet cells and mucins in the active defense against rotavirus infection. We found that during rotavirus infection goblet cells, in contrast to enterocytes, are spared from apoptosis, intestinal mucin Muc2 expression is up-regulated and mucin structure is changed. This suggests that mucins and in particular Muc2, play an important role in the active defense against rotavirus infection. In this chapter, we further show that age-dependent differences in mucin composition and increased occurrence of sialylated mucins after infection alter the inhibitory capabilities of mucins isolated from the mouse small intestine. This suggests that posttranslational modification in glycosylation of mucins during infection alters their anti-viral capabilities and ultimately can affect their specific epithelial barrier function against intestinal pathogens. In **chapter 4**, the role of prostaglandins in mucin expression during rotavirus infection was examined. We found that Cox2 mRNA expression is strongly enhanced during rotavirus infection in neonatal mice, implying increased PG production. Infected mice also showed increased levels of Muc2, Muc3 and Muc5AC mRNAs. *In vitro* experiments were performed to evaluate the role of PGs in mucin transcription. As an enterocyte model, Caco-2 cells “mirrored” the observations in mice and showed increased enterocyte-specific MUC3 mRNA expression during rotavirus infection. In the goblet cell line LS174T, PGE₁ and PGE₂ were able to induce MUC2 and MUC3 mRNA. However, PGE₂ failed to induce MUC5AC mRNA, whereas the PGE₁ was only able to moderately increase MUC5AC mRNA levels, indicating that other pathways and/or other PGs are likely to be involved in the induction of this mucin. In particular, these findings suggest that mucin up regulation during rotavirus infection is mediated at least in part through up regulation of rotavirus-induced Cox2 and PG levels. Moreover, the rotavirus-induced prostaglandin production and subsequent mucin induction could have beneficial effects on the gut by supporting mucosal barrier integrity. **Chapter 5** describes the immune responses in infant mice following oral inoculation with murine

rotavirus as a model for natural infection and heterologous simian rotavirus (SA11) as a model for vaccination. For the heterologous infections, three different fractions (with dissimilar composition) obtained after purification by cesium chloride density gradient centrifugation were used for inoculation. Diarrhea was observed after inoculation with EDIM and all three SA11 fractions. Viral shedding was observed in the group inoculated with the murine virus, but not in any of the mice inoculated with the heterologous virus. Moreover, in contrast to the homologous infection, heterologous virus replication could not be detected in the mouse small intestine using various techniques. The homologous virus and the heterologous virus fractions induced similar IgG responses but only minor IgA responses were found in the mice infected with the heterologous virus compared to the murine virus. The rotavirus specific IgG1/2a ratios differed between the three heterologous virus fractions. The results suggest that the polarization of the immune response (Th1/Th2) against heterologous rotavirus is depending on the composition of the inoculum used. Furthermore, the level and possible site of replication of heterologous rotavirus differs from wild-type rotavirus infection, whereas the mucosal immune response is lacking after a heterologous infection. These factors should be evaluated with respect to the development of novel rotavirus vaccines as they may have a significant impact on the neonatal immune system. In **chapter 6** we aimed to identify cellular proteins that interact with the rotavirus enterotoxin NSP4. Using the two-hybrid technique as an approach, we isolated cDNAs encoding the extracellular matrix (ECM) proteins laminin- β 3 and fibronectin. By means of deletion analyses, we mapped the regions of NSP4 and Laminin- β 3 responsible for interaction. Interaction of NSP4 with either laminin- β 3 or fibronectin was further confirmed by coimmunoprecipitation. Additionally, NSP4 was present in the basement membrane (BM) of infected mice and colocalized with laminin- β 3, indicating a physiological interaction. Binding to the ECM and localization at the BM suggests that NSP4 is released from the basal side of infected epithelial cells. These findings may denote a new mechanism by which rotavirus disease is established.

Discussion

Rotavirus induced diarrhea is thought to be a multifactorial process that is caused by a combination of factors (369), which include a reduction in epithelial surface area, replacement of mature enterocytes by immature (crypt-like) cells (84), down regulation of genes involved in digestion and absorption of nutrients, salt and water, an osmotic effect resulting from incomplete absorption of carbohydrates from the intestinal lumen in combination with bacterial fermentation of these non-absorbed compounds, secretion of intestinal fluid and electrolytes through activation of the enteric nervous system (ENS)(246), and the effect of the rotavirus non-structural protein 4 (NSP4), which is thought to act as a viral enterotoxin (16). An overview showing established (see also chapter 1) or speculative events that are or might be involved in the multifactorial process of rotavirus pathogenesis is presented in figure 1. The speculative events are also pointed out in the next sections.

The epithelium is the primary target of rotavirus infection, and it is not surprising that epithelial dysfunction plays an important role in rotavirus pathogenesis (84, 162, 209, 306, 355, 389). Although there have been various reports regarding the effect of rotavirus infection on epithelial homeostasis *in vivo* (84, 162, 209, 389), none of these studies did

present a more complete and overall picture of rotavirus infection but rather they presented fragmentary data. In **chapter 2**, we performed an elaborate study in order to obtain a more comprehensive and complete understanding of rotavirus infection *in vivo*. We found that during homologous rotavirus (EDIM) infection in mice, villus atrophy and an increase in crypt depth are accompanied by highly induced epithelial apoptotic- and proliferation rates. Along with this, epithelial cell turnover also increased. In addition to these processes, we found that rotavirus caused a strong down regulation of enterocyte specific gene expression at the mRNA and protein level (SGLT1, Lactase, LFABP) in infected cells. The shut off of gene expression has been demonstrated for various viruses (HIV, influenza, poliovirus, adenovirus, and herpes simplex (35, 223, 244, 258, 463)), but was not shown previously for rotavirus *in vivo*. The rotavirus non-structural protein NSP3 is known to induce the shut off of host cell translation during *in vitro* rotavirus infection, by interacting with the eukaryotic initiation factor eIF4GI, which is part of the eIF4F holoenzyme complex (326). Since eIF4F modulates mRNA stability (343), the shut off of enterocyte gene expression during rotavirus infection we observed in **chapter 2**, might also be mediated by NSP3. Furthermore, we hypothesize that NSP3 could mediate this shut off by removing eIF4F from cellular mRNA resulting in decreased stability of these mRNAs and subsequently a decreased translation (see also Box in **chapter 1**). The shut off of enterocyte gene expression is further in accordance with earlier studies in mice and rabbits where the enzymatic activity (dissacharidase activity, amino acid uptake, solute co-transport) in the brush border was markedly decreased (84, 162, 209). Our data further showed that there are reduced levels of the sodium glucose co-transporter SGLT1 transcripts and protein in the brush border of enterocytes. This might be an important mechanism underlying the reduced Na⁺ solute transport activity observed during rotavirus infection in rabbits (162). Based on the findings stated above, and with respect to one of the established mechanisms leading to rotavirus diarrhea that is decreased solute absorption and water reabsorption in the intestine through substitution of mature enterocytes by non-transporting crypt cells (164, 212, 350), we propose that in addition to the direct inhibition of Na (+)-solute co-transport activities through NSP4 (163), at least 3 sequential processes are implicated in this mechanism of rotavirus-induced diarrhea. 1) Early on during infection, enterocyte specific gene expression is directly down regulated in infected cells at the mRNA level. This results in reduction of mature enterocyte specific protein levels and thus in a functional less differentiated status relatively early during infection while there is still little histological damage. 2) Mature enterocytes are lost from the villi through apoptosis and shedding. 3) These mature enterocytes are replaced by immature and actively dividing cells.

Adult Mice

Mice usually do not develop any symptoms when infected beyond 2 weeks of age, and infection of adult mice occurs without diarrheal disease or histopathological lesions (59, 130, 306, 341, 402, 453). As part of the *in vivo* studies we performed in young mice, we did a comparative study of rotavirus infection in adult (> 6 weeks) mice (the same standardized amount of EDIM virus inoculum was used; unpublished data). As for the suckling mice, we examined the pathogenesis of rotavirus infection in the adult mice by examining the induction of diarrhea, and timing and extent of rotavirus replication in the gastrointestinal epithelium. During the course of our experiment (14 days), the adult mice, in contrast to the suckling mice, did not experience diarrhea. We used *in situ* hybridization and immunohistochemistry to detect viral replication in the small intestinal epithelium and found,

in contrast to the massive replication in young mice, that only a few enterocytes were infected at day 2 and 4 post infection.

Age-dependent diarrhea has been explained by various hypotheses (126, 280). For example, the decrease in net fluid absorption may especially have an impact at young age at the time when the absorptive capacity of the colon is not yet fully developed, and changes in the osmotic permeability of the mucosa secondary to destruction, and changes in fluid and electrolyte secretion may be different in adults and young. Since the mice in our experiments were naïve and did not encounter rotavirus before, the (maturation of) immune system may be of little importance, at least in mice. The absence of diarrhea in the adult mice seems to be directly related to the amount of infected cells and virus replication. This may be explained by age-dependent differences in expression or appearance of molecules involved in the different stages of infection and replication (various stages of binding, entry, replication, mechanisms of secondary infection). Gangliosides, sialic acid-containing glycosphingolipids, are found in the outer layer of the plasma membrane of all vertebrate tissue cells and gangliosides like GM1 and GM3 have been suggested to play a role as possible receptors for rotavirus (161, 356). Interestingly, GM1 and GM3 ganglioside contents increase in mouse small intestine during the suckling period, and decreased after weaning (375). Like GM1 and GM3, integrins which are also involved in rotavirus binding, appear to be differentially expressed throughout development as well, (21, 89, 418), indicating that all these molecules could be implicated in age-dependent differences in susceptibility towards rotavirus infections.

In agreement with what we found in mice, rotavirus-infected human adults were shown to shed 10–100 times less rotavirus than do infected children (41, 449). We have to bear in mind however, that the mechanisms of age-dependent diarrhea in humans is most likely very different from naïve mice, since in humans the acquired immune system plays a pivotal role in protection (31, 444, 473).

Role of Mucins and Prostaglandins during rotavirus infection

In **chapter 2**, we demonstrated that rotavirus infection has a profound effect on small intestinal epithelial homeostasis and induces apoptosis at the tips of the villi, increases epithelial cell turnover and hampers enterocyte gene expression. In **chapter 3** and **chapter 4**, we evaluated the role of goblet cells and mucins in the active defense against homologous rotavirus (EDIM) infection in mice. We focused our attention on goblet cell homeostasis during infection in conjunction with the expression of specific gene products that are secreted by these cells. Goblet cells are characteristic for the intestinal epithelium and are known to secrete molecules such as mucins and trefoil factor family peptides that serve protective and healing functions in the gut, respectively (419, 438).

We found that in the ileum, the intestinal region with highest levels of viral replication, goblet cells in contrast to enterocytes, are spared from apoptosis during severe rotavirus infection. The sparing of goblet cells could uphold their protective function in epithelial defense and this event has also been observed in rats after intestinal damage has been induced by the cytostatic drug methotrexate (446). Muc2, Muc3 and Muc5AC mRNA levels were increased in the ileum during infection, whereas Muc2 protein expression was maintained during infection. In contrast, protein expression of goblet cell specific protein TFF3 was strongly affected.

Many rotavirus strains use sialic acid (SA) residues on the surface of target cells for initial attachment (107, 356, 410). Mucins of various origins have previously been implicated in the inhibition of rotavirus infection *in vivo* and *in vitro* via binding of rotavirus to sialic acid moieties (72, 289, 323, 440, 459, 471, 472).

In **chapter 3**, we found that the number of goblet cells containing sulfated mucins was reduced whereas the fraction of heavily sialylated mucins was strongly increased. A reduction in the number of sulfated mucin-containing cells was also found during infection of simian SA11 rotavirus in rats (156). One of the possible explanations for this observation is that sulfated mucins could have been preferentially secreted into the intestinal lumen, or that the mucin molecules are undersulfated as has been observed in patients with ulcerative colitis or in a rat model for colitis (191, 345, 442). As sulfate content of mucins is thought to present resistance to (bacterial) enzymatic degradation of the mucus layer (293, 352), a decrease in sulfated mucins during rotavirus infection could therefore influence the consistency of the mucus layer. Changes in mucin sulfation particularly will be of relevance in the colon where sulfate-reducing bacteria reside. It will therefore be of special interest to determine whether sulfation is also reduced in the colon during rotavirus infection.

Changes in the glycosylation and sialylation of mucins are observed during bacterial or parasite infections (100, 170). *In vitro*, cytokines have been implicated in the sialylation of mucins (106). In particular, TNF- α was shown to upregulate mRNA levels of sialyl- and of fucosyl-transferases and increases the sialylation of mucins in a human respiratory gland cell line. Prostaglandins (PGs) were also shown to alter the terminal glycosylation and sialylation of mucins (117). Interestingly both prostaglandins (see also below) and TNF- α levels were found increased in rotavirus-infected children (193, 466).

The changes in mucin sulfation and especially sialylation during rotavirus infection in mice suggested that these mucins would have an altered competence to inhibit rotavirus infection. As described in **chapter 3**, we isolated mucins from the small intestines of control and infected mice at several time-points and tested these mucins for neutralization of rotavirus in an *in vitro* infection system. We show that age-dependent differences in mucin composition and increased occurrence of sialylated mucins alter the inhibitory capabilities of mucins isolated from the mouse small intestine. This suggests that posttranslational modification in glycosylation and sialylation of mucins during infection alters their anti-viral capabilities and ultimately can affect their specific epithelial barrier function against intestinal pathogens.

PGs are lipid mediators that are produced through cyclooxygenases (COXs). A number of studies have shown that COX and PGs are involved in rotavirus replication and pathogenesis. Prostaglandin E₂ (PGE₂) levels rise early after rotavirus infection in pigs (481) and elevated levels of prostaglandin PGE₂ and PGF₂ have been observed in the plasma and stool of rotavirus-infected children (466). Moreover, Rossen et al. showed that COX2 mRNA and PGE₂ levels are increased after rotavirus infection *in vitro* (358). PGE₂ and COX activity were shown to be crucial for rotavirus replication in Caco-2 cells and rotavirus illness in young children is reduced after oral aspirin, a non-specific COX inhibitor (358, 466). PGs were previously shown to play a role in the production and secretion of mucins, as PGE₂ enhanced mucin release via a cAMP-dependent mechanism in LS174T cells and in the rat colon (25), and MUC2 protein expression is enhanced by short chain fatty acids through PGE₁ and PGE₂ produced by myofibroblasts (458).

In **chapter 4**, we examined whether PGs could be involved in the induced mucin expression during rotavirus infection. We found that Cox2 mRNA expression is strongly enhanced during rotavirus infection in mice, implying increased PG production. The enhancement of

Cox2 mRNA expression largely followed the course of infection as expression of mRNA was provoked at both peaks of viral replication. The increased levels of Cox2 were accompanied by elevated levels of Muc2, Muc3 and Muc5AC mRNAs. We performed *in vitro* experiments to evaluate the role of PGs in mucin transcription. By using Caco-2 cells as an enterocyte model, enterocyte-specific MUC3 mRNA expression was also increased during rotavirus infection *in vitro*. PGE1 and PGE2 were shown to be inducers of mucin expression in the goblet cells. PGE1 was able to induce MUC2, MUC3 and MUC5AC mRNA levels, whereas PGE2 was able to induce MUC2 and MUC3 mRNA levels. The *in vitro* induction of MUC2 and MUC3 mRNA by PGE₁ and PGE₂ mirrored the *in vivo* induction in mice. Although MUC5AC expression could be induced by PGE₁ in LS174T cells, the increase was only moderate, indicating that other pathways or other PGs (e.g. PGF) are likely to be important in the induction of Muc5ac in infected mice. These data suggest that rotavirus-induced Cox2 and PG levels are involved in mucin upregulation.

The increased mucin expression observed during infection (**chapter 3** and **4**) could be mediated through several other mechanisms apart from PGs. Induction of mucins can be directly affected by viral double stranded RNA (dsRNA) (238). This signaling pathway includes the activation of mitogen-activated protein kinases (MAPK) and nuclear factor κ B (NF- κ B)(238). Rotavirus was indeed shown to activate NF- κ B (355). However, instead of via dsRNA, activation is most likely provoked primarily via binding of its outer capsid protein VP4 to the TNFR-associated factor 2 (TRAF2) and activation of TRAF signaling (226). NF- κ B and various cytokines also are involved in the induction of mucin transcription by bacteria (110, 113, 232, 250). Among the many (pro-inflammatory) cytokines that stimulate mucin gene expression are IL-1, IL-4, IL-6, IL-9 and tumor necrosis factor α (TNF- α), (110, 443). TNF- α is particularly interesting, since this cytokine is involved in the induction of Muc5ac in infected mice. TNF- α is found increased in rotavirus infected children (15) and is able to upregulate MUC5AC in airways via an epidermal growth factor receptor mediated route. Moreover TNF- α increases MUC5AC mRNA half-life (42) and induces MUC5AC secretion in HT29-MTX cells (397).

Other than the induction of mucins, rotavirus-induced PGs are doubtlessly implicated in various other processes during rotavirus infection (See figure 1). PGs could participate in the inflammatory response and result in impaired intestinal absorption and the initiation of a prosecretory state in the intestine (128). Rotavirus infection in mice has been correlated with changes in vascular circulation and ischemia (306, 307, 402). The authors proposed that diarrhea was likely to result from the release of a vasoactive substance causing villus ischemia and functional damage to enterocytes (307). It later was proposed that VIP and/or prostaglandins could embody this vasoactive agent (279). Thus, there possibly exist prostaglandin-dependent mechanisms that mediate the histological changes observed during rotavirus infections and contribute to diarrhea.

Implications of a basal release of NSP4 and binding to the ECM

Cell signaling

The rotavirus non-structural protein 4 (NSP4) is an enterotoxin that was identified as an important agent in symptomatic rotavirus infection (16). In **chapter 6**, we showed that NSP4 interacts with the ECM proteins laminin- β 3 and fibronectin and colocalizes with laminin- β 3

in the BM of infected mice suggesting that NSP4 is released from the basal side of infected epithelial cells. Laminin and fibronectin are multifunctional proteins that can be found in association with each other (422, 475). They can influence cell adhesion, growth, morphology, differentiation, migration, and agglutination as well as the assembly of the ECM (86, 311, 329). Laminin-5, a heterotrimer of $\alpha 2$, $\beta 3$, and $\gamma 2$ chain subunits, can bind to $\alpha 3\beta 1$, $\alpha 6\beta 4$, and $\alpha 6\beta 1$ integrins (64, 253, 292), whereas fibronectin can be a ligand for other members of the integrin receptor family, including $\alpha 5\beta 1$, $\alpha 4\beta 1$, $\alpha 4\beta 7$, $\alpha 9\beta 1$ (329). The fibronectin insert that we found using the two-hybrid system contains a domain called the HepII region that is involved in cell binding and spreading (38, 462). The HepII region also binds to heparan sulfate proteoglycans like syndecan-4 (17, 60, 185, 462), tenascin-C (181), and integrins $\alpha 4\beta 1$ and $\alpha \text{IIb}\beta 3$, (274, 284), (17, 60, 185). By binding to the HepII region in fibronectin, syndecan-4 has been shown to function as a co-receptor in integrin signaling (462). It might be possible that NSP4, through binding to fibronectin, could interfere with this sort of interactions and influence integrin mediated signaling pathways. This has been observed for tenascin-C as binding of tenascin-C interfered with fibronectin-syndecan-4 interaction and influenced cell signaling and proliferation (181).

Thus from this knowledge, it is possible that NSP4 could intervene and mediate several physiological processes through binding to the ECM underneath the intestinal epithelium, thereby influencing epithelial differentiation, migration, and cell survival/apoptosis, processes that are apparently disturbed during rotavirus infection in mice, as we have established in **chapter 2**.

Possible effect on virus entry and binding

Recently, it was reported that integrins are involved in rotavirus binding and that the rotavirus capsid proteins VP4 and VP7 contain integrin ligand sequences (89, 150, 476). VP4 (VP5 part) contains the DGE tripeptide sequence motif and interacts with integrin $\alpha 2\beta 1$ (150), while VP7 binds to $\alpha \text{x}\beta 2$ and $\alpha \text{v}\beta 3$ via its integrin ligand site GPR and CNP region (150, 476), and contains a $\alpha 4\beta 1$ binding motif LDV (89). Most rotavirus strains use integrins for cell-binding and infection, although all porcine viruses seem to be integrin independent (150).

The role of integrins as one of the receptors for rotavirus remains however conflicting with their almost exclusive basal localization at intestinal cells (20, 322). For example $\alpha 2\beta 1$ integrin was found at the basal domain of human intestinal cells according to strict complementary staining patterns (20, 322).

Integrins can adopt inactive and active configurations, which differ by change in relative orientation of the α - and β - subunits. The active orientation has enhanced affinity for both external and cytoplasmic (talin and α -actinin) ligands. Binding of ligand on either side promotes the change to active form, so cytoplasmic ligands can promote binding to ECM, and ECM binding can enhance interaction with cytoplasmic ligands or binding partners. (380).

Administration of NSP4 was found to cause a reduction in the transepithelial electrical resistance (TER) in MDCK-1 cells (411) indicating that it can increase epithelial permeability as has been observed during rotavirus infection in piglets, mice and humans (168, 211, 405). Together with our finding of binding of NSP4 to the ECM, we hypothesize that NSP4 could simultaneously increase epithelial permeability during rotavirus infection and interfere with integrin ECM interactions. This interference would yield additional unbound integrins. Consequently, via the cooperative effects on conformation, this

interference would result in a lower affinity of the integrins for cytoplasmic ligands. In this way, integrins could become more readily accessible for rotavirus particles at the more apical surfaces of the intestinal cells. Since NSP4 is not present in the infectious rotavirus particles during primary infection, this mechanism would play a role to expedite secondary infections.

Chloride secretion and diarrhea

The mechanism contributing to diarrheal disease involving NSP4 is thought to occur through release of NSP4, or its cleavage product NSP4 (112-175), from infected cells and binding to a yet-unidentified apical membrane receptor. Binding would directly or indirectly trigger a signal transduction pathway to enhance chloride secretion, eventually resulting in diarrhea (16, 126, 279, 480). This secretory mechanism however is thought to act in the intestinal crypts (247). It is still not clear if and how NSP4 reaches the intestinal crypts. However, it seems unlikely that this occurs via the luminal route since continuous abundant secretion from the crypts results in a hydrodynamic flow against which NSP4 has to diffuse (247). The data presented in **chapter 6** suggest that NSP4 or a cleavage product (containing the enterotoxic domain aa 114-135) is released from the basal side of infected enterocytes and colocalizes with the ECM. From these data, we hypothesize that via a route involving the ECM, NSP4 could travel towards the crypt region where it can induce fluid secretion. In concurrence with this hypothesis and with our results, Ball and coworkers found that NSP4 is able to cause chloride secretion when added to the submucosal (basal) surface of mouse mucosal sheets and in vivo when injected intraperitoneally into mice (16).

The extraintestinal rotavirus

Numerous studies indicate that rotavirus infection is not confined to the intestine and is able to enter the circulatory system (40, 282). Rotavirus has been detected in cerebral spinal fluid ((188, 248, 294, 310, 474)), liver and kidney (145), extra-intestinal lymphoid tissue (54), and serum of infected children and animals (40, 431). The data presented in **Chapter 6** imply that NSP4 could be able to get into the circulatory system, as it is apparently secreted into the tissue underlying the enterocytes. If NSP4 is also able to get into the circulatory system, it is likely that it does so through release from the basal side of infected epithelial cells. Additional evidence for this possible scenario comes from our unpublished data. Using the 2-hybrid system, we found that NSP4 also interacts with the ECM and acute phase protein fibrinogen. In this system NSP4 interacts with both the fibrinogen α subunit (5 clones of which 2 independent) and the fibrinogen β subunits (3 clones of which 2 independent). Like the other ECM molecules we found with the 2-hybrid system laminin- β 3 and fibronectin, fibrinogen is known to bind to integrins (e.g. α (IIb) β 3, α M β 2 and α 5 β 1 (234, 428)), and the fibrinogen α subunit insert contains two integrin ligand sequences (RGD).

Fibrinogen plays a key role in platelet aggregation, the final step of the coagulation cascade (37, 281). It is questionable whether NSP4 could have any effect on for example blood clotting, or that NSP4 merely uses fibrinogen as a vehicle to get into the circulatory system to exert some secondary effects.

Fibrinogen is also known to play a role in immune and inflammatory responses (234, 428). Directed migration of phagocytic leukocytes through the extracellular matrix for example, requires the engagement of integrin leukocyte adhesion receptors to fibrinogen (234). The integrin α 4 β 7 is expressed by B and T cells responsible for immunity to intestinal antigens and α 4 β 7 expressing lymphocytes have been shown to play a part in the defense against rotavirus (37, 281). α 4 β 7 mediates lymphocyte attachment within the ECM by adhering to

one of the other ECM proteins found to interact with NSP4, fibronectin (66, 361). Since both fibronectin and fibrinogen play a role in the inflammatory response through mediating the attachment and recruitment of lymphocytes to the ECM, it is tempting to speculate that NSP4 could modulate these processes.

Further studies are therefore needed to determine the significance of the above findings while it still has to be determined whether NSP4 binds to fibrinogen *in vitro* and *in vivo* using, among others, the co-immunoprecipitation technique.

Immune response after rotavirus infection in neonatal mice

There has been variable efficacy with the use of live-attenuated rotaviruses developed for oral administration (18, 186). A live attenuated tetravalent rhesus-human reassortant rotavirus vaccine (Rotashield) seemed to produce the best results and prevented about half of rotavirus infections, while it was particularly effective in preventing severe disease (194, 321). In 1998 this vaccine, the first licensed rotavirus vaccine, was recommended for routine immunization of U.S. infants. Shortly after the vaccine was approved however, the use of Rotashield was suspended because of the possible association with intussusception (287). This side effect draws attention to possible effects of childhood infection or vaccination on the maturation of the immune system early in life.

Immune responses against heterologous rotavirus infections are usually studied using crude concentrates of cell-culture grown virus (129, 140, 187, 209, 267, 270). Obviously, this approach implies that in addition to the virus, animals are inoculated with viral preparations containing unknown and non-standardized amounts of cellular proteins. From this standpoint, we proposed that the type of purification of the viruses used in such infection experiments might influence subsequent immune responses.

The study presented in **chapter 5** was designed to assess the influence of different preparations of simian rotavirus (SA11) on the immune response following oral delivery to suckling mice as a model for vaccination. Using cesium chloride density gradient centrifugation, we purified three different fractions of simian rotavirus, corresponding with the two forms of virus particles (triple layered and double layered) and infected-cell components. These fractions are enriched, but did not exclusively contain the specified components; while infectious virus was present in all fractions administered but in different amounts. We found that all three fractions of SA11, as well as the homologous mouse rotavirus strain EDIM, were able to induce diarrhea in suckling mice but with different kinetics. Standardization of the SA11 preparations resulted in notable differences in antigen content. In mice, the different preparations however produced very similar serum IgG antibody responses that were comparable to responses after infection with EDIM. Interestingly, the IgG subtype responses of the different fractions were not similar. We found a significantly higher IgG1/2a ratio in the animals inoculated with the infected-cell component fraction compared to the other fractions and the EDIM infected animals. This means that the presence of cell associated proteins results in a skewed Th2-type immune response (134) and indicates that the composition of the inoculum determines the sort of the immune response following infection with the same amount of infectious virus. The presence of high amounts of antigen in the virus preparation could result in an adjuvant effect. Another possibility is that unknown components of infected cells, like cytokines that are produced during infection *in vitro*, could influence the immune response in mice.

As was found in a previous study (385), we observed that the SA11 fractions produced only minor IgA titers when compared to the homologous EDIM strain. Since replication is an important determinant of IgA responses to rotavirus (385), the low levels of IgA are most likely caused by the inferior intestinal replication of the heterologous SA11 strain, with respect to the EDIM strain. In fact, we did not find measurable virus shedding in the SA11-infected animals and in contrast to EDIM inoculated mice, could not detect virus replication in the small intestine either by immunohistochemistry or *in situ* hybridization. Paradoxically, we did observe diarrhea in animals up to 1 week after oral delivery of the SA11 virus. Moreover, mice inoculated with UV-treated triple layered fraction did not experience diarrhea or show an immune response. The results therefore suggest that there was indeed replication of SA11, but that replication occurred extraintestinally.

As stated above, extraintestinal spread of rotavirus might be a common event (40, 282). In case of extraintestinal replication of the virus, the histological damage and diarrhea might be induced by a secreted viral factor and not by direct viral cytopathological effect (CPE) (77, 306). Again, a plausible candidate for this effect would be NSP4. We can also not exclude the possibility that the fractions used for inoculation were contaminated with a small amount of NSP4 protein produced during virus growth in cell culture. This mechanism however, could only account for diarrhea observed on day 1 after inoculation, since it was reported that mice inoculated with purified NSP4, do not experience diarrhea beyond 24 hours after inoculation (16).

The following question still remains; where did SA11 replication occur in the inoculated mice and how did the virus escape the intestine? Rotavirus has been detected in cerebral spinal fluid (188, 248, 294, 310, 474), liver and kidney (145), macrophages in (extra-) intestinal lymphoid tissue (54), serum (40, 431) and heart (282). Moreover, Coulson et al. found that pancreatic islet cells are susceptible to rotavirus infection suggesting that rotavirus can also infect the pancreas (90). It still has to be determined where the SA11 virus replicates in mice, and whether extraintestinal replication is perhaps a common event for heterologous rotaviruses.

It was suggested that rotavirus, gets into the circulatory system through M cells that are present in the epithelium that overlies the Peyer's patches (40, 282). Intestinal replication of rotavirus has been correlated with production of IgA (385), and we found very low levels of IgA after infection with the SA11 strain. From this, we therefore propose that the uptake of SA11 probably occurs via the epithelium of the Peyer's patches and that the virus is subsequently transported to the underlying lymphoid follicles. Replication of SA11 would only occur beyond the intestinal epithelium and Peyer's patches, accounting for the lack of intestinal specific IgA induction, despite the high levels of serum IgG.

The described data might also have important implications with respect to the as yet unexplained adverse effects (i.e. intussusception) of oral rotavirus vaccines (287) and should be evaluated with respect to the development of novel rotavirus vaccines as they have a significant impact on the neonatal immune system. Currently no effective rotavirus vaccine is available. Together with the adverse effects of live attenuated (reassortant) rotavirus vaccines, there is need for alternative strategies for prevention of rotavirus infection and disease. In this light, several studies indicate that a more feasible target for vaccination might prove to be NSP4 (16, 214). Additionally cyclooxygenase inhibitors may also be useful as an antiviral drug, since PGE₂ and COX activity were shown to be crucial for rotavirus replication *in vitro* and rotavirus illness in young children is reduced after oral aspirin, (358, 466).

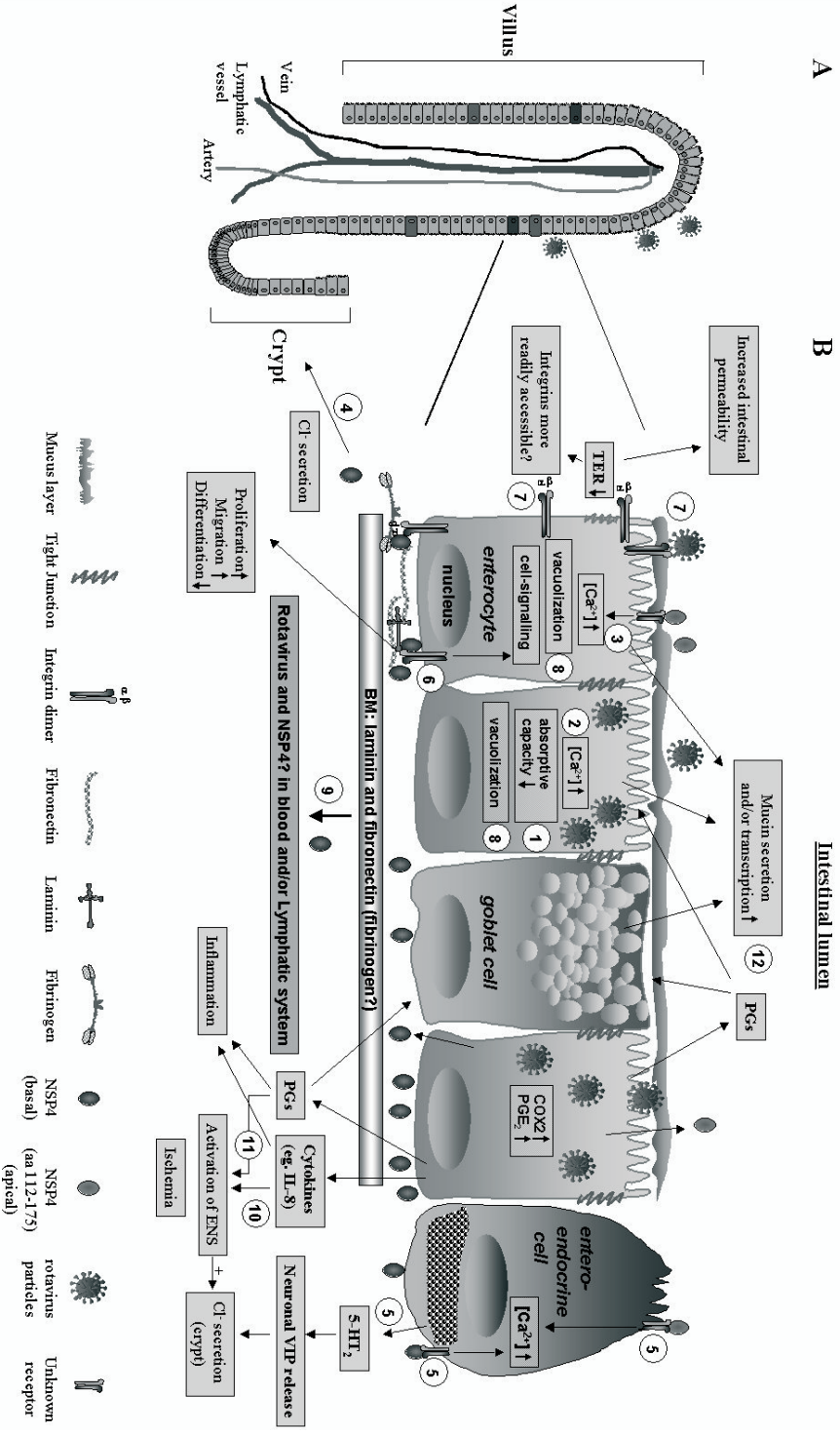


Figure 1. Speculative hypotheses of rotavirus-induced pathogenesis.

The anatomy of the villus is shown in panel A. Intestinal mucosal epithelial cells are formed by division from undifferentiated cells in the villus crypt region. Crypt cells function primarily to secrete fluid into the intestinal lumen. As they mature the cells migrate up the lateral surface of the villus toward the tip. During this process the cells develop microvilli and specialized enzyme systems and carrier proteins for the digestion and absorption of certain nutrients. Rotavirus predominantly infects the more mature enterocytes in the mid and upper part of the villi of the small intestine. In panel B the pleiotropic cellular effects of rotavirus infection and NSP4 are depicted. Different simultaneous effects of rotavirus on cellular homeostasis may achieve the decreased capacity of the intestinal epithelium to absorb solutes and reabsorb water [1].

- 1) Early on during infection, enterocyte specific gene expression is directly down regulated in infected cells at the mRNA level. This results in reduction of mature enterocyte specific protein levels and thus in a functional less differentiated status relatively early during infection while there is still little histological damage.
- 2) Mature enterocytes are lost from the villi through apoptosis and shedding.
- 3) The mature enterocytes are replaced by immature and actively dividing cells.
- 4) NSP4 directly inhibits SGLT1 thereby impairing Na (+)-solute co-transport activities (162, 163). NSP4 can affect cells through its effect on intracellular Ca²⁺. It can increase calcium levels in both infected cells (by acting as a Ca²⁺ channel in the ER (421)) [2], and in neighboring uninfected cells (secreted NSP4 (aa 112-175) binds to an unidentified apical receptor and mediates PLC dependent Ca²⁺ increase (16, 114, 480) [3]. NSP4 may also disperse into the crypts to directly influence the secretory epithelium (Cl⁻ secretion) through its effect on intracellular calcium [4]. By binding to Laminin-β3 and fibronectin (and fibrinogen?), NSP4 could reach the crypt region via a route involving the ECM. NSP4 or rotavirus may also be involved in enteric nervous system (ENS)-mediated disease. For example similar to cholera toxin, NSP4 induced increases the intracellular calcium concentration may cause the release of 5-hydroxytryptamine (5-HT) from enteroendocrine cells (247, 320) [5]. 5-HT activates nervous dendrites to release vasoactive intestinal polypeptide (VIP), this results in both PKC and phosphoinositol hydrolysis-dependent increases in Cl⁻ (or HCO₃⁻) and fluid secretion in crypts as well as decreases in transmucosal absorption (279, 320). NSP4 may influence integrin mediated signaling through binding to the ECM (Laminin-β3, fibronectin, and fibrinogen?), thereby affecting epithelial proliferation, differentiation, migration, and cell survival/apoptosis [6]. NSP4 causes a reduction in the transepithelial electrical resistance (TER) (411) indicating that it can increase epithelial permeability. NSP4 could simultaneously increase epithelial permeability during rotavirus infection and interfere with integrin ECM interactions. This would yield additional unbound integrins that are more readily accessible for rotavirus particles at the more apical surfaces of the intestinal cells [7]. By its effect on intracellular Ca²⁺ or possibly integrin mediated signaling, NSP4 could cause the extensive vacuolization observed during rotavirus infection in mice [8]. Rotavirus is able to enter the circulatory system (40, 282). Like rotavirus, NSP4 could possibly be able to get into the circulatory system (blood and lymphatic system) via release from the basal side of infected epithelial cells [9]. Inflammatory mediators like cytokines, prostaglandins and nitrous oxide, may participate in the inflammatory response and result in impaired intestinal absorption and the initiation of a prosecretory state in the intestine. Rotavirus promotes the synthesis and release of chemokines, such as interleukin (IL)-8 (65, 355). This can enhance the inflammatory cascade producing mucosal and epithelial damage by release of reactive oxygen species. Moreover, activation of the ENS might be accomplished by these chemokines (355) [10]. COX2 and PGE₂ levels are increased after rotavirus infection *in vitro* (358) and elevated levels of prostaglandins have been observed in the plasma and stool of rotavirus-infected children (466). As high levels of PGs (PGE₂) can enhance VIP (accomplished by NSP4?), acetylcholine and substance P-induced chloride secretion in intestinal crypts (208), elevated levels of PGs during rotavirus infection might augment ENS mediated fluid secretion [11].

Rotavirus infection increases mucin transcription and alters mucin glycosylation (and sialylation). These events are mediated by the rotavirus-induced prostaglandins and most probably also by rotavirus-induced cytokines [12]. The alteration in mucin expression and glycosylation probably affect the epithelial barrier function against intestinal pathogens.

Concluding remarks and future directions

There are many unanswered questions regarding the multifactorial rotavirus-induced diarrheal disease and yet more questions have arisen from the work presented in this thesis. In the recent years, many promising and advanced new methods were developed that could shed more light on these questions. One of the most promising methods is RNA interference (RNAi). This technique was already successfully used to study rotavirus proteins and silence VP4 gene expression in virus-infected cells (103). RNAi is a double-stranded RNA-triggered mechanism for suppressing gene expression, which is conserved in evolution and has emerged as a powerful tool to study gene function. Especially for rotavirus, RNAi is an excellent technique to study the role of individual rotavirus proteins like NSP4, as reverse genetic techniques for rotavirus are not available. By silencing cellular proteins, rotavirus-cell interactions can also be studied. Most importantly however, RNAi may additionally prove important for therapeutic approaches for rotavirus and many other viruses (8, 103). In figure 1, an overview is presented showing established (see also **chapter 1**) and speculative events that are or might be involved in the multifactorial process of rotavirus pathogenesis. In view of the processes presented in figure 1 the following questions remain:

- ▶ It was shown that NSP4 mobilizes intracellular calcium ($[Ca^{2+}]_i$) in human intestinal cells through receptor-mediated phospholipase C activation (114). Does this mechanism involve a specific receptor and is this receptor specifically localized at the apical or basal side of epithelial cell?
- ▶ What is the role of the basal release of NSP4 in the induction of diarrhea? Is the entire NSP4 protein or a cleavage product secreted from the basal side of infected enterocytes?
- ▶ Does NSP4 induce a signalling cascade through binding to ECM molecules at the BM (eg. can NSP4 elicit for example integrin mediated cell signalling by disturbing ECM/integrin interactions.) and what cell types are affected (enterocytes, enteroendocrine cells, goblet cells)?
- ▶ Have intracellular NSP4 and extracellular NSP4 (112-175) different roles in rotavirus induced pathogenesis?
- ▶ In order to induce fluid secretion, can NSP4 travel towards the crypt region via a route involving the ECM? With respect to this, NSP4 fails to cause diarrheal disease in CFTR knockout mice (280). Rotavirus-induced secretory diarrhea is therefore probably not mediated by CFTR. What is the molecular identity of the channel(s) responsible for chloride transport?

- ▶ Does a specific cell type (enteroendocrine?) transfer NSP4 mucosal signalling effects into the ENS through release of a mucosal cell neuroactive substance?
- ▶ Is NSP4 able to get into the circulatory system?
- ▶ Our data suggest that posttranslational modification in glycosylation and sialylation of mucins during infection, affect the specific epithelial barrier function against intestinal pathogens. Which specific modifications in mucin structure take place and are PGs involved in these alterations (glycosylation and sialylation)?
- ▶ There are four prostaglandin E type receptors (EP1-4), which of these receptors is involved in the PG-mediated increase in mucin expression during infection?

Chapter 8

Samenvatting

Rotavirussen maken deel uit van de familie van de *Reoviridae* en danken hun naam aan de vorm van de virus deeltjes zoals die met een elektronenmicroscop kunnen worden waargenomen. De deeltjes lijken op een wiel met spaken, vandaar de naam *rota* wat in het Latijn wiel betekent.

Rotavirussen zijn de belangrijkste veroorzakers van ernstige en soms levensbedreigende virale gastro-enteritis en diarree bij de mens. Symptomen zoals koorts, overgeven, diarree en uitdroging worden voornamelijk waargenomen bij jonge kinderen onder de 5 jaar. Rotavirus wordt verspreid via de ontlasting en komt via de mond het lichaam weer binnen. Jaarlijks sterven wereldwijd naar schatting gemiddeld 440.000 kinderen onder de 5 jaar ten gevolge van een rotavirus infectie. Dit houdt in dat wereldwijd 1 op de 293 kinderen die geïnfecteerd worden met rotavirus hieraan sterven. Hierbij moet dan worden opgemerkt dat veruit de meeste slachtoffers vallen in ontwikkelingslanden. De sterke ziektegerelateerde morbiditeit en mortaliteit maakt het noodzakelijk een beter inzicht te krijgen in het ontstaan van symptomen en het ziekteverloop tijdens een rotavirus infectie. Bovendien is de ontwikkeling van een effectief vaccin van groot belang. Er zijn tot nu toe verscheidene vaccins ontwikkeld op basis van eiwitten die de buitenste laag van het virus vormen (VP4 en VP7), maar helaas is er op dit moment geen effectief vaccin tegen rotavirus beschikbaar. In 1999 werd in de Verenigde Staten licentie verleend aan een tetravalent rotavirus vaccin (Rotashield). Dit vaccin werd echter al na enige maanden uit de handel genomen vanwege een verhoogde incidentie van intussusceptie (invaginatie of instulping van de darm) die gecorreleerd bleek te zijn aan de vaccinatie.

Ondanks de hoge prevalentie van rotavirus infecties en de vele uitgebreide studies in verschillende diermodellen, is het inzicht in de mechanismen die leiden tot ziekte beperkt. Het onderzoek dat in dit proefschrift wordt beschreven richt zich in het bijzonder op verschillende factoren die leiden tot rotavirus geïnduceerde ziekte en symptomen.

Hoofdstuk 1 geeft een overzicht van de literatuur betreffende de mechanismen die betrokken zijn bij rotavirus pathogenese. Het dunne darm epitheel bestaat uit verschillende celtypen waaronder enterocyten en slijmbekercellen (goblet cellen). Enterocyten zijn betrokken bij de vertering, opname en transport van voedingsstoffen (zoals suikers en vetten) en deze cellen worden door het rotavirus geïnfecteerd. Slijmbekercellen produceren en scheiden eiwitten zoals mucines uit die belangrijk zijn voor de bescherming van het epitheel. Het mucine Muc2 bijvoorbeeld is de belangrijkste component van de beschermende slijmlaag in de darm.

Het darmepitheel wordt constant vernieuwd en de darmcellen ontstaan uit stamcellen die gelegen zijn in darm instulpingen (crypten). Deze cellen migreren dieper de instulping in of in de richting van de darmholte waar de darm vlokken (villi; deze uitstulpingen zorgen voor een vergroting van de oppervlakte van het darmepitheel) zich bevinden (voor een overzicht van een crypt en villus zie figuur 1 in **hoofdstuk 7**). Tijdens deze migratie differentiëren de cellen tot de verschillende gespecialiseerde celtypen van het darmepitheel. De gespecialiseerde en gedifferentieerde cellen in de crypt en op de darmvlokken gaan na verloop van tijd dood of worden in de darmholte uitgestoten en vervangen door jongere cellen. Op deze manier is er een constante aanmaak en aanstroom van nieuwe cellen. Het is de homeostase van de epitheelcellen waar het rotavirus op ingrijpt.

In **hoofdstuk 2** van dit proefschrift gebruiken we een muizenmodel om het effect van rotavirus infectie op darm homeostase en disfunctie te bestuderen. In dit onderzoek werden 7-dagen oude zogende muisjes geïnfecteerd met een muizen rotavirus. De replicatie van het virus vond plaats in twee pieken, namelijk op dag 1 en dag 4 na infectie. De histologische en morfologische veranderingen werden gekarakteriseerd door het ontstaan van vacuoles in de

enterocyten. We vonden dat door de infectie het aantal apoptotische cellen (celdood) en delende cellen was toegenomen. Bovendien was in geïnfecteerde muizen de snelheid verhoogd waarmee het darmepitheel werd vernieuwd. Het gevolg van deze veranderingen was dat de diepte van de crypten toenam en de darm villi (vlokken) korter werden en daardoor de totale oppervlakte van het darmepitheel kleiner werd. In rotavirus geïnfecteerde enterocyten werd een sterke afname gevonden van de expressie (op zowel eiwit- en RNA niveau) van specifieke eiwitten die betrokken zijn bij de opname en het transport van suikers, zouten, vetten en water. Verschillende factoren, zoals de uitschakeling van genexpressie in enterocyten samen met het verlies van gedifferentieerde enterocyten door apoptose en de vervanging van deze cellen door minder gedifferentieerde cellen, zijn waarschijnlijk verantwoordelijk voor een gebrekkige opname functie van het darmepitheel. Deze gebrekkige opname functie levert vervolgens een belangrijke bijdrage aan het ontstaan van diarree tijdens een rotavirus infectie.

Veel rotavirus stammen gebruiken siaalzuur residuen, die aanwezig zijn op verschillende moleculen in de celmembraan als een soort opstapplaats voor binding aan de gastheercel. Ook veel mucines waaronder Muc2 bevatten veel siaalzuur residuen en er wordt aangenomen dat deze siaalzuren erg belangrijk zijn voor de rotavirus remmende eigenschappen die mucines bezitten. In **hoofdstuk 3** hebben we de rol die slijmbekercellen en mucines spelen bij de bescherming van het darmepitheel tegen een rotavirus infectie geëvalueerd. We laten zien dat tijdens een rotavirus infectie in jonge muizen de slijmbekercellen, in tegenstelling tot enterocyten, niet massaal in apoptose gaan. Bovendien vonden we dat de expressie van intestinale mucine Muc2 was verhoogd tijdens infectie met rotavirus en dat de structuur van deze mucines was veranderd, wat er op duidt dat mucines en in het bijzonder Muc2 een belangrijke rol spelen bij de bescherming tegen infectie. We laten tevens zien dat leeftijdsafhankelijke verschillen in de samenstelling van mucines en een verhoogde aanwezigheid van sterk gesialyleerde mucines tijdens infectie een rol spelen bij hun beschermende capaciteit. De resultaten suggereren dat posttranslationele veranderingen in de glycosylering en sialylering van mucines tijdens rotavirus infectie hun beschermende capaciteit kunnen veranderen. Dit kan uiteindelijk een invloed hebben op de barrière functie van de slijmlaag tegen darm pathogenen.

Hoofdstuk 4 beschrijft een onderzoek naar de rol van prostaglandines (PGs) in de toename van mucine expressie tijdens rotavirus infectie. We vonden dat de expressie van cyclooxygenase 2 (Cox2) mRNA, een eiwit dat essentieel is voor de synthese van PGs, sterk verhoogd is tijdens infectie in muizen. Dit impliceert tevens dat er tijdens infectie zeer waarschijnlijk ook een verhoogde productie van PGs moet zijn geweest.

In geïnfecteerde muizen werden verhoogde niveaus van Muc2, Muc3 en Muc5AC mRNA gemeten. Om de rol van PGs in de transcriptie van mucines te bestuderen werd gebruik gemaakt van 2 celweek modellen. Als een model voor enterocyten werd de humane colon adenocarcinoma cellijn Caco-2 gebruikt. Net als in geïnfecteerde muizen kwam het mucine MUC3 mRNA verhoogd tot expressie tijdens een rotavirus infectie. De PGs PGE₁ en PGE₂ waren in staat om MUC2 and MUC3 specifieke mRNA niveaus te verhogen in LS174T cellen. Deze cellen werden gebruikt als model voor slijmbekercellen. De expressie van MUC5AC werd in mindere mate verhoogd door PGE₁ en helemaal niet door PGE₂. Dit suggereert dat de inductie van dit mucine tijdens rotavirus infectie in muizen niet uitsluitend wordt bewerkstelligd door PGs, maar ook door andere mediators en mechanismen. De bevindingen in hoofdstuk 4 impliceren dat de inductie van mucine expressie tijdens een

rotavirus infectie in ieder geval deels het gevolg zijn van de door rotavirus verhoogde niveaus van Cox2 en PGs.

De meeste rotavirus vaccins worden ontwikkeld op basis van zogenaamde heterologe virussen voor de mens. Dit houdt in dat de mens normaal gesproken geen gastheer is voor deze virussen. Kennis over heterologe infecties in diermodellen zoals de muis is meestal beperkt tot de inductie van diarree en het meten van de aanwezigheid van het virus in de ontlasting. Replicatie van heterologe virussen wordt zelden bestudeerd en bevestigd in het darmweefsel. Daarentegen wordt een toegenomen hoeveelheid (infectieus) virus in de ontlasting gebruikt als maat voor replicatie in de darm.

In **hoofdstuk 5** is onderzocht of er verschillen bestaan in de afweerreactie na infectie met een muizen rotavirus (EDIM stam) als model voor een natuurlijke infectie en een heteroloog apen rotavirus (SA11 stam) als model voor vaccinatie. Voor de heterologe infectie werden drie verschillende fracties van het SA11 virus (met verschillende samenstelling) gebruikt die waren verkregen met behulp van cesium chloride gradiënt zuivering. EDIM en alle drie geteste fracties van SA11 bleken in staat om diarree te veroorzaken in jonge muizen, terwijl fecale uitscheiding van het virus alleen werd waargenomen bij het EDIM virus. In tegenstelling tot EDIM, werd er met behulp van verschillende technieken geen replicatie van SA11 gedetecteerd in het dunne darmweefsel van geïnfecteerde muizen. Er bestaan dus grote verschillen in de mate van virus replicatie en het (mogelijke) weefsel tropisme van het homologe EDIM virus en het heterologe SA11 virus. Dit gegeven is waarschijnlijk verantwoordelijk voor het feit dat er werd aangetoond dat de specifieke mucosale afweerreactie (ontwikkeling van IgA antilichamen) niet tot stand komt na de heterologe infectie, dit in tegenstelling tot de homologe infectie. Het EDIM virus en de drie verschillende SA11 fracties induceerden dezelfde hoeveelheid IgG. De rotavirus specifieke IgG1/IgG2a ratio verschilde echter tussen de verschillende SA11 fracties. Dit betekent dat het type immuun respons (Th1/Th2) dat wordt opgewekt tegen een heteroloog virus afhankelijk is van de exacte samenstelling van het inoculum dat gebruikt is voor de infectie van de muizen. Het is derhalve van groot belang om met deze factoren rekening te houden met betrekking tot de ontwikkeling van nieuwe rotavirus vaccines.

Het rotavirus genoom codeert voor zowel eiwitten die een onderdeel uitmaken van het virus deeltje (structurele eiwitten), als eiwitten die geen deel uitmaken van het virus maar alleen tot expressie komen als het virus zich vermenigvuldigt in de gastheercel (niet structurele eiwitten). De niet structurele eiwitten spelen een belangrijke rol bij de morfogenese en vermenigvuldiging van het virus. Eén van de niet structurele eiwitten, NSP4, is recentelijk geïdentificeerd als het eerste virale enterotoxine. NSP4 is in staat om diarree te veroorzaken als het in de buikholte of in de darm van jonge dieren wordt ingespoten. De inductie van diarree door NSP4 is leeftijdsafhankelijk en lijkt in die zin op de leeftijdsafhankelijke diarree veroorzaakt door een rotavirus infectie. Deze gegevens tonen aan dat NSP4 dus voor een belangrijk deel verantwoordelijk is voor de diarree die ontstaat tijdens een rotavirus infectie. In **hoofdstuk 6** is onderzocht met welke cellulaire eiwitten NSP4 een interactie aangaat. Die eiwitten spelen mogelijk een rol bij het ontstaan van diarree. Met behulp van de zogenaamde two-hybrid techniek in gist cellen, waarmee eiwit interacties kunnen worden aangetoond, vonden we twee extracellulaire matrix (ECM) eiwitten, laminine- β 3 en fibronectine. De interactie van deze twee eiwitten met NSP4 werd vervolgens ook aangetoond door middel van co-immunoprecipitatie. Bovendien kon NSP4 samen met laminine- β 3 in de basale

membraan van geïnfecteerde muizen worden aangetoond. Dit duidt er op dat er een fysiologische interactie plaatsvindt. De binding van NSP4 aan extracellulaire matrix eiwitten in de basale membraan duidt er op dat NSP4 vrijkomt vanuit de basale kant van geïnfecteerde cellen. De beschreven bevindingen wijzen mogelijk op een nieuw mechanisme waarop rotavirus diarree en ziekte ontstaat.

Hoofdstuk 7 tenslotte, geeft een opsomming en bediscussieert de resultaten van de voorgaande hoofdstukken. De figuur in dit hoofdstuk geeft een overzicht van gevestigde en speculatieve gebeurtenissen die betrokken (kunnen) zijn bij het ontstaan van rotavirus pathogenese.

References

1. Adams, W. R., and L. M. Kraft. 1963. Epizootic diarrhea of infant mice: identification of the etiologic agent. *Science* 141:359-60.
2. Afrikanova, I., E. Fabbretti, M. C. Miozzo, and O. R. Burrone. 1998. Rotavirus NSP5 phosphorylation is up-regulated by interaction with NSP2. *J Gen Virol* 79 (Pt 11):2679-86.
3. Afrikanova, I., M. C. Miozzo, S. Giambiagi, and O. Burrone. 1996. Phosphorylation generates different forms of rotavirus NSP5. *J Gen Virol* 77 (Pt 9):2059-65.
4. Anderson, E. J., and S. G. Weber. 2004. Rotavirus infection in adults. *Lancet Infect Dis* 4:91-9.
5. Angel, J., B. Tang, N. Feng, H. B. Greenberg, and D. Bass. 1998. Studies of the role for NSP4 in the pathogenesis of homologous murine rotavirus diarrhea. *J Infect Dis* 177:455-8.
6. Ansari, S. A., S. A. Sattar, V. S. Springthorpe, G. A. Wells, and W. Tostowaryk. 1988. Rotavirus survival on human hands and transfer of infectious virus to animate and nonporous inanimate surfaces. *J Clin Microbiol* 26:1513-8.
7. Aponte, C., N. M. Mattion, M. K. Estes, A. Charpilienne, and J. Cohen. 1993. Expression of two bovine rotavirus non-structural proteins (NSP2, NSP3) in the baculovirus system and production of monoclonal antibodies directed against the expressed proteins. *Arch Virol* 133:85-95.
8. Arias, C. F., M. A. Dector, L. Segovia, T. Lopez, M. Camacho, P. Isa, R. Espinosa, and S. Lopez. 2004. RNA silencing of rotavirus gene expression. *Virus Res* 102:43-51.
9. Arias, C. F., S. Lopez, and R. T. Espejo. 1982. Gene protein products of SA11 simian rotavirus genome. *J Virol* 41:42-50.
10. Arias, C. F., P. Romero, V. Alvarez, and S. Lopez. 1996. Trypsin activation pathway of rotavirus infectivity. *J Virol* 70:5832-9.
11. Au, K. S., W. K. Chan, J. W. Burns, and M. K. Estes. 1989. Receptor activity of rotavirus nonstructural glycoprotein NS28. *J Virol* 63:4553-62.
12. Au, K. S., N. M. Mattion, and M. K. Estes. 1993. A subviral particle binding domain on the rotavirus nonstructural glycoprotein NS28. *Virology* 194:665-73.
13. Audie, J. P., A. Janin, N. Porchet, M. C. Copin, B. Gosselin, and J. P. Aubert. 1993. Expression of human mucin genes in respiratory, digestive, and reproductive tracts ascertained by in situ hybridization. *J Histochem Cytochem* 41:1479-85.
14. Awad, A. B., A. Kamei, P. J. Horvath, and C. S. Fink. 1995. Prostaglandin synthesis in human cancer cells: influence of fatty acids and butyrate. *Prostaglandins Leukot Essent Fatty Acids* 53:87-93.
15. Azim, T., S. M. Ahmad, E. K. Sefat, M. S. Sarker, L. E. Unicomb, S. De, J. D. Hamadani, M. A. Salam, M. A. Wahed, and M. J. Albert. 1999. Immune response of children who develop persistent diarrhea following rotavirus infection. *Clin Diagn Lab Immunol* 6:690-5.
16. Ball, J. M., P. Tian, C. Q. Zeng, A. P. Morris, and M. K. Estes. 1996. Age-dependent diarrhea induced by a rotaviral nonstructural glycoprotein. *Science* 272:101-4.
17. Barkalow, F. J., and J. E. Schwarzbauer. 1991. Localization of the major heparin-binding site in fibronectin. *J Biol Chem* 266:7812-8.
18. Barnes, G. L., J. S. Lund, S. V. Mitchell, L. De Bruyn, L. Piggford, A. L. Smith, J. Furnedge, P. J. Masendycz, H. C. Bugg, N. Bogdanovic-Sakran, J. B. Carlin, and R. F. Bishop. 2002. Early phase II trial of human rotavirus vaccine candidate RV3. *Vaccine* 20:2950-6.
19. Bass, D., E. Cordoba, C. Dekker, A. Schuind, and C. Cassady. 2004. Intestinal imaging of children with acute rotavirus gastroenteritis. *J Pediatr Gastroenterol Nutr* 39(3):270-274.
20. Beaulieu, J. F. 1992. Differential expression of the VLA family of integrins along the crypt-villus axis in the human small intestine. *J Cell Sci* 102 (Pt 3):427-36.
21. Beaulieu, J. F. 1999. Integrins and human intestinal cell functions. *Front Biosci* 4:D310-21.
22. Beaulieu, J. F., P. H. Vachon, and S. Chartrand. 1991. Immunolocalization of extracellular matrix components during organogenesis in the human small intestine. *Anat Embryol (Berl)* 183:363-9.
23. Beisner, B., D. Kool, A. Marich, and I. H. Holmes. 1998. Characterisation of G serotype dependent non-antibody inhibitors of rotavirus in normal mouse serum. *Arch Virol* 143:1277-94.
24. Bell, L. M., H. F. Clark, E. A. O'Brien, M. J. Kornstein, S. A. Plotkin, and P. A. Offit. 1987. Gastroenteritis caused by human rotaviruses (serotype three) in a suckling mouse model. *Proc Soc Exp Biol Med* 184:127-32.
25. Belley, A., and K. Chadee. 1999. Prostaglandin E(2) stimulates rat and human colonic mucin exocytosis via the EP(4) receptor. *Gastroenterology* 117:1352-62.
26. Berghem, L. E., and K. J. Johanson. 1983. Effect of ¹³⁷Cs gamma radiation on the fibronectin content in basement membrane of mouse small intestine. *Acta Radiol Oncol* 22:389-93.

27. Bern, C., and R. I. Glass. 1994. Impact of diarrheal diseases worldwide. *In* A. Z. Kapikian (ed.), *Viral Infections of the Gastrointestinal Tract*. Marcel Dekker, New York.
28. Bern, C., J. Martinez, I. de Zoysa, and R. I. Glass. 1992. The magnitude of the global problem of diarrhoeal disease: a ten-year update. *Bull World Health Organ* 70:705-14.
29. Bernstein, D. I., M. M. McNeal, G. M. Schiff, and R. L. Ward. 1989. Induction and persistence of local rotavirus antibodies in relation to serum antibodies. *J Med Virol* 28:90-5.
30. Bican, P., J. Cohen, A. Charpilienne, and R. Scherrer. 1982. Purification and characterization of bovine rotavirus cores. *J Virol* 43:1113-7.
31. Bishop, R. F., G. L. Barnes, E. Cipriani, and J. S. Lund. 1983. Clinical immunity after neonatal rotavirus infection. A prospective longitudinal study in young children. *N Engl J Med* 309:72-6.
32. Bishop, R. F., G. P. Davidson, I. H. Holmes, and B. J. Ruck. 1974. Detection of a new virus by electron microscopy of faecal extracts from children with acute gastroenteritis. *Lancet* 1:149-51.
33. Bishop, R. F., G. P. Davidson, I. H. Holmes, and B. J. Ruck. 1973. Virus particles in epithelial cells of duodenal mucosa from children with acute non-bacterial gastroenteritis. *Lancet* 2:1281-3.
34. Black, R. E., M. H. Merson, A. S. Rahman, M. Yunus, A. R. Alim, I. Huq, R. H. Yolken, and G. T. Curlin. 1980. A two-year study of bacterial, viral, and parasitic agents associated with diarrhea in rural Bangladesh. *J Infect Dis* 142:660-4.
35. Black, T. L., G. N. Barber, and M. G. Katze. 1993. Degradation of the interferon-induced 68,000-M(r) protein kinase by poliovirus requires RNA. *J Virol* 67:791-800.
36. Blackhall, J., A. Fuentes, K. Hansen, and G. Magnusson. 1997. Serine protein kinase activity associated with rotavirus phosphoprotein NSP5. *J Virol* 71:138-44.
37. Blomback, B., B. Hessel, D. Hogg, and L. Therkildsen. 1978. A two-step fibrinogen--fibrin transition in blood coagulation. *Nature* 275:501-5.
38. Bloom, L., K. C. Ingham, and R. O. Hynes. 1999. Fibronectin regulates assembly of actin filaments and focal contacts in cultured cells via the heparin-binding site in repeat III13. *Mol Biol Cell* 10:1521-36.
39. Blutt, S. E., S. E. Crawford, K. L. Warfield, D. E. Lewis, M. K. Estes, and M. E. Conner. 2004. The VP7 outer capsid protein of rotavirus induces polyclonal B-cell activation. *J Virol* 78:6974-81.
40. Blutt, S. E., C. D. Kirkwood, V. Parreno, K. L. Warfield, M. Ciarlet, M. K. Estes, K. Bok, R. F. Bishop, and M. E. Conner. 2003. Rotavirus antigenaemia and viraemia: a common event? *Lancet* 362:1445-9.
41. Bolivar, R., R. H. Conklin, J. J. Vollet, L. K. Pickering, H. L. DuPont, D. L. Walters, and S. Kohl. 1978. Rotavirus in travelers' diarrhea: study of an adult student population in Mexico. *J Infect Dis* 137:324-7.
42. Borchers, M. T., M. P. Carty, and G. D. Leikauf. 1999. Regulation of human airway mucins by acrolein and inflammatory mediators. *Am J Physiol* 276:L549-55.
43. Boshuizen, J. A., J. H. Reimerink, A. M. Korteland-Van Male, V. J. Van Ham, M. P. Koopmans, H. A. Buller, J. Dekker, and A. W. Einerhand. 2003. Changes in Small Intestinal Homeostasis, Morphology, and Gene Expression during Rotavirus Infection of Infant Mice. *J Virol* 77:13005-16.
44. Boshuizen, J. A., J. W. Rossen, C. K. Sitaram, F. F. Kimenai, Y. Simons-Oosterhuis, C. Lafféber, H. A. Buller, and A. W. Einerhand. 2004. Rotavirus enterotoxin NSP4 binds to the extracellular matrix proteins laminin-beta3 and fibronectin. *J Virol* 78:10045-53.
45. Both, G. W., J. S. Mattick, and A. R. Bellamy. 1983. Serotype-specific glycoprotein of simian 11 rotavirus: coding assignment and gene sequence. *Proc Natl Acad Sci U S A* 80:3091-5.
46. Both, G. W., L. J. Siegman, A. R. Bellamy, and P. H. Atkinson. 1983. Coding assignment and nucleotide sequence of simian rotavirus SA11 gene segment 10: location of glycosylation sites suggests that the signal peptide is not cleaved. *J Virol* 48:335-9.
47. Bowman, G. D., I. M. Nodelman, O. Levy, S. L. Lin, P. Tian, T. J. Zamb, S. A. Udem, B. Venkataraghavan, and C. E. Schutt. 2000. Crystal structure of the oligomerization domain of NSP4 from rotavirus reveals a core metal-binding site. *J Mol Biol* 304:861-71.
48. Boyle, J. F., and K. V. Holmes. 1986. RNA-binding proteins of bovine rotavirus. *J Virol* 58:561-8.
49. Brandt, C. D., H. W. Kim, W. J. Rodriguez, J. O. Arrobio, B. C. Jeffries, E. P. Stallings, C. Lewis, A. J. Miles, R. M. Chanock, A. Z. Kapikian, and R. H. Parrott. 1983. Pediatric viral gastroenteritis during eight years of study. *J Clin Microbiol* 18:71-8.
50. Bresee, J. S., R. I. Glass, B. Ivanoff, and J. R. Gentsch. 1999. Current status and future priorities for rotavirus vaccine development, evaluation and implementation in developing countries. *Vaccine* 17:2207-22.
51. Bridger, J. C., W. Dhaliwal, M. J. Adamson, and C. R. Howard. 1998. Determinants of rotavirus host range restriction--a heterologous bovine NSP1 gene does not affect replication kinetics in the pig. *Virology* 245:47-52.

52. Bridger, J. C., G. A. Hall, and K. R. Parsons. 1992. A study of the basis of virulence variation of bovine rotaviruses. *Vet Microbiol* 33:169-74.
53. Broome, R. L., P. T. Vo, R. L. Ward, H. F. Clark, and H. B. Greenberg. 1993. Murine rotavirus genes encoding outer capsid proteins VP4 and VP7 are not major determinants of host range restriction and virulence. *J Virol* 67:2448-55.
54. Brown, K. A., and P. A. Offit. 1998. Rotavirus-specific proteins are detected in murine macrophages in both intestinal and extraintestinal lymphoid tissues. *Microb Pathog* 24:327-31.
55. Buisine, M. P., P. Desreumaux, E. Leteurtre, M. C. Copin, J. F. Colombel, N. Porchet, and J. P. Aubert. 2001. Mucin gene expression in intestinal epithelial cells in Crohn's disease. *Gut* 49:544-51.
56. Buisine, M. P., J. L. Desseyn, N. Porchet, P. Degand, A. Laine, and J. P. Aubert. 1998. Genomic organization of the 3'-region of the human MUC5AC mucin gene: additional evidence for a common ancestral gene for the 11p15.5 mucin gene family. *Biochem J* 332 (Pt 3):729-38.
57. Buller, H. A., M. J. Kothe, D. A. Goldman, S. A. Grubman, W. V. Sasak, P. T. Matsudaira, R. K. Montgomery, and R. J. Grand. 1990. Coordinate expression of lactase-phlorizin hydrolase mRNA and enzyme levels in rat intestine during development. *J Biol Chem* 265:6978-83.
58. Burke, B., and U. Desselberger. 1996. Rotavirus pathogenicity. *Virology* 218:299-305.
59. Burns, J. W., A. A. Krishnaney, P. T. Vo, R. V. Rouse, L. J. Anderson, and H. B. Greenberg. 1995. Analyses of homologous rotavirus infection in the mouse model. *Virology* 207:143-53.
60. Busby, T. F., W. S. Argraves, S. A. Brew, I. Pechik, G. L. Gilliland, and K. C. Ingham. 1995. Heparin binding by fibronectin module III-13 involves six discontinuous basic residues brought together to form a cationic cradle. *J Biol Chem* 270:18558-62.
61. Bushell, M., and P. Sarnow. 2002. Hijacking the translation apparatus by RNA viruses. *J Cell Biol* 158:395-9.
62. Campbell, I. D., and C. Spitzfaden. 1994. Building proteins with fibronectin type III modules. *Structure* 2:333-7.
63. Carpio, M. M., L. A. Babiuk, V. Misra, and R. M. Blumenthal. 1981. Bovine rotavirus-cell interactions: effect of virus infection on cellular integrity and macromolecular synthesis. *Virology* 114:86-97.
64. Carter, W. G., M. C. Ryan, and P. J. Gahr. 1991. Epiligrin, a new cell adhesion ligand for integrin alpha 3 beta 1 in epithelial basement membranes. *Cell* 65:599-610.
65. Casola, A., M. K. Estes, S. E. Crawford, P. L. Ogra, P. B. Ernst, R. P. Garofalo, and S. E. Crowe. 1998. Rotavirus infection of cultured intestinal epithelial cells induces secretion of CXC and CC chemokines. *Gastroenterology* 114:947-55.
66. Chan, B. M., M. J. Elices, E. Murphy, and M. E. Hemler. 1992. Adhesion to vascular cell adhesion molecule 1 and fibronectin. Comparison of alpha 4 beta 1 (VLA-4) and alpha 4 beta 7 on the human B cell line JY. *J Biol Chem* 267:8366-70.
67. Chan, W. K., K. S. Au, and M. K. Estes. 1988. Topography of the simian rotavirus nonstructural glycoprotein (NS28) in the endoplasmic reticulum membrane. *Virology* 164:435-42.
68. Chang, K. O., Y. J. Kim, and L. J. Saif. 1999. Comparisons of nucleotide and deduced amino acid sequences of NSP4 genes of virulent and attenuated pairs of group A and C rotaviruses. *Virus Genes* 18:229-33.
69. Chang, S. K., A. F. Dohrman, C. B. Basbaum, S. B. Ho, T. Tsuda, N. W. Toribara, J. R. Gum, and Y. S. Kim. 1994. Localization of mucin (MUC2 and MUC3) messenger RNA and peptide expression in human normal intestine and colon cancer. *Gastroenterology* 107:28-36.
70. Charpilienne, A., M. J. Abad, F. Michelangeli, F. Alvarado, M. Vasseur, J. Cohen, and M. C. Ruiz. 1997. Solubilized and cleaved VP7, the outer glycoprotein of rotavirus, induces permeabilization of cell membrane vesicles. *J Gen Virol* 78 (Pt 6):1367-71.
71. Chemello, M. E., O. C. Aristimuno, F. Michelangeli, and M. C. Ruiz. 2002. Requirement for vacuolar H⁺-ATPase activity and Ca²⁺ gradient during entry of rotavirus into MA104 cells. *J Virol* 76:13083-7.
72. Chen, C. C., M. Baylor, and D. M. Bass. 1993. Murine intestinal mucins inhibit rotavirus infection. *Gastroenterology* 105:84-92.
73. Chen, D., C. L. Luongo, M. L. Nibert, and J. T. Patton. 1999. Rotavirus open cores catalyze 5'-capping and methylation of exogenous RNA: evidence that VP3 is a methyltransferase. *Virology* 265:120-30.
74. Chen, N., and C. S. Reis. 2002. Distinct roles of eicosanoids in the immune response to viral encephalitis: or why you should take NSAIDS. *Viral Immunol* 15:133-46.
75. Cheng, Y. S., M. F. Champlaud, R. E. Burgeson, M. P. Marinkovich, and P. D. Yurchenco. 1997. Self-assembly of laminin isoforms. *J Biol Chem* 272:31525-32.

76. Chien, C. T., P. L. Bartel, R. Sternglanz, and S. Fields. 1991. The two-hybrid system: a method to identify and clone genes for proteins that interact with a protein of interest. *Proc Natl Acad Sci U S A* 88:9578-82.
77. Ciarlet, M., M. E. Conner, M. J. Finegold, and M. K. Estes. 2002. Group A Rotavirus Infection and Age-Dependent Diarrheal Disease in Rats: a New Animal Model To Study the Pathophysiology of Rotavirus Infection. *J Virol* 76:41-57.
78. Ciarlet, M., S. E. Crawford, and M. K. Estes. 2001. Differential infection of polarized epithelial cell lines by sialic acid-dependent and sialic acid-independent rotavirus strains. *J Virol* 75:11834-50.
79. Ciarlet, M., and M. K. Estes. 1999. Human and most animal rotavirus strains do not require the presence of sialic acid on the cell surface for efficient infectivity. *J Gen Virol* 80:943-8.
80. Ciarlet, M., F. Liprandi, M. E. Conner, and M. K. Estes. 2000. Species specificity and interspecies relatedness of NSP4 genetic groups by comparative NSP4 sequence analyses of animal rotaviruses. *Arch Virol* 145:371-83.
81. Clark, S. M., J. R. Roth, M. L. Clark, B. B. Barnett, and R. S. Spendlove. 1981. Trypsin enhancement of rotavirus infectivity: mechanism of enhancement. *J Virol* 39:816-22.
82. Coelho, K. I., A. S. Bryden, C. H. Hall, and T. H. Flewett. 1981. Pathology of rotavirus infection in suckling mice: a study by conventional histology, immunofluorescence, ultrathin sections, and scanning electron microscopy. *Ultrastruct Pathol* 2:59-80.
83. Cohen, J., A. Charpilienne, S. Chilmonczyk, and M. K. Estes. 1989. Nucleotide sequence of bovine rotavirus gene 1 and expression of the gene product in baculovirus. *Virology* 171:131-40.
84. Collins, J., W. G. Starkey, T. S. Wallis, G. J. Clarke, K. J. Worton, A. J. Spencer, S. J. Haddon, M. P. Osborne, D. C. Candy, and J. Stephen. 1988. Intestinal enzyme profiles in normal and rotavirus-infected mice. *J Pediatr Gastroenterol Nutr* 7:264-72.
85. Collins, J. E., D. A. Benfield, and J. R. Duimstra. 1989. Comparative virulence of two porcine group-A rotavirus isolates in gnotobiotic pigs. *Am J Vet Res* 50:827-35.
86. Colognato, H., and P. D. Yurchenco. 2000. Form and function: the laminin family of heterotrimers. *Dev Dyn* 218:213-34.
87. Control, C. f. D. 1999. Rotavirus vaccine for prevention of rotavirus gastroenteritis among children. Recommendations of the Advisory Committee on Immunization Practices (ACIP). *Morb Mortal Wkly Rep* 48:1-20.
88. Corpe, C. P., and C. F. Burant. 1996. Hexose transporter expression in rat small intestine: effect of diet on diurnal variations. *Am J Physiol* 271:G211-6.
89. Coulson, B. S., S. L. Londrigan, and D. J. Lee. 1997. Rotavirus contains integrin ligand sequences and a disintegrin-like domain that are implicated in virus entry into cells. *Proc Natl Acad Sci U S A* 94:5389-94.
90. Coulson, B. S., P. D. Witterick, Y. Tan, M. J. Hewish, J. N. Mountford, L. C. Harrison, and M. C. Honeyman. 2002. Growth of rotaviruses in primary pancreatic cells. *J Virol* 76:9537-44.
91. Cox, K. H., D. V. DeLeon, L. M. Angerer, and R. C. Angerer. 1984. Detection of mnas in sea urchin embryos by in situ hybridization using asymmetric RNA probes. *Dev Biol* 101:485-502.
92. Cox, M. J., and G. F. Medley. 2003. Serological survey of anti-group A rotavirus IgM in UK adults. *Epidemiol Infect* 131:719-26.
93. Crawford, S. E., M. Labbe, J. Cohen, M. H. Burroughs, Y. J. Zhou, and M. K. Estes. 1994. Characterization of virus-like particles produced by the expression of rotavirus capsid proteins in insect cells. *J Virol* 68:5945-52.
94. Crawford, S. E., S. K. Mukherjee, M. K. Estes, J. A. Lawton, A. L. Shaw, R. F. Ramig, and B. V. Prasad. 2001. Trypsin cleavage stabilizes the rotavirus VP4 spike. *J Virol* 75:6052-61.
95. Crawley, J. M., R. F. Bishop, and G. L. Barnes. 1993. Rotavirus gastroenteritis in infants aged 0-6 months in Melbourne, Australia: implications for vaccination. *J Paediatr Child Health* 29:219-21.
96. Cuadras, M. A., D. A. Feigelstock, S. An, and H. B. Greenberg. 2002. Gene expression pattern in Caco-2 cells following rotavirus infection. *J Virol* 76:4467-82.
97. Davidson, G. P., and G. L. Barnes. 1979. Structural and functional abnormalities of the small intestine in infants and young children with rotavirus enteritis. *Acta Paediatr Scand* 68:181-6.
98. Davidson, G. P., R. F. Bishop, R. R. Townley, and I. H. Holmes. 1975. Importance of a new virus in acute sporadic enteritis in children. *Lancet* 1:242-6.
99. Davidson, G. P., D. G. Gall, M. Petric, D. G. Butler, and J. R. Hamilton. 1977. Human rotavirus enteritis induced in conventional piglets. Intestinal structure and transport. *J Clin Invest* 60:1402-9.

100. Davril, M., S. Degroote, P. Humbert, C. Galabert, V. Dumur, J. J. Lafitte, G. Lamblin, and P. Roussel. 1999. The sialylation of bronchial mucins secreted by patients suffering from cystic fibrosis or from chronic bronchitis is related to the severity of airway infection. *Glycobiology* 9:311-21.
101. de Wit, M. A., M. P. Koopmans, L. M. Kortbeek, N. J. van Leeuwen, J. Vinje, and Y. T. van Duynhoven. 2001. Etiology of gastroenteritis in sentinel general practices in the Netherlands. *Clin Infect Dis* 33:280-8.
102. de Wit, M. A., M. P. Koopmans, J. F. van der Blij, and Y. T. van Duynhoven. 2000. Hospital admissions for rotavirus infection in the Netherlands. *Clin Infect Dis* 31:698-704.
103. Dector, M. A., P. Romero, S. Lopez, and C. F. Arias. 2002. Rotavirus gene silencing by small interfering RNAs. *EMBO Rep* 3:1175-80.
104. Dekker J, E., AWC, Büller HA. 2002. Carbohydrate malabsorption, p. 339-374. *In* L. CH (ed.), *Pediatric gastroenterology and nutrition in clinical practice*. Marcel Dekker Inc, New York.
105. Dekker, J., J. W. Rossen, H. A. Buller, and A. W. Einerhand. 2002. The MUC family: an obituary. *Trends Biochem Sci* 27:126-31.
106. Delmotte, P., S. Degroote, M. D. Merten, I. Van Seuning, A. Bernigaud, C. Figarella, P. Roussel, and J. M. Perini. 2001. Influence of TNFalpha on the sialylation of mucins produced by a transformed cell line MM-39 derived from human tracheal gland cells. *Glycoconj J* 18:487-97.
107. Delorme, C., H. Brussow, J. Sidoti, N. Roche, K. A. Karlsson, J. R. Neeser, and S. Teneberg. 2001. Glycosphingolipid binding specificities of rotavirus: identification of a sialic acid-binding epitope. *J Virol* 75:2276-87.
108. Denisova, E., W. Dowling, R. LaMonica, R. Shaw, S. Scarlata, F. Ruggeri, and E. R. Mackow. 1999. Rotavirus capsid protein VP5* permeabilizes membranes. *J Virol* 73:3147-53.
109. Deo, R. C., C. M. Groft, K. R. Rajashankar, and S. K. Burley. 2002. Recognition of the rotavirus mRNA 3' consensus by an asymmetric NSP3 homodimer. *Cell* 108:71-81.
110. Deplancke, B., and H. R. Gaskins. 2001. Microbial modulation of innate defense: goblet cells and the intestinal mucus layer. *Am J Clin Nutr* 73:1131S-1141S.
111. Desselberger, U. 1999. Rotavirus infections: guidelines for treatment and prevention. *Drugs* 58:447-52.
112. Dickman, K. G., S. J. Hempson, J. Anderson, S. Lippe, L. Zhao, R. Burakoff, and R. D. Shaw. 2000. Rotavirus alters paracellular permeability and energy metabolism in Caco-2 cells. *Am J Physiol Gastrointest Liver Physiol* 279:G757-66.
113. Dohrman, A., S. Miyata, M. Gallup, J. D. Li, C. Chapelin, A. Coste, E. Escudier, J. Nadel, and C. Basbaum. 1998. Mucin gene (MUC 2 and MUC 5AC) upregulation by Gram-positive and Gram-negative bacteria. *Biochim Biophys Acta* 1406:251-9.
114. Dong, Y., C. Q. Zeng, J. M. Ball, M. K. Estes, and A. P. Morris. 1997. The rotavirus enterotoxin NSP4 mobilizes intracellular calcium in human intestinal cells by stimulating phospholipase C-mediated inositol 1,4,5-trisphosphate production. *Proc Natl Acad Sci U S A* 94:3960-5.
115. Dormitzer, P. R., and H. B. Greenberg. 1992. Calcium chelation induces a conformational change in recombinant herpes simplex virus-1-expressed rotavirus VP7. *Virology* 189:828-32.
116. Einerhand, A. W., I. B. Renes, M. K. Makkink, M. van der Sluis, H. A. Buller, and J. Dekker. 2002. Role of mucins in inflammatory bowel disease: important lessons from experimental models. *Eur J Gastroenterol Hepatol* 14:757-65.
117. Enss, M. L., H. K. Heim, S. Wagner, W. Beil, R. Eisenblatter, K. F. Sewing, and H. J. Hedrich. 1998. Effects of PGE2 and of different synthetic PGE derivatives on the glycosylation of pig gastric mucins. *Prostaglandins Leukot Essent Fatty Acids* 59:49-54.
118. Ericson, B. L., D. Y. Graham, B. B. Mason, and M. K. Estes. 1982. Identification, synthesis, and modifications of simian rotavirus SA11 polypeptides in infected cells. *J Virol* 42:825-39.
119. Ericson, B. L., D. Y. Graham, B. B. Mason, H. H. Hanssen, and M. K. Estes. 1983. Two types of glycoprotein precursors are produced by the simian rotavirus SA11. *Virology* 127:320-32.
120. Escande, F., N. Porchet, A. Bernigaud, D. Petitprez, J. P. Aubert, and M. P. Buisine. 2004. The mouse secreted gel-forming mucin gene cluster. *Biochim Biophys Acta* 1676:240-50.
121. Espejo, R. T., S. Lopez, and C. Arias. 1981. Structural polypeptides of simian rotavirus SA11 and the effect of trypsin. *J Virol* 37:156-60.
122. Estes, M. K. 2001. Rotaviruses and their replication, p. 1747-1785. *In* D. M. Knipe and P. M. Howley (ed.), *Fields virology*. Lippincott-Raven Publishers, Philadelphia.
123. Estes, M. K., and J. Cohen. 1989. Rotavirus structure and function. *Microbiological reviews* 53:410-449.
124. Estes, M. K., S. E. Crawford, M. E. Penaranda, B. L. Petrie, J. W. Burns, W. K. Chan, B. Ericson, G. E. Smith, and M. D. Summers. 1987. Synthesis and immunogenicity of the rotavirus major capsid antigen using a baculovirus expression system. *J Virol* 61:1488-94.

125. Estes, M. K., D. Y. Graham, and B. B. Mason. 1981. Proteolytic enhancement of rotavirus infectivity: molecular mechanisms. *J Virol* 39:879-88.
126. Estes, M. K., and A. P. Morris. 1999. A viral enterotoxin. A new mechanism of virus-induced pathogenesis. *Adv Exp Med Biol* 473:73-82.
127. Fabbretti, E., I. Afrikanova, F. Vascotto, and O. R. Burrone. 1999. Two non-structural rotavirus proteins, NSP2 and NSP5, form viroplasm-like structures in vivo. *J Gen Virol* 80 (Pt 2):333-9.
128. Farthing, M. J. 1993. Pathophysiology of infective diarrhoea. *Eur J Gastroenterol Hepatol* 5:796-807.
129. Feng, N., J. W. Burns, L. Bracy, and H. B. Greenberg. 1994. Comparison of mucosal and systemic humoral immune responses and subsequent protection in mice orally inoculated with a homologous or a heterologous rotavirus. *J Virol* 68:7766-73.
130. Feng, N., M. A. Franco, and H. B. Greenberg. 1997. Murine model of rotavirus infection. *Adv Exp Med Biol* 412:233-40.
131. French-Constant, C. 1995. Alternative splicing of fibronectin--many different proteins but few different functions. *Exp Cell Res* 221:261-71.
132. Fields, S., and O. Song. 1989. A novel genetic system to detect protein-protein interactions. *Nature* 340:245-6.
133. Fiore, L., H. B. Greenberg, and E. R. Mackow. 1991. The VP8 fragment of VP4 is the rhesus rotavirus hemagglutinin. *Virology* 181:553-63.
134. Fireman, P. 2003. Understanding asthma pathophysiology. *Allergy Asthma Proc* 24:79-83.
135. Flewett, T. H., A. S. Bryden, and H. Davies. 1973. Letter: Virus particles in gastroenteritis. *Lancet* 2:1497.
136. Flewett, T. H., A. S. Bryden, H. Davies, G. N. Woode, J. C. Bridger, and J. M. Derrick. 1974. Relation between viruses from acute gastroenteritis of children and newborn calves. *Lancet* 2:61-3.
137. Forstner, J. F., and G. G. Forstner. 1994. Gastrointestinal mucus, p. 1255-1284. *In* J. L.R. (ed.), *Physiology of the Gastrointestinal Tract*, 3rd ed. Raven, New York.
138. Franco, M. A., and H. B. Greenberg. 2000. Immunity to homologous rotavirus infection in adult mice. *Trends Microbiol* 8:50-2.
139. Franco, M. A., I. Prieto, M. Labbe, D. Poncet, F. Borrás-Cuesta, and J. Cohen. 1993. An immunodominant cytotoxic T cell epitope on the VP7 rotavirus protein overlaps the H2 signal peptide. *J Gen Virol* 74 (Pt 12):2579-86.
140. Fromantin, C., L. Piroth, I. Petitpas, P. Pothier, and E. Kohli. 1998. Oral delivery of homologous and heterologous strains of rotavirus to BALB/c mice induces the same profile of cytokine production by spleen cells. *Virology* 244:252-60.
141. Fukuhara, N., O. Yoshie, S. Kitaoka, and T. Konno. 1988. Role of VP3 in human rotavirus internalization after target cell attachment via VP7. *J Virol* 62:2209-18.
142. Furness, J. B. 1987. *The enteric nervous system*. Churchill Livingstone, New York.
143. Gache, Y., M. Allegra, C. Bodemer, A. Pisani-Spadafora, Y. de Prost, J. P. Ortonne, and G. Meneguzzi. 2001. Genetic bases of severe junctional epidermolysis bullosa presenting spontaneous amelioration with aging. *Hum Mol Genet* 10:2453-61.
144. Gietz, D., A. St Jean, R. A. Woods, and R. H. Schiestl. 1992. Improved method for high efficiency transformation of intact yeast cells. *Nucleic Acids Res* 20:1425.
145. Gilger, M. A., D. O. Matson, M. E. Conner, H. M. Rosenblatt, M. J. Finegold, and M. K. Estes. 1992. Extraintestinal rotavirus infections in children with immunodeficiency. *J Pediatr* 120:912-7.
146. Golantsova, N. E., E. E. Gorbunova, and E. R. Mackow. 2004. Discrete domains within the rotavirus VP5* direct peripheral membrane association and membrane permeability. *J Virol* 78:2037-44.
147. Gonzalez, R. A., M. A. Torres-Vega, S. Lopez, and C. F. Arias. 1998. In vivo interactions among rotavirus nonstructural proteins. *Arch Virol* 143:981-96.
148. Gonzalez, S. A., and O. R. Burrone. 1991. Rotavirus NS26 is modified by addition of single O-linked residues of N-acetylglucosamine. *Virology* 182:8-16.
149. Gouvea, V. S., A. A. Alencar, O. M. Barth, L. de Castro, A. M. Fialho, H. P. Araujo, S. Majerowicz, and H. G. Pereira. 1986. Diarrhoea in mice infected with a human rotavirus. *J Gen Virol* 67:577-81.
150. Graham, K. L., P. Halasz, Y. Tan, M. J. Hewish, Y. Takada, E. R. Mackow, M. K. Robinson, and B. S. Coulson. 2003. Integrin-using rotaviruses bind alpha2beta1 integrin alpha2 I domain via VP4 DGE sequence and recognize alphaXbeta2 and alphaVbeta3 by using VP7 during cell entry. *J Virol* 77:9969-78.
151. Greenberg, H. B., H. F. Clark, and P. A. Offit. 1994. Rotavirus pathology and pathophysiology. *Curr Top Microbiol Immunol* 185:255-83.

152. Grimwood, K., J. C. Lund, B. S. Coulson, I. L. Hudson, R. F. Bishop, and G. L. Barnes. 1988. Comparison of serum and mucosal antibody responses following severe acute rotavirus gastroenteritis in young children. *J Clin Microbiol* 26:732-8.
153. Grohmann, G. S., R. I. Glass, H. G. Pereira, S. S. Monroe, A. W. Hightower, R. Weber, and R. T. Bryan. 1993. Enteric viruses and diarrhea in HIV-infected patients. Enteric Opportunistic Infections Working Group. *N Engl J Med* 329:14-20.
154. Guarino, A., R. B. Canani, S. Russo, F. Albano, M. B. Canani, F. M. Ruggeri, G. Donelli, and A. Rubino. 1994. Oral immunoglobulins for treatment of acute rotaviral gastroenteritis. *Pediatrics* 93:12-6.
155. Guarino, A., R. B. Canani, M. I. Spagnuolo, F. Albano, and L. Di Benedetto. 1997. Oral bacterial therapy reduces the duration of symptoms and of viral excretion in children with mild diarrhea. *J Pediatr Gastroenterol Nutr* 25:516-9.
156. Guerin-Danan, C., J. C. Meslin, A. Chambard, A. Charpilienne, P. Relano, C. Bouley, J. Cohen, and C. Andrieux. 2001. Food supplementation with milk fermented by *Lactobacillus casei* DN-114 001 protects suckling rats from rotavirus-associated diarrhea. *J Nutr* 131:1111-7.
157. Guerin-Danan, C., J. C. Meslin, F. Lambre, A. Charpilienne, M. Serezat, C. Bouley, J. Cohen, and C. Andrieux. 1998. Development of a heterologous model in germfree suckling rats for studies of rotavirus diarrhea. *J Virol* 72:9298-302.
158. Guerrero, C. A., D. Bouyssouade, S. Zarate, P. Isa, T. Lopez, R. Espinosa, P. Romero, E. Mendez, S. Lopez, and C. F. Arias. 2002. Heat shock cognate protein 70 is involved in rotavirus cell entry. *J Virol* 76:4096-102.
159. Gum, J. R., J. W. Hicks, D. M. Swallow, R. L. Lagace, J. C. Byrd, D. T. Lamport, B. Siddiki, and Y. S. Kim. 1990.
160. Gum, J. R., Jr., J. W. Hicks, N. W. Toribara, B. Siddiki, and Y. S. Kim. 1994. Molecular cloning of human intestinal mucin (MUC2) cDNA. Identification of the amino terminus and overall sequence similarity to prepro-von Willebrand factor. *J Biol Chem* 269:2440-6.
161. Guo, C. T., O. Nakagomi, M. Mochizuki, H. Ishida, M. Kiso, Y. Ohta, T. Suzuki, D. Miyamoto, K. I. Hidari, and Y. Suzuki. 1999. Ganglioside GM(1a) on the cell surface is involved in the infection by human rotavirus KUN and MO strains. *J Biochem (Tokyo)* 126:683-8.
162. Halaihel, N., V. Lievin, F. Alvarado, and M. Vasseur. 2000. Rotavirus infection impairs intestinal brush-border membrane Na(+)-solute cotransport activities in young rabbits. *Am J Physiol Gastrointest Liver Physiol* 279:G587-96.
163. Halaihel, N., V. Lievin, J. M. Ball, M. K. Estes, F. Alvarado, and M. Vasseur. 2000. Direct inhibitory effect of rotavirus NSP4(114-135) peptide on the Na(+)-D-glucose symporter of rabbit intestinal brush border membrane. *J Virol* 74:9464-70.
164. Hamilton, J. R. 1988. Viral enteritis. *Pediatr Clin North Am* 35:89-101.
165. Heimer, G. V., and C. E. Taylor. 1974. Improved mountant for immunofluorescence preparations. *J Clin Pathol* 27:254-6.
166. Hershey, J. W. B., and W. C. Merrick. 2000. The pathway and mechanism of initiation of protein synthesis, p. 33-88. *In* N. Sonenberg, J. W. B. Hershey, and M. B. Mathews (ed.), *Translational control of gene expression*. Cold Spring Harbor Press, New York.
167. Hewish, M. J., Y. Takada, and B. S. Coulson. 2000. Integrins alpha2beta1 and alpha4beta1 can mediate SA11 rotavirus attachment and entry into cells. *J Virol* 74:228-36.
168. Heyman, M., G. Corthier, A. Petit, J. C. Meslin, C. Moreau, and J. F. Desjeux. 1987. Intestinal absorption of macromolecules during viral enteritis: an experimental study on rotavirus-infected conventional and germ-free mice. *Pediatr Res* 22:72-8.
169. Hirayama, B. A., M. P. Lostao, M. Panayotova-Heiermann, D. D. Loo, E. Turk, and E. M. Wright. 1996. Kinetic and specificity differences between rat, human, and rabbit Na⁺-glucose cotransporters (SGLT-1). *Am J Physiol* 270:G919-26.
170. Holmen, J. M., F. J. Olson, H. Karlsson, and G. C. Hansson. 2002. Two glycosylation alterations of mouse intestinal mucins due to infection caused by the parasite *Nippostrongylus brasiliensis*. *Glycoconj J* 19:67-75.
171. Holmes, I. H., B. J. Ruck, R. F. Bishop, and G. P. Davidson. 1975. Infantile enteritis; morphogenesis and morphology. *J Virol* 16:937-943.
172. Homaidan, F. R., A. Torres, M. Donowitz, and G. W. Sharp. 1991. Electrolyte transport in piglets infected with transmissible gastroenteritis virus. Stimulation by verapamil and clonidine. *Gastroenterology* 101:895-901.

173. Horie, Y., O. Nakagomi, Y. Koshimura, T. Nakagomi, Y. Suzuki, T. Oka, S. Sasaki, Y. Matsuda, and S. Watanabe. 1999. Diarrhea induction by rotavirus NSP4 in the homologous mouse model system. *Virology* 262:398-407.
174. Hoshino, Y., L. J. Saif, S. Y. Kang, M. M. Sereno, W. K. Chen, and A. Z. Kapikian. 1995. Identification of group A rotavirus genes associated with virulence of a porcine rotavirus and host range restriction of a human rotavirus in the gnotobiotic piglet model. *Virology* 209:274-80.
175. Hoshino, Y., L. J. Saif, M. M. Sereno, R. M. Chanock, and A. Z. Kapikian. 1988. Infection immunity of piglets to either VP3 or VP7 outer capsid protein confers resistance to challenge with a virulent rotavirus bearing the corresponding antigen. *J Virol* 62:744-8.
176. Hoshino, Y., M. M. Sereno, K. Midthun, J. Flores, A. Z. Kapikian, and R. M. Chanock. 1985. Independent segregation of two antigenic specificities (VP3 and VP7) involved in neutralization of rotavirus infectivity. *Proc Natl Acad Sci U S A* 82:8701-4.
177. Hoshino, Y., R. G. Wyatt, H. B. Greenberg, J. Flores, and A. Z. Kapikian. 1984. Serotypic similarity and diversity of rotaviruses of mammalian and avian origin as studied by plaque-reduction neutralization. *J Infect Dis* 149:694-702.
178. Hrdy, D. B. 1987. Epidemiology of rotaviral infection in adults. *Rev Infect Dis* 9:461-9.
179. Hsu, K. T., and J. Storch. 1996. Fatty acid transfer from liver and intestinal fatty acid-binding proteins to membranes occurs by different mechanisms. *J Biol Chem* 271:13317-23.
180. Hua, J., and J. T. Patton. 1994. The carboxyl-half of the rotavirus nonstructural protein NS53 (NSP1) is not required for virus replication. *Virology* 198:567-76.
181. Huang, W., R. Chiquet-Ehrismann, J. V. Moyano, A. Garcia-Pardo, and G. Orend. 2001. Interference of tenascin-C with syndecan-4 binding to fibronectin blocks cell adhesion and stimulates tumor cell proliferation. *Cancer Res* 61:8586-94.
182. Hunter, I., T. Schulthess, M. Bruch, K. Beck, and J. Engel. 1990. Evidence for a specific mechanism of laminin assembly. *Eur J Biochem* 188:205-11.
183. Ikeshima-Kataoka, H., J. B. Skeath, Y. Nabeshima, C. Q. Doe, and F. Matsuzaki. 1997. Miranda directs Prospero to a daughter cell during *Drosophila* asymmetric divisions. *Nature* 390:625-9.
184. Inaba, T., H. Sano, Y. Kawahito, T. Hla, K. Akita, M. Toda, I. Yamashina, M. Inoue, and H. Nakada. 2003. Induction of cyclooxygenase-2 in monocyte/macrophage by mucins secreted from colon cancer cells. *Proc Natl Acad Sci U S A* 100:2736-41.
185. Ingham, K. C., S. A. Brew, and D. H. Atha. 1990. Interaction of heparin with fibronectin and isolated fibronectin domains. *Biochem J* 272:605-11.
186. Iosef, C., T. Van Nguyen, K. Jeong, K. Bengtsson, B. Morein, Y. Kim, K. O. Chang, M. S. Azevedo, L. Yuan, P. Nielsen, and L. J. Saif. 2002. Systemic and intestinal antibody secreting cell responses and protection in gnotobiotic pigs immunized orally with attenuated Wa human rotavirus and Wa 2/6-rotavirus-like-particles associated with immunostimulating complexes. *Vaccine* 20:1741-53.
187. Ishida, S. I., N. Feng, J. M. Gilbert, B. Tang, and H. B. Greenberg. 1997. Immune responses to individual rotavirus proteins following heterologous and homologous rotavirus infection in mice. *J Infect Dis* 175:1317-23.
188. Iturriza-Gomara, M., I. A. Auchterlonie, W. Zaw, P. Molyneaux, U. Desselberger, and J. Gray. 2002. Rotavirus gastroenteritis and central nervous system (CNS) infection: characterization of the VP7 and VP4 genes of rotavirus strains isolated from paired fecal and cerebrospinal fluid samples from a child with CNS disease. *J Clin Microbiol* 40:4797-9.
189. Iturriza-Gomara, M., J. Green, D. W. Brown, M. Ramsay, U. Desselberger, and J. J. Gray. 2000. Molecular epidemiology of human group A rotavirus infections in the United Kingdom between 1995 and 1998. *J Clin Microbiol* 38:4394-401.
190. Jarvis, W. R., P. J. Middleton, and E. W. Gelfand. 1983. Significance of viral infections in severe combined immunodeficiency disease. *Pediatr Infect Dis* 2:187-92.
191. Jass, J. R., and A. M. Robertson. 1994. Colorectal mucin histochemistry in health and disease: a critical review. *Pathol Int* 44:487-504.
192. Jiang, B., J. R. Gentsch, and R. I. Glass. 2002. The role of serum antibodies in the protection against rotavirus disease: an overview. *Clin Infect Dis* 34:1351-61.
193. Jiang, B., L. Snipes-Magaldi, P. Dennehy, H. Keyserling, R. C. Holman, J. Bresee, J. Gentsch, and R. I. Glass. 2003. Cytokines as mediators for or effectors against rotavirus disease in children. *Clin Diagn Lab Immunol* 10:995-1001.

194. Joensuu, J., E. Koskenniemi, X. L. Pang, and T. Vesikari. 1997. Randomised placebo-controlled trial of rhesus-human reassortant rotavirus vaccine for prevention of severe rotavirus gastroenteritis. *Lancet* 350:1205-9.
195. Johnson, C. A., T. G. Snider, 3rd, W. G. Henk, and R. W. Fulton. 1986. A scanning and transmission electron microscopic study of rotavirus-induced intestinal lesions in neonatal gnotobiotic dogs. *Vet Pathol* 23:443-53.
196. Jolly, C. L., B. M. Beisner, and I. H. Holmes. 2000. Rotavirus infection of MA104 cells is inhibited by Ricinus lectin and separately expressed single binding domains. *Virology* 275:89-97.
197. Jonckheere, N., M. Van Der Sluis, A. Velghe, M. P. Buisine, M. Suttmuller, M. P. Ducourouble, P. Pigny, H. A. Buller, J. P. Aubert, A. W. Einerhand, and I. Van Seuningen. 2004. Transcriptional activation of the murine Muc5ac mucin gene in epithelial cancer cells by TGF-beta/Smad4 signalling pathway is potentiated by Sp1. *Biochem J* 377:797-808.
198. Jourdan, N., M. Maurice, D. Delautier, A. M. Quero, A. L. Servin, and G. Trugnan. 1997. Rotavirus is released from the apical surface of cultured human intestinal cells through nonconventional vesicular transport that bypasses the Golgi apparatus. *J Virol* 71:8268-78.
199. Kabcenell, A. K., and P. H. Atkinson. 1985. Processing of the rough endoplasmic reticulum membrane glycoproteins of rotavirus SA11. *J Cell Biol* 101:1270-80.
200. Kalica, A. R., J. Flores, and H. B. Greenberg. 1983. Identification of the rotaviral gene that codes for hemagglutination and protease-enhanced plaque formation. *Virology* 125:194-205.
201. Kaljot, K. T., R. D. Shaw, D. H. Rubin, and H. B. Greenberg. 1988. Infectious rotavirus enters cells by direct cell membrane penetration, not by endocytosis. *J Virol* 62:1136-44.
202. Kapikian, A. Z. 1993. Viral gastroenteritis.
203. Kapikian, A. Z., and R. M. Chanock. 1990. Rotaviruses, p. 1353-1404. *In* B. N. Fields, D. M. Knipe, R. M. Chanock, M. S. Hirsch, J. L. Melnick, and B. Roizman (ed.), *Virology*, 2nd ed. Raven press, New York.
204. Kapikian, A. Z., Y. Hoshino, and R. M. Chanock. 2001. Rotaviruses, p. 1787-1833. *In* D. M. Knipe and P. M. Howley (ed.), *Fields' virology*, 4th ed. Lippincott Williams and Wilkins, Philadelphia.
205. Kapikian, A. Z., Y. Hoshino, R. M. Chanock, and I. Perez-Schael. 1996. Jennerian and modified Jennerian approach to vaccination against rotavirus diarrhea using a quadrivalent rhesus rotavirus (RRV) and human-RRV reassortant vaccine. *Arch Virol Suppl* 12:163-75.
206. Kapikian, A. Z., H. W. Kim, R. G. Wyatt, W. L. Cline, J. O. Arrobio, C. D. Brandt, W. J. Rodriguez, D. A. Sack, R. M. Chanock, and R. H. Parrott. 1976. Human reovirus-like agent as the major pathogen associated with "winter" gastroenteritis in hospitalized infants and young children. *N Engl J Med* 294:965-72.
207. Kapikian, A. Z., H. W. Kim, R. G. Wyatt, W. J. Rodriguez, S. Ross, W. L. Cline, R. H. Parrott, and R. M. Chanock. 1974. Reoviruslike agent in stools: association with infantile diarrhea and development of serologic tests. *Science* 185:1049-53.
208. Karaki, S. I., and A. Kuwahara. 2004. Regulation of intestinal secretion involved in the interaction between neurotransmitters and prostaglandin E2. *Neurogastroenterol Motil* 16 Suppl 1:96-9.
209. Katyal, R., S. V. Rana, K. Vaiphei, S. Ohja, K. Singh, and V. Singh. 1999. Effect of rotavirus infection on small gut pathophysiology in a mouse model. *J Gastroenterol Hepatol* 14:779-84.
210. Keenan, K. P., H. R. Jervis, R. H. Marchwicki, and L. N. Binn. 1976. Intestinal infection of neonatal dogs with canine coronavirus 1-71: studies by virologic, histologic, histochemical, and immunofluorescent techniques. *Am J Vet Res* 37:247-56.
211. Keljo, D. J., D. G. Butler, and J. R. Hamilton. 1985. Altered jejunal permeability to macromolecules during viral enteritis in the piglet. *Gastroenterology* 88:998-1004.
212. Keljo, D. J., R. J. MacLeod, M. H. Perdue, D. G. Butler, and J. R. Hamilton. 1985. D-Glucose transport in piglet jejunal brush-border membranes: insights from a disease model. *Am J Physiol* 249:G751-60.
213. Kerzner, B., M. H. Kelly, D. G. Gall, D. G. Butler, and J. R. Hamilton. 1977. Transmissible gastroenteritis: sodium transport and the intestinal epithelium during the course of viral enteritis. *Gastroenterology* 72:457-61.
214. Kim, T. G., N. Befus, and W. H. Langridge. 2004. Co-immunization with an HIV-1 Tat transduction peptide-rotavirus enterotoxin fusion protein stimulates a Th1 mucosal immune response in mice. *Vaccine* 22:431-8.
215. Kim, Y. D., E. J. Kwon, D. W. Park, S. Y. Song, S. K. Yoon, and S. H. Baek. 2002. Interleukin-1beta induces MUC2 and MUC5AC synthesis through cyclooxygenase-2 in NCI-H292 cells. *Mol Pharmacol* 62:1112-8.

216. Kirkwood, C. D., B. S. Coulson, and R. F. Bishop. 1996. G3P2 rotaviruses causing diarrhoeal disease in neonates differ in VP4, VP7 and NSP4 sequence from G3P2 strains causing asymptomatic neonatal infection. *Arch Virol* 141:1661-76.
217. Konno, T., H. Suzuki, N. Katsushima, A. Imai, F. Tazawa, T. Kutsuzawa, S. Kitaoka, M. Sakamoto, N. Yazaki, and N. Ishida. 1983. Influence of temperature and relative humidity on human rotavirus infection in Japan. *J Infect Dis* 147:125-8.
218. Kordasti, S., H. Sjovall, O. Lundgren, and L. Svensson. 2004. Serotonin and vasoactive intestinal peptide antagonists attenuate rotavirus diarrhoea. *Gut* 53:952-7.
219. Korhonen, M., M. Ormio, R. E. Burgeson, I. Virtanen, and E. Savilahti. 2000. Unaltered distribution of laminins, fibronectin, and tenascin in celiac intestinal mucosa. *J Histochem Cytochem* 48:1011-20.
220. Kosmehl, H., A. Berndt, and D. Katenkamp. 1996. Molecular variants of fibronectin and laminin: structure, physiological occurrence and histopathological aspects. *Virchows Arch* 429:311-22.
221. Krasinski, S. D., G. Estrada, K. Y. Yeh, M. Yeh, P. G. Traber, E. H. Rings, H. A. Buller, M. Verhave, R. K. Montgomery, and R. J. Grand. 1994. Transcriptional regulation of intestinal hydrolase biosynthesis during postnatal development in rats. *Am J Physiol* 267:G584-94.
222. Kujubu, D. A., B. S. Fletcher, B. C. Varnum, R. W. Lim, and H. R. Herschman. 1991. TIS10, a phorbol ester tumor promoter-inducible mRNA from Swiss 3T3 cells, encodes a novel prostaglandin synthase/cyclooxygenase homologue. *J Biol Chem* 266:12866-72.
223. Kwong, A. D., and N. Frenkel. 1987. Herpes simplex virus-infected cells contain a function(s) that destabilizes both host and viral mRNAs. *Proc Natl Acad Sci U S A* 84:1926-30.
224. Laan, M. P., M. R. Baert, A. M. Bijl, A. E. Vredendaal, F. B. De Waard-van der Spek, A. P. Oranje, H. F. Savelkoul, and H. J. Neijens. 2000. Markers for early sensitization and inflammation in relation to clinical manifestations of atopic disease up to 2 years of age in 133 high-risk children. *Clin Exp Allergy* 30:944-53.
225. Labbe, M., P. Baudoux, A. Charpilienne, D. Poncet, and J. Cohen. 1994. Identification of the nucleic acid binding domain of the rotavirus VP2 protein. *J Gen Virol* 75 (Pt 12):3423-30.
226. LaMonica, R., S. S. Kocer, J. Nazarova, W. Dowling, E. Geimonen, R. D. Shaw, and E. R. Mackow. 2001. VP4 differentially regulates TRAF2 signaling, disengaging JNK activation while directing NF-kappa B to effect rotavirus-specific cellular responses. *J Biol Chem* 276:19889-96.
227. Larralde, G., and M. Gorziglia. 1992. Distribution of conserved and specific epitopes on the VP8 subunit of rotavirus VP4. *J Virol* 66:7438-43.
228. Laurie, G. W., C. P. Leblond, and G. R. Martin. 1982. Localization of type IV collagen, laminin, heparan sulfate proteoglycan, and fibronectin to the basal lamina of basement membranes. *J Cell Biol* 95:340-4.
229. Le, P. U., and I. R. Nabi. 2003. Distinct caveolae-mediated endocytic pathways target the Golgi apparatus and the endoplasmic reticulum. *J Cell Sci* 116:1059-71.
230. Leivo, I., T. Tani, L. Laitinen, R. Bruns, E. Kivilaakso, V. P. Lehto, R. E. Burgeson, and I. Virtanen. 1996. Anchoring complex components laminin-5 and type VII collagen in intestine: association with migrating and differentiating enterocytes. *J Histochem Cytochem* 44:1267-77.
231. Lewis, H. M., J. V. Parry, H. A. Davies, R. P. Parry, A. Mott, R. R. Dourmashkin, P. J. Sanderson, D. A. Tyrrell, and H. B. Valman. 1979. A year's experience of the rotavirus syndrome and its association with respiratory illness. *Arch Dis Child* 54:339-46.
232. Li, J. D., W. Feng, M. Gallup, J. H. Kim, J. Gum, Y. Kim, and C. Basbaum. 1998. Activation of NF-kappaB via a Src-dependent Ras-MAPK-pp90rsk pathway is required for *Pseudomonas aeruginosa*-induced mucin overproduction in epithelial cells. *Proc Natl Acad Sci U S A* 95:5718-23.
233. Lindenbergh-Kortleve, D. J., R. R. Rosato, J. W. van Neck, J. Nauta, M. van Kleffens, C. Groffen, E. C. Zwarthoff, and S. L. Drop. 1997. Gene expression of the insulin-like growth factor system during mouse kidney development. *Mol Cell Endocrinol* 132:81-91.
234. Lishko, V. K., V. P. Yakubenko, and T. P. Ugarova. 2003. The interplay between integrins alpha5beta1 and alpha5beta2 during cell migration to fibronectin. *Exp Cell Res* 283:116-26.
235. Little, E., P. Bork, and R. F. Doolittle. 1994. Tracing the spread of fibronectin type III domains in bacterial glycohydrolases. *J Mol Evol* 39:631-43.
236. Little, L. M., and J. A. Shaddock. 1982. Pathogenesis of rotavirus infection in mice. *Infect Immun* 38:755-63.
237. Liu, M., N. M. Mattion, and M. K. Estes. 1992. Rotavirus VP3 expressed in insect cells possesses guanylyltransferase activity. *Virology* 188:77-84.
238. Londhe, V., N. McNamara, H. Lemjabbar, and C. Basbaum. 2003. Viral dsRNA activates mucin transcription in airway epithelial cells. *FEBS Lett* 553:33-8.

239. Longman, R. J., J. Douthwaite, P. A. Sylvester, D. O'Leary, B. F. Warren, A. P. Corfield, and M. G. Thomas. 2000. Lack of mucin MUC5AC field change expression associated with tubulovillous and villous colorectal adenomas. *J Clin Pathol* 53:100-4.
240. Lopez, S., and C. F. Arias. 2004. Multistep entry of rotavirus into cells: a Versaillesque dance. *Trends Microbiol* 12:271-8.
241. Lopez, S., C. F. Arias, J. R. Bell, J. H. Strauss, and R. T. Espejo. 1985. Primary structure of the cleavage site associated with trypsin enhancement of rotavirus SA11 infectivity. *Virology* 144:11-9.
242. Losonsky, G. A., J. P. Johnson, J. A. Winkelstein, and R. H. Yolken. 1985. Oral administration of human serum immunoglobulin in immunodeficient patients with viral gastroenteritis. A pharmacokinetic and functional analysis. *J Clin Invest* 76:2362-7.
243. Lu, W., K. Miyazaki, H. Mizushima, and N. Nemoto. 2001. Immunohistochemical distribution of laminin-5 gamma2 chain and its developmental change in human embryonic and foetal tissues. *Histochem J* 33:629-37.
244. Lu, Y., M. Wambach, M. G. Katze, and R. M. Krug. 1995. Binding of the influenza virus NS1 protein to double-stranded RNA inhibits the activation of the protein kinase that phosphorylates the eIF-2 translation initiation factor. *Virology* 214:222-8.
245. Ludert, J. E., A. A. Krishnaney, J. W. Burns, P. T. Vo, and H. B. Greenberg. 1996. Cleavage of rotavirus VP4 in vivo. *J Gen Virol* 77 (Pt 3):391-5.
246. Lundgren, O., A. T. Peregrin, K. Persson, S. Kordasti, I. Uhnoo, and L. Svensson. 2000. Role of the enteric nervous system in the fluid and electrolyte secretion of rotavirus diarrhea. *Science* 287:491-5.
247. Lundgren, O., and L. Svensson. 2001. Pathogenesis of rotavirus diarrhea. *Microbes Infect* 3:1145-56.
248. Lynch, M., B. Lee, P. Azimi, J. Gentsch, C. Glaser, S. Gilliam, H. G. Chang, R. Ward, and R. I. Glass. 2001. Rotavirus and central nervous system symptoms: cause or contaminant? Case reports and review. *Clin Infect Dis* 33:932-8.
249. Maass, D. R., and P. H. Atkinson. 1990. Rotavirus proteins VP7, NS28, and VP4 form oligomeric structures. *J Virol* 64:2632-41.
250. Mack, D. R., and P. M. Sherman. 1991. Mucin isolated from rabbit colon inhibits in vitro binding of *Escherichia coli* RDEC-1. *Infect Immun* 59:1015-23.
251. Majerowicz, S., C. F. Kubelka, P. Stephens, and O. M. Barth. 1994. Ultrastructural study on experimental infection of rotavirus in a murine heterologous model. *Mem Inst Oswaldo Cruz* 89:395-402.
252. Makkink, M. K., N. M. Schwerbrock, M. Mahler, J. A. Boshuizen, I. B. Renes, M. Cornberg, H. J. Hedrich, A. W. Einerhand, H. A. Buller, S. Wagner, M. L. Enss, and J. Dekker. 2002. Fate of goblet cells in experimental colitis. *Dig Dis Sci* 47:2286-97.
253. Marchisio, P. C., O. Cremona, P. Savoia, G. Pellegrini, J. P. Ortonne, P. Verrando, R. E. Burgeson, R. Cancedda, and M. De Luca. 1993. The basement membrane protein BM-600/nicein codistributes with kalinin and the integrin alpha 6 beta 4 in human cultured keratinocytes. *Exp Cell Res* 205:205-12.
254. Marquet, F., D. Pansu, and M. Descroix-Vagne. 1999. Distant intestinal stimulation by cholera toxin in rat in vivo. *Eur J Pharmacol* 374:103-11.
255. Mashimo, H., D. C. Wu, D. K. Podolsky, and M. C. Fishman. 1996. Impaired defense of intestinal mucosa in mice lacking intestinal trefoil factor. *Science* 274:262-5.
256. Mason, B. B., D. Y. Graham, and M. K. Estes. 1980. In vitro transcription and translation of simian rotavirus SA11 gene products. *J Virol* 33:1111-21.
257. Mathan, M. M., G. Chandy, and V. I. Mathan. 1995. Ultrastructural changes in the upper small intestinal mucosa in patients with cholera. *Gastroenterology* 109:422-30.
258. Mathews, M. B., and T. Shenk. 1991. Adenovirus virus-associated RNA and translation control. *J Virol* 65:5657-62.
259. Matricardi, P. M., F. Rosmini, V. Panetta, L. Ferrigno, and S. Bonini. 2002. Hay fever and asthma in relation to markers of infection in the United States. *J Allergy Clin Immunol* 110:381-7.
260. Matricardi, P. M., F. Rosmini, S. Riondino, M. Fortini, L. Ferrigno, M. Rapicetta, and S. Bonini. 2000. Exposure to foodborne and orofecal microbes versus airborne viruses in relation to atopy and allergic asthma: epidemiological study. *Bmj* 320:412-7.
261. Mattion, N. M., J. Cohen, C. Aponte, and M. K. Estes. 1992. Characterization of an oligomerization domain and RNA-binding properties on rotavirus nonstructural protein NS34. *Virology* 190:68-83.
262. Mattion, N. M., J. Cohen, and M. K. Estes. 1994. The rotavirus proteins, p. 169-249. *In* A. Z. Kapikian (ed.), *Viral Infections of the Gastrointestinal Tract*. Marcel Dekker, New York.

263. Mattion, N. M., J. Cohen, and M. K. Estes. 1994. Viral infections of the gastrointestinal tract, p. 169-249. *In* A. Z. Kapikian (ed.). Marcel Dekker, New York.
264. Mattion, N. M., D. B. Mitchell, G. W. Both, and M. K. Estes. 1991. Expression of rotavirus proteins encoded by alternative open reading frames of genome segment 11. *Virology* 181:295-304.
265. McClung, H. J., D. G. Butler, B. Kerzner, D. G. Gall, and J. R. Hamilton. 1976. Transmissible gastroenteritis. Mucosal ion transport in acute viral enteritis. *Gastroenterology* 70:1091-5.
266. McNeal, M. M., K. S. Barone, M. N. Rae, and R. L. Ward. 1995. Effector functions of antibody and CD8⁺ cells in resolution of rotavirus infection and protection against reinfection in mice. *Virology* 214:387-97.
267. McNeal, M. M., R. L. Broome, and R. L. Ward. 1994. Active immunity against rotavirus infection in mice is correlated with viral replication and titers of serum rotavirus IgA following vaccination. *Virology* 204:642-50.
268. Mebus, C. A., M. Kono, N. R. Underdahl, and M. J. Twiehaus. 1971. Cell culture propagation of neonatal calf diarrhea (scours) virus. *Can Vet J* 12:69-72.
269. Medicine, I. o. 1986. New vaccine development:establishing priorities. *In* Diseases of importance in developing countries. Natl. Acad. Press, Washington DC.
270. Merchant, A. A., W. S. Groene, E. H. Cheng, and R. D. Shaw. 1991. Murine intestinal antibody response to heterologous rotavirus infection. *J Clin Microbiol* 29:1693-701.
271. Meyer, J. C., C. C. Bergmann, and A. R. Bellamy. 1989. Interaction of rotavirus cores with the nonstructural glycoprotein NS28. *Virology* 171:98-107.
272. Michel, Y. M., D. Poncet, M. Piron, K. M. Kean, and A. M. Borman. 2000. Cap-Poly(A) synergy in mammalian cell-free extracts. Investigation of the requirements for poly(A)-mediated stimulation of translation initiation. *J Biol Chem* 275:32268-76.
273. Mirazimi, A., M. Nilsson, and L. Svensson. 1998. The molecular chaperone calnexin interacts with the NSP4 enterotoxin of rotavirus in vivo and in vitro. *J Virol* 72:8705-9.
274. Mohri, H., J. Tanabe, K. Katoh, and T. Okubo. 1996. Identification of a novel binding site to the integrin alpha11beta3 located in the C-terminal heparin-binding domain of human plasma fibronectin. *J Biol Chem* 271:15724-8.
275. Moon, A., and R. E. Kleinman. 1995. Allergic gastroenteropathy in children. *Ann Allergy Asthma Immunol* 74:5-12.
276. Mori, Y., M. A. Borgan, N. Ito, M. Sugiyama, and N. Minamoto. 2002. Diarrhea-inducing activity of avian rotavirus NSP4 glycoproteins, which differ greatly from mammalian rotavirus NSP4 glycoproteins in deduced amino acid sequence in suckling mice. *J Virol* 76:5829-34.
277. Mori, Y., M. A. Borgan, M. Takayama, N. Ito, M. Sugiyama, and N. Minamoto. 2003. Roles of outer capsid proteins as determinants of pathogenicity and host range restriction of avian rotaviruses in a suckling mouse model. *Virology* 316:126-34.
278. Morris, A. P. 1999. The regulation of the epithelial cell cAMP-and calcium-dependent chloride channels. *Adv Pharmacol* 46:209-251.
279. Morris, A. P., and M. K. Estes. 2001. Microbes and microbial toxins: paradigms for microbial-mucosal interactions. VIII. Pathological consequences of rotavirus infection and its enterotoxin. *Am J Physiol Gastrointest Liver Physiol* 281:G303-10.
280. Morris, A. P., J. K. Scott, J. M. Ball, C. Q. Zeng, W. K. O'Neal, and M. K. Estes. 1999. NSP4 elicits age-dependent diarrhea and Ca(2+)-mediated I(-) influx into intestinal crypts of CF mice. *Am J Physiol* 277:G431-44.
281. Mosesson, M. W., K. R. Siebenlist, and D. A. Meh. 2001. The structure and biological features of fibrinogen and fibrin. *Ann N Y Acad Sci* 936:11-30.
282. Mossel, E. C., and R. F. Ramig. 2003. A lymphatic mechanism of rotavirus extraintestinal spread in the neonatal mouse. *J Virol* 77:12352-6.
283. Mota-Hernandez, F., J. J. Calva, C. Gutierrez-Camacho, S. Villa-Contreras, C. F. Arias, L. Padilla-Noriega, H. Guiscafre-Gallardo, M. de Lourdes Guerrero, S. Lopez, O. Munoz, J. F. Contreras, R. Cedillo, I. Herrera, and F. I. Puerto. 2003. Rotavirus diarrhea severity is related to the VP4 type in Mexican children. *J Clin Microbiol* 41:3158-62.
284. Mould, A. P., A. Komoriya, K. M. Yamada, and M. J. Humphries. 1991. The CS5 peptide is a second site in the IIICS region of fibronectin recognized by the integrin alpha 4 beta 1. Inhibition of alpha 4 beta 1 function by RGD peptide homologues. *J Biol Chem* 266:3579-85.
285. Munro, S., and H. R. Pelham. 1987. A C-terminal signal prevents secretion of luminal ER proteins. *Cell* 48:899-907.

286. Murakami, M., K. Nakashima, D. Kamei, S. Masuda, Y. Ishikawa, T. Ishii, Y. Ohmiya, K. Watanabe, and I. Kudo. 2003. Cellular prostaglandin E2 production by membrane-bound prostaglandin E synthase-2 via both cyclooxygenases-1 and -2. *J Biol Chem* 278:37937-47.
287. Murphy, T. V., P. M. Gargiullo, M. S. Massoudi, D. B. Nelson, A. O. Jumaan, C. A. Okoro, L. R. Zanardi, S. Setia, E. Fair, C. W. LeBaron, M. Wharton, J. R. Livengood, and J. R. Livingood. 2001. Intussusception among infants given an oral rotavirus vaccine. *N Engl J Med* 344:564-72.
288. Nakajima, H., T. Nakagomi, T. Kamisawa, N. Sakaki, K. Muramoto, T. Mikami, H. Nara, and O. Nakagomi. 2001. Winter seasonality and rotavirus diarrhoea in adults. *Lancet* 357:1950.
289. Newburg, D. S., J. A. Peterson, G. M. Ruiz-Palacios, D. O. Matson, A. L. Morrow, J. Shults, M. L. Guerrero, P. Chaturvedi, S. O. Newburg, C. D. Scallan, M. R. Taylor, R. L. Ceriani, and L. K. Pickering. 1998. Role of human-milk lactadherin in protection against symptomatic rotavirus infection. *Lancet* 351:1160-4.
290. Newton, K., J. C. Meyer, A. R. Bellamy, and J. A. Taylor. 1997. Rotavirus nonstructural glycoprotein NSP4 alters plasma membrane permeability in mammalian cells. *J Virol* 71:9458-65.
291. Nibert, M. L., D. B. Furlong, and B. N. Fields. 1991. Mechanisms of viral pathogenesis. Distinct forms of reoviruses and their roles during replication in cells and host. *J Clin Invest* 88:727-34.
292. Niessen, C. M., F. Hogervorst, L. H. Jaspars, A. A. de Melker, G. O. Delwel, E. H. Hulsman, I. Kuikman, and A. Sonnenberg. 1994. The alpha 6 beta 4 integrin is a receptor for both laminin and kalinin. *Exp Cell Res* 211:360-7.
293. Nieuw Amerongen, A. V., J. G. Bolscher, E. Bloemena, and E. C. Veerman. 1998. Sulfomucins in the human body. *Biol Chem* 379:1-18.
294. Nishimura, S., H. Ushijima, H. Shiraishi, C. Kanazawa, T. Abe, K. Kaneko, and Y. Fukuyama. 1993. Detection of rotavirus in cerebrospinal fluid and blood of patients with convulsions and gastroenteritis by means of the reverse transcription polymerase chain reaction. *Brain Dev* 15:457-9.
295. Niv, Y., J. C. Byrd, S. B. Ho, R. Dahiya, and Y. S. Kim. 1992. Mucin synthesis and secretion in relation to spontaneous differentiation of colon cancer cells in vitro. *Int J Cancer* 50:147-52.
296. Obert, G., I. Peiffer, and A. L. Servin. 2000. Rotavirus-induced structural and functional alterations in tight junctions of polarized intestinal Caco-2 cell monolayers. *J Virol* 74:4645-51.
297. O'Brien, J. A., J. A. Taylor, and A. R. Bellamy. 2000. Probing the structure of rotavirus NSP4: a short sequence at the extreme C terminus mediates binding to the inner capsid particle. *J Virol* 74:5388-94.
298. Offit, P. A. 1996. Host factors associated with protection against rotavirus disease: the skies are clearing. *J Infect Dis* 174 Suppl 1:S59-64.
299. Offit, P. A. 1994. Immunologic determinants of protection against rotavirus disease. *Curr Top Microbiol Immunol* 185:229-54.
300. Offit, P. A., G. Blavat, H. B. Greenberg, and H. F. Clark. 1986. Molecular basis of rotavirus virulence: role of gene segment 4. *J Virol* 57:46-9.
301. Offit, P. A., D. B. Boyle, G. W. Both, N. L. Hill, Y. M. Svoboda, S. L. Cunningham, R. J. Jenkins, and M. A. McCrae. 1991. Outer capsid glycoprotein vp7 is recognized by cross-reactive, rotavirus-specific, cytotoxic T lymphocytes. *Virology* 184:563-8.
302. Offit, P. A., H. F. Clark, M. J. Kornstein, and S. A. Plotkin. 1984. A murine model for oral infection with a primate rotavirus (simian SA11). *J Virol* 51:233-6.
303. Oishi, I., T. Kimura, T. Murakami, K. Haruki, K. Yamazaki, Y. Seto, Y. Minekawa, and H. Funamoto. 1991. Serial observations of chronic rotavirus infection in an immunodeficient child. *Microbiol Immunol* 35:953-61.
304. Okada, J., N. Kobayashi, K. Taniguchi, and S. Urasawa. 1999. Analysis on reassortment of rotavirus NSP1 genes lacking coding region for cysteine-rich zinc finger motif. *Arch Virol* 144:345-53.
305. O'Neal, C. M., G. R. Harriman, and M. E. Conner. 2000. Protection of the villus epithelial cells of the small intestine from rotavirus infection does not require immunoglobulin A. *J Virol* 74:4102-9.
306. Osborne, M. P., S. J. Haddon, A. J. Spencer, J. Collins, W. G. Starkey, T. S. Wallis, G. J. Clarke, K. J. Worton, D. C. Candy, and J. Stephen. 1988. An electron microscopic investigation of time-related changes in the intestine of neonatal mice infected with murine rotavirus. *J Pediatr Gastroenterol Nutr* 7:236-48.
307. Osborne, M. P., S. J. Haddon, K. J. Worton, A. J. Spencer, W. G. Starkey, D. Thornber, and J. Stephen. 1991. Rotavirus-induced changes in the microcirculation of intestinal villi of neonatal mice in relation to the induction and persistence of diarrhea. *J Pediatr Gastroenterol Nutr* 12:111-20.

308. Owens, J. R., R. Broadhead, R. G. Hendrickse, O. P. Jaswal, and R. N. Gangal. 1981. Loperamide in the treatment of acute gastroenteritis in early childhood. Report of a two centre, double-blind, controlled clinical trial. *Ann Trop Paediatr* 1:135-41.
309. Padilla-Noriega, L., S. J. Dunn, S. Lopez, H. B. Greenberg, and C. F. Arias. 1995. Identification of two independent neutralization domains on the VP4 trypsin cleavage products VP5* and VP8* of human rotavirus ST3. *Virology* 206:148-54.
310. Pang, X. L., J. Joensuu, and T. Vesikari. 1996. Detection of rotavirus RNA in cerebrospinal fluid in a case of rotavirus gastroenteritis with febrile seizures. *Pediatr Infect Dis J* 15:543-5.
311. Pankov, R., and K. M. Yamada. 2002. Fibronectin at a glance. *J Cell Sci* 115:3861-3.
312. Parashar, U. D., J. S. Bresee, J. R. Gentsch, and R. I. Glass. 1998. Rotavirus. *Emerg Infect Dis* 4:561-70.
313. Parashar, U. D., E. G. Hummelman, J. S. Bresee, M. A. Miller, and R. I. Glass. 2003. Global illness and deaths caused by rotavirus disease in children. *Emerg Infect Dis* 9:565-72.
314. Patel, R. S., E. Odermatt, J. E. Schwarzbauer, and R. O. Hynes. 1987. Organization of the fibronectin gene provides evidence for exon shuffling during evolution. *Embo J* 6:2565-72.
315. Patton, J. T. 1996. Rotavirus VP1 alone specifically binds to the 3' end of viral mRNA, but the interaction is not sufficient to initiate minus-strand synthesis. *J Virol* 70:7940-7.
316. Patton, J. T., M. T. Jones, A. N. Kalbach, Y. W. He, and J. Xiaobo. 1997. Rotavirus RNA polymerase requires the core shell protein to synthesize the double-stranded RNA genome. *J Virol* 71:9618-26.
317. Patton, J. T., and E. Spencer. 2000. Genome replication and packaging of segmented double-stranded RNA viruses. *Virology* 277:217-25.
318. Pediatrics, A. A. o. 2003. Rotavirus infections, p. 536. *In* L. K. Pickering (ed.), Red book 2003 report of Committee on Infectious Diseases, vol. 26. American Academy of Pediatrics, Elk Grove Village.
319. Peigue-Lafeuille, H., C. Henquell, M. Chambon, N. Gazuy, C. De Champs, and R. Cluzel. 1991. Nosocomial rotavirus infections in adult renal transplant recipients. *J Hosp Infect* 18:67-70.
320. Peregrin, A. T., H. Ahlman, M. Jodal, and O. Lundgren. 1999. Involvement of serotonin and calcium channels in the intestinal fluid secretion evoked by bile salt and cholera toxin. *Br J Pharmacol* 127:887-94.
321. Perez-Schael, I., M. J. Guntinas, M. Perez, V. Pagone, A. M. Rojas, R. Gonzalez, W. Cunto, Y. Hoshino, and A. Z. Kapikian. 1997. Efficacy of the rhesus rotavirus-based quadrivalent vaccine in infants and young children in Venezuela. *N Engl J Med* 337:1181-7.
322. Perreault, N., P. H. Vachon, and J. F. Beaulieu. 1995. Appearance and distribution of laminin A chain isoforms and integrin alpha 2, alpha 3, alpha 6, beta 1, and beta 4 subunits in the developing human small intestinal mucosa. *Anat Rec* 242:242-50.
323. Peterson, J. A., C. D. Scallan, R. L. Ceriani, and M. Hamosh. 2001. Structural and functional aspects of three major glycoproteins of the human milk fat globule membrane. *Adv Exp Med Biol* 501:179-87.
324. Petrie, B. L., M. K. Estes, and D. Y. Graham. 1983. Effects of tunicamycin on rotavirus morphogenesis and infectivity. *J Virol* 46:270-4.
325. Piron, M., T. Delaunay, J. Grosclaude, and D. Poncet. 1999. Identification of the RNA-binding, dimerization, and eIF4GI-binding domains of rotavirus nonstructural protein NSP3. *J Virol* 73:5411-21.
326. Piron, M., P. Vende, J. Cohen, and D. Poncet. 1998. Rotavirus RNA-binding protein NSP3 interacts with eIF4GI and evicts the poly(A) binding protein from eIF4F. *Embo J* 17:5811-21.
327. Pizarro, J. L., A. M. Sandino, J. M. Pizarro, J. Fernandez, and E. Spencer. 1991. Characterization of rotavirus guanylyltransferase activity associated with polypeptide VP3. *J Gen Virol* 72 (Pt 2):325-32.
328. Pizarro, J. M., J. L. Pizarro, J. Fernandez, A. M. Sandino, and E. Spencer. 1991. Effect of nucleotide analogues on rotavirus transcription and replication. *Virology* 184:768-72.
329. Plow, E. F., T. A. Haas, L. Zhang, J. Loftus, and J. W. Smith. 2000. Ligand binding to integrins. *J Biol Chem* 275:21785-8.
330. Poncet, D., C. Aponte, and J. Cohen. 1993. Rotavirus protein NSP3 (NS34) is bound to the 3' end consensus sequence of viral mRNAs in infected cells. *J Virol* 67:3159-65.
331. Poncet, D., S. Laurent, and J. Cohen. 1994. Four nucleotides are the minimal requirement for RNA recognition by rotavirus non-structural protein NSP3. *Embo J* 13:4165-73.
332. Poncet, D., P. Lindenbaum, R. L'Haridon, and J. Cohen. 1997. In vivo and in vitro phosphorylation of rotavirus NSP5 correlates with its localization in viroplasm. *J Virol* 71:34-41.
333. Poruchynsky, M. S., and P. H. Atkinson. 1988. Primary sequence domains required for the retention of rotavirus VP7 in the endoplasmic reticulum. *J Cell Biol* 107:1697-706.
334. Poruchynsky, M. S., and P. H. Atkinson. 1991. Rotavirus protein rearrangements in purified membrane-enveloped intermediate particles. *J Virol* 65:4720-7.

335. Poruchynsky, M. S., D. R. Maass, and P. H. Atkinson. 1991. Calcium depletion blocks the maturation of rotavirus by altering the oligomerization of virus-encoded proteins in the ER. *J Cell Biol* 114:651-6.
336. Poruchynsky, M. S., C. Tyndall, G. W. Both, F. Sato, A. R. Bellamy, and P. H. Atkinson. 1985. Deletions into an NH₂-terminal hydrophobic domain result in secretion of rotavirus VP7, a resident endoplasmic reticulum membrane glycoprotein. *J Cell Biol* 101:2199-209.
337. Prasad, B. V., J. W. Burns, E. Marietta, M. K. Estes, and W. Chiu. 1990. Localization of VP4 neutralization sites in rotavirus by three-dimensional cryo-electron microscopy. *Nature* 343:476-9.
338. Prasad, B. V., R. Rothnagel, C. Q. Zeng, J. Jakana, J. A. Lawton, W. Chiu, and M. K. Estes. 1996. Visualization of ordered genomic RNA and localization of transcriptional complexes in rotavirus. *Nature* 382:471-3.
339. Quaroni, A., and K. J. Isselbacher. 1985. Study of intestinal cell differentiation with monoclonal antibodies to intestinal cell surface components. *Dev Biol* 111:267-79.
340. Quaroni, A., K. J. Isselbacher, and E. Ruoslahti. 1978. Fibronectin synthesis by epithelial crypt cells of rat small intestine. *Proc Natl Acad Sci U S A* 75:5548-52.
341. Ramig, R. F. 1988. The effects of host age, virus dose, and virus strain on heterologous rotavirus infection of suckling mice. *Microb Pathog* 4:189-202.
342. Ramig, R. F. 2004. Pathogenesis of intestinal and systemic rotavirus infection. *Journal of Virology* In Press.
343. Ramirez, C. V., C. Vilela, K. Berthelot, and J. E. McCarthy. 2002. Modulation of eukaryotic mRNA stability via the cap-binding translation complex eIF4F. *J Mol Biol* 318:951-62.
344. Rao, G. G. 1995. Control of outbreaks of viral diarrhoea in hospitals--a practical approach. *J Hosp Infect* 30:1-6.
345. Renes, I. B., J. A. Boshuizen, D. J. Van Nispen, N. P. Bulsing, H. A. Buller, J. Dekker, and A. W. Einerhand. 2002. Alterations in Muc2 biosynthesis and secretion during dextran sulfate sodium-induced colitis. *Am J Physiol Gastrointest Liver Physiol* 282:G382-9.
346. Renes, I. B., M. Verburg, N. P. Bulsing, S. Ferdinandusse, H. A. Buller, J. Dekker, and A. W. Einerhand. 2002. Protection of the Peyer's patch-associated crypt and villus epithelium against methotrexate-induced damage is based on its distinct regulation of proliferation. *J Pathol* 198:60-8.
347. Reynolds, D. J., G. A. Hall, T. G. Debney, and K. R. Parsons. 1985. Pathology of natural rotavirus infection in clinically normal calves. *Res Vet Sci* 38:264-9.
348. Rhoads, J. M., E. O. Keku, J. Quinn, J. Woosely, and J. G. Lecce. 1991. L-glutamine stimulates jejunal sodium and chloride absorption in pig rotavirus enteritis. *Gastroenterology* 100:683-91.
349. Rhoads, J. M., R. J. MacLeod, and J. R. Hamilton. 1986. Alanine enhances jejunal sodium absorption in the presence of glucose: studies in piglet viral diarrhea. *Pediatr Res* 20:879-83.
350. Rhoads, J. M., R. J. MacLeod, and J. R. Hamilton. 1989. Diminished brush border membrane Na-dependent L-alanine transport in acute viral enteritis in piglets. *J Pediatr Gastroenterol Nutr* 9:225-31.
351. Rijke, R. P., W. R. Hanson, H. M. Plaisier, and J. W. Osborne. 1976. The effect of ischemic villus cell damage on crypt cell proliferation in the small intestine: evidence for a feedback control mechanism. *Gastroenterology* 71:786-92.
352. Robertson, A. M., and D. P. Wright. 1997. Bacterial glycosulphatases and sulphomucin degradation. *Can J Gastroenterol* 11:361-6.
353. Robinson, J. W., V. Mirkovitch, B. Winistorfer, and F. Saegesser. 1981. Response of the intestinal mucosa to ischaemia. *Gut* 22:512-27.
354. Rodriguez, W. J., H. W. Kim, J. O. Arrobio, C. D. Brandt, R. M. Chanock, A. Z. Kapikian, R. G. Wyatt, and R. H. Parrott. 1977. Clinical features of acute gastroenteritis associated with human reovirus-like agent in infants and young children. *J Pediatr* 91:188-93.
355. Rollo, E. E., K. P. Kumar, N. C. Reich, J. Cohen, J. Angel, H. B. Greenberg, R. Sheth, J. Anderson, B. Oh, S. J. Hempson, E. R. Mackow, and R. D. Shaw. 1999. The epithelial cell response to rotavirus infection. *J Immunol* 163:4442-52.
356. Rolsma, M. D., T. B. Kuhlenschmidt, H. B. Gelberg, and M. S. Kuhlenschmidt. 1998. Structure and function of a ganglioside receptor for porcine rotavirus. *J Virol* 72:9079-91.
357. Rose, J., M. A. Franco, and H. B. Greenberg. 1998. The immunology of rotavirus infection in the mouse. *Adv Virus Res* 51:203-235.
358. Rossen, J. W., J. Bouma, R. H. Raatgeep, H. A. Buller, and A. W. Einerhand. 2004. Inhibition of cyclooxygenase activity reduces rotavirus infection at a postbinding step. *J Virol* 78:9721-30.

359. Roth, K. A., J. M. Hertz, and J. I. Gordon. 1990. Mapping enteroendocrine cell populations in transgenic mice reveals an unexpected degree of complexity in cellular differentiation within the gastrointestinal tract. *J Cell Biol* 110:1791-801.
360. Rothenberg, M. E., A. Mishra, M. H. Collins, and P. E. Putnam. 2001. Pathogenesis and clinical features of eosinophilic esophagitis. *J Allergy Clin Immunol* 108:891-4.
361. Ruegg, C., A. A. Postigo, E. E. Sikorski, E. C. Butcher, R. Pytela, and D. J. Erle. 1992. Role of integrin alpha 4 beta 7/alpha 4 beta P in lymphocyte adherence to fibronectin and VCAM-1 and in homotypic cell clustering. *J Cell Biol* 117:179-89.
362. Ruggeri, F. M., and H. B. Greenberg. 1991. Antibodies to the trypsin cleavage peptide VP8 neutralize rotavirus by inhibiting binding of virions to target cells in culture. *J Virol* 65:2211-9.
363. Ruiz, M. C., M. J. Abad, A. Charpilienne, J. Cohen, and F. Michelangeli. 1997. Cell lines susceptible to infection are permeabilized by cleaved and solubilized outer layer proteins of rotavirus. *J Gen Virol* 78 (Pt 11):2883-93.
364. Ruiz, M. C., S. R. Alonso-Torre, A. Charpilienne, M. Vasseur, F. Michelangeli, J. Cohen, and F. Alvarado. 1994. Rotavirus interaction with isolated membrane vesicles. *J Virol* 68:4009-16.
365. Sachs, A. B. 2000. Physical and functional interactions between the mRNA cap structure and the poly(A) tail, p. 447-465. *In* N. Sonenberg, J. W. B. Hershey, and M. B. Mathews (ed.), *Translational control of gene expression*. Cold Spring Harbor Press, New York.
366. Sachs, A. B., and G. Varani. 2000. Eukaryotic translation initiation: there are (at least) two sides to every story. *Nat Struct Biol* 7:356-61.
367. Saif, L. J., B. I. Rosen, and A. V. Parwani. 1994. Animal Rotaviruses, p. 279-367. *In* A. Z. Kapikian (ed.), *Viral Infections of the Gastrointestinal Tract*. Marcel Dekker, New York.
368. Salazar-Lindo, E., J. Santisteban-Ponce, E. Chea-Woo, and M. Gutierrez. 2000. Racecadotril in the treatment of acute watery diarrhea in children. *N Engl J Med* 343:463-7.
369. Salim, A. F., A. D. Phillips, and M. J. Farthing. 1990. Pathogenesis of gut virus infection. *Baillieres Clin Gastroenterol* 4:593-607.
370. Salim, A. F., A. D. Phillips, J. A. Walker-Smith, and M. J. Farthing. 1995. Sequential changes in small intestinal structure and function during rotavirus infection in neonatal rats. *Gut* 36:231-8.
371. Sanchez-San Martin, C., T. Lopez, C. F. Arias, and S. Lopez. 2004. Characterization of rotavirus cell entry. *J Virol* 78:2310-8.
372. Sandino, A. M., M. Jashes, G. Faundez, and E. Spencer. 1986. Role of the inner protein capsid on in vitro human rotavirus transcription. *J Virol* 60:797-802.
373. Sapin, C., O. Colard, O. Delmas, C. Tessier, M. Breton, V. Enouf, S. Chwetzoff, J. Ouanich, J. Cohen, C. Wolf, and G. Trugnan. 2002. Rafts promote assembly and atypical targeting of a nonenveloped virus, rotavirus, in Caco-2 cells. *J Virol* 76:4591-602.
374. Sasaki, S., Y. Horie, T. Nakagomi, M. Oseto, and O. Nakagomi. 2001. Group C rotavirus NSP4 induces diarrhea in neonatal mice. *Arch Virol* 146:801-6.
375. Sato, E., T. Uezato, M. Fujita, and K. Nishimura. 1982. Developmental profiles of glycolipids in mouse small intestine. *J Biochem (Tokyo)* 91:2013-9.
376. Sattar, S. A., N. Lloyd-Evans, V. S. Springthorpe, and R. C. Nair. 1986. Institutional outbreaks of rotavirus diarrhoea: potential role of fomites and environmental surfaces as vehicles for virus transmission. *J Hyg (Lond)* 96:277-89.
377. Saulsbury, F. T., J. A. Winkelstein, and R. H. Yolken. 1980. Chronic rotavirus infection in immunodeficiency. *J Pediatr* 97:61-5.
378. Saxena, S. K., J. S. Thompson, D. A. Crouse, and J. G. Sharp. 1991. Epithelial cell proliferation and uptake of radiolabeled urogastone in the intestinal tissues following abdominal irradiation in the mouse. *Radiat Res* 128:37-42.
379. Schiestl, R. H., and R. D. Gietz. 1989. High efficiency transformation of intact yeast cells using single stranded nucleic acids as a carrier. *Curr Genet* 16:339-46.
380. Schwartz, M. A. 2001. Integrin signaling revisited. *Trends Cell Biol* 11:466-70.
381. Shahrabadi, M. S., and P. W. Lee. 1986. Bovine rotavirus maturation is a calcium-dependent process. *Virology* 152:298-307.
382. Shaoul, R., Y. Okada, E. Cutz, and M. A. Marcon. 2004. Colonic expression of MUC2, MUC5AC, and TFF1 in inflammatory bowel disease in children. *J Pediatr Gastroenterol Nutr* 38:488-93.
383. Sharma, A., J. A. Askari, M. J. Humphries, E. Y. Jones, and D. I. Stuart. 1999. Crystal structure of a heparin- and integrin-binding segment of human fibronectin. *Embo J* 18:1468-79.

384. Sharma, R., M. L. Hudak, B. R. Premachandra, G. Stevens, C. B. Monteiro, J. A. Bradshaw, A. M. Kaunitz, and R. A. Hollister. 2002. Clinical manifestations of rotavirus infection in the neonatal intensive care unit. *Pediatr Infect Dis J* 21:1099-105.
385. Shaw, R. D., and S. J. Hempson. 1996. Replication as a determinant of the intestinal response to rotavirus. *J Infect Dis* 174:1328-31.
386. Sheahan, D. G., and H. R. Jervis. 1976. Comparative histochemistry of gastrointestinal mucosubstances. *Am J Anat* 146:103-31.
387. Shekels, L. L., D. A. Hunninghake, A. S. Tisdale, I. K. Gipson, M. Kieliszewski, C. A. Kozak, and S. B. Ho. 1998. Cloning and characterization of mouse intestinal MUC3 mucin: 3' sequence contains epidermal-growth-factor-like domains. *Biochem J* 330 (Pt 3):1301-8.
388. Shekels, L. L., C. Lyftogt, M. Kieliszewski, J. D. Filie, C. A. Kozak, and S. B. Ho. 1995. Mouse gastric mucin: cloning and chromosomal localization. *Biochem J* 311 (Pt 3):775-85.
389. Shepherd, R. W., D. G. Butler, E. Cutz, D. G. Gall, and J. R. Hamilton. 1979. The mucosal lesion in viral enteritis. Extent and dynamics of the epithelial response to virus invasion in transmissible gastroenteritis of piglets. *Gastroenterology* 76:770-7.
390. Shepherd, R. W., D. G. Gall, D. G. Butler, and J. R. Hamilton. 1979. Determinants of diarrhea in viral enteritis. The role of ion transport and epithelial changes in the ileum in transmissible gastroenteritis in piglets. *Gastroenterology* 76:20-4.
391. Sherman, M. P., and K. L. Cox. 1982. Neonatal eosinophilic colitis. *J Pediatr* 100:587-9.
392. Shornikova, A. V., I. A. Casas, H. Mykkanen, E. Salo, and T. Vesikari. 1997. Bacteriotherapy with *Lactobacillus reuteri* in rotavirus gastroenteritis. *Pediatr Infect Dis J* 16:1103-7.
393. Shukry, S., A. M. Zaki, H. L. DuPont, I. Shoukry, M. el Tagi, and Z. Hamed. 1986. Detection of enteropathogens in fatal and potentially fatal diarrhea in Cairo, Egypt. *J Clin Microbiol* 24:959-62.
394. Simon, T. C., K. A. Roth, and J. I. Gordon. 1993. Use of transgenic mice to map cis-acting elements in the liver fatty acid-binding protein gene (*Fabpl*) that regulate its cell lineage- specific, differentiation-dependent, and spatial patterns of expression in the gut epithelium and in the liver acinus. *J Biol Chem* 268:18345-58.
395. Simon-Assmann, P., O. Lefebvre, A. Bellissent-Waydelich, J. Olsen, V. Orian-Rousseau, and A. De Arcangelis. 1998. The laminins: role in intestinal morphogenesis and differentiation. *Ann N Y Acad Sci* 859:46-64.
396. Singer, II, D. W. Kawka, S. Schloemann, T. Tessner, T. Riehl, and W. F. Stenson. 1998. Cyclooxygenase 2 is induced in colonic epithelial cells in inflammatory bowel disease. *Gastroenterology* 115:297-306.
397. Smirnova, M. G., J. P. Birchall, and J. P. Pearson. 2000. TNF-alpha in the regulation of MUC5AC secretion: some aspects of cytokine-induced mucin hypersecretion on the in vitro model. *Cytokine* 12:1732-6.
398. Snodgrass, D. R., K. W. Angus, and E. W. Gray. 1977. Rotavirus infection in lambs: pathogenesis and pathology. *Arch Virol* 55:263-74.
399. Snodgrass, D. R., A. Ferguson, F. Allan, K. W. Angus, and B. Mitchell. 1979. Small intestinal morphology and epithelial cell kinetics in lamb rotavirus infections. *Gastroenterology* 76:477-81.
400. Soriano-Brucher, H., P. Avendano, M. O'Ryan, S. D. Braun, M. D. Manhart, T. K. Balm, and H. A. Soriano. 1991. Bismuth subsalicylate in the treatment of acute diarrhea in children: a clinical study. *Pediatrics* 87:18-27.
401. Starkey, W. G., J. Collins, D. C. Candy, A. J. Spencer, M. P. Osborne, and J. Stephen. 1990. Transport of water and electrolytes by rotavirus-infected mouse intestine: a time course study. *J Pediatr Gastroenterol Nutr* 11:254-60.
402. Starkey, W. G., J. Collins, T. S. Wallis, G. J. Clarke, A. J. Spencer, S. J. Haddon, M. P. Osborne, D. C. Candy, and J. Stephen. 1986. Kinetics, tissue specificity and pathological changes in murine rotavirus infection of mice. *J Gen Virol* 67:2625-34.
403. Steer, S. A., and J. A. Corbett. 2003. The role and regulation of COX-2 during viral infection. *Viral Immunol* 16:447-60.
404. Steer, S. A., J. M. Moran, L. B. Maggi, Jr., R. M. Buller, H. Perlman, and J. A. Corbett. 2003. Regulation of cyclooxygenase-2 expression by macrophages in response to double-stranded RNA and viral infection. *J Immunol* 170:1070-6.
405. Stintzing, G., K. Johansen, K. E. Magnusson, L. Svensson, and T. Sundqvist. 1986. Intestinal permeability in small children during and after rotavirus diarrhoea assessed with different-size polyethyleneglycols (PEG 400 and PEG 1000). *Acta Paediatr Scand* 75:1005-9.
406. Strachan, D. P. 1989. Hay fever, hygiene, and household size. *Bmj* 299:1259-60.

407. Strous, G. J., and J. Dekker. 1992. Mucin-type glycoproteins. *Crit Rev Biochem Mol Biol* 27:57-92.
408. Suemori, S., K. Lynch-Devaney, and D. K. Podolsky. 1991. Identification and characterization of rat intestinal trefoil factor: tissue- and cell-specific member of the trefoil protein family. *Proc Natl Acad Sci U S A* 88:11017-21.
409. Superti, F., M. G. Ammendolia, A. Tinari, B. Bucci, A. M. Giammarioli, G. Rainaldi, R. Rivabene, and G. Donelli. 1996. Induction of apoptosis in HT-29 cells infected with SA-11 rotavirus. *J Med Virol* 50:325-34.
410. Superti, F., and G. Donelli. 1991. Gangliosides as binding sites in SA-11 rotavirus infection of LLC-MK2 cells. *J Gen Virol* 72 (Pt 10):2467-74.
411. Tafazoli, F., C. Q. Zeng, M. K. Estes, K. E. Magnusson, and L. Svensson. 2001. NSP4 enterotoxin of rotavirus induces paracellular leakage in polarized epithelial cells. *J Virol* 75:1540-6.
412. Taraporewala, Z., D. Chen, and J. T. Patton. 1999. Multimers formed by the rotavirus nonstructural protein NSP2 bind to RNA and have nucleoside triphosphatase activity. *J Virol* 73:9934-43.
413. Targan, S. R., and L. K. Murphy. 1995. Clarifying the causes of Crohn's. *Nat Med* 1:1241-3.
414. Taylor, J. A., J. C. Meyer, M. A. Legge, J. A. O'Brien, J. E. Street, V. J. Lord, C. C. Bergmann, and A. R. Bellamy. 1992. Transient expression and mutational analysis of the rotavirus intracellular receptor: the C-terminal methionine residue is essential for ligand binding. *J Virol* 66:3566-72.
415. Taylor, J. A., J. A. O'Brien, V. J. Lord, J. C. Meyer, and A. R. Bellamy. 1993. The RER-localized rotavirus intracellular receptor: a truncated purified soluble form is multivalent and binds virus particles. *Virology* 194:807-14.
416. Taylor, J. A., J. A. O'Brien, and M. Yeager. 1996. The cytoplasmic tail of NSP4, the endoplasmic reticulum-localized non-structural glycoprotein of rotavirus, contains distinct virus binding and coiled coil domains. *Embo J* 15:4469-76.
417. Telch, J., R. W. Shepherd, D. G. Butler, M. Perdue, J. R. Hamilton, and D. G. Gall. 1981. Intestinal glucose transport in acute viral enteritis in piglets. *Clin Sci (Lond)* 61:29-34.
418. Teller, I. C., and J. F. Beaulieu. 2001. Interactions between laminin and epithelial cells in intestinal health and disease. *Expert Rev Mol Med* 2001:1-18.
419. Thim, L. 1997. Trefoil peptides: from structure to function. *Cell Mol Life Sci* 53:888-903.
420. Tian, P., J. M. Ball, C. Q. Zeng, and M. K. Estes. 1996. The rotavirus nonstructural glycoprotein NSP4 possesses membrane destabilization activity. *J Virol* 70:6973-81.
421. Tian, P., M. K. Estes, Y. Hu, J. M. Ball, C. Q. Zeng, and W. P. Schilling. 1995. The rotavirus nonstructural glycoprotein NSP4 mobilizes Ca²⁺ from the endoplasmic reticulum. *J Virol* 69:5763-72.
422. Timpl, R., and J. C. Brown. 1996. Supramolecular assembly of basement membranes. *Bioessays* 18:123-32.
423. Torpier, G., J. F. Colombel, C. Mathieu-Chandelier, M. Capron, J. P. Dessaint, A. Cortot, J. C. Paris, and A. Capron. 1988. Eosinophilic gastroenteritis: ultrastructural evidence for a selective release of eosinophil major basic protein. *Clin Exp Immunol* 74:404-8.
424. Torres-Vega, M. A., R. A. Gonzalez, M. Duarte, D. Poncet, S. Lopez, and C. F. Arias. 2000. The C-terminal domain of rotavirus NSP5 is essential for its multimerization, hyperphosphorylation and interaction with NSP6. *J Gen Virol* 81:821-30.
425. Tossier, G., T. Delaunay, E. Kohli, J. Grosclaude, P. Pothier, and J. Cohen. 1994. Topology of bovine rotavirus (RF strain) VP6 epitopes by real-time biospecific interaction analysis. *Virology* 204:8-16.
426. Tytgat, K. M., H. A. Buller, F. J. Opdam, Y. S. Kim, A. W. Einerhand, and J. Dekker. 1994. Biosynthesis of human colonic mucin: Muc2 is the prominent secretory mucin. *Gastroenterology* 107:1352-63.
427. Tytgat, K. M., J. W. van der Wal, A. W. Einerhand, H. A. Buller, and J. Dekker. 1995. Muc2 in ulcerative colitis: a quantitative study. *Biochem Soc Trans* 23:531S.
428. Ugarova, T. P., and V. P. Yakubenko. 2001. Recognition of fibrinogen by leukocyte integrins. *Ann N Y Acad Sci* 936:368-85.
429. Uhnou, I., T. Dharakul, M. Riepenhoff-Talty, and P. L. Ogra. 1988. Immunological aspects of interaction between rotavirus and the intestine in infancy. *Immunol Cell Biol* 66:135-45.
430. Uhnou, I., M. Riepenhoff-Talty, T. Dharakul, P. Chegas, J. E. Fisher, H. B. Greenberg, and P. L. Ogra. 1990. Extramucosal spread and development of hepatitis in immunodeficient and normal mice infected with rhesus rotavirus. *J Virol* 64:361-8.
431. Ushijima, H., K. Q. Xin, S. Nishimura, S. Morikawa, and T. Abe. 1994. Detection and sequencing of rotavirus VP7 gene from human materials (stools, sera, cerebrospinal fluids, and throat swabs) by reverse transcription and PCR. *J Clin Microbiol* 32:2893-7.

432. Utani, A., M. Nomizu, R. Timpl, P. P. Roller, and Y. Yamada. 1994. Laminin chain assembly. Specific sequences at the C terminus of the long arm are required for the formation of specific double- and triple-stranded coiled-coil structures. *J Biol Chem* 269:19167-75.
433. Valenzuela, S., J. Pizarro, A. M. Sandino, M. Vasquez, J. Fernandez, O. Hernandez, J. Patton, and E. Spencer. 1991. Photoaffinity labeling of rotavirus VP1 with 8-azido-ATP: identification of the viral RNA polymerase. *J Virol* 65:3964-7.
434. Van Beers, E. H., H. A. Buller, R. J. Grand, A. W. Einerhand, and J. Dekker. 1995. Intestinal brush border glycohydrolases: structure, function, and development. *Crit Rev Biochem Mol Biol* 30:197-262.
435. Van De Bovenkamp, J. H., A. M. Korteland-Van Male, H. A. Buller, A. W. Einerhand, and J. Dekker. 2003. Metaplasia of the duodenum shows a *Helicobacter pylori*-correlated differentiation into gastric-type protein expression. *Hum Pathol* 34:156-65.
436. Van De Bovenkamp, J. H., A. M. Korteland-Van Male, C. Warson, H. A. Buller, A. W. Einerhand, N. L. Ectors, and J. Dekker. 2003. Gastric-type mucin and TFF-peptide expression in Barrett's oesophagus is disturbed during increased expression of MUC2. *Histopathology* 42:555-65.
437. Van den Brink, G. R., K. M. Tytgat, R. W. Van der Hulst, C. M. Van der Loos, A. W. Einerhand, H. A. Buller, and J. Dekker. 2000. *H pylori* colocalises with MUC5AC in the human stomach. *Gut* 46:601-7.
438. Van Klinken, B. J., J. Dekker, H. A. Buller, and A. W. Einerhand. 1995. Mucin gene structure and expression: protection vs. adhesion. *Am J Physiol* 269:G613-27.
439. van Klinken, B. J., J. Dekker, S. A. van Gool, J. van Marle, H. A. Buller, and A. W. Einerhand. 1998. MUC5B is the prominent mucin in human gallbladder and is also expressed in a subset of colonic goblet cells. *Am J Physiol* 274:G871-8.
440. van Klinken, B. J., A. W. Einerhand, L. A. Duits, M. K. Makkink, K. M. Tytgat, I. B. Renes, M. Verburg, H. A. Buller, and J. Dekker. 1999. Gastrointestinal expression and partial cDNA cloning of murine Muc2. *Am J Physiol* 276:G115-24.
441. van Klinken, B. J., E. Oussoren, J. J. Weenink, G. J. Strous, H. A. Buller, J. Dekker, and A. W. Einerhand. 1996. The human intestinal cell lines Caco-2 and LS174T as models to study cell-type specific mucin expression. *Glycoconj J* 13:757-68.
442. Van Klinken, B. J., J. W. Van der Wal, A. W. Einerhand, H. A. Buller, and J. Dekker. 1999. Sulphation and secretion of the predominant secretory human colonic mucin MUC2 in ulcerative colitis. *Gut* 44:387-93.
443. Van Seuning, I., P. Pigny, M. Perrais, N. Porchet, and J. P. Aubert. 2001. Transcriptional regulation of the 11p15 mucin genes. Towards new biological tools in human therapy, in inflammatory diseases and cancer? *Front Biosci* 6:D1216-34.
444. Velazquez, F. R., D. O. Matson, J. J. Calva, L. Guerrero, A. L. Morrow, S. Carter-Campbell, R. I. Glass, M. K. Estes, L. K. Pickering, and G. M. Ruiz-Palacios. 1996. Rotavirus infections in infants as protection against subsequent infections. *N Engl J Med* 335:1022-8.
445. Vende, P., M. Piron, N. Castagne, and D. Poncet. 2000. Efficient translation of rotavirus mRNA requires simultaneous interaction of NSP3 with the eukaryotic translation initiation factor eIF4G and the mRNA 3' end. *J Virol* 74:7064-71.
446. Verburg, M., I. B. Renes, H. P. Meijer, J. A. Taminiau, H. A. Buller, A. W. Einerhand, and J. Dekker. 2000. Selective sparing of goblet cells and paneth cells in the intestine of methotrexate-treated rats. *Am J Physiol Gastrointest Liver Physiol* 279:G1037-47.
447. Verburg, M., I. B. Renes, D. J. Van Nispen, S. Ferdinandusse, M. Jorritsma, H. A. Buller, A. W. Einerhand, and J. Dekker. 2002. Specific responses in rat small intestinal epithelial mRNA expression and protein levels during chemotherapeutic damage and regeneration. *J Histochem Cytochem* 50:1525-36.
448. Vesikari, T., T. Rautanen, T. Varis, G. M. Beards, and A. Z. Kapikian. 1990. Rhesus Rotavirus candidate vaccine. Clinical trial in children vaccinated between 2 and 5 months of age. *Am J Dis Child* 144:285-9.
449. Vollet, J. J., C. D. Ericsson, G. Gibson, L. K. Pickering, H. L. DuPont, S. Kohl, and R. H. Conklin. 1979. Human rotavirus in an adult population with travelers' diarrhea and its relationship to the location of food consumption. *J Med Virol* 4:81-7.
450. Walsh, R. E., and T. S. Gaginella. 1991. The eosinophil in inflammatory bowel disease. *Scand J Gastroenterol* 26:1217-24.
451. Ward, L. A., B. I. Rosen, L. Yuan, and L. J. Saif. 1996. Pathogenesis of an attenuated and a virulent strain of group A human rotavirus in neonatal gnotobiotic pigs. *J Gen Virol* 77 (Pt 7):1431-41.
452. Ward, R. L. 2003. Possible mechanisms of protection elicited by candidate rotavirus vaccines as determined with the adult mouse model. *Viral Immunol* 16:17-24.

453. Ward, R. L., M. M. McNeal, and J. F. Sheridan. 1990. Development of an adult mouse model for studies on protection against rotavirus. *J Virol* 64:5070-5.
454. Welch, S. K., S. E. Crawford, and M. K. Estes. 1989. Rotavirus SA11 genome segment 11 protein is a nonstructural phosphoprotein. *J Virol* 63:3974-82.
455. Westerwoudt, R. J., A. M. Naipal, and C. M. Harrison. 1984. Improved fusion technique. II. Stability and purity of hybrid clones. *J Immunol Methods* 68:89-101.
456. Whitfeld, P. L., C. Tyndall, S. C. Stirzaker, A. R. Bellamy, and G. W. Both. 1987. Location of sequences within rotavirus SA11 glycoprotein VP7 which direct it to the endoplasmic reticulum. *Mol Cell Biol* 7:2491-7.
457. Wilde, J., R. Yolken, R. Willoughby, and J. Eiden. 1991. Improved detection of rotavirus shedding by polymerase chain reaction. *Lancet* 337:323-6.
458. Willemsen, L. E., M. A. Koetsier, S. J. van Deventer, and E. A. van Tol. 2003. Short chain fatty acids stimulate epithelial mucin 2 expression through differential effects on prostaglandin E(1) and E(2) production by intestinal myofibroblasts. *Gut* 52:1442-7.
459. Willoughby, R. E., and R. H. Yolken. 1990. SA11 rotavirus is specifically inhibited by an acetylated sialic acid. *J Infect Dis* 161:116-9.
460. Wong, W. M., R. Poulosom, and N. A. Wright. 1999. Trefoil peptides. *Gut* 44:890-5.
461. Wood, D. J., T. J. David, I. L. Chrystie, and B. Totterdell. 1988. Chronic enteric virus infection in two T-cell immunodeficient children. *J Med Virol* 24:435-44.
462. Woods, A., R. L. Longley, S. Tumova, and J. R. Couchman. 2000. Syndecan-4 binding to the high affinity heparin-binding domain of fibronectin drives focal adhesion formation in fibroblasts. *Arch Biochem Biophys* 374:66-72.
463. Xiao, H., C. Neuveut, M. Benkirane, and K. T. Jeang. 1998. Interaction of the second coding exon of Tat with human EF-1 delta delineates a mechanism for HIV-1-mediated shut-off of host mRNA translation. *Biochem Biophys Res Commun* 244:384-9.
464. Xu, A., A. R. Bellamy, and J. A. Taylor. 1998. BiP (GRP78) and endoplasmic reticulum chaperone (GRP94) are induced following rotavirus infection and bind transiently to an endoplasmic reticulum-localized virion component. *J Virol* 72:9865-72.
465. Xu, A., A. R. Bellamy, and J. A. Taylor. 2000. Immobilization of the early secretory pathway by a virus glycoprotein that binds to microtubules. *Embo J* 19:6465-74.
466. Yamashiro, Y., T. Shimizu, S. Oguchi, and M. Sato. 1989. Prostaglandins in the plasma and stool of children with rotavirus gastroenteritis. *J Pediatr Gastroenterol Nutr* 9:322-7.
467. Yeager, M., J. A. Berriman, T. S. Baker, and A. R. Bellamy. 1994. Three-dimensional structure of the rotavirus haemagglutinin VP4 by cryo-electron microscopy and difference map analysis. *Embo J* 13:1011-8.
468. Yolken, R., S. Arango-Jaramillo, J. Eiden, and S. Vonderfecht. 1988. Lack of genomic reassortment following infection of infant rats with group A and group B rotaviruses. *J Infect Dis* 158:1120-3.
469. Yolken, R., and J. Wilde. 1994. Assays for detecting human rotavirus, p. 251-278. *In* A. Z. Kapikian (ed.), *Viral infections of the gastrointestinal tract*, 2 ed. Marcel Dekker, New York.
470. Yolken, R. H., C. A. Bishop, T. R. Townsend, E. A. Bolyard, J. Bartlett, G. W. Santos, and R. Saral. 1982. Infectious gastroenteritis in bone-marrow-transplant recipients. *N Engl J Med* 306:1010-2.
471. Yolken, R. H., C. Ojeh, I. A. Khatri, U. Sajjan, and J. F. Forstner. 1994. Intestinal mucins inhibit rotavirus replication in an oligosaccharide-dependent manner. *J Infect Dis* 169:1002-6.
472. Yolken, R. H., R. Willoughby, S. B. Wee, R. Miskuff, and S. Vonderfecht. 1987. Sialic acid glycoproteins inhibit in vitro and in vivo replication of rotaviruses. *J Clin Invest* 79:148-54.
473. Yolken, R. H., R. G. Wyatt, G. Zisis, C. D. Brandt, W. J. Rodriguez, H. W. Kim, R. H. Parrott, J. J. Urrutia, L. Mata, H. B. Greenberg, A. Z. Kapikian, and R. M. Chanock. 1978. Epidemiology of human rotavirus Types 1 and 2 as studied by enzyme-linked immunosorbent assay. *N Engl J Med* 299:1156-61.
474. Yoshida, A., T. Kawamitsu, R. Tanaka, M. Okumura, S. Yamakura, Y. Takasaki, H. Hiramatsu, T. Momoi, M. Iizuka, and O. Nakagomi. 1995. Rotavirus encephalitis: detection of the virus genomic RNA in the cerebrospinal fluid of a child. *Pediatr Infect Dis J* 14:914-6.
475. Yurchenco, P. D., and J. J. O'Rear. 1994. Basement membrane assembly. *Methods Enzymol* 245:489-518.
476. Zarate, S., M. A. Cuadras, R. Espinosa, P. Romero, K. O. Juarez, M. Camacho-Nuez, C. F. Arias, and S. Lopez. 2003. Interaction of rotaviruses with Hsc70 during cell entry is mediated by VP5. *J Virol* 77:7254-60.

477. Zarate, S., P. Romero, R. Espinosa, C. F. Arias, and S. Lopez. 2004. VP7 Mediates the Interaction of Rotaviruses with Integrin $\alpha v\beta 3$ through a Novel Integrin-Binding Site. *J Virol* 78:10839-10847.
478. Zeng, C. Q., M. K. Estes, A. Charpilienne, and J. Cohen. 1998. The N terminus of rotavirus VP2 is necessary for encapsidation of VP1 and VP3. *J Virol* 72:201-8.
479. Zhang, M., C. Q. Zeng, Y. Dong, J. M. Ball, L. J. Saif, A. P. Morris, and M. K. Estes. 1998. Mutations in rotavirus nonstructural glycoprotein NSP4 are associated with altered virus virulence. *J Virol* 72:3666-72.
480. Zhang, M., C. Q. Zeng, A. P. Morris, and M. K. Estes. 2000. A functional NSP4 enterotoxin peptide secreted from rotavirus-infected cells. *J Virol* 74:11663-70.
481. Zijlstra, R. T., B. A. McCracken, J. Odle, S. M. Donovan, H. B. Gelberg, B. W. Petschow, F. A. Zuckermann, and H. R. Gaskins. 1999. Malnutrition modifies pig small intestinal inflammatory responses to rotavirus. *J Nutr* 129:838-43.

**Dankwoord
&
Curriculum
vitae**

Dankwoord

Een proefschrift produceer je niet alleen en dat geldt zeker ook voor dit proefschrift. Om het mezelf eenvoudig te maken en bij voorbaat niemand te vergeten wil ik graag iedereen bedanken die, op welke manier dan ook, heeft bijgedragen tot de totstandkoming van dit proefschrift. De volgende mensen wil ik echter in het bijzonder bedanken voor hun bijdrage. Als eerste wil ik natuurlijk mijn begeleidster en co-promotor dr. Sandra Einerhand bedanken voor haar bijdrage en betrokkenheid bij mijn promotieonderzoek. Bedankt voor je nimmer aflatende enthousiasme en inzet. Vlak voor het afronden van mijn promotie heb je het lab Kindergeneeskunde verlaten en ben je naar het bedrijfsleven vertrokken, heel veel succes in je nieuwe carrière.

Dr. Jan Dekker, je bent tijdens de duur van mijn onderzoek verhuisd naar het Rudolf Magnus Instituut in Utrecht. Vanuit je nieuwe functie ben je altijd bereid geweest om mijn manuscripten te corrigeren en te voorzien van commentaar. Zowel je “professionele” als persoonlijke betrokkenheid heb ik zeer gewaardeerd en ik wil je hiervoor hartelijk danken.

Mijn promotor professor Büller. Beste Hans, je hebt mijn onderzoek natuurlijk altijd van een wat grotere afstand gadeslagen. Ik bewonder de manier waarop je tijdens de besprekingen over de voortgang van het werk altijd “knopen kon doorhakken”.

Beste Johan, ik ben altijd met groot plezier naar Bilthoven gereden voor onze gezamenlijke experimenten. Bedankt voor alle hulp en ik wens je veel succes met het afronden van je eigen promotie.

Vanessa, Rahena en Cynthia ik heb jullie met veel plezier begeleid tijdens jullie stage. Jullie werk is van groot belang geweest voor ons onderzoek, bedankt voor jullie bijdrage. Anita Korteland, dank je voor alle (immuno-)histochemische kleuringen en dat je, tot misselijkheid toe, achter de microscoop al die vervelende tellingen hebt volbracht. Janneke Bouma, je hebt in mijn laatste jaar nog heel wat praktisch werk afgerond, hartelijk dank daarvoor. John Rossen, bedankt voor het opzetten van het 2-hybrid systeem, de puntjes op de i tijdens de werkbesprekingen en de gezelligheid tijdens het congres in Parijs. Maria van der Sluis en Danielle van Nispen, bedankt voor de gezelligheid en technische ondersteuning. Charlie bedankt voor de enthousiaste inzet en schitterende dubbelkleuringen. Frank en Ytje, bedankt voor jullie inzet.

Alle (ex) collega’s van het laboratorium Kindergeneeskunde: Ad, Amy, Anita, Arantza, Arlène, Barbara, Bas, Charlie, Cynthia, Daniëlle, Debby, Dicky, Edward, Freek, Gerard, Ingrid, Jessica, Jules, Karin, Marcel, Maria, Marrit, Monique, Marcel, Natasja, Nathalie, Paul, Peter & Peter & Peter, Rolien, Ronald, Saskia, Sebastiaan, Silvia, Theo, Thomas & Thomas, Vesna, Vishal, Wendy, Wim, Wouter, alle stagiaires die ik hier vergeten ben, en natuurlijk de ex-KG&V AIO’s Jeroen en Melissa. Bedankt voor jullie hulp, collegialiteit en gezelligheid. Ada, speciale dank voor al het regelwerk, het lab zal je missen.

Mijn paranimfen Wim Rietveld en Ingrid Renes. Wim, dank je voor alle gezellige gesprekken over onze gezamenlijke hobby’s en je betrokkenheid. We moeten maar weer

eens afspreken om te gaan blokfluiten. Bedankt dat je mijn paranimf wilde zijn. Ingrid, je bent een onderzoeker in hart en nieren met je tomeloze enthousiasme en inzet. Ondanks je volle agenda wilde je toch nog tijd vrijmaken, bedankt daarvoor.

Amos en Andre, jungs bedankt voor de vriendschap en de survival ontspanningstochten.

Ik wil de hele familie, en met name tante Annie, bedanken voor de belangstelling en support.

Helmoed & Anneke, heel hartelijk bedankt voor alle steun het afgelopen decennium!

Pa & Ma, bedankt voor het feit dat jullie altijd achter mij staan en zullen staan!

Sam “mini-man” je bent een ongelofelijke bron van vreugde en energie. Het is een genot om je te zien opgroeien! En als laatste,...Mireille. Allerliefste, dank je voor al je steun en liefde!

That’s all I have to say about that.

Curriculum Vitae

The author of this thesis was born on December 29th, 1971 in Boxmeer (The Netherlands). After graduating from the Rijksscholengemeenschap Ter Apel in 1989, he attended teacher-training education at the Algemene Hogeschool Amsterdam. From 1992 to 1998 he studied biology at the University of Amsterdam, where he did research at the department of Virology, Laboratory of Medical Microbiology (head: dr. J ter Schegget) and the Laboratory of Pediatric Gastroenterology & Nutrition (head: prof. dr. H.A. Büller) at the Academic Medical Center (AMC), Amsterdam (The Netherlands). He obtained his Master of Sciences degree (drs) in oktober 1998 and in 1999 began working at the Laboratory of Pediatrics at the Erasmus MC in Rotterdam. Under supervision of dr. A.W.C. Einerhand and prof.dr. H.A. Büller the research resulted in this thesis. The author is married to Mireille Makkink with whom he has a child: Sam, born in 2002.

Publications

1. **J.A. Boshuizen**, J. Reimerink, A.M. Korteland-van Male, V.J.J. van Ham, M.P.G. Koopmans, H.A. Büller, J. Dekker, A.W.C. Einerhand, Changes in small intestinal homeostasis, morphology, and gene expression during rotavirus infection in infant mice. *Journal of Virology*, December 2003, Vol. 77, No. 24, p. 13005-13016.
2. **J.A. Boshuizen**, J.W.A. Rossen, C.K. Sitaram, F.F.P Kimenai, Y. Oosterhuis, H.A. Büller, J. Dekker and A.W.C. Einerhand. Rotavirus enterotoxin NSP4 interacts with the extracellular matrix proteins fibronectin and laminin beta 3 subunit. *Journal of Virology*, September 2004, Vol. 78, No 18, p. 10045-10053.
3. **J.A. Boshuizen**, J. Reimerink, A.M. Korteland-van Male, V.J.J. van Ham, M.P.G. Koopmans, H.A. Büller, J. Dekker, A.W.C. Einerhand. Goblet cell homeostasis during rotavirus infection in infant mice. *Virology* 2005; *in press*.
4. **J.A. Boshuizen**, J. Bouma, H.A. Büller, J. Dekker, A.W.C. Einerhand. Rotavirus infection induces mucin gene expression via a prostaglandin-mediated mechanism. Manuscript submitted.
5. J. Reimerink, **J.A. Boshuizen**, A.W.C. Einerhand, G van Amerongen, N Schmidt, M.P.G. Koopmans. Polarization of the mucosal and systemic immune response following oral inoculation of neonatal mice with rotavirus depends on source and level of purification of the virus: implications for the use of heterologous vaccine candidates. Manuscript submitted.
6. I.B. Renes, **J.A. Boshuizen**, D.J.P.M. van Nispen, H.A. Buller, J. Dekker, A.W.C. Einerhand. Alterations in Muc2 biosynthesis and secretion during dextran sulfate sodium-induced colitis. *Am J Physiol Gastrointest Liver Physiol* 2002 Feb; 282(2):G382-G389.
7. M.K. Makkink, N.M. Schwerbrock, M. Mähler, **J.A. Boshuizen**, I.B. Renes, M. Cornberg, H.J. Hedrich, A.W.C. Einerhand, H.A. Buller, S. Wagner, M.L. Enss, J. Dekker. Fate of goblet cells in experimental colitis. *Dig Dis Sci* 2002 Oct;47(10):2286-2297.

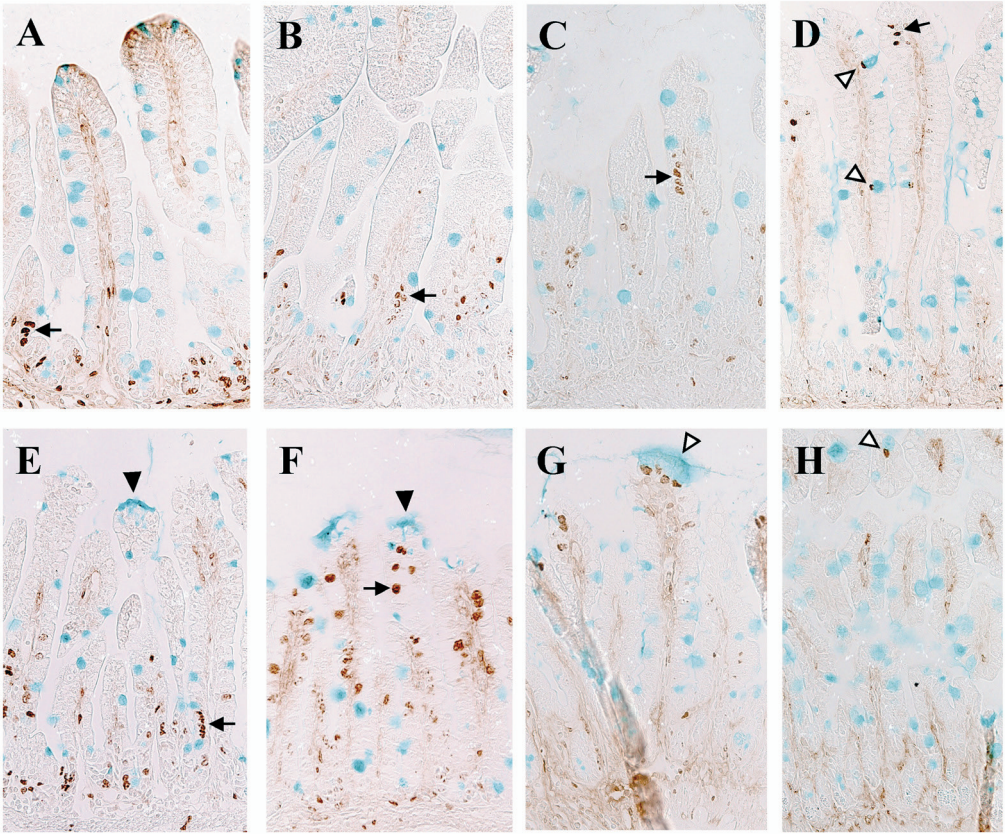
Appendix

Color Figures

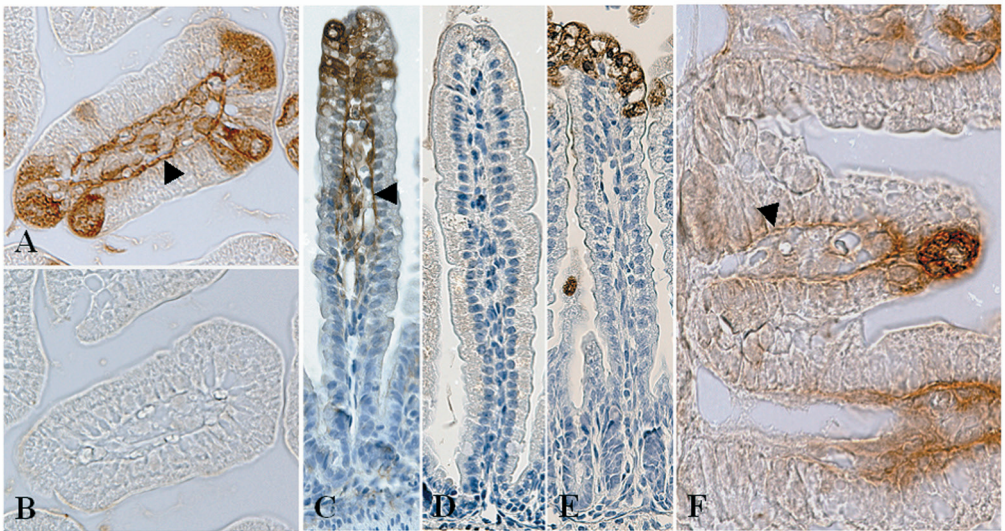
Chapter 3, Figure 7. (page 166, top) The number of goblet cells containing sulfated mucins and acidic mucins during rotavirus infection. Using a combined AB-PAS staining, goblet cells in control tissue (A; at 4 dpi) stained pink, whereas goblet cells stained blue in the crypt region or dark purple on the villi in infected tissue (B; at 4 dpi). This phenomenon was observed from 1 to 4 dpi in all analyzed sections from infected animals. Using a combined HID-AB staining (C-E), goblet cells in control mice stained black/brown indicating that they contained sulfated mucins (C; at 7 dpi). In infected mice, goblet cells stained blue indicating that they predominantly contained sialomucin (D; at 7 dpi). During infection, the percentage of HID-stained goblet cells was significantly decreased at 1 and 7 dpi (E). a $P < .005$, ‡ $P < .001$ vs. control using Student's *t*-test.

Chapter 6, Figure 2. (page 166, bottom) NSP4 associates with the epithelial basement membrane in mouse jejunum during rotavirus infection in neonatal mice. Using the anti-NSP4 (114-135) rabbit polyclonal serum, NSP4 protein was detected in epithelial cells at the tips of intestinal villi at 4 days post infection and at the epithelial BM of infected- and non-infected cells (A and C, arrowheads). Localization of NSP4 at the BM was not observed with pre-immune serum (B). NSP4 protein expression was not detected in control mice (D). An antibody that recognizes rotavirus structural proteins stained infected epithelial cells, but failed to stain the epithelial basement membranes (E). NSP4 could occasionally be detected in the BM of lower villus- and crypt cells (F, arrowhead). Panels A and B are cross-sectional slides, original magnification, X 400. Panels C to F are longitudinal slides, original magnification, X 200 (C to E) and X 600 (F).

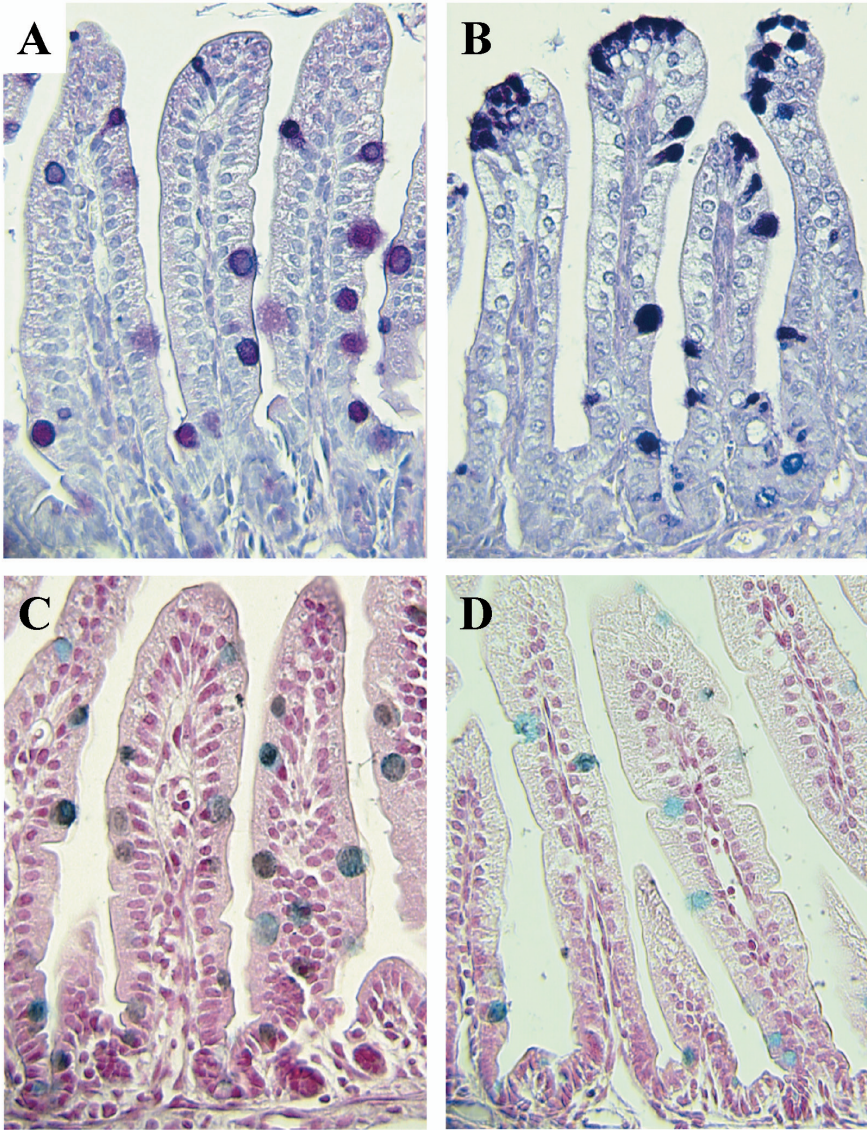
Chapter 3, Figure 3. (page 167) Goblet cell migration kinetics in the ileum during rotavirus infection. Just before inoculation, mice were injected with BrdU. Goblet cells in control (A-D) and infected mice (E-H) at 1 (A and E), 2 (B and F), 4 (C and G), and 7 dpi (D and H) were detected by AB staining. From 1 to 7 dpi, BrdU-labeled enterocytes (arrows) in infected mice migrated faster up the villus than in control animals. In infected mice, goblet cells (solid arrowheads or open arrowheads when BrdU-labeled) tended to accumulate at the tips of the villi (E-H), whereas in control mice goblet cells appeared evenly distributed in the villus epithelium.



Chapter 3, Figure 3.



Chapter 6, Figure 2.



E

| | Percentage of IID positive goblet cells | | | | | |
|----------|---|-----------|-------------|------------|------------|------------|
| | 6 hpi | 1 dpi | 2 dpi | 4 dpi | 7 dpi | 14 dpi |
| control | 52.8±9.4 | 74.7±3.2 | 61.0±29.7 | 58.2±14.0 | 68.9±20.6 | 57.6±18.0 |
| Infected | 50.0± 25.3 | 44.8± 9.9 | 38.6± 19.7a | 64.2± 30.1 | 23.2± 3.9‡ | 57.3± 11.4 |

Chapter 3, Figure 7.

